Green chemistry in Ireland

This editorial is being written at the time of the European Catalysis Conference ('Europacat')—one of the major events in the calendar for academic and industrial chemists interested in catalysis, regularly attracting over 1000 delegates. For the first time Europacat is being held in Ireland at the University of Limerick, and also for the first time a Green Chemistry Session has been included, with a large number of oral and poster presentations. In the light of this, one of Limerick's most senior professors Kieran Hodnett has co-authored this editorial to give us an outline of green chemistry in Ireland, and especially at the University of Limerick.

The chemical industry in Ireland is dominated by the pharmaceuticals sector with smaller numbers of plants in fine and bulk chemicals; in the last 10 years the electronics manufacturing sector has also become very important. Manufacturing licenses, however, are being issued by the Environmental Protection Agency with ever more stringent conditions.

An increasing number of projects at universities in Ireland are under way in the general area of green chemistry addressing the twin aspects of clean and end-of-pipe technologies. Several research groups in Limerick are involved in such green chemistry research projects. A novel low-waste Friedel–Crafts acylation process based on trifluoroacetic anhydride–phosphoric acid has been developed by T. Smyth and successfully applied to an intermediate in the manufacture of Tamoxifen; it has also recently been applied to the synthesis of 2-tetralones (Scheme 1).

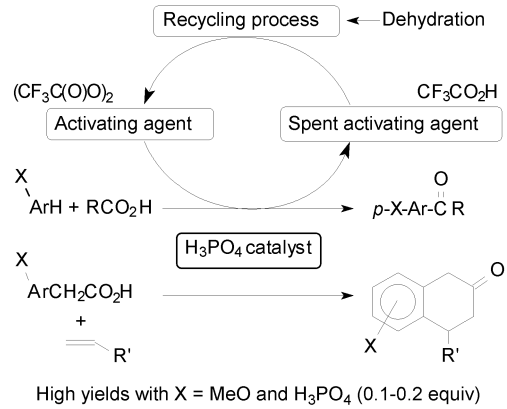

Scheme 1 Synthesis of 2-tetralones, involving a low-waste Friedel–Crafts acylation process.

The high cost of virgin vegetable oil as well as EU land use policies has restricted the utilisation of biodiesel, but this can be overcome by using waste cooking oil and tallow as alternative low-cost feedstocks. Research work at Limerick led by J. J. Leahy focuses on pretreating the waste cooking oil to reduce moisture, free fatty acids and peroxides so as to increase the yield and quality of the methyl ester.

Several research groups at Limerick are involved in research on catalytic oxidation. These include low-temperature catalytic oxidation over hydrophobic catalysts (J. B. McMonagle); the selective oxidation of hydrocarbons to olefins and oxygenates (J. R. H. Ross); the CuO/Al_2O_3 catalysed oxidation of SO_2 to SO_3, followed by capture of the latter species to form $CuSO_4/Al_2O_3$ (B. K. Hodnett); and the study of adsorption and activity of proteins and enzymes on and inside mesoporous silicates (E. Magner and G. Wall). The last of these is directed towards developing the next generation of heterogeneous catalysts with selectivities in excess of those that can be achieved with current catalysts. Peroxidative activity profiles over a range of adsorbed protein concentrations is typically twice that of the free protein in aqueous solution.

T. Curtin and P. O'Sullivan are researching the vapour phase Beckmann rearrangement of cyclohexanone oxime to caprolactam using a range of solid acid catalysts varying from boron oxide-treated aluminas to zeolites. They have shown that there is a direct relationship between the amount of coke that forms on the surface and the loss in catalytic activity. They have postulated that polymerisation of caprolactam and the condensation of aniline with cyclohexanone to a Schiff base on basic sites represents a possible starting point for coke formation.

The management of industrial waste is a topic of major concern to industry, government and the public. Many industries have adopted new processing technologies to reduce or eliminate waste, but some, *e.g.* the alumina industry, continue to produce very large quantities of waste residue. For every tonne of alumina produced, 500–700 kg of waste red mud is generated. The vast majority of this is stockpiled close to the production plant. Though much research has been done throughout the world, no viable use for the red mud has been found to make any appreciable impact on the quantities generated. However, one technology that has spread from Australia is to use the red mud waste to treat another industrial waste—tailings from mines. The latter contain high levels of heavy metals such as lead and arsenic, contaminating soil and water and posing a major environmental threat. Red mud can adsorb up to 99.99% of these heavy metals, producing a very inert and stable material that supports plant growth and vegetation; the run-off water is of drinkable quality. This technology is now a commercial reality with a number of projects starting in Europe. Given the number of mining tailing areas throughout Europe, possibly in the thousands, the use of red mud to rehabilitate these sites may be a cost-effective means of solving two problems at once. Aughinish Alumina and the University of Limerick are working together to apply this technology in Ireland and work under the direction of R. Moles at the university and M. Fennel of Aughinish Alumina is under way.

James Clark and Kieran Hodnett
Limerick, September 2001

DOI: 10.1039/b108143h

Running fuel cells on biogas – a renewable fuel

Biogas represents a renewable but largely under-exploited energy reserve often ignored because of the variable composition and often low level of methane that prevents its use in conventional power systems. As part of our continuing series of front-section articles on renewable waste energy, John Staniforth and Mark Ormerod from the Birchall Centre for Inorganic Chemistry and Materials Science at Keele University, UK, describe how biogas can be used directly in a solid oxide fuel cell even at remarkably low levels of methane thus offering a valuable use for poor-quality biogas that is currently wasted.

Introduction to biogas

Biogas is a complex and variable mixture of methane, carbon dioxide and other gases.[1] It is cheap and readily available and should be considered as a very under-exploited energy reserve. It is currently used for heating and cooking purposes in Third World countries such as India and China.[2] One of the principal limitations of biogas in certain applications is its variability of composition, not only in different locations but also over time, which presents major difficulties in its use.[3] As the proportion of carbon dioxide in the biogas increases the fuel becomes progressively more difficult to ignite, and eventually the proportion of CO_2 becomes such that ignition can no longer be maintained; this occurs when the ratio of CO_2 to methane is about 3 : 1.[4] Because of this situation, large quantities of biogas are presently vented to the atmosphere, making a significant contribution to greenhouse gas emissions, whilst at the same time wasting a potentially clean, renewable energy resource.

Solid oxide fuel cells (SOFCs)

Fuel cells are currently attracting tremendous interest because of their huge potential in stationary, portable and transport applications,[5-9] in terms of sustainability of our energy use. They also offer environmental advantages, combining significantly higher efficiency with very much lower emissions of SO_x, NO_x and residual hydrocarbons, and significantly reduced CO_2 emissions, compared to conventional power generation. Solid oxide fuel cells (SOFCs) (which use a hard ceramic material instead of a liquid electrolyte, and operate at a very high temperature) offer potential advantages in terms of efficiency, flexibility and cost over other types of fuel cells, because of their tolerance to carbon monoxide, their increased resistance to poisons and impurities in the fuel and because their high operating temperatures allow the possibility of running the fuel cell directly on natural gas or other practical hydrocarbon fuels, catalytically reforming the fuel to CO and H_2 within the fuel cell.[8,9] It is generally accepted that for SOFCs to be cost-effective, internal reforming of the fuel within the fuel cell is essential, since this both increases efficiency and reduces the complexity of the system.[8] Although natural gas is the most common fuel for SOFCs, other hydrocarbon fuels such as propane and butane are particularly suitable for certain applications.

Biogas as a fuel source for SOFCs

From the above it follows that biogas can be considered as a possible source of fuel for the solid oxide fuel cell. At CO_2 levels which are too high for conventional power generation systems, SOFCs could, in theory, still extract the power available from the methane content of biogas. Thus, in principle, SOFCs offer the possibility of using even biogas that is depleted in methane, consuming methane which would otherwise be vented wastefully and harmfully to the atmosphere, thus acting as an environmental clean-up device, significantly reducing the contribution to greenhouse gas emissions (methane being a 26-fold greenhouse gas than CO_2), whilst at the same time producing useful energy.

Conventionally in SOFCs steam is added to the natural gas and the natural gas is catalytically converted to CO and H_2 *via* steam reforming [eqn. (1)], either externally, or preferably internally, either indirectly using a reforming catalyst or directly on the nickel anode.[10]

$$CH_4 + H_2O \rightarrow 3H_2 + CO \qquad (1)$$

There are still several major problems associated with internal reforming in SOFCs, which contribute to a loss of cell performance and lead to poor durability. There is therefore much interest in developing and evaluating optimised anode formulations for internally reforming SOFCs.[11] Partial oxidation of the natural gas to H_2 and CO using oxygen [eqn. (2)], or potentially air, is a possible alternative to steam reforming,[12] though it does lead to an inherent inefficiency due to the large energy loss in oxidising methane, and carbon deposition is a particular problem.

$$CH_4 + {}^1/_2O_2 \rightarrow 2H_2 + CO \qquad (2)$$

Carbon dioxide or 'dry' reforming of methane [eqn. (3)] has attracted much attention in recent years as a potentially very attractive route for methane conversion,[13] not least for environmental reasons, though again carbon deposition is a major problem.

$$CH_4 + CO_2 \rightarrow 2H_2 + 2CO \qquad (3)$$

Carbon dioxide is inherently present in biogas, in addition to methane, and hence **in principle biogas may be used directly in the SOFC without the addition of either steam or oxygen**. One obvious potential drawback is the variable composition of biogas, and hence the variable CO_2/methane ratio.

DOI: 10.1039/b108144f

SOFC test system

At Keele we have recently demonstrated that it is possible to run a solid oxide fuel cell directly on biogas, using a small tubular SOFC and test system developed in our laboratory.

The SOFC test system, shown schematically in Fig. 1, is based on a small diameter, thin-walled tubular solid electrolyte reactor. The test cell inlet is linked to a gas handling system which enables evaluation over a full range of operating conditions and fuel compositions. The exhaust gas from the SOFC is monitored by gas chromatography. Hence, the test system allows the performance and durability of the fuel cell to be evaluated, whilst simultaneously directly studying the reforming catalysis and reactions of biogas in the actual working SOFC. We have previously demonstrated the value of such *in situ* catalytic measurements on SOFCs.[14]

The SOFC has a two-layer anode, both layers consisting of nickel oxide and yttria-stabilised zirconia physically mixed in specified proportions in a solvent slurry. Ceria was also added to the outer layer anode. The anode was applied to the inside of the electrolyte tubes and dried in air before high temperature firing. Strontium-doped lanthanum manganite was used as the cathode material and again applied in two layers. Gas mixtures were made up to cover the full composition range of all biogas sources. The anodes were not pre-reduced but were exposed directly to the biogas feed at operating temperature.

Fig. 2 shows the power obtained from an SOFC operating at 850 °C as a function of methane content of the biogas, whilst Fig. 3 shows the corresponding exit gas composition from the SOFC under the same experimental conditions, except that the measurements were made with the cell not under load in order to prevent interference from the electrochemical cell reactions. The changes in the power output can be attributed to the gas composition at the anode and hence the availability and type of fuel.

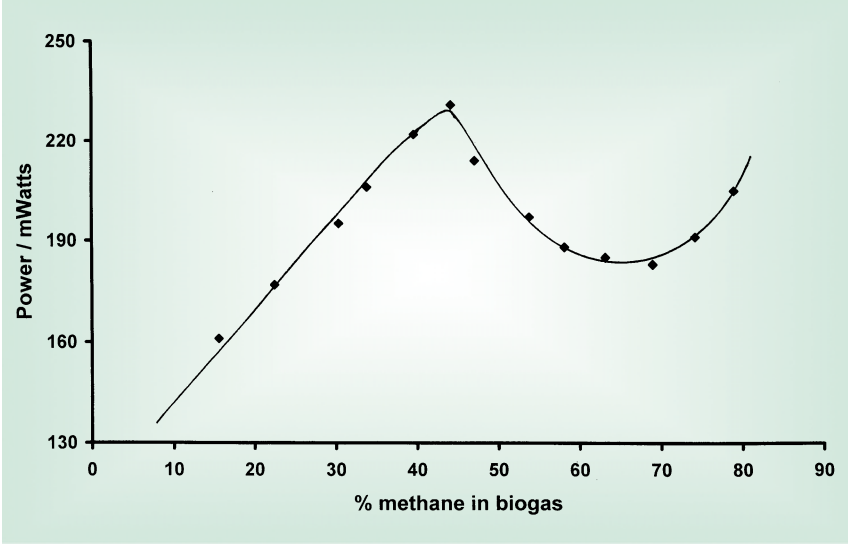

Fig. 2 Power output from a small tubular solid oxide fuel cell running on biogas at 850 °C, as a function of methane content.

There is a steady increase in power output from the cell over the range 15–45% methane content in the biogas, with a maximum power output for biogas with a methane content of 45%. As the methane content in the biogas exceeds 45% the power output decreases, initially quite quickly and then more slowly, reaching a minimum for biogas with a methane content around 70%, with an increase in power output being observed for biogas with methane content exceeding 70%.

For biogas samples with methane contents of 15–45% the exit gas composition from the fuel cell shows that complete consumption of the methane occurs, together with the formation of H_2 and CO, the amount of which parallel the increase in power output, and significant consumption of the CO_2 in the biogas. Maximum formation of CO and H_2 occurs at almost exactly the same fuel composition at which maximum power output is observed, close to equimolar quantities of methane and CO_2. At this biogas composition essentially complete consumption of CO_2 was observed. The exit gas compositions thus clearly show that internal dry reforming of the methane present in the biogas [eqn. (3)] is occurring effectively. As the methane content of the biogas exceeds 45% and the CO_2 content decreases, the amount of H_2 and CO formed start to decrease. This behaviour again precisely mirrors the power output over this composition range. The quantity of methane in the exit gas continues to increase. This clearly demonstrates that it is electrochemical oxidation of H_2 and CO which lead to power production, and that direct electrochemical oxidation of methane does not therefore make any significant contribution to power production.

For biogas with methane content around 75% the amount of H_2 in the exit gas reaches a minimum, with H_2 production increasing at higher methane contents, with a parallel increase in the

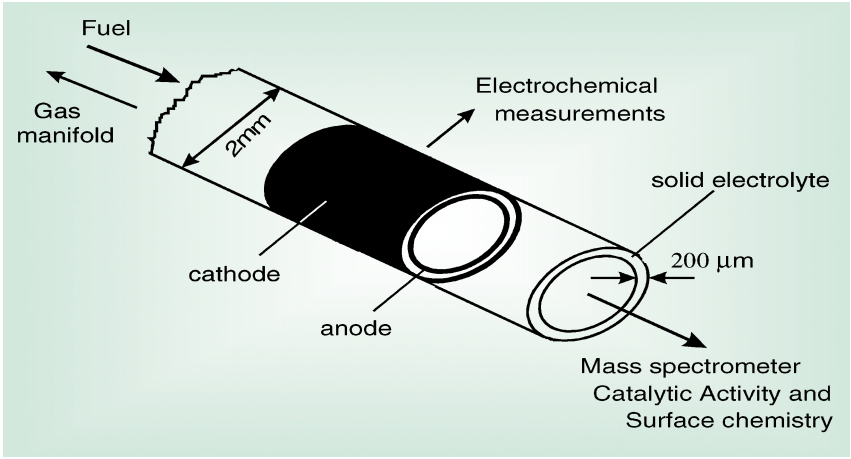

Fig. 1 Schematic of a solid oxide fuel cell running on biogas.

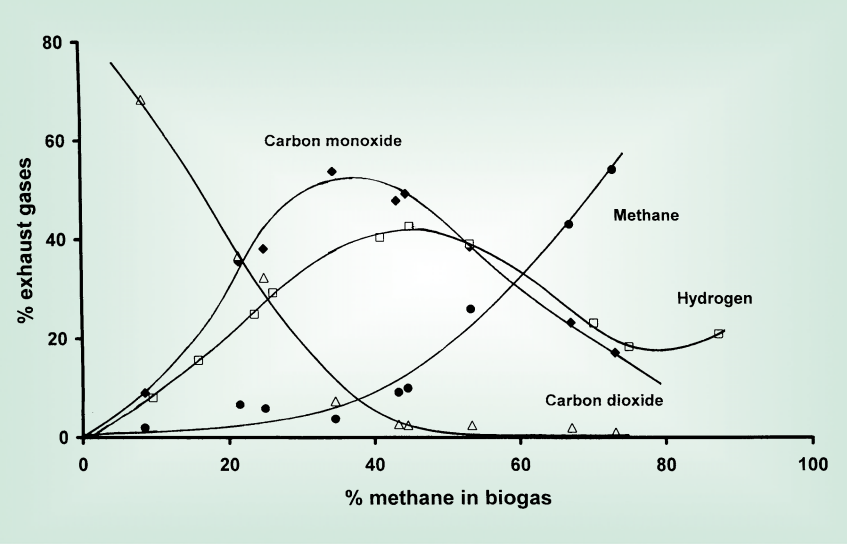

Fig. 3 Exit gas compositions from an unloaded solid oxide fuel cell running on biogas at 850 °C, as a function of methane content.

power output from the cell also being observed. This can be rationalised in terms of catalytic methane decomposition [eqn. (4)] becoming progressively more important at high methane levels, providing an additional route to H_2 production, which is then electrochemically oxidised.

$$CH_4 \rightarrow C_{(ad)} + 2H_2 \qquad (4)$$

Thus the power output and exit gas compositions from the fuel cell over the entire biogas compositional range can be accounted for. For biogas with lower methane contents, and high CO_2 levels, dry reforming of the methane [eqn. (3)] should predominate over methane decomposition [eqn. (4)]. Further, any carbon that is deposited may be removed by reaction with carbon dioxide [eqn. (5)].

$$CO_2 + C_{(ad)} \rightarrow 2CO \qquad (5)$$

For biogas with high methane contents, significant carbon deposition will occur through catalytic methane decomposition [eqn. (4)], leading to eventual deactivation.

Conclusion

We have shown that it is possible to run a solid oxide fuel cell directly on biogas a truly renewable fuel, over a wide compositional range of methane and carbon dioxide. It is particularly worth noting that the amount of power produced within the SOFC from biogas is still very reasonable at methane contents as low as 15%, being ~70% of the maximum power output. Thus at methane contents below which conventional heat engines would have long since stopped working (~45%), the SOFC is able not only to function but to produce a significant amount of power from poor-quality biogas, which is presently disposed of by simply venting wastefully and detrimentally to the atmosphere. Electricity and useful energy are produced, with significant reduction in greenhouse gas emissions. Our current research is directed towards longer-term durability experiments using biogas, with a particular emphasis on biogas with a low methane content.[15]

References

1 M. Hammad, D. Badarneh and K. Tahboub, *Energy Convers. Manage.*, 1999, **40**, 1463.
2 C. Bell, S. Boulter, D. Dunlop and P. Keiller, in *Methane: Fuel of the Future*, 1973 Andrew Singer, Bottisham, UK.
3 J. Huang and R. J. Crookes, *Fuel*, 1998, **77**, 1793.
4 S. Neyeloff and W. W. Gungel, in *Energy, Agriculture and Waste Management*, Ann Arbor Science, 1975.
5 R. Kingston, *Chem. Brit.*, June 2000, 24.
6 G. Hoogers and D. Thompsett, *Chem. Ind.*, 1999, 796.
7 C. K. Dyer, *Sci. Am.*, 1999, **281**, 70.
8 D. Hart, *Chem. Ind.*, 1998, 344.
9 A. C. Lloyd, *Sci. Am.*, 1999, **281**, 64.
10 C. M. Finnerty, N. J. Coe, R. H. Cunningham and R. M. Ormerod, *Catal. Today*, 1998, **46**, 137.
11 C. M. Finnerty and R. M. Ormerod, *J. Power Sources*, 2000, **86**, 390.
12 A. T. Ashcroft, A. K. Cheetham, J. S. Foord, M. L. H. Green, C. P. Grey, A. J. Murrell and P. D. F. Vernon, *Nature*, 1990, **344**, 319.
13 F. Besenbacher, I. Chorkendorff, B. S. Clausen, B. Hammer, A. M. Molenbroek, J. K. Norskov and I. Stensgaard, *Science*, 1998, **279**, 1913.
14 C. M. Finnerty, R. H. Cunningham, K. Kendall and R. M. Ormerod, *Chem. Commun.*, 1998, 915.
15 J. Staniforth and R. M. Ormerod, in preparation.

Professor Mark Ormerod is an EPSRC Advanced Research Fellow and is Professor of Catalysis and Materials Chemistry. He and Dr John Staniforth are based in the Birchall Centre for Inorganic Chemistry and Materials Science, at Keele University, UK.

Highlights

Duncan Macquarrie reviews the latest research in green chemistry

Mannich reactions

The Mannich reaction represents a powerful method for the formation of advanced synthons, especially when carried out in an enantioselective manner. Two papers from the group led by Karl Anker Jørgensen of Aarhus University in Denmark are of great interest in this respect. The first (*Angew. Chem., Int. Ed.*, 2001, **40**, 2992) describes the addition of nitroalkanes to iminoesters, using chiral bisoxazoline copper catalysts. This protocol allows the formation of the

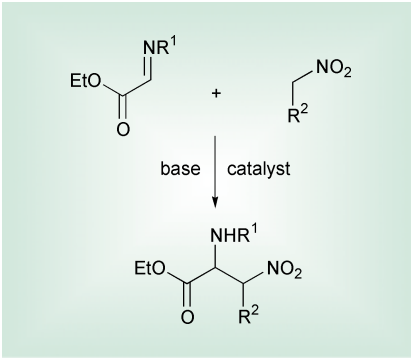

addition products in high yield (typically >80%) and with de and ee both above 90%. The fact that the reactions can be run at, or close to, room temperature avoids the need for difficult (and energy-intensive) cooling to the very low temperatures often required for such enantioselective methodologies. A range of nitro compounds have been used and, while the de can vary significantly, the ee remains high.

The second paper describes the direct Mannich reaction of carbonyl compounds with imino esters, again utilising the bisoxazoline copper catalysts described in the first paper (*Angew. Chem., Int. Ed.*, 2001, **40**, 2995). Here again the reactions are carried out advantageously at or around ambient temperature, and the ee's and de's are typically good. A further important feature of the reaction, perhaps the most innovative, is that the carbonyl component can be used directly, avoiding the wasteful preparation of very sensitive silyl enol esters. This makes the procedure shorter, more robust and much less wasteful.

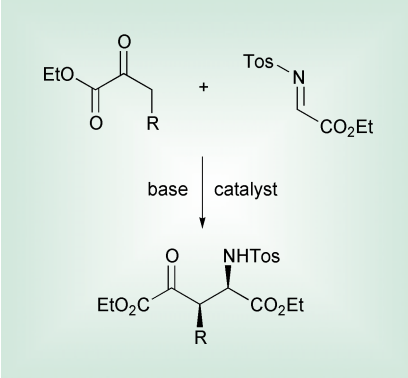

LASC technique

Another contribution to synthetic methodology has been provided by the group of Shu Kobayashi in the University of Tokyo (*Angew. Chem., Int. Ed.*, 2001, **40**, 2815). This research involved the use of the so-called Lewis Acid Surfactant Combined catalyst (LASC) technique, which has already been successfully applied to other C–C bond-forming processes. In this process, colloidal particles are formed in water, inside which the desired reaction takes place. In

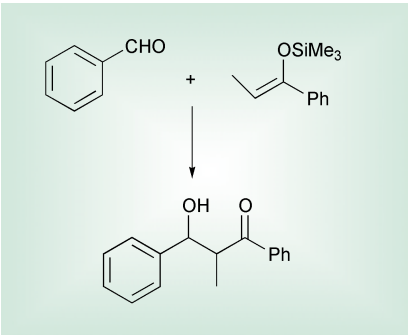

this case, the reaction is the Mukaiyama aldol reaction of a silyl enol ether and an aldehyde, catalysed by diphenylboronic acid and 1 mol% of benzoic acid. Yields are generally high, and diastereoselectivity was also very good in most cases. The reaction proceeds *via* exchange of the silyl group for the boron species, making the real reagent a boron enolate. The method described represents the first example where such species can be formed catalytically *in situ*, and thus may prove to be of general utility.

Molecular aggregates

The construction of molecular aggregates, based on supramolecular host–guest chemistry is a burgeoning area of research. Work carried out by Colin Raston and his group at Monash University. Australia, and latterly at Leeds University, has demonstrated such chemistry (*Eur. J. Org. Chem.*, 2001, 3227) based on green synthetic procedures for the construction of the building blocks. They have shown that inclusion of guest molecules can take place inside molecular capsules based on terpyridines and calixarenes, prepared using solvent-free syntheses, avoiding the more wasteful routes originally employed.

Ionic liquids and supercritical fluids

Ionic liquids and supercritical fluids represent two classes of solvents possessing excellent properties for green processing. A very innovative combination of these two solvents has led to a very elegant methodology for hydrovinylation reactions. Hydrovinylation of alkanes is an addition reaction leading to new alkenes, and can be carried out enantioselectively using Wilkes catalysts, a nickel-based catalyst where the nickel is coordinated to a chiral

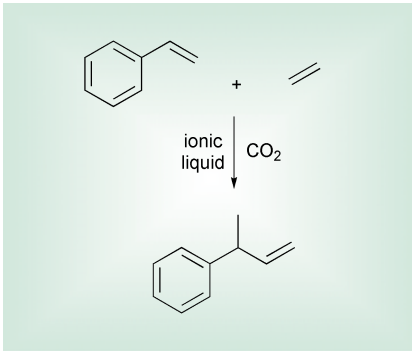

phosphorus centre. Walter Leitner of the Max-Planck Institut in Mulheim, and Peter Wasserscheid of the RWTH Aachen have joined forces to develop a continuous process based on this reaction in ionic liquids and compressed CO_2 (*Angew. Chem., Int. Ed.*, 2001, **40**, 2697). They have immobilised an ionic version of Wilkes catalyst by making it the

DOI: 10.1039/b108144f

counterion of an ionic liquid, and carried out a continuous hydrovinylation and separation using compressed CO_2 as the mobile phase, simultaneously reducing the viscosity of the system and improving mass transport. Conversions and ee values were good and dropped only slightly over tens of hours of processing.

Carbonylations

Pd-catalysed carbonylation reactions are a versatile route to a range of acid derivatives, but are less well developed than other C–C bond forming analogues such as the Heck and Suzuki coupling reactions. Matthias Beller and co-workers from the University of Rostock have now published details of an exciting new catalyst system which allows the highly efficient carbonylation of aryl chlorides, the cheapest and most readily available class of aryl halides (*Angew. Chem., Int. Ed.,* 2001, **40**, 2856). They have shown that monodentate phosphines do not produce catalysts with acceptable activity

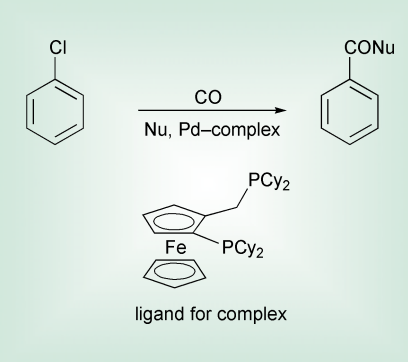

in the carbonylation of aryl chlorides, but bidentate phosphines are excellent in this respect. After screening some ferrocenyl phosphines (a well-developed class of diphosphines) they found that the diphosphine shown was an excellent catalyst, and carbonylations could be carried out in essentially quantitative yield and with selectivities often >90%. They showed that the carbonylated intermediate could be trapped with alcohols, water and amines, leading to esters, acids and amides, all in high yield.

Tertiary C9–C11 carboxylic acids are used in a variety of applications such as coatings. They are produced by carbonylation of alkenes using extremely acidic liquids. The search for solid acids capable of carrying out this transformation has met with limited success, but Jean-Paul Lange of Shell, Amsterdam, and Leo Petrus of Resolution Performance Products (Amsterdam) have published details of their investigations into this reaction (*Appl. Catal. A*, 2001, **216**, 285). They found that under optimal conditions, sulfonated resins such as Nafion and Amberlyte resins were able to give good yields of acid using the product as solvent, and a relatively low concentration of reactants under CO pressure and temperatures of *ca.* 150 °C. Interestingly inorganic solid acids were not effective.

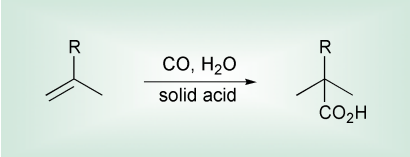

Heterogeneous catalysis

A further use of ionic liquids relies on the potential to complex a Lewis acid to the counterion to provide an ionic liquid solution of Lewis acid, which can then be used to catalyse for example the Friedel–Crafts reaction. Analogous complexes can also be immobilised on silica and used as heterogeneous catalysts. The group led by Wolfgang Hölderich at the RWTH in Aachen has published details of such catalysts based on imidazolium chloride complexes of

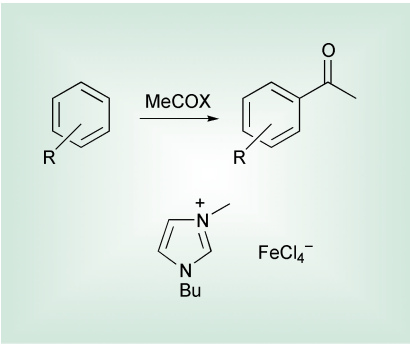

ferric chloride (*Appl. Catal. A,* 2001, **215**, 185). These are excellent catalysts for the acylation of anisole and alkylbenzenes but the heterogeneous catalysts are subject to leaching of the iron chloride into solution. Reactions carried out in a gas phase flow reactor were also attempted, and showed interesting results, although some loss of acetyl chloride was observed. Nonetheless these materials are genuinely catalytic in this reaction type.

Oxidations

Selective oxidations using oxygen are one of the most important technologies

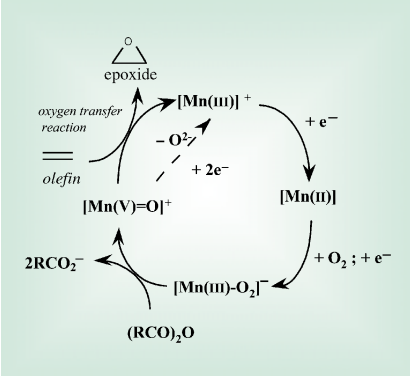

available to green chemistry. However, the direct activation of oxygen without adjuncts such as bromide or aldehydes is often difficult. Laurent Gaillon and Fethi Bedioui of the CNRS in Paris have now demonstrated the potential of electrochemical activation of oxygen *via* Jacobsen's catalyst in ionic liquids (*Chem. Commun*., 2001, 1458). They have shown that the key steps in the activation of oxygen can be achieved using carbon electrodes, indicating that this method may be able to activate oxygen, and transfer it to an olefin selectively without the need for other auxiliary reagents.

A contribution to the oxidation of alkanes by hydrogen peroxide has appeared from Georg Süss-Fink and co-workers from Neuchajtel in Switzerland and Moscow. They have shown that a range of alkanes can be oxidised to the hydroperoxide (and then subsequently decomposed to the alcohol and ketone) with hydrogen peroxide using vanadium-containing polyphosphomolybdates (*Appl. Catal. A,* 2001, **217**, 111). Using this system in acetonitrile at moderate temperatures, they achieved good turnover numbers and high yields (>30%) in the case of cyclooctane, *n*-octane, adamantane and even ethane. Only traces of methane oxidation could be observed, and in this case solvent breakdown was observed.

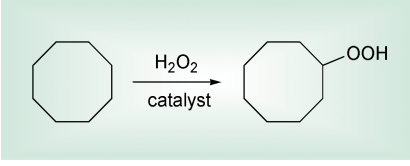

Another paper dealing with the oxidation of hydrocarbons has been published by the group of Laureano Canoira on the Polytechnic University of Madrid (*Appl. Catal. A*, 2001, **218**, 269). The reaction investigated here is the nickel-catalysed oxidation of

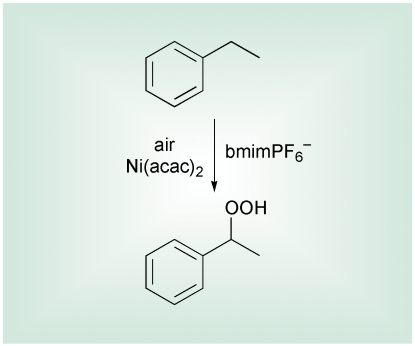

ethylbenzene. The group had previously found that quaternary ammonium salts are excellent co-catalysts for the production of ethylbenzene hydroperoxide (an intermediate in the synthesis of phenethyl alcohol, acetophenone and styrene) using soluble $Ni(acac)_2$ complexes and oxygen. They now present results which indicate that the use of 1-butyl-3-methylimidazolium hexafluorophosphate gives better results than the simpler tetraalkylammonium salts used up to now.

Phase-transfer catalysis

The use of phase-transfer catalysis can often be a very attractive synthetic protocol, but one which is made much less attractive by the catalysts' inherently good solubility in both aqueous and organic phases. This property make the catalysts difficult to recover, reducing its attractiveness industrially and environmentally. The group led by Sathinder Luthra from Imperial College, London, has now published details of a potential breakthrough in this respect (*Chem. Commun.*, 2001, 1468). They have found that nanofiltration membranes can be successfully used to recover phase-transfer catalysts from a toluene/water mixture after reaction. Catalyst recovery was excellent and reuse was demonstrated over three cycles. Some fouling of the membrane was noted, but was easily reversible.

Centre for Green Chemistry, Monash University

A report on the official opening

The new facilities of the Australian Research Council (ARC), Special Research Centre (SRC), the Centre for Green Chemistry were officially opened by Senator Kay Patterson on Monday 9th July 2001. Among the 80 or so guests was Professor Colin Raston, whose enthusiasm led to the establishment of the Centre, but who has since moved to a chair at Leeds University, UK. Other distinguished guests included Dr Denny Hjeresen, Director of the American Green Chemical Institute, Professor Pietro Tundo, Director of the European based Inter-University Consortium for Chemistry and the Environment and a number of visitors from the UK, China, Portugal, Italy, South Africa, Sweden and Australia.

Distinguished guests at the official opening of the new facility of the Centre for Green Chemistry. From left, Professor W. Roy Jackson, Director, Centre for Green Chemistry; Dr Geoff Knights, Chair, Centre for Green Chemistry Advisory Board; Hon. Kay Patterson, Senator for Victoria; Mr Jerry Ellis, Chancellor, Monash University.

The Centre for Green Chemistry (CGC) commenced operation in January 2000 and has grown rapidly since its inception. There are now more than 24 Ph.D. students and visiting scholars, 10 postdoctoral research fellows and 4 staff within the Centre and a large number of associated researchers from diverse scientific backgrounds, working on green chemistry research projects. These include a number of faculty from the School of Chemistry as well as Monash University Departments of Materials Engineering, Biochemistry, Earth Sciences, (and it is hoped soon Chemical Engineering); faculty at other universities in Australia and researchers from divisions of CSIRO including Forestry and Forestry Products, Minerals, Molecular Sciences and Manufacturing Science. International collaborations with scientists in the UK, USA, Japan, Sweden and South Africa are well developed and expected to grow from strength to strength and other opportunities for extending links are being actively explored, as are possibilities for student exchange.

The purpose of the Special Research Centre is to engage in fundamental research and development towards the design, manufacture and use of clean

ARC Special Research Centres in context

The Australian Research Council (ARC) is the main funding agency in Australia for basic research. It supports research in essentially all fields from science, engineering and new technologies through to social sciences, humanities and the creative arts (except clinical medicine and dentistry). Special Research Centres are funded by the Australian Federal Government *via* the Australian Research Council and are designed to 'enable special concentrations of staff and resources for research and research training of a longer term nature'. The Centres are funded for up to nine years, with reviews every three years. Eleven new Centres were identified from 76 applications to receive funding beginning in 2000. AU$135 million funding is allocated for these Centres over their lifetime.

chemical processes that have little or no pollution potential or environmental risk and are both economically and technologically feasible. Clearly, interaction with Australian industry is of paramount importance and collaborations with companies representing industries as apparently diverse as mining, pulp and paper processing and pharmaceutical development are in place, whilst others are being explored. Evidence that Australian industry is actively exploring the concepts of sustainability and green chemistry comes from a number of invitations to address company boards and future planning workshops received by Centre representatives.

The CGC aims to provide a scientific base for future chemical technology, identifying niche areas in the Australian context and beyond for global initiatives, as well as providing valuable training of future workers in this area through postgraduate scholarships and postdoctoral fellowships. It will provide a common focus, build up a critical mass of researchers, and provide the synergy and creativity expected of a SRC. In addition, the CGC must work to become financially independent to ensure its continued existence beyond the period of the ARC funding.

To meet these aims within the timeframe allowed, four main research streams have been identified to provide a suitable mix of:

- fundamental research
- strategic research with unencumbered intellectual property
- research for the public good
- industrial collaborations

This is designed to provide a sustainable mix of high-profile fundamental scientific research, new opportunities and income-generating segments with the goal of providing the best possible research training for students and fulfilling the mission statement with regard to 'becoming internationally recognised for research and teaching in the field of green chemistry'.

Current projects may be broadly divided into 3 groups:

- Those associated with the design and synthesis of more benign products such as: Novel Boron-based Wood Preservatives; Non-addictive Opioid Analgesics; Supramolecular Polymers; Soil Remediation Products and Green Corrosion Inhibitors (for use in recycling water systems or with replacement of toxic reagents); Benign Mineral Processing Methods; Alternative Routes to Isocyanates (phosgene replacement)
- Those centred around the development of green synthetic protocols and enabling methodologies: Understanding Solvent-free Reactions and Supramolecular Reaction Control; Microwave Heating and High-Temperature Aqueous Reactions; Green Nucleophilic Addition and Ring Closure (NARC) reactions; Green Medicinal Chemistry (simultaneous development of new therapeutic agents and clean synthetic routes); Electrochemical Methodologies; Use of Ionic Liquids as Green Reaction Media and a number of projects relating to catalysis. Many of these projects are fundamental studies leading to a greater understanding of the science underlying the technologies.
- Projects with the goal of facilitating the use of renewable raw materials: FIA/FTIR/Raman methods for of real-time monitoring of chemicals in fermentation processes; Biotechnology in Green Chemistry and the Development of Drug Products from Plant-Derived Chemicals.

Part of the Centre for Green Chemistry Laboratories nearing completion early in 2001. The laboratories are no longer quite this spotless but now buzz with productive activity.

While Special Research Centre funding is granted for the purpose of development of research in a specific field, education in green chemistry is also considered to be an important part of the Centre's role and a number of programmes are being developed. A course in green chemistry is offered at 3rd year level at Monash University and green chemistry laboratory exercises are incorporated into the practical component of the final year courses. Postgraduate courses are under development and a part time Community Outreach Officer has recently been

Dr Ulf Kreher, a postdoctoral fellow, assembling the reaction vessel of the custom designed microwave batch reactor which allows continual monitoring of temperature and pressure, removal of samples for monitoring and rapid well-controlled cooling via **a cold-finger.**

employed to increase the capacity of the Centre to offer lectures to schools and community groups. Interactions with secondary school students and teachers are deemed especially important as, in common with many other countries, enrolment in science courses at tertiary level shows a downward trend. Exciting lectures, which demonstrate the application and importance of green chemistry by way of everyday examples and chemical demonstrations, are under development and will be delivered by the Community Outreach Officer at individual schools. Expanded versions of these lectures will be presented this year as the Hartung Youth Lectures and Tasmanian Youth Lectures, sponsored by the Royal Australian Chemical Institute (RACI). Teachers from the Science Teachers Association of Victoria (STAV) and the Chemical Education Association (CEA) are collaborating with key researchers in the Centre for Green Chemistry to develop resources to aid teachers who wish to incorporate green chemistry into their high school courses.

As the Centre expands further and develops both its educational, research and industrial projects the challenge will be to maintain focus and ensure that the strategic goals of the Centre are met whilst remaining flexible and open to innovation. Sound science, a commitment to education and close relationships with all the players in this developing field will ensure the future of this exciting project.

For further information see the Centre for Green Chemistry website: http://web.chem.monash.edu.au/GreenChem/ and to receive electronic copies of the Newsletter send an e-mail to Green.Chemistry@sci.monash.edu.au.

From plant to plastic, Renewables are fantastic!

Elinor Scott and her colleagues at ATO describe their research in the area of polymers and plastics aims at integrating health, safety and environmental aspects with a high product performance and economic sustainability. ATO continues to be naturally inspired in order to explore the synergy between resources, materials and technologies from synthetic and natural origin.

Introduction

The large demand for petrochemical-based polymers and plastics has led to optimized product chains in terms of the economics and performance of the product, as well as in aspects such as process optimization and environmental impact. However, there is a current resurgence of interest in sustainable natural products for the preparation of alternative plasticisers, alternatives to diols, diacids and aromatic molecules. It is proposed that biosynthetic systems can be thought of as a useful (bio-) chemical and technological toolbox. For example, biological reactions may lead to more efficient routes to materials or allow incorporation of a naturally occurring chemical structure, which offers better functionality of the material.

Considerations such as resource sustainability, (bio-) chemistry, engineering technology and environmental impact are given special attention. From a chemical or technological perspective, by adopting a combined biosynthetic methodology and petrochemical technology approach there is an important complementary and synergistic effect. Therefore materials can be designed with a desired composition, structure and property and prepared by an effective, energy-efficient and safe method.

Aspects of monomer, polymer and wood additives, biopolymer technology and post-consumer life research are described below.

(Bio-) chemical monomer and polymer synthesis

Recent advances in combining conventional and novel (bio-)chemical transformations and use of sustainable resources, make it possible to enter existing product chains with chemicals prepared from a sustainable natural

origin. One such entrance point is the synthesis of chemical building blocks for the preparation of polymers. These building blocks may have:

- Existing functionality

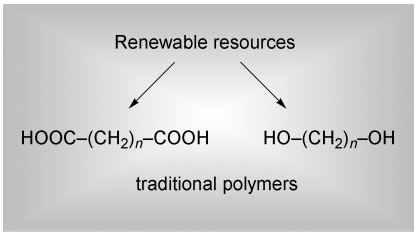

- Alternative functionality, characteristics *similar* to traditional petrochemically derived aromatic monomers, *e.g.* terephthalic acid.

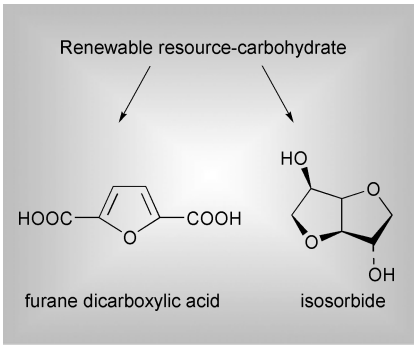

These compounds, for example, have rigid structures and can undergo polycondensation reactions to produce polyesters with specific properties. As well as this, isosorbide has been esterified and behaves as an effective plasticiser. Other activities in (bio-) chemical monomer and polymer synthesis include fermentation, biocatalysis and protein engineering.

Polymer additives–plasticisers

Many conventional plasticisers are based on phthalate esters.[1,2] Currently there is concern over the use of phthalates as certain derivatives are suspected of being carcinogens or endocrine disrupters. Environmental studies have shown that they can be found in the food chain, in sediments and water supplies.[3] Most are monomeric and eventually, depending on conditions, migrate out of the polymer. These problems may be overcome using polymeric plasticisers, but these tend to have low efficiency and high costs.[2] Some monomeric non-toxic alternatives for phthalates such as citrates, benzoates and adipates are currently commercially available, but with some limitations for widespread use.[2]

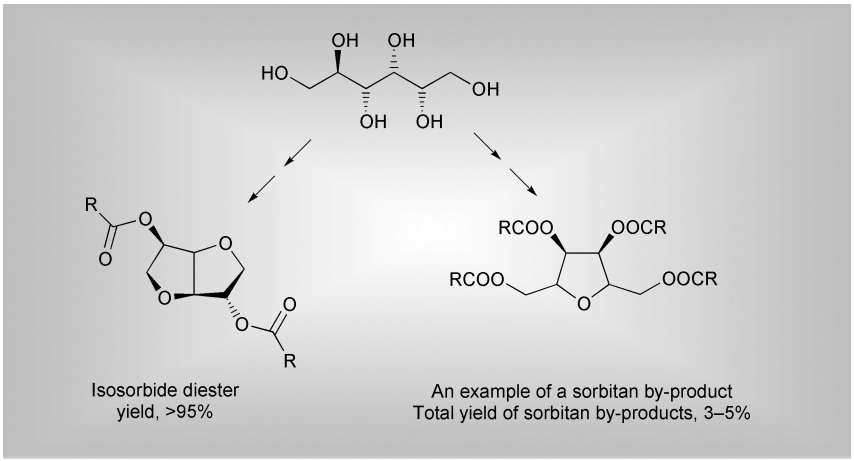

The use of isosorbide diesters as plasticisers was first mentioned as early as 1953, but limited yields and high price of isosorbide proved detrimental to further development.[4] At ATO isosorbide plasticisers have been developed using a new method.[5] Isosorbide diesters show similar plasticising behaviour to phthalate (esters) and are compatible with poly(vinyl chloride) over a wide concentration range.

Recently a one-pot procedure to prepare isosorbide diesters, from inexpensive sorbitol, has been developed. The proprietary technology uses a specific catalyst making it possible to do *in-situ* dehydration of sorbitol and esterification of isosorbide using the alkanoic acid as the solvent. By careful control of some reaction parameters sorbitan byproducts are minimised.

One-pot procedure

Currently the reaction mechanism is being investigated to determine the influence of reaction parameters on product distribution. These compounds are currently undergoing an extensive testing program.

Other polymer additives being developed include:

- Halogen-free flame retardant chemicals for electric cables and equipment.
- Antioxidants of natural origin for use in polymers

Wood–flame retardants

Wood has many properties which makes it a very useful building material, however its flammability can be a disadvantage in some applications. To reduce flammability, chemicals, *e.g.* phosphorus compounds, can be impregnated to reduce the temperature of the pyrolysis and form a protective char layer.[6] However, current flame-retardant chemicals have some negative aspects. For example under the influence of humidity they tend to slowly migrate out of the material and they increase the level of water absorption causing faster degradation of the wood due to fungal growth. In co-operation with industrial partners[7] a project on development of more environmentally friendly flame retardants has recently started. The use of these new compounds combines both flame retardancy and durability of wood or wood-based products (Fig. 1).

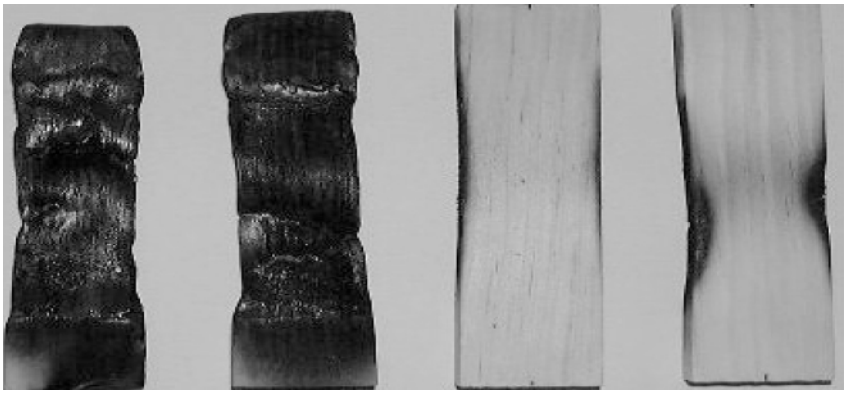

Fig. 1 Untreated wood (2× left) and newly developed treated wood (2× right) after flame test.

Fig. 2 Film blowing of co-extruded biopolymer multi-layered films.

In some building situations, *e.g.* escape routes, the use of wood may not meet the required levels required for flame retardancy. When the wood materials can be modified to meet these requirements, there becomes a possibility of using wood-based products.

Within this project chemicals, which are directly bonded on to the reactive groups of wood, and treatments, are being developed. As well as this, the wood also becomes intrinsically more hydrophobic and so a more resilient and durable product can be made. An additional benefit is the swelling of the wood may be reduced—an important feature in construction materials. Presently there are a series of compounds and treatments with promising results.

Biopolymer products–starch-based packaging

Polymers from natural resources are finding more and more applications in various markets. Food packaging is a potential market for these bio-based polymers. The aim of this research is to show that it is possible to produce packaging materials totally from bio-based polymers that do not only meet the requirements of the food packaging industry, but also give additional advantages over conventional packaging materials. The properties of starch make it a suitable alternative to conventional packaging materials. However, there are some aspects of using starch which need to be overcome. For example the water sensitivity of starch may limit the application and should be improved.

To overcome this problem, an approach has been to chosen where starch is coated with (biodegradable) polyesters. While this approach is useful in improving water resistance, the adhesion between the surfaces of the starch and the polyester in the layered foil is a very important aspect in developing a durable product. This has been a focus in the research programs. One successful approach to reduce the water sensitivity and improve adhesion has been the development of a co-extruded multi-layered film (Fig. 2).

The performance of these barrier laminate films has been evaluated in real life packaging tests. Results show that the developed packagings have a positive effect on the shelf life of Modified Atmosphere (MA)-packed cut vegetables and fresh salads when compared to conventional packaging materials. Little to no negative influence on the product quality during the shelf life of the packed products was observed in MA packaging of fresh bread rolls, meat and cheese.

Other activities in the biopolymer area include:

- Biosynthetic polymer synthesis
- Foam and injection moulding technology of biopolymers
- Product development with compostable polymers

Post-consumer product life

The test below (Fig. 3) simulates conditions in a municipal solid waste treatment plant. This is just one on the many conditions that are studied to understand the relationships between polymer structure and (bio-)degradation behavior. Insight in to these relationships can then be used to predict degradation of newly developed materials and provides a tool for selectively engineered degradable products. At ATO research has been performed to improve existing tests and develop new tests to assess biodegradation, mineralisation and disintegration of products under specific (simulated) environmental conditions.

Other activities in post-consumer product studies include additives and technology to aid recycling.

Fig. 3 Laboratory composting test.

E. Scott, R. van Tuil, D. van Es, R. Bezemer, G. Schennink and M. van der Zee are based at ATO, PO Box 17, 6700 AA Wageningen, The Netherlands Tel: +31 317 475029.

Acknowledgements

Stephan Hulleman and his group Polymers, Composites and Additives. Industrial partners and funding bodies that participate in the work.

References

1 R. Gächter and H. Müller, *Plastic Additives Handbook*, 4th edn.; Carl Hanser Verlag, Munich, 1993.
2 A. S. Wilson, *Plasticisers; Principles and Practice*, Cambridge, The Institute of Materials, 1995.
3 Reports of the National Toxicology Program (U.S. Dept. of Health and Human Services) by the Center for the Evaluation of Risks to Human Reproduction (CERHR): http://cerhr.niehs.nih.gov
4 I. Hayashi, S. Hamada and Y. Hachihama, Kogyo Kagaku Zasshi, 1953, **56**, 623–625.
5 J. C. Jansen and H. Luitjes, *Bicyclooctane derivatives as plasticisers*; Inst. voor Agrotechnologisch Onderzoek, EP1058711, 1998.
6 W. D. Ellis and R. M. Rowell, *Wood Fiber Sci.*, 1989, **21**(4), 367–375.
7 In co-operation with SHR, Houtbedrijf Van Hout b.v., Kegro Deuren b.v., Heraklith b.v., IVAM Environmental Research b.v., Wageningen UR and Dick Peters b.v.

ATO (The Agrotechnological Research Institute) in Wageningen is situated in the 'green valley' of Dutch agricultural innovation. As one of its activities, ATO successfully performs developments in collaboration with industry leading to the future of renewable resources in non-food markets. See http://www.ato.wageningen-ur.nl/

RSC Clean Technology Monographs

SERIES EDITOR: J H CLARK, UNIVERSITY OF YORK, UK

Clean Synthesis Using Porous Inorganic Solid Catalysts and Supported Reagents

BY J H CLARK & C N RHODES
University of York, UK

Clean Synthesis Using Porous Inorganic Solid Catalysts and Supported Reagents is concerned with the use of solid catalysts in the clean synthesis of organic chemicals. The emphasis is on chemical processes of importance to the manufacture/preparation of fine and speciality chemicals, chemical intermediates and pharmaceutical intermediates, especially where catalysis is not currently used or where current catalysts are homogeneous, leading to difficult separation procedures and unacceptable levels of waste. This book focuses on solid catalysts based on inorganic supports and covers the emerging area of chemically modified mesoporous solid catalysts.

Hardcover · x + 108 pages · ISBN 0 85404 526 0 · 2000 · £55.00

Price for this volume for customers placing a standing order for the series is £49.50

The Sulfur Problem

Cleaning Up Industrial Feedstocks

BY D STIRLING
University of Glasgow, UK

The main objectives of *The Sulfur Problem: Cleaning Up Industrial Feedstocks* are to demonstrate the importance of eliminating sulfur contaminants from the environment and the measures necessary to effect this. Using a systematic and pedagogical approach, the reader is first presented with the problem. Current technology for solving it is then outlined together with appropriate theory on the synthesis, structure and sorption behaviour of the materials used. Relevant characterisation techniques are described with reference to typical sorbents, to demonstrate how the sorption behaviour of the materials correlates with their properties. The book is unique in blending together aspects of environmental chemistry, materials/solid state chemistry, surface chemistry, catalysis and separation processes to address the problem of sulfur contaminants in a wide range of feedstocks.

Hardcover · x + 94 pages · ISBN 0 85404 541 4 · 2000 · £55.00

Price for this volume for customers placing a standing order for the series is £49.50

Applications of Hydrogen Peroxide and Derivatives

BY C W JONES

Beginning with an historical overview, and guidelines for the safe handling of peroxygens, *Applications of Hydrogen Peroxide and Derivatives* goes on to cover key activation mechanisms, organic functional group oxidations and the use of hydrogen peroxide with heterogeneous catalysts. The clean-up of environmental pollutants; chemical purification; and extraction of metals from their ores are also discussed in detail, using actual examples from industry.

"… well-organized and enjoyable overview … this useful book is strongly recommended to anyone interested in oxidation or peroxygen chemistry …"

Journal of the American Chemical Society, Vol 122, No 26, 2000

Hardcover · x + 264 pages · ISBN 0 85404 536 8 · 1999 · £59.50

Price for this volume for customers placing a standing order for the series is £53.50

Feedstock Recycling of Plastic Wastes

BY J AGUADO & D SERRANO
Universidad Complutense, Madrid, Spain

Feedstock Recycling of Plastic Wastes looks at the conversion of plastic wastes into valuable chemicals useful as fuels or raw materials. Looking at both scientific and technical aspects of the recycling developments, this book describes the alternatives available. Areas include chemical depolymerization, thermal processes, oxidation and hydrogenation. Besides conventional treatments, new technological approaches for the degradation of plastics, such as conversion under supercritical conditions and coprocessing with coal are discussed.

"… a clear, extensive review … essential reading for all those concerned with plastics recycling."

Warmer Bulletin, January 2000, No 70

Hardcover · xiv + 192 pages · ISBN 0 85404 531 7 · 1999 · £59.50

Price for this volume for customers placing a standing order for the series is £53.50

For RSC member prices, contact Sales & Customer Care as below

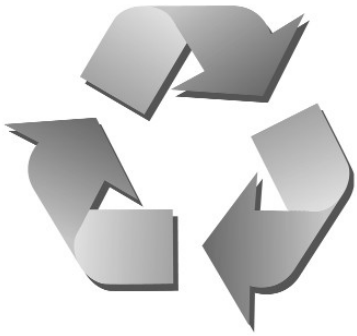

RSC·C
ROYAL SOCIETY OF CHEMISTRY

Royal Society of Chemistry · Thomas Graham House · Science Park
Milton Road · Cambridge · CB4 0WF · T +44(0)1223 432360
F +44(0)1223 423429 · E sales@rsc.org
Or visit our website: www.rsc.org
Part of the chemistry societies' network: www.chemsoc.org

Registered Charity No. 207890

ROYAL SOCIETY OF CHEMISTRY *Investing in Chemistry*

RSC-29086028

Sugar-derived building blocks. Part 26.† Hydrophilic pyrroles, pyridazines and diazepinones from D-fructose and isomaltulose

Frieder W. Lichtenthaler,* Andreas Brust and Eckehard Cuny

Institut für Organische Chemie, Technische Universität Darmstadt, Petersenstraße 22, D-64287 Darmstadt, Germany. E-mail: fwlicht@sugar.oc.chemie.tu-darmstadt.de

Received 27th June 2001
First published as an Advance Article on the web 13th September 2001

Efficient, large scale-adaptable protocols are described for the straightforward conversion of D-fructose-derived 5-hydroxymethylfurfural (HMF) and of 5-glucosyloxymethylfurfural (αGMF, from isomaltulose) into hydrophilically substituted N-heterocycles of the pyrrole, pyridazine, thiophene and benzodiazepine type. Key intermediates are 1,6-dihydroxy-2,5-hexenediones, readily generated by oxidative furan ring-opening.

Introduction

As carbohydrates are by far the most abundant organic compounds on earth and represent the major portion of the annually renewable biomass, their utilization for the production of low cost and eco-friendly chemicals of versatile industrial applicability is of central importance for relieving and eventually terminating the reliance of chemical industry on petrochemical raw materials.[2,3] Unlike fossil resources, which essentially are devoid of oxygen, carbohydrates are overfunctionalized with hydroxyl groups, thus requiring efficient methodologies for the simultaneous reduction of their oxygen content and introduction of C=C and C=O unsaturation. As such methodologies meeting process chemistry demands are exceedingly scarce, the systematic elaboration of practical, large-scale adaptable *reaction channels* from cheap, ton-scale accessible sugars to building blocks with industrial application profiles is an urgent necessity.[3,4]

Prototypes of such industrially useful building blocks are furan-type oxygen heterocycles as, *e.g. furfural*, already produced on an industrial scale from biomass-derived xylose,[5] *5-hydroxymethylfurfural* (HMF, **1**), for which a pilot plant process to produce it from D-fructose or inulin is available,[6] and *5-α-D-glucosyloxymethyl-furfural* (α-GMF, **2**), readily accessible from sucrose-derived isomaltulose.[7] By contrast, technically viable reaction channels from carbohydrates to nitrogen heterocycles, which would be of similar industrial importance, have not been systematically exploited, some recent investigations on the transformation of sugars into pyridinols[8] and pyrazoles[9] being first endeavors towards this end. In continuation of our efforts to convert cheap, bulk-scale available sugars simply and efficiently into N-heterocycles with inherent hydrophilic substituents, we here detail oxidative conditions that allow the direct conversion of HMF (**1**) and its *O*-glucosylated analog **2** into derivatives of 2,5-hexanedione (**I**) and 4-ketopentanoic acid (**II**), then to be cyclized with amines, diamines and hydrazine to N-heterocycles of the pyrrole (**III**), pyridazine (**IV**) and diazepine type (**V**) (Scheme 1).

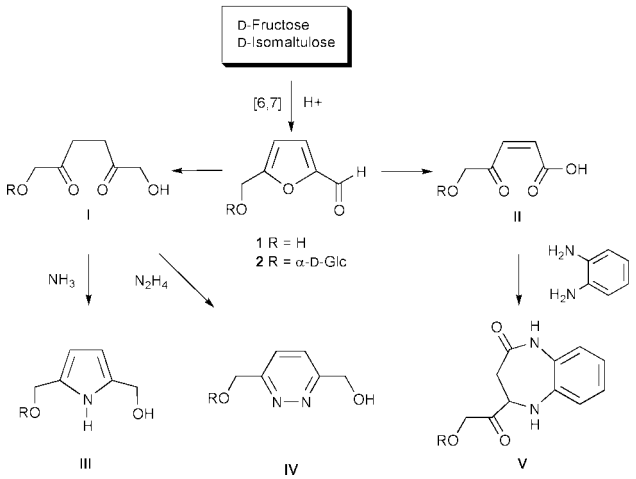

Scheme 1 General approach to hydrophilic pyrroles, pyridazines and diazepines from fructose and isomaltulose (R = H or α-D-glucosyl).

Results and discussion

Conversion of furans into N-heterocycles of the pyrrole and pyridazine type presupposes that the furan ring opening to 1,4-dicarbonyl compounds can be effected in a preparatively satisfactory manner, as the subsequent introduction of a nitrogen functionality and recyclization would follow standard methodologies. Of the various oxidants that have previously been used for this purpose,[10] *i.e.* pyridinium chlorochromate,[11] dimethyldioxirane,[12] 3-chloroperbenzoic acid,[13] singlet oxygen,[14] and bromine in water–methanol[15] or aqueous acetone,[16] we selected the latter three for evaluation of their applicability to the HMF-derived, *O*-blocked 2,5-bis(hydroxymethyl)furans **3** and **4** (Scheme 2).

Indeed, on exposure of the acetyl-protected **3** or its benzyl analog **4** to bromine in aqueous acetone (−30 → +25 °C, 2 h), addition to the dibromide **5** is directly followed by hydrolysis to

Green Context

Carbohydrates are by far the most abundant organic compounds on earth and their effective utilisation for the production of chemical products and intermediates is of fundamental importance to green chemistry. In this article practical reaction methods are described for the conversion of sugar-derived furans into pyrrole, pyridazine and benzodiazepine chemicals. These have value as intermediates and products for the pharmaceutical and agrochemical industries. ***JHC***

† Part 25. See ref. 1.

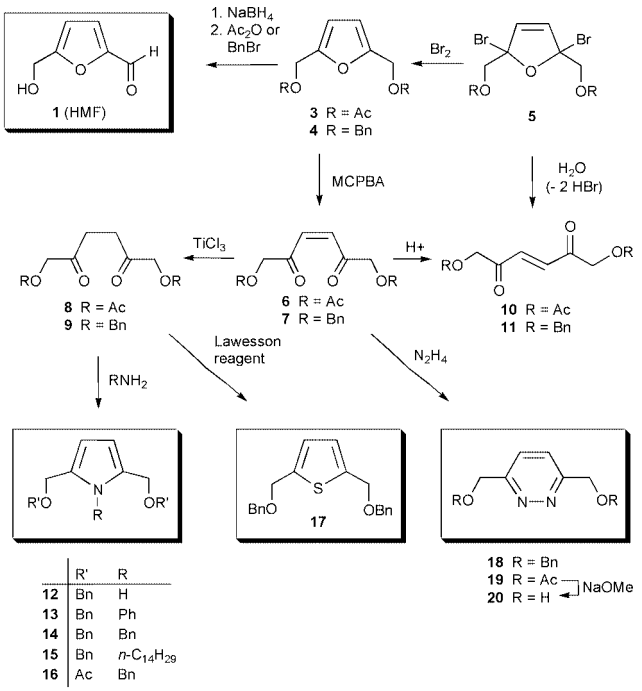

Scheme 2 Conversions of 5-hydroxymethylfurfural (HMF, **1**) into pyrroles, thiophenes and pyridazines (Ac = acetyl, Bn = benzyl).

the respective *cis*-hexenediones **6** and **7**, which under the strongly acidic conditions (HBr formed) undergo rearrangement to the corresponding *trans*-isomers **10** and **11**. Both are isolable in crystalline form albeit modest yields (~35%).

Preparatively more favorable proved to be the use of 3-chloroperbenzoic acid or singlet oxygen for oxidative ring opening in the furans **3** and **4**, since not only the oxidations proceeded cleanly (TLC, ^{1}H NMR), but due to the slightly acidic conditions no *cis* → *trans*-isomerization occured, allowing the isolation of the *cis*-hexenediones **6** and **7** in high yields (>90%).

The structural assignment to the *cis*- (**6**) and *trans*-enedione **10** – both were obtained in nicely crystalline form – were based on ^{1}H NMR data, which are identical except for the chemical shift of the 2H-singlet for the olefinic protons H-3 and H-4: 6.40 ppm for the *cis*-olefin **6** *vs*. 7.00 for the *trans*-isomer **10**, in accord with analogous shift differences in the *cis*/*trans*-isomers of hex-3-ene-2,5-dione.[17]

Saturation of the olefinic double bond in either of the hexenediones **6**–**11** could be effected catalytically (Ni/H_2) yet in some cases, obviously depending on the activity of the catalyst, concomitant hydrogenation of one of the carbonyl groups was also observed. By contrast, reductions with $TiCl_3$[18] or zinc/acetic acid[19] proceeded uniformly providing the desired hexanediones **8** and **9** in yields >90%.

With the versatile 1,4-diketo building blocks **8** and **9** now readily at hand—yields based on HMF (**1**) amounted to a satisfactory 75% for the four steps involved—their Paal–Knorr type cyclo-condensation with ammonia, and various amines to pyrroles was to follow standard methodology. Here, the bis(benzyloxy)hexanedione **9** performed exceptionally well, providing the N-unsubstituted pyrrole **12** on a 3 h reflux with ammonium acetate in methanol (70%), the N-blocked pyrroles **13**–**15** on reaction with aniline, benzylamine and *n*-tetradecylamine (85–93%), and the corresponding 2,5-bis(benzyloxy)thiophene **17** (74%) on exposure to Lawesson's thiation reagent.[20] Treatment of the unsaturated analog, *i.e*. *cis*-hexenedione **7** with hydrazine furnished the pyridazine **18** (73%).

Less opportune in cyclocondensations to pyrroles proved to be the bis(acetoxy)hexanedione **8**, since its terminal ester groups are partially saponified in the necessarily basic reaction medium, entailing pyranoid side products *via* cycloacetalization of the respective intermediates. Thus, on reaction of **8** with benzylamine in chloroform brought to pH 4 by the addition of acetic acid (2 h reflux), the *N*-benzyl-bis(acetoxymethyl)pyrrole **16** could be isolated in modest yield (28%) only.

On exposure of enedione **6** to hydrazine, however, the acetoxy groups survived, straightforwardly generating the bis(acetoxymethyl)pyridazine **19** (90%), which could be readily de-*O*-acetylated under Zemplén conditions (NaOMe–MeOH) to give **20**.

Glucosylated analogs from α-GMF

Gratifyingly, the methodology elaborated for the conversion of HMF (**1**) into hydrophilic pyrroles could directly be transferred to its α-glucosylated analog α-GMF (**2**). Thus, the 3-chloroperbenzoic acid oxidation of the peracetylated or perbenzylated GMF-alcohols **22** and **23** proceeded smoothly to give in excellent yields (97 and 90%) the glucosylated *cis*-hexenediones **24** and **25**, respectively (Scheme 3). Likewise, the subsequent saturation of the olefinic double bond to the hexanediones **26** and **27** was readily accomplished. The ensuing N-cyclizations with ammonium acetate (→**28**), aniline (→**29**), benzylamine (→**30**) and dodecylamine (→**31**), however, are preferably performed with the perbenzylated diketone **25** which allows yields in the 70–85% range, since the peracetylated analog **24** suffers substantial de-*O*-acetylation under the amination condition (3 h reflux in methanol) despite of maintaining a pH of 4 during the reaction.

Bromine water, an admittedly less 'green' reagent than peracids, can also be used for conversion of the furan ring in α-GMF into the respective hexenedione—*via* a dibromide

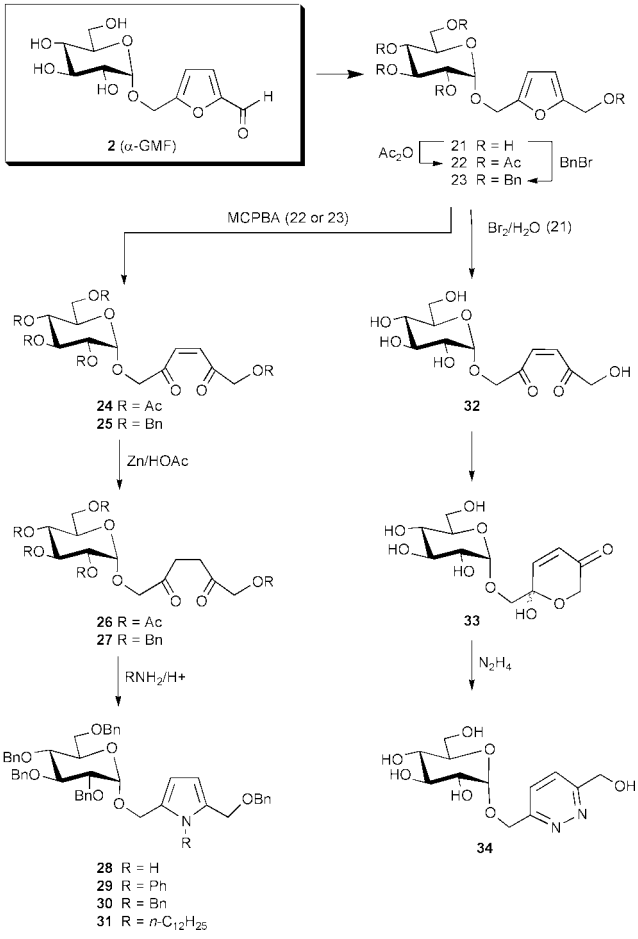

Scheme 3 α-GMF-derived pyrroles and pyridazines carrying hydrophilic glucosyl residues.

intermediate of type **5** and subsequent hydrolysis. As this oxidant leaves hydroxyl groups unaffected,[21] it can be applied to the unprotected GMF-alcohol **21**, first providing the glucosyloxy-*cis*-hexenedione **32** which due to its terminal hydroxyl group undergoes spontaneous cycloacetalisation to the dihydropyranone **33** (95%), rather than isomerizing to the *trans*-isomer as observed for **6** and **7** under acidic conditions. When reacted with hydrazine in water, **33** smoothly elaborated the mono-glucosylated 3,6-dihydroxymethylpyridazine **34** (68%) thus establishing a most convenient water-based three-step reaction channel from α-GMF to a highly hydrophilic, easily water-soluble N-heterocycle.

Elaboration of another, preparatively efficient reaction channel leading to hydrophilic diazepinones from α-GMF started with the oxidation of its peracetate **35** by either 3-chloroperbenzoic acid or by singlet oxygen – in adaptation of a photooxygenation procedure for 5-acetoxymethylfurfural[22] – to afford the glucosylated hydroxybutenolide **36** in yields of 70 and 95%, respectively (Scheme 4). It proved to be a versatile intermediate for generating benzodiazepinones on reaction with *o*-phenylenediamine (→**37**, 65%) and dehydrogenation (→**39**, 89%). Both could easily be de-*O*-acetylated with methoxide/methanol, the resulting products **38** and **40** constituting water-soluble, pharmaceutically interesting compounds. They are presently being biologically evaluated.

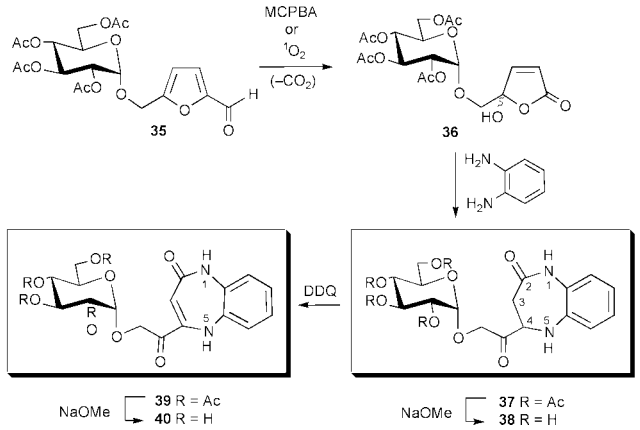

Scheme 4 α-GMF-derived benzodiazepinones.

Conclusion

Practical, large scale-adaptable reaction channels have been developed for the conversion of the sugar-derived furans HMF (**1**) and α-GMF (**2**) into N-heterocycles of the pyrrole, pyridazine and benzodiazepine type, their hydrophilic substituents rendering them water-soluble as well as readily biodegradable. Accordingly, they are assumed to be versatile intermediate chemicals of particular use in pharma- and agro-industry.

Future work will focus on the conversion of bulk-sugars into imidazoles carrying hydrophilic substituents, which are thought to be of similar industrial relevance.

Experimental

Melting points (uncorrected values): Bock monoskop instrument. Spectral measurements: Perkin Elmer 241 (rotations), Varian MAT 311 A (MS), and Bruker WM 300 instruments (^{1}H at 300, ^{13}C NMR at 75.5 MHz, respectively). TLC on Kieselgel 60 F_{254} plastic sheets (Merck) was used to monitor the reactions and to ascertain the purity of the products; eluants employed are given in the appropriate experiment; detection with UV-light or by charring with sulfuric acid. Column chromatography: Kieselgel 60 (63-200 mesh, Macherey-Nagel).

2,5-Bis(acetoxymethyl)furan (3)

To a suspension of $NaBH_4$ (0.85 g, 24 mmol) in 50 mL of Pr^{i}OH was added dropwise a solution of 5.8 g (46 mmol) of HMF (**1**) in 50 mL of MeOH. After stirring for 12 h, excessive $NaBH_4$ was decomposed with a few drops of HOAc. Removal of the solvent under reduced pressure left a syrup, which was acetylated by refluxing in a mixture of Ac_2O (20 mL), NaOAc (5 g) and $CHCl_3$ (50 mL) for 5 h. Ice (40 g) was then added and the reaction mixture was diluted with $CHCl_3$ (200 mL). The organic layer was washed with satd. $NaHCO_3$ solution (2 × 100 mL) and water (2 × 100 mL), dried ($MgSO_4$) and evaporated to dryness, the resulting syrup crystallizing from a mixture of *n*-hexane–diethyl ether: 8.1 g (83%) of **3** as colorless needles; mp. 64–66 °C (lit.[23] mp 63.5–65.5 °C). ^{1}H NMR ($CDCl_3$): δ 2.09 (s, 6 H, 2 AcCH_3), 5.04 (s, 4 H, 2-CH_2, 5-CH_2), 6.38 (s, 2 H, 3-H, 4-H).

2,5-Bis(benzyloxymethyl)furan (4)

To a suspension of $NaBH_4$ (1.8 g, 50 mmol) in 50 mL of Pr^{i}OH was added dropwise a solution of 12.6 g (0.1 mol) of HMF (**1**) in 50 mL of MeOH. After stirring for additional 2 h excessive $NaBH_4$ was decomposed with a few drops of HOAc. Removal of the solvent under reduced pressure left a syrup which was dissolved in dry dioxane (150 mL). After addition of benzyl bromide (50 mL, 0.4 mol) and of crushed KOH (50 g, 0.88 mol) the mixture was refluxed for 4 h. Then, 100 mL of ice were added and the mixture was extracted with CH_2Cl_2 (3 × 100 mL). The combined organic layers were washed with water (3 × 100 mL) and dried ($MgSO_4$). Evaporation of the solvent furnished a yellow syrup, which was purified by elution from a silica gel column (10 × 25 cm) with toluene–EtOAc (20 : 1). Concentration of the appropriate eluates *in vacuo* gave a colorless syrup, which crystallized within a few hours: 25 g (82%) of **4**, mp 43 °C (lit.[24]: mp 44 °C, 74%). ^{1}H NMR ($CDCl_3$): δ 4.55 (s, 4 H, 2 CH_2Ph), 4.62 (s, 4 H, 2-CH_2, 5-CH_2), 6.35 (s, 2 H, 3-H, 4-H).

(*Z*)-1,6-Bis(acetoxy)hex-3-ene-2,5-dione (6)

(a) Photooxidation of 3 with singlet oxygen. A stirred and cooled (−40 °C) solution of **3** (5.0 g, 24 mmol) in dry CH_2Cl_2 (50 mL) was irradiated with a halogen lamp (Tungsram, 500 W) in the presence of methylene blue. Dry oxygen was bubbled through the mixture (5 h) followed by degassing (N_2) and addition of Me_2S (2.2 mL, 30 mmol). The mixture was allowed to warm to room temperature, was decolored with charcoal and then evaporated to dryness *in vacuo*. The resulting residue crystallized from diethyl ether to afford 4.8 g (88%) of **6** as stout prisms of mp 75–76 °C.[25,26] ^{1}H NMR ($CDCl_3$): δ 2.12 (s, 6 H, 2 AcCH_3), 4.75 (s, 4 H, 1-CH_2, 6-CH_2), 6.42 (s, 2 H, 3-H, 4-H). ^{13}C NMR ($CDCl_3$): δ 20.6 (AcCH_3), 67.6 (C-1, C-6), 133.9 (C-3, C-4), 170.3 (Ac*C*O), 196.1 (C-2, C-5). Calc. for $C_{10}H_{12}O_6$ (324.4): C, 52.63; H, 5.30. Found: C, 52.52; H, 5.40%.

(b) Oxidation of furan 3 with 3-*chloroperbenzoic acid (MCPBA).* A mixture of furan **3** (10.0 g, 47 mmol) and of anhydrous MCPBA[27] (15.0 g, 88 mmol) in dry CH_2Cl_2 (300 mL) was stirred at ambient temperature for 18 h. After filtration of the crystallized 3-chlorobenzoic acid, the reaction mixture was washed with satd. $NaHCO_3$ solution (5 × 100 mL) and water (2 × 100 mL). After drying ($MgSO_4$) and evaporation of

the solvent the crude product was purified by crystallization from diethyl ether afforded 9.6 g (90%) of **6** as well-formed prisms identical with respect to mp, ^{1}H and ^{13}C NMR data with the product described above.

(*Z*)-1,6-Bis(benzyloxy)hex-3-ene-2,5-dione (7)

Oxidation of **4** (0.8 g, 2.6 mmol) with anhydrous MCPBA[27] (0.52 g, 3 mmol) in CH_2Cl_2 (50 mL) as described for **3** → **6** and purification of the crude product by elution from a silica gel column (4 × 20 cm) with toluene–EtOAc (10 : 1) gave 590 mg (70%) of **7** as a colorless syrup; R_f 0.3 (toluene–EtOAc, 10 : 1). ^{1}H NMR ($CDCl_3$): δ 4.20 (s, 4 H, 1-C*H*$_2$, 6-C*H*$_2$), 4.62 (s, 4 H, 2 C*H*$_2$Ph), 6.18 (s, 2 H, 3-H, 4-H). ^{13}C NMR ($CDCl_3$): δ 72.2 (C-1, C-6), 73.5 (*C*H$_2$Ph), 128.2–128.7, 136.7 (C_6H_5), 130.0 (C-3, C-4), 201.2 (C-2, C-5). Calc. for $C_{20}H_{20}O_4$ (324.4): C, 74.05; H 6.22. Found: C, 74.00; H, 6.17%.

1,6-Bis(acetoxy)hexane-2,5-dione (8)

(a) By reduction of *Z*-hexenedione 6 with $TiCl_3$. To a vigorously stirred mixture of **6** (1.1 g, 5.0 mmol) in 70 mL of acetone and under a nitrogen atmosphere was added 8.5 mL (10 mmol) of an ice-cold, (15%) aqueous solution of $TiCl_3$. The mixture was stirred at room temperature for 10 min and then extracted with CH_2Cl_2 (3 × 100 mL). The combined organic layers were washed with satd. $NaHCO_3$ solution (2 × 100 mL), and water (2 × 100 mL), dried ($MgSO_4$) and evaporated to dryness *in vacuo*. Crystallization of the residue from diethyl ether afforded 1.0 g (90%) of **8** as colorless needles; mp 93 °C. ^{1}H NMR ([D$_6$]DMSO): δ 2.16 (s, 6 H, 2 AcC*H*$_3$), 2.76 (s, 4 H, 3-C*H*$_2$, 4-C*H*$_2$), 4.71 (s, 4 H, 1-C*H*$_2$, 6-C*H*$_2$). ^{13}C NMR ([D$_6$]DMSO): δ 20.9 (Ac*C*H$_3$), 32.0 (C-3, C-4), 68.0 (C-1, C-6), 170.0 (Ac*C*O), 202.7 (C-2, C-5). Calc. for $C_{10}H_{14}O_6$ (230.2): C, 52.17; H, 6.13. Found: C, 52.23; H, 6.18%.

(b) By reduction of *Z*- (6) or *E*-hexenedione (10) with Zn/HOAc. To a solution of enediones **6** or **10** (1.1 g, 5 mmol) in 50 mL of glacial acetic acid was added zinc powder (1.7 g, 25 mmol) and the mixture was stirred at room temperature for 2 h. After filtration, the zinc cake was washed with CH_2Cl_2 (200 mL) and the combined filtrates were vigorously shaken with 200 mL of brine. The organic layer was separated and washed with water (3 × 100 mL), satd. $NaHCO_3$ solution (3 × 100 mL), and water (2 × 100 mL). After drying ($MgSO_4$) and evaporation of the solvent the crude product was purified by crystallization from diethyl ether to afford 1.0 g (90%) of **8** as colorless needles with the same physical data (^{1}H, ^{13}C) as the product yielded under procedure (a).

1,6-Bis(benzyloxy)hexane-2,5-dione (9)

To a vigorously stirred mixture of enedione **7** (1.62 g, 5 mmol) in 70 mL of acetone and under a nitrogen atmosphere was added 8.5 mL (10 mmol) of an ice-cold aqueous solution of $TiCl_3$ (15%). The mixture was stirred at room temperature for 10 min and then extracted with CH_2Cl_2 (3 × 100 mL). The combined organic layers were washed with satd. $NaHCO_3$ solution (2 × 100 mL), and water (2 × 100 mL), dried ($MgSO_4$), and evaporated *in vacuo*: 1.55 g (95%) of **9** as a colorless syrup. ^{1}H NMR ($CDCl_3$): δ 2.65 (s, 4 H, 3-CH$_2$, 4-CH$_2$), 4.00 (s, 4 H, 1-C*H*$_2$, 6-C*H*$_2$), 4.47 (s, 4 H, 2 C*H*$_2$Ph). ^{13}C NMR ($CDCl_3$): δ 32.3 (C-3, C-4), 72.2 (C-1, C-6), 75.0 (*C*H$_2$Ph), 207.5 (C-2, C-5). Calc. for $C_{20}H_{22}O_4$ (326.4): C, 73.60; H, 6.79. Found: C, 73.58; H, 6.81%.

(*E*)-1,6-Bis(acetoxy)hex-3-ene-2,5-dione (10)

To a vigorously stirred and cooled solution (−30 °C) of furan **3** (2.3 g, 10 mmol) in acetone–water (5 : 1, 60 mL) a solution of bromine (0.5 mL, 10 mmol) in CH_2Cl_2 (10 mL) was added dropwise. The reaction mixture was then allowed to warm to room temperature with continued stirring (2 h) and poured into diethyl ether. The organic layer was washed with satd. $NaHCO_3$ solution (4 × 100 mL), and water (2 × 100 mL), followed by drying ($MgSO_4$), and evaporation to dryness *in vacuo*. Elution of the crude product from silica gel (3 × 15 cm) with CH_2Cl_2–EtOAc (5 : 1) and standing of the appropriate eluates (R_f 0.57 in $CHCl_3$–MeOH, 5 : 1) in a freezer (−40 °C) resulted in crystallization to give 0.85 g (37%) of **10** as colorless needles; mp 91–92 °C.[25,26] ^{1}H NMR ($CDCl_3$): δ 2.10 (6 H-s, 2 AcC*H*$_3$), 4.83 (s, 4 H, 1-C*H*$_2$, 6-C*H*$_2$), 7.00 (s, 2 H, 3-H, 4-H). ^{13}C NMR ($CDCl_3$): δ 20.1 (Ac*C*H$_3$), 67.7 (C-1, C-6), 132.7 (C-3, C-4), 169.7 (Ac*C*O), 194.0 (C-2, C-5). Calc. for $C_{10}H_{12}O_6$ (228.2): C, 52.63; H, 5.30. Found: C, 52.57; H, 5.21%.

(*E*)-1,6-Bis(benzyloxy)hex-3-ene-2,5-dione (11)

A solution of bromine (0.5 mL, 10 mmol) in CH_2Cl_2 (10 mL) was added dropwise to a vigorously stirred and cooled solution (−30 °C) of furan **4** (3.1 g, 10 mmol) in acetone–water (5 : 1, 60 mL). The mixture was then allowed to warm to room temperature with continued stirring for another 2 h and subsequently poured into diethyl ether. The organic layer was washed with satd. $NaHCO_3$ solution (4 × 100 mL) and water (2 × 100 mL), followed by drying ($MgSO_4$), evaporation of the solvent *in vacuo* and crystallization of the residue from diethyl ether: 1.13 g (35%) of **11** as needles; mp 35 °C. ^{1}H NMR ($CDCl_3$): δ 4.26 (s, 4 H, 1-C*H*$_2$, 6-C*H*$_2$), 4.61 (s, 4 H, 2 C*H*$_2$Ph), 7.15 (s, 2 H, 3-H, 4-H). ^{13}C NMR ($CDCl_3$): δ 73.7 (C-1, C-6), 74.8 (*C*H$_2$Ph), 128.2–128.7, 136.7 (C_6H_5), 133.2 (C-3, C-4), 197.3 (C-2, C-5). Calc. for $C_{20}H_{20}O_4$ (324.4): C, 74.05; H, 6.22. Found: C, 74.00; H, 6.17%.

2,5-Bis(benzyloxymethyl)pyrrole (12)

To a solution of **9** (0.33 g, 1 mmol) and NH_4OAc (230 mg, 3 mmol) in dry MeOH (30 mL) was added glacial acetic acid (0.18 ml, 3 mmol) and the mixture was refluxed for 3 h. The mixture was diluted with CH_2Cl_2 (100 mL), washed with satd. $NaHCO_3$ solution (3 × 100 mL), water (2 × 100 mL) and dried ($MgSO_4$). Evaporation to dryness left a syrup, which was purified by elution from a silica gel column (4 × 25 cm) with toluene–EtOAc (9 : 1) to give 215 mg (70%) of **12** as a yellow syrup of R_f 0.53 (toluene–EtOAc, 9 : 1). ^{1}H NMR ($CDCl_3$): δ 4.48, 4.49 (2 s, 4 H each, 2-C$_2$, 5-C*H*$_2$, 2 C*H*$_2$Ph), 6.05 (d, $J_{3,NH}$ = $J_{4,NH}$ = 2.6 Hz, 2 H, 3-H, 4-H), 8.51 (br s, 1 H, NH). ^{13}C NMR ($CDCl_3$): δ 64.9 (2-C$_2$, 5-CH$_2$), 71.6 (2 *C*H$_2$Ph), 108.4 (C-3, C-4), 127.1, 128.2, 128.6, 138.2 (C_6H_5), 129.2 (C-2, C-5). MS (FD): *m*/*z* 307 (M^+).

2,5-Bis(benzyloxymethyl)-*N*-phenylpyrrole (13)

To a stirred solution of **9** (0.33 g, 1 mmol) and of aniline (0.16 g, 1.7 mmol) in dry CH_2Cl_2 (30 mL) was added acetic acid (0.24 mL, 4.0 mmol) and the mixture refluxed for 3 h. Then, the mixture was diluted with CH_2Cl_2 (100 mL), washed with satd. $NaHCO_3$ solution (3 × 100 mL), water (2 × 100 mL) and dried ($MgSO_4$). Evaporation to dryness left a syrup, which was purified by elution from a silica gel column (4 × 25 cm) with toluene–EtOAc (10 : 1) to give 327 mg (85%) of **13** as a yellow syrup; R_f 0.69 (toluene–EtOAc, 10 : 1). ^{1}H NMR ($CDCl_3$): δ 4.25 (s, 4 H, 2-C*H*$_2$, 5-C*H*$_2$), 4.36 (s, 4 H, 2 C*H*$_2$Ph), 6.29 (s,

2 H, 3-H, 4-H). ^{13}C NMR ($CDCl_3$): δ 64.4 (2-CH_2, 5-CH_2), 72.3 (2 CH_2Ph), 111.1 (C-3, C-4), 132.4 (C-2, C-5). MS (FD): *m*/*z* 383 (M^+).

2,5-Bis(benzyloxymethyl)-*N*-benzylpyrrole (14)

Cyclization of **9** (0.33 g, 1 mmol) with benzylamine (0.18 g, 1.7 mmol) in CH_2Cl_2–HOAc was effected as described for **9** → **13**: 361 mg (93%) of **14** as a yellow oil; R_f 0.62 (toluene–EtOAc, 10 : 1). ^{1}H NMR ($CDCl_3$): δ 4.40 (s, 4 H, 2-CH_2, 5-CH_2), 4.46 (s, 4 H, 2 OCH_2Ph), 5.32 (s, 2 H, NCH_2Ph), 6.21 (s, 2 H, 3-H, 4-H). ^{13}C NMR ($CDCl_3$): δ 47.5 (NCH_2Ph), 63.9 (2-CH_2, 5-CH_2), 71.3 (2 OCH_2Ph), 109.9 (C-3, C-4), 130.7 (C-2, C-5). MS (FD): *m*/*z* 398 (M^+). Calc. for $C_{27}H_{27}NO_2$ (397.5): C, 81.58; H, 6.85; N, 3.52. Found: C, 81.47; H, 6.80; N, 3.47%.

2,5-Bis(benzyloxymethyl)-*N*-*n*-tetradecylpyrrole (15)

Generation from **9** and tetradecylamine by refluxing in CH_2Cl_2 containing HOAc analogous to **9** → **13** gave 430 mg (86%) of **15** as a yellow oil; R_f 0.64 (toluene–EtOAc, 10 : 1). ^{1}H NMR ($CDCl_3$): δ 0.88 (t, J = 6.7 Hz, 3 H, CH_3), 1.2–1.3 (m, 22 H, 11 CH_2), 1.66 (m, 2 H, NCH_2CH_2), 3.92 (t, J = 8.1 Hz, 2 H, NCH_2), 4.47 (s, 8 H, 2-CH_2, 5-CH_2, 2 CH_2Ph), 6.08 (s, 2 H, 3-H, 4-H). MS (FD): *m*/*z* 503 (M^+).

2,5-Bis(acetoxymethyl)-*N*-benzylpyrrole (16)

Hexanedione **8** (345 mg, 1.5 mmol) was added to a solution of benzylamine (1.0 mL, 9.1 mmol) in $CHCl_3$ (25 ml), which had been brought to pH 4 by the dropwise addition of acetic acid (2–3 ml). The mixture was refluxed for 2 h, then diluted with $CHCl_3$ (100 mL), followed by washings with water (100 mL), satd. $NaHCO_3$ solution (2 × 100 mL) and water (100 mL). Drying ($MgSO_4$) and removal of the solvent *in vacuo* gave a syrupy residue which crystallized on trituration with methanol: 125 mg (28%) of **16** as colorless needles of mp 99–101 °C. ^{1}H NMR ($CDCl_3$): δ 1.79 (6H-s, 2 AcCH_3), 4.99 (s, 4 H, 2-CH_2, 5-CH_2), 5.20 (2H-s, CH_2Ph), 6.30 (2H-s, 3-H, 4-H). Calc. for $C_{17}H_{19}NO_4$ (301.3): C, 67.76; H, 4.65. Found: C, 67.70; H, 6.39; N, 4.66%.

2,5-Bis(benzyloxymethyl)thiophene (17)

A suspension of 310 mg (1 mmol) of hexanedione **9** and 200 mg (0.5 mmol) of commercially available Lawesson reagent[20] (4-methoxyphenylthiophenic acid dithioanhydride) in toluene (30 mL) was stirred at ambient temperature for 3 h and subsequently refluxed for 1 h. Evaporation to dryness *in vacuo* and elution of the residue from a silica gel column (3 × 26 cm) with toluene–EtOAc (15 : 1) gave 220 mg (74%) of **17** as a colorless oil. ^{1}H NMR ($CDCl_3$): δ 4.56 (s, 4 H, CH_2Ph), 4.66 (s, 4 H, 2-CH_2, 5-CH_2), 6.87 (s, 2 H, 3-H, 4-H). ^{13}C NMR ($CDCl_3$): δ 66.8 (2-CH_2, 5-CH_2), 71.8 (2 CH_2Ph), 126.2 (C-3, C-4), 141.8 (C-2, C-5). Calc. for $C_{20}H_{20}O_2S$ (324.4): C, 74.04; H, 20.16. Found: C, 73.95; H, 20.10%.

3,6-Bis(benzyloxymethyl)pyridazine (18)

To a stirred and cooled solution (0 °C) of 0.33 g (1.0 mmol) of **7** in THF (30 mL) was added 0.1 mL (2.0 mmol) of hydrazine monohydrate. After 2 h, TLC indicating the absence of educt, the mixture was diluted with CH_2Cl_2 (100 mL), washed with water (3 × 100 mL) and dried ($MgSO_4$). Evaporation to drynessleft a syrup, which was purified by elution from a silica gel column (4 × 25 cm) with toluene–EtOAc (2 : 1). Removal of the solvent from the appropriate eluates furnished **18** (231 mg, 73%) as a syrup; R_f 0.20 (toluene–EtOAc, 2 : 1). ^{1}H NMR ($CDCl_3$): δ 4.64 (s, 4 H, 3-CH_2, 5-CH_2), 4.90 (s, 4 H, 2 CH_2Ph), 7.69 (s, 2 H, 4-H, 5-H). ^{13}C NMR ($CDCl_3$): δ 71.1 (2 CH_2Ph), 73.1 (3-CH_2, 5-CH_2), 125.8 (C-4, C-5), 160.1 (C-3, C-6). MS (FD): *m*/*z* 320 (M^+). Calc. for $C_{20}H_{20}N_2O_2$ (320.4): C, 74.97; H, 6.29; N, 8.74. Found: C, 74.90; H, 6.19; N, 8.69%.

3,6-Bis(acetoxymethyl)pyridazine (19)

To a stirred and cooled suspension (0 °C) of 0.8 g (3.5 mmol) of **6** in water (30 mL) was added 0.2 mL (4.0 mmol) of hydrazine monohydrate. Monitoring of the reaction (TLC) indicated the disappearance of the enedione **6** within 10 min. To prevent subsequent cleavage of the ester groups, the mixture was neutralized with a strongly acidic resin (Amberlite IR120, H^+-form). Filtration and evaporation to dryness left a brown syrup, which was purified by elution from a silica gel column (3 × 20 cm) with $CHCl_3$–MeOH (10 : 1). Removal of the solvent from the appropriate eluates furnished **19** (0.41 g, 90%) as a syrup; R_f 0.52 ($CHCl_3$–MeOH, 5 : 1) ^{1}H NMR (CD_3OD): δ 2.10 (6 H-s, 2 AcCH_3), 5.38 (s, 4 H, 3-CH_2, 6-CH_2), 7.80 (2H-s, 4-H, 5-H). ^{13}C NMR (CD_3OD): δ 65.8 (3-CH_2, 6-CH_2), 128.4 (C-4, C-5), 159.8 (C-3, C-6). Calc. for $C_{10}H_{12}N_2O_4$ (224.2): C, 53.57; H, 5.39; N, 12.50. Found: C, 53.49; H, 5.31; N, 12.40%.

3,6-Bis(hydroxymethyl)pyridazine (20)

To a solution of 100 mg (0.45 mmol) of pyridazine **19** in dry MeOH (5 mL) was added NaOMe (10 mg, 0.2 mmol) and the mixture was kept at room temperature for 4 h. Neutralization by stirring with Amberlite IR120, H^+-form, filtration and evaporation to dryness left a syrup, which crystallized on trituration with EtOAc: 48 mg (70%) of **20** of mp 105–106 °C (lit. mp 105–105.5[28] and 105.5–106 °C[15]). ^{1}H NMR (CD_3OD): δ 4.84 (s, 4 H, 3-CH_2, 6-CH_2), 7.78 (2 H-s, 4-H, 5-H). ^{13}C NMR (CD_3OD): δ 63.8 (3-CH_2, 6-CH_2), 127.8 (C-4, C-5), 159.8 (C-3, C-6).

2-Acetoxymethyl-5-(2,3,4,6-tetra-*O*-acetyl-α-D-glucopyranosyloxymethyl)furan (22)

Reduction of the aldehyde group in α-GMF (**2**)[7a] (10.0 g, 35.0 mmol) was effected with $NaBH_4$ (0.66 g, 17.3 mmol) in Pr^{i}OH (50 mL), as described for **1** (HMF) → **4**. The resulting syrupy **21** was dissolved in pyridine (100 mL), followed by cooling (0 °C), addition of acetic anhydride (40 mL, 0.42 mol), and stirring for about 12 h. Crushed ice (40 g) was then added with vigorous stirring (2 h) and the resulting mixture was taken to dryness *in vacuo*. The residue was dissolved in CH_2Cl_2 (200 mL) and the organic layer was washed with 2 M HCl (2 × 100 mL), satd. $NaHCO_3$ solution (3 × 100 mL) and water (2 × 100 mL). Drying ($MgSO_4$) and evaporation to dryness afforded 16.5 g (95%) of **22** as a colorless syrup; $[\alpha]_D^{20}$ + 110 (*c* 1.0, $CHCl_3$). ^{1}H NMR ($CDCl_3$): δ 2.01–2.10 (five 3-H-s, 5 AcCH_3), 4.05 (m, 2H, 5′-H, 6′-H_a), 4.28 (dd, J = 4 and 12.4 Hz, 1 H, 6′-H_b), 4.53, 4.61 (2 d, J = 13.2 Hz, 2 H, 5-CH_2), 4.86 (dd, J = 3.8 and 10.2 Hz, 1 H, 2′-H), 5.03 (s, 2 H, 2-CH_2), 5.08 (dd, J = 9.8 and 9.9 Hz, 1 H, 4′-H), 5.19 (d, J = 3.8, 1-H, 1′-H), 5.49 (dd, J = 10.2 and 9.8 Hz, 1 H, 3′-H), 6.32, 6.37 (2 d, J = 3.2 Hz, 1 H each, 3-H, 4-H). Calc. for $C_{22}H_{28}O_{13}$ (500.45): C, 52.80; H, 5.64. Found: C, 53.15; H, 5.69%.

2-Benzyloxymethyl-5-(2,3,4,6-tetra-*O*-benzyl-α-D-glucopyranosyloxymethyl)furan (23)

A mixture of α-GMF[7a] (**2**) in MeOH (10.0 g, 35 mmol, in 10 mL) and $NaBH_4$ in Pr^iOH (0.66 g, 17.3 mmol, in 50 mL) was stirred for 2 h at ambient temperature and processed as described for **1** → **3**. The resulting syrupy **21** was dissolved in dioxane (500 mL), benzyl bromide (29 g, 0.17 mol) and crushed KOH (18 g, 0.32 mol) was added and the mixture was refluxed for 6 h. Then, ice (100 mL) was added and the mixture was extracted with CH_2Cl_2 (3 × 100 mL). The combined organic layers were washed with water (3 × 100 mL) and dried ($MgSO_4$). Evaporation of the solvent afforded a yellow syrup which was purified by elution from a silica gel column (8 × 25 cm) with toluene–EtOAc (20 : 1) furnished 22.8 g (88%) of **23** as a colorless syrup; R_f 0.29 (toluene–EtOAc, 20 : 1); $[\alpha]_D^{20}$ + 118 (*c* 1.0, $CHCl_3$). ^{1}H NMR ($CDCl_3$): δ 3.60 (dd, *J* = 3.7 and 9.2 Hz, 1 H, 2′-H), 3.60–3.81 (m, 4 H, 4′-H, 5′-H, 6′-H_2), 4.00 (t, *J* = 9.2 Hz, 1 H, 3′-H), 4.43–4.62 (m, 12 H, 2-CH_2, 5 CH_2Ph), 4.80 (dd, *J* = 9 and 9.1 Hz, 2 H, 5-CH_2), 4.91 (d, *J* = 3.8 Hz, 1 H, 1′-H), 6.28, 6.31 (2 d, *J* = 3.4 Hz, 1 H each, 3-H, 4-H). ^{13}C NMR ($CDCl_3$): δ 61.0, 64.1, 72.1, 72.8, 73.5 (5 CH_2Ph), 68.4 (C-6′), 70.4 (C-5′), 75.1, 75.8 (2CH_2, 5-CH_2), 76.7 (C-4′), 79.6 (C-2′), 82.1 (C-3′), 95.1 (C-1′), 110.2, 111.1 (C-3, C-4), 151.1, 152.4 (C-2, C-5). MS (FD): *m*/*z* 741 (M^+).

(*Z*)-1-Acetoxy-6-(2,3,4,6-tetra-*O*-acetyl-α-D-glucopyranosyloxy)hex-3-ene-2,5-dione (24)

Anhydrous MCPBA[27] (0.85 g, 5 mmol) was added to a solution of furan **22** (2.5 g, 5 mmol) in CH_2Cl_2 (50 mL) and the mixture was refluxed for 5 h, followed by another addition of MCPBA (0.85 g) and further refluxing (total 12 h). Subsequent washing with satd. $NaHCO_3$ solution (3 × 100 mL) and water (2 × 100 mL). After drying ($MgSO_4$) and evaporation of the solvent the crude product was purified by elution from a silica gel column (4 × 20 cm) with toluene–EtOAc (1 : 1). Removal of the solvents from the appropriate eluates gave 2.4 g (93%) of **24** as a colorless syrup; R_f 0.33 (toluene–EtOAc, 1 : 1); $[\alpha]_D^{20}$ + 84.3 (*c* 1.16, $CHCl_3$). ^{1}H NMR ($CDCl_3$): δ 1.86–2.15 (5 s, 15 H, 5 AcCH_3), 4.05-4.10 (m, 2 H, 5′-H, 6′-H_a), 4.25 (m, 1 H, 6′-H_b), 4.83 (s, 2 H, 6-CH_2), 4.90 (dd, *J* = 3.8 and 10.2 Hz, 1 H, 2′-H), 5.09 (t, *J* = 9.8 Hz; 1 H, 4′-H), 5.36 (d, *J* = 3.8 Hz, 1 H, 1′-H), 5.47 (m, 3 H, 3′-H, 1-CH_2), 6.15, 6.53 (2 d, *J* = 12.2 Hz, 1 H each, 3-H, 4-H). ^{13}C NMR ($CDCl_3$): δ 18.3–18.6 (5 AcCH_3), 59.6 (C-6′), 65.1 (C-5′), 66.2 (C-6), 66.5 (C-4′), 67.7 (C-2′), 84.1 (C-3′), 88.0 (C-1), 93.0 (C-1′), 123.9 (C-4), 137.7 (C-3), 167.4–168.5 (5 Ac*C*O), 194.7 (C-2, C-5).

(*Z*)-1-Benzyloxy-6-(2,3,4,6-tetra-*O*-benzyl-α-D-glucopyranosyloxy)hex-3-ene-2,5-dione (25)

Oxidation of **23** (3.7 g, 5 mmol) with anhydrous MCPBA[27] (0.86 g, 5 mmol) in CH_2Cl_2 (50 mL) as described for **22** → **24** furnished after purification by elution from a silica gel column (4 × 20 cm) with toluene–EtOAc (10 : 1) **25** (3.4 g, 90%) as a colorless syrup; R_f 0.50 (toluene–EtOAc, 10 : 1). ^{1}H NMR ($CDCl_3$): δ 3.57 (dd, *J* = 3.5 and 9.3 Hz, 1 H, 2′-H), 3.63 (br d, 1 H, 6′-H_a), 3.64 (t, *J* = 9.0, 1 H, 4′-H), 3.65 (dd, *J* = 2.0 and 10.5 Hz, 1 H, 6′-H_b), 3.75 (ddd, *J* = 2.0, 3.6 and 9.0 Hz, 1 H, 5′-H), 3.96 (t, *J* = 9.3 Hz, 1 H, 3′-H), 4.10 (s, 2 H, 1-CH_2), 4.17, 4.23 (two 1H-d, *J* = 13.2 Hz, 6-CH_2), 4.42–4.91 (6 d, 2 s, 10 H, 5 CH_2Ph), 5.13 (d, *J* = 3.5 Hz, 1 H, 1′-H), 6.27, 6.35 (two s, 2 H, 3-H, 4-H). ^{13}C NMR ($CDCl_3$): δ 67.3 (C-6′), 70.2 (C-5′), 70.9, 71.9, 72.3, 73.8, 74.5 (5 CH_2Ph), 72.0 (C-1), 76.2 (C-4′), 76.4 (C-6), 78.2 (C-2′), 80.4 (C-3′), 95.7 (C-1′), 128.2, 129.2 (C-3, C-4), 201.3, 203.3 (C-2, C-5). MS (FD): *m*/*z* 757 ($M+1^+$).

1-Acetoxy-6-(2,3,4,6-tetra-*O*-acetyl-α-D-glucopyranosyloxy)hexane-2,5-dione (26)

To a solution of enedione **24** (5.16 g, 10 mmol) in 250 mL of acetic acid was added zinc powder (3.3 g, 50 mmol) and the mixture was stirred at room temperature for 2 h. After filtration, the zinc cake was washed with CH_2Cl_2 (500 mL) and the combined filtrates were vigorously shaken with 200 mL of brine. The organic layer was separated and washed with water (3 × 100 mL), satd. $NaHCO_3$ solution (3 × 100 mL), and water (2 × 100 mL). After drying ($MgSO_4$) and evaporation of the solvent the crude product was purified by elution from a silica gel column (4 × 20 cm) with CH_2Cl_2–EtOAc (10 : 1). Removal of the solvents from the appropriate eluates gave **26** (4.6 g, 89%) as a colorless syrup; R_f 0.16 (CH_2Cl_2–EtOAc, 10 : 1); $[\alpha]_D^{20}$ + 88.6 (*c* 1.1, $CHCl_3$). ^{1}H NMR ($CDCl_3$): δ 1.94–2.09 (5 s, 15 H, 5 AcCH_3), 2.59 (m, 2 H, 3-H_2), 2.71 (m, 2 H, 4-H_2), 4.03 (m, 2 H, 5′-H, 6′-H_a), 4.20 (dd, *J* = 2.3 and 12.4 Hz, 1 H, 6′-H_b), 4.63 (s, 2 H, 6H_2), 4.79 (dd, *J* = 3.8 and 10.2 Hz, 1 H, 2′-H), 5.01 (dd, *J* = 9.8 Hz, 1 H, 4′-H), 5.28-5.32 (m, 3-H, 1′-H, 1-H_2), 5.42 (dd, *J* = 10.2 and 9.8 Hz, 1 H, 3′-H). ^{13}C NMR ($CDCl_3$): δ 21.7–22.0 (5 AcCH_3), 28.7 (C-3), 34.4 (C-4′), 63.0 (C-6′), 71.2 (C-6), 71.3 (C-5′), 71.7 (C-4′), 72.5 (C-3′), 72,7 (C-2′), 87.0 (C-1), 96.2 (C-1′), 170.9–172.8 (5 AcCO), 203.5 (C-2, C-5). MS (FD): *m*/*z* 475 (M^+ − 43).

1-Benzyloxy-6-(2,3,4,6-tetra-*O*-benzyl-α-D-glucopyranosyloxy)hexane-2,5-dione (27)

Reduction of **25** (7.56 g, 10 mmol) with zinc powder (3.3 g, 50 mmol) in 250 mL of glacial acetic acid, as described for **24** → **26,** furnished 5.3 g (70%) of **27** as a colorless syrup; R_f 0.31 (toluene–EtOAc, 10 : 1); $[\alpha]_D^{20}$ + 50.3 (*c* 1.1, $CHCl_3$). ^{1}H NMR ($CDCl_3$): δ 2.7–2.9 (br 4-H-m, 3-H_2, 4-H_2), 3.58 (dd, *J* = 3.6 and 9.3 Hz, 1 H, 2′-H), 3.63 (br d, *J* = 10.5 Hz, 1 H, 6′-H_a), 3.64 (t, *J* = 9.3 Hz; 1 H, 4′-H), 3.66 (dd, 1 H, 6′-H_b), 3.76 (ddd, *J* = 2.0, 3.6 and 9.0 Hz, 1 H, 5′-H), 3.97 (t, *J* = 9.3 Hz, 1 H, 3′-H), 4.10 (s, 2 H, 1-CH_2), 4.17, 4.23 (two 1H-d, *J* = 10.3 Hz, 6-CH_2), 4.44-4.97 (6 d, 2 s, 10 H, 5 CH_2Ph), 5.10 (d, *J* = 3.6 Hz, 1 H, 1′-H). ^{13}C NMR ($CDCl_3$): δ 32.6 (C-3, C-4), 68.4 (C-6′), 71.3 (C-5′), 71.9 (C-6), 73.1, 73.5, 73.9, 75.1, 75.8 (5 CH_2Ph), 76.1 (C-1), 78.5 (C-4′), 80.3 (C-2′), 81.7 (C-3′), 97.5 (C-1′), 206.8, 207.7 (C-2, C-5). MS (FD): *m*/*z* 758 (M^+). Calc. for $C_{47}H_{50}O_9$ (758.87): C, 74.38; H, 6.64. Found: C, 74.30; H, 6.59%.

2-Benzyloxymethyl-5-(2,3,4,6-tetra-*O*-benzyl-α-D-glucopyranosyloxymethyl)pyrrole (28)

Refluxing **27** (0.76 g, 1 mmol) to NH_4OAc (230 mg, 3 mmol) in dry MeOH (30 mL) in the presence of acetic acid (0.18 mL, 3 mmol), for 3 h and work-up, as described for **9** → **12**, afforded, after purification by elution from a silica gel column (4 × 25 cm) with toluene–EtOAc (20 : 1), containing 1% Et_3N, 510 mg (70%) of **28** as a pale yellow syrup; $[\alpha]_D^{20}$ + 70 (*c* 1.0, $CHCl_3$). ^{1}H NMR ($CDCl_3$): δ 3.52 (dd, *J* = 3.7 and 9.5 Hz, 1 H, 2′-H), 3.57 (dd, *J* = 9.2 and 10.5 Hz, 1 H, 4′-H), 3.65 (d, 2 H, 6′-H_2), 3.84 (dt, *J* = 10.5 and 3.0 Hz, 1 H, 5′-H), 3.99 (t, *J* = 9.5 Hz, 1 H, 3′-H), 4.40 (s, 2 H, 2 CH_2), 4.4–4.8 (m, 12 H, 5 CH_2Ph, 5-CH_2), 4.88 (d, *J* = 3.7 Hz, 1 H, 1′-H), 6.06 (m, 2 H, 3-H, 4-H), 8.72 (br s, 1 H, 1-H). ^{13}C NMR ($CDCl_3$): δ 62.3 (2-CH_2), 64.8 (5-CH_2) 68.7 (C-6′), 70.5 (C-5′), 71.5, 72.9, 73.5, 75.0, 75.7 (5 CH_2Ph) 77.9 (C-4′), 79.6 (C-2′), 82.2 (C-3′), 95.3 (C-1′), 108.3, 109.2 (C-3, C-4), 127.6–129.4 and 137.9–138.8 (5 C_6H_5, C-2, C-5). MS (FD): *m*/*z* 739 [M^+], 648 [M^+−C_7H_7]. Calc. for $C_{47}H_{49}NO_7$ (739.9): C, 76.30; H, 6.68; N, 1.89. Found: C, 76.16; H, 6.73; N, 1.92%.

2-Benzyloxymethyl-5-(2,3,4,6-tetra-*O*-benzyl-α-D-glucopyranosyloxymethyl)-*N*-phenylpyrrole (29)

Reaction of **27** (0.76 g, 1 mmol) with aniline (0.28 g, 3 mmol) in dry MeOH (30 mL) in the presence of acetic acid (0.18 mL, 3 mmol), as described for **9** → **13** gave upon purification by elution from a silica gel column (4 × 25 cm) with toluene–EtOAc (20:1), containing 1% Et_3N, 606 mg (75%) of **29** as a syrup; R_f 0.29 (toluene–EtOAc, 20:1); $[\alpha]_D^{20}$ + 77 (*c* 1.0, $CHCl_3$). ^1H NMR ($CDCl_3$): δ 3.43–3.47 (m, 2H, 6′-H_2), 3.52 (dd, *J* = 3.6 and 9.4 Hz, 1 H, 2′-H), 3.57–3.63 (m, 2 H, 4′-H, 5′-H), 3.92 (t, *J* = 9.4 Hz, 1 H, 3′-H), 4.19, 4.24 (2 d, *J* = 12.0 Hz, 1 H each, 5-CH_2), 4.34 (s, 2 H, 2-C_2), 4.18–4.97 (m, 10 H, 5 CH_2Ph), 4.87 (d, *J* = 3.6 Hz, 1 H, 1′-H), 6.30, 6.32 (2 d, *J* = 3.6 Hz, 1H each, 3-H, 4-H). Calc. for $C_{53}H_{53}NO_7$ (825.96): C, 78.01; H, 6.55; N, 1.72. Found: C, 78.07; H, 6.53; N, 1.79%.

2-Benzyloxymethyl-5-(2,3,4,6-tetra-*O*-benzyl-α-D-glucopyranosyloxymethyl)-*N*-benzylpyrrole (30)

Exposure of **27** (0.76 g, 1 mmol) to benzylamine (0.32 g, 3 mmol) in dry MeOH (30 mL) in the presence of acetic acid (0.18 mL, 3 mmol), as described for **9** → **14** gave upon purification by elution from a silica gel column (4 × 25 cm) with toluene–EtOAc (30:1) 692 mg (84%) of **30** as a colorless syrup; $[\alpha]_D^{20}$ + 62 (*c* 1.1, $CHCl_3$). ^1H NMR ($CDCl_3$): δ 3.52 (dd, *J* = 3.5 and 9.4 Hz, 1 H, 2′-H), 3.57 (dd, *J* = 10.5 and 1.8 Hz, 1 H, 6′-H_a), 3.61 (t, *J* = 9.4 Hz, 1 H, 4′-H), 3.68 (dd, *J* = 10.5 and 3.5 Hz, 1 H, 6′-H_b), 3.74 (ddd, *J* = 1.8, 3.5 and 9.6 Hz, 1 H, 5′-H), 3.92 (t, *J* = 9.4 Hz, 1 H, 3′-H), 4.29, 4.34 (2 d, *J* = 12.5 Hz, 1 H each, 5-CH_2), 4.39 (s, 2 H, 2-CH_2), 4.33–4.94 (m, 10 H, OCH_2Ph), 4.90 (d, *J* = 3.5 Hz, 1 H, 1′-H), 5.25, 5.37 (2 d, *J* = 17.0 Hz; 1 H each, NCH_2Ph), 6.16, 6.19 (2 d, *J* = 3.5 Hz, 1 H each, 3-H, 4-H). ^{13}C NMR ($CDCl_3$): δ 47.5 (NCH_2Ph), 61.4 (5-CH_2) 63.8 (2-CH_2), 68.6 (C-6′), 70.6 (C-5′), 71.4, 72.6, 73.6, 75.1, 75.8 (5 OCH_2Ph) 77.8 (C-4′), 79.8 (C-2′), 82.1 (C-3′), 95.1 (C-1′), 109.9, 110.3 (C-3, C-4), 129.9, 130.9 (C-2, C-5). Calc. for $C_{54}H_{55}NO_7$ (830.0): C, 78.14; H, 6.68; N, 1.68. Found: C, 78.25; H, 6.77; N, 1.72%.

2-Benzyloxymethyl-5-(2,3,4,6-tetra-*O*-benzyl-α-D-glucopyranosyloxymethyl)-*N*-*n*-dodecylpyrrole (31)

Reaction of **27** (0.76 g, 1 mmol) with dodecylamine (0.55 g, 3 mmol) in dry MeOH (30 mL) and in the presence of acetic acid (0.18 mL, 3 mmol) as described for **8** → **16** afforded, after purification by elution from a silica gel column (4 × 25 cm) with toluene–EtOAc (30:1), 752 mg (83%) of **31** as a colorless syrup; R_f 0.26 (toluene–EtOAc, 30:1); $[\alpha]_D^{20}$ + 50 (*c* 1.1, $CHCl_3$). ^1H NMR ($CDCl_3$): δ 0.87 (t, 3 H, CH_3), 1.00–1.29 (m, 18 H, $(CH_2)_9$), 1.71 (m, 2 H, NCH_2CH_2-), 3.52 (dd, *J* = 3.6 and 9.3 Hz, 1 H, 2′-H), 3.59–3.65 (m, 2 H, 4′-H, 6′-H_a), 3.71 (dd, *J* = 10.6 and 3.6 Hz, 1 H, 6′-H_b), 3.81 (ddd, *J* = 2.0, 3.6 and 10.0 Hz, 1 H, 5′-H), 3.86–4.06 (m, 2 H, NCH_2), 3.98 (t, *J* = 9.3 Hz, 1 H, 3′-H), 4.40, 4.45 (2 d, *J* = 12.5 Hz, 1 H each, 5-CH_2), 4.46 (s, 2 H, 2-C_2), 4.40-4.97 (m, 10 H, 5 CH_2Ph), 4.94 (d, *J* = 3.6 Hz, 1 H, 1′-H), 6.07, 6.10 (2 d, *J* = 3.5 Hz, 1 H each, 3-H, 4-H), 7.12–7.34 (m, 25 H, 5 C_6H_5). Calc. for $C_{59}H_{73}NO_7$ (908.24): C, 78.03; H, 8.10; N, 1.54. Found: C, 78.16; H, 8.18; N, 1.60%.

2-(α-D-Glucopyranosyloxymethyl)-2-hydroxy-2*H*-pyran-5(6*H*)-one (33)

To a stirred and cooled suspension (0 °C) of $NaBH_4$ (200 mg, 5 mmol) in Pr^iOH (200 mL) was added dropwise a solution of 3.5 g (12 mmol) of α-GMF[7a] (**2**) in MeOH (80 mL). After 2 h excessive $NaBH_4$ was decomposed by addition of a few drops of HOAc and the solvent removed *in vacuo*. The remaining syrupy **21** was dissolved in water (100 mL), followed by adding dropwise a solution of bromine (0.6 mL, 12 mmol) in 5 mL of MeOH. The mixture was then stirred at ambient temperature for 2 h, neutralized with a weakly basic ion exchange resin (Amberlite IRA-68, OH form), and excess bromine was removed *in vacuo* on a rotary evaporator (< 30 °C). The resulting solution was evaporated to dryness under reduced pressure to yield 3.5 g (95 %) of **33** as an amorphous solid. ^1H NMR (D_2O): δ 3.29–3.35 (m, 1 H, 5′-H), 3.50–3.85 (m, 9 H, 2-CH_2, 6-H_2, 2′-H, 3′-H, 4′-H, 6′-H_2), 5.00 (m, 1 H, 1′-H), 6.28 (two 1H-d of diasteriomer I and II, $J_{3,4}$ = 10.5 Hz, 4-H), 7.25 (two 1H-d of diasteriomer I and II, $J_{4,3}$ = 10.5 Hz, 3-H). ^{13}C NMR (D_2O): δ 63.2 (2-CH_2), 68.8 (C-6′), 72.3 (C-6), 74.0 (C-5′), 74.2 (C-2′), 74.9 (C-3′), 75.7 (C-4′), 101.6 (C-1′), 130.4, 130.6 (C-4), 150.6, 150.9 (C-3), 183.9, 200.5 (C-2, C-5).

6-(α-D-Glucopyranosyloxymethyl)-3-hydroxymethylpyridazine (34)

Hydrazine monohydrate (0.1 mL, 1 mmol) was added to an aqueous solution of freshly prepared **33** (350 mg, 1.1 mmol) and the mixture was stirred for 2 h, followed by evaporation to dryness *in vacuo* afforded a yellow syrup, which was purified by elution from a column of silica gel (3 × 15 cm) with $CHCl_3$–MeOH (2:1). Removal of the solvents *in vacuo* gave **34** (0.24 g, 68%) as a colorless foam; R_f 0.13 ($CHCl_3$–MeOH, 2:1); $[\alpha]_D^{20}$ + 110.6 (*c* 1.0, MeOH). ^1H NMR (CD_3OD): δ 3.29–3.35 (m, 1 H, 5′-H), 3.45 (dd, *J* = 3.7 and 9.6 Hz, 1 H, 2′-H), 3.64–3.80 (m, 4 H, 3′-H, 4′-H, 6′-CH_2), 4.79 (s, 2 H, 3-CH_2), 4.80 (d, *J* = 19.9 Hz, 1 H, 6-CH_{2a}), 4.89 (d, *J* = 3.7 Hz, 1 H, 1′-H), 5.03 (d, *J* = 19.9 Hz, 1 H, 6-CH_{2b}), 7.86, 7.97 (2 d, *J* = 8.7, 1 H each, 4-H, 5-H). ^{13} C NMR (CD_3OD): δ 61.5 (C-6′), 62.8 (3-CH_2), 67.9 (6-CH_2), 70.6 (C-5′), 72.4 (C-2′), 73.2 (C-4′), 73.9 (C-3′), 99.3 (C-1′), 126.5, 127.7 (C-4, C-5), 159.7, 163.2 (C-3, C-6). MS (FD): *m*/*z* = 302 (M^+). Calc. for $C_{17}H_{18}N_2O_7$ (302.3): C, 47.68; H, 6.00; N, 9.27. Found: C, 47.59; H, 6.07; N, 9.22%.

5-Hydroxy-5-(2,3,4,6-tetra-*O*-acetyl-α-D-glucopyranosyloxymethyl)-furan-2(5*H*)-one (36)

Photooxidation of α-GMF-tetraacetate 35 with singlet oxygen. A stirred and cooled (−40 °C) solution of **35** [7a] (2.5 g, 5.5 mmol) in dry CH_2Cl_2 (50 mL) was irradiated with a halogen lamp (Tungsram, 500 W) in the presence of methylene blue. Dry oxygen was bubbled through the mixture (5 h) followed by degassing (N_2) and addition of Me_2S (0.37 g, 6 mmol). The mixture was allowed to warm to room temperature, was decolored with charcoal and then evaporated to dryness to afford 2.31 g (95%) of chromatographically uniform **36** as a colorless foam; R_f 0.14 (CH_2Cl_2–EtOAc, 10:1). ^1H NMR ($CDCl_3$): δ 2.01–2.14 (4 s, 12 H, 4 AcCH_3), 4.07–4.15 (m, 5 H, 5′-H, 6′-CH_2, 5-CH_2), 4.91 (dd, *J* = 3.8 and 10.3 Hz, 1 H, 2′-H), 4.95 (dd, *J* = 10.3 and 10.4 Hz, 1 H, 4′-H), 5.07 (d, *J* = 3.8 Hz, 1 H, 1′-H), 5.46 (dd, *J* = 10.3 Hz, 1 H, 3′-H), 6.23 (d, *J* = 6 Hz, 1 H, 3-H), 7.26 (d, *J* = 6 Hz, 1 H, 4-H). ^{13}C NMR ($CDCl_3$): δ 20.5–20.7 (4 AcCH_3), 61.8 (5-CH_2), 62.1 (C-6′), 67.9 (C-5′), 68.3 (C-4′), 69.7 (C-3′), 69.9 (C-2′), 97.2 (C-1′), 105.5 (C-5), 124.9 (C-3), 151.9 (C-4), 169.5, 169.7, 169.9, 170.4, 170.9 (4 Ac*C*O, C-2). MS (FD): *m*/*z* 461 (M^+ + 1).

Oxidation of 35 with 3-chloroperbenzoic acid (MCPBA). To a stirred solution of **35** (2.5 g, 5.5 mmol) in dry CH_2Cl_2 (200 mL) was added anhydrous MCPBA[27] (2.5 g, 14 mmol) in several portions and stirring was continued for 18 h whereafter TLC indicated absence of educt in favor of **36** (R_f 0.14, CH_2Cl_2–EtOAc, 10:1). The mixture was concentrated to about half its volume, resulting in a precipitate of 3-chlorobenzoic acid which

was filtered off. The filtrate was washed with satd. $NaHCO_3$ solution (3 × 100 mL), water (2 × 100 mL), dried ($MgSO_4$), and evaporated to dryness *in vacuo*. The remaining syrup was purified by elution from a silica gel column (4 × 25 cm) with CH_2Cl_2–EtOAc (10×1) → EtOAc. Concentration of the appropriate eluates gave 1.7 g (70%) of **36** as a colorless foam, identical (R_f, ^1H, ^{13}C NMR) with the product described above.

4-[(2,3,4,6-Tetra-*O*-acetyl-α-D-glucopyranosyloxy)acetyl]-1,3,4,5-tetrahydro-2*H*-1,5-benzodiazepin-2-one (37)

To a cooled (0 °C), stirring solution of **36** (0.60 g, 1.3 mmol) in $CHCl_3$ (10 mL) was added in several portions 0.14 g (1.3 mmol) of *o*-phenylenediamine. The mixture was stirred at room temperature for 3 h, filtered, and evaporated. The residue was purified by elution from a silica gel column (3 × 25 cm) with CH_2Cl_2–EtOAc (2:1). Removal of the solvents from the appropriate eluates afforded **37** (0.46 g, 65%) as a syrup; R_f 0.24 (CH_2Cl_2–EtOAc, 2:1). ^1H NMR ($CDCl_3$): δ 2.00–2.10 (four 3-H-s, 4 AcCH_3), 2.55 and 3.11 (two 0.5 H-dd, $J_{3,3}$ = 16.8, $J_{3,4}$ = 5.8 Hz, 3-H_2 of diastereomer I), 2.61 and 3.21 (two 0.5 H-dd, $J_{3,3}$ = 17.8, $J_{3,4}$ = 5.8 Hz, 3-H_2 of diastereomer II), 4.07–4.15 (m, 4 H, 2-H, 5′-H, OCH_2CO), 4.17–4.37 (m, 2 H, 6′-H_a, 6′-H_b), 4.93 (dd, J = 3.8 and 10.3 Hz, 1 H, 2′-H), 5.12 (dd, J = 9.7 and 9.8 Hz, 1 H, 4′-H), 5.18 (d, J = 3.8 Hz, 1 H, 1′-H), 5.52 (t, J = 9.7 Hz, 1 H, 3′-H), 6.90–7.31 (m, 4 H, C_6H_4), 9.29, 9.33 (2 br s, 1 H each, NH). ^{13}C NMR ($CDCl_3$): δ 20.5–20.7 (4 AcCH_3), 37.0 (C-3), 52.1 (C-4), 61.9 (C-6′), 68.0 (C-5′), 68.5 (C-4′), 70.0 (C-3′), 70.5 (C-2′), 72.3 (OCH_2CO), 96.2, 96.4 (C-1′- of diastereomers I and II), 117.6, 124.2, 127.8, 128.1 (C-6, C-7, C-8, C-9), 133.7, 136.2 (C-6a, C-9a), 167.7 (C-2), 169.8, 170.2, 170.8, 171.4 (4 Ac*C*O), 202.8, 203.2 (4-CO of diastereomer I and II). MS (FD): *m*/*z* 550 (M^+).

4-[(α-D-Glucopyranosyloxy)-acetyl]-1,3,4,5-tetrahydro-2*H*-1,5-benzodiazepin-2-one (38)

To a solution of 0.31 g (0.5 mmol) of benzodiazepinone **37** in dry MeOH (5 mL) was added NaOMe (10 mg, 0.2 mmol). The mixture was kept for 4 h at room temperature, neutralized with a strongly acidic exchange resin (Amberlite IR120, H^+-form), filtered and evaporated to dryness: 250 mg (75 %) of **38** as a syrup. ^1H NMR (CD_3OD): δ 2.85 (m,1 H, 3-H_a), 3.05 (m,1 H, 3-H_b), 3.12-3.50 (m, 6 H, 2′-H, 3′-H, 4′-H, 5′-H, 6′-H_2), 4.20–4.52 (m, 3 H, 4-H, OCH_2CO), 4.85 (d, J = 3.8 Hz, 1 H, 1′-H), 6.68–7.36 (m, 4 H, C_6H_4). ^{13}C NMR ($CDCl_3$): δ 40.3 (C-3), 50.7, 50.8 (C-4 of diastereomer I and II), 60.9 (C-6′), 70.0 (C-2′,C-5′), 71.7 (OCH_2CO), 73.0 (C-4′), 73.1 (C-3′), 98.7 (C-1′), 117.6, 124.1, 127.7, 128.0 (C-6, C-7, C-8, C-9), 133.5, 136.2 (C-6a, C-9a), 168.3 (C-2), 205.8, 205.9 (4-*C*O of diastereomer I and II).

1,5-Dihydro-4-[(2,3,4,6-tetra-*O*-acetyl-α-D-glucopyranosyloxymethyl)acetyl]-2*H*-1,5-benzodiazepin-2-one (39)

To a solution of **37** (0.3 g, 0.55 mmol) in 10 mL of $CHCl_3$ was added 290 mg (1.3 mmol) of DDQ and 100 mg of *p*-toluenesulfonic acid and the mixture was stirred for 2 h. Water (50 mL) was added and the mixture was extracted with $CHCl_3$ (3 × 20 mL). The combined extracts were washed with water (2 × 30 mL) and dried ($MgSO_4$). Evaporation of the solvent afforded a yellow oil, which was purified by elution from a column of silica gel (2 × 15 cm) with CH_2Cl_2–EtOAc (2:1). Removal of the solvent from the appropriate eluates gave **39** (0.17 g, 50%) as a pale yellow syrup; R_f 0.25 (CH_2Cl_2–EtOAc; 2:1). ^1H NMR ($CDCl_3$): δ 1.97–2.20 (four 3-H-s, 4 AcCH_3), 4.11–4.27 (m, 3 H, 6′-H_a, OCH_2CO), 4.32 (m, 2 H, 6′-H_b, 5′-H), 5.08 (dd, J = 3.8 and 10.3 Hz, 1 H, 2′-H), 5.12 (dd, J = 9.7 and 9.8 Hz, 1 H, 4′-H), 5.15 (d, J = 3.8 Hz, 1 H, 1′-H), 5.63 (t, J = 10.3 Hz, 1 H, 3′-H), 6.45 (s, 1 H, 3-H), 11.20, 13.33 (br s, 1 H each, 2 N*H*). ^{13}C NMR ($CDCl_3$): δ 20.1–20.7 (4 AcCH_3), 61.9 (C-6′), 67.8 (C-5′), 68.6 (C-4′), 69.9 (C-3′), 70.2 (C-2′), 70.7 (OCH_2CO), 89.9 (C-3), 96.0 (C-1′), 116.1, 116.4, 124.5, 124.8 (C-6, C-7, C-8, C-9), 125.9 (C-4), 144.7, 144.9 (C-6a, C-9a), 157.3 (C-2), 169.6, 169.8 170.3, 170.6 (4 Ac*C*O), 195.8 (4-*C*OCH_2). MS (FD): *m*/*z* 548 (M^+).

1,5-Dihydro-4-[(α-D-glucopyranosyloxy)-acetyl]-2*H*-1,5-benzodiazepin-2-one (40)

To a solution of 0.27 g (0.5 mmol) of benzodiazepinone **39** in dry MeOH (5 mL) was added NaOMe (5 mg, 0.1 mmol). The mixture was kept for 2 h at room temperature, neutralized with a strongly acidic exchange resin (Amberlite IR120, H^+-form), filtered and evaporated to dryness: 170 mg (89 %) of **40** as a syrup. ^1H NMR (CD_3OD): δ 3.08 (m, 1 H, 5′-H), 3.25 (dd, J = 3.5 and 9.6 Hz, 2′-H), 3.39–3.48 (m, 3 H, 3′-H, 4′-H, 6′-H_a), 3.62 (m, 1 H, 6′-H_b), 4.27 (s, 2 H, OCH_2CO), 4.74 (d, J = 3.5 Hz, 1 H, 1′-H), 6.45 (s, 1 H, 3-H). ^{13}C NMR (CD_3OD): δ 60.9 (C-6′), 69.8 (C-2′), 69.9 (C-5′), 70.7 (OCH_2CO), 73.9 (C-4′), 73.5 (C-3′), 90.9 (C-3), 98.9 (C-1′), 116.1, 116.4, 124.5, 124.8 (C-6, C-7, C-8, C-9), 127.6 (C-4), 145.7, 146.1 (C-6a, C-9a), 159.0 (C-2), 196.8 (4-*C*OCH_2). MS (FD): *m*/*z* 380 (M^+).

Acknowledgments

This work was financially supported by the Südzucker AG, Mannheim/Ochsenfurt, and by Grant 94 NR 078-F and 99 NR 063 from the Ministry of Nutrition, Agriculture and Forestry, Bonn, administered by the Fachagentur Nachwachsende Rohstoffe, Gülzow.

References

1 F. W. Lichtenthaler and B. Werner, *Carbohydr. Res.*, 1999, **319**, 47.
2 D. L. Klass, *Biomass for Renewable Energy, Fuels and Chemicals*, Academic Press, San Diego / London, 1998, 608 pp.; particularly ch. 13, pp. 495–546.
3 *Carbohydrates as Organic Raw Materials*, ed. F. W. Lichtenthaler, VCH Publ., Weinheim/New York, 1991, 367 pp.
4 F. W. Lichtenthaler and S. Mondel, *Pure Appl.Chem.*, 1997, **69**, 1833; F. W. Lichtenthaler, *Carbohydr. Res.*, 1998, **313**, 69.
5 W. J. McKillip, in *Ullmann's Encyclopedia of Industrial Chemistry*, VCH Publ., Weinheim/New York, 5th edn., 1989, vol. **A12**, p. 122 ff.
6 B. F. M. Kuster, *Starch/Stärke*, 1990, **43**, 314; H. Schiweck, M. Munir, K. M. Rapp, B. Schneider and M. Vogel, in *Carbohydrates as Organic Raw Materials*, ed. F. W. Lichtenthaler, VCH Publ., Weinheim/New York, 1991, p. 78 ff; M. J. Antal Jr, W. S. L. Mok and G. N. Richards, *Carbohydr. Res.*, 1990, **199**, 91; L. Cottier and G. Descotes, *Trends Heterocyclic Chem.*, 1991, **2**, 233.
7 (*a*) F. W. Lichtenthaler, D. Martin, T. Weber and H. Schiweck, *Liebigs Ann.Chem.*, 1993, 967; (*b*) Ger. *Offen.*, 3.936.522, 1989; *Chem. Abstr.*, 1991, **115**, P 92826 t; (*c*) M. Kunz, in *Ullmann's Encyclopedia Industrial Chemistry*, VCH Publ., Weinheim/New York, 5th edn., 1994, **A25**, pp.426-429.
8 C. Müller, V. Diehl and F. W. Lichtenthaler, *Tetrahedron*, 1998, **54**, 10703.
9 (*a*) V. Diehl, E. Cuny and F. W. Lichtenthaler, *Heterocycles*, 1998, **48**, 1193; (*b*) N. Oikawa, C. Müller, M. Kunz and F. W. Lichtenthaler, *Carbohydr. Res.*, 1998, **309**, 269.

10 G. Piancatelli, M. D'Auria and F. D'Onofrio, *Synthesis*, 1994, 867.
11 G. Piancatelli, A. Scettri and M. D'Auria, *Tetrahedron*, 1980, **36**, 661.
12 B. M. Adger, C. Barret, J. Brennan, M. A. McKervey and R. W. Murray, *J. Chem. Soc., Chem. Commun*., 1991, 1553.
13 P. D. Williams and E. LeGoff, *J. Org. Chem*., 1981, **46**, 4143; P. D. Williams and E. Le Goff, *Tetrahedron Lett*., 1985, **26**, 1867; S. P. Tannis, Y. H. Chuang and D. B. Head, *Tetrahedron Lett*., 1985, **26**, 6147.
14 J. H. Kuo, *J. Chin. Chem. Soc*., 1986, **33**, 95.
15 M-I. Chung and H. H. Szmant, *Macromolecules*, 1986, **19**, 25.
16 J. Jurczak and S. Pikul, *Tetrahedron Lett*., 1985, **26**, 3039.
17 K. Gollnick and A. Griesbeck, *Tetrahedron*, 1985, **41**, 2057 (*cis*-hex-3-ene-2,5-dione); A. Del Zotto, W. Baratta, G. Verardo and P. Rigo, *Eur. J. Org. Chem*., 2000, 2799 (*trans* isomer).
18 L. C. Blaszczak and J. E. McMurry, *J. Org. Chem*., 1974, **39**, 258.
19 A. P. Marchand and G. M. Reddy, *Synthesis*, 1991, 198.
20 R. A. Cherkasov, G. A. Kutyrev and A. N. Padovik, *Tetrahedron*, 1985, **41**, 2567.
21 J. W. Green, *Adv. Carbohydr. Chem*., 1960, **3**, 129; D. R. Williams, F. D. Klingler, E. E. Allen and F. W. Lichtenthaler, *Tetrahedron Lett*., 1988, **29**, 5087.
22 L. Cottier, G. Descotes, L. Eymard and K. Rapp, *Synthesis*, 1995, 303.
23 R. F. Hartman and S. D. Rose, *J. Org. Chem*., 1981, **46**, 4340.
24 M. Majdoub, A. Loupy, A. Petit and S. Roudesli, *Tetrahedron*, 1996, **52**, 617.
25 For products believed to be the *cis* (*Z*)-enedione **6**, melting points of 106–108 °C[14] and 91.5–92 °C[15] have been reported. Whilst the identity of the former product obtained by photooxidation of **3**,[14] remains obscure, the latter undoubtedly constitutes the *trans* (*E*)-isomer **10**, which the authors[15] had unknowingly acquired on bromination of **3** in KOAc-buffered aqueous methanol.
26 TLC ($CHCl_3$–MeOH, 5 : 1) and ^{1}H NMR inspection of the mp sample of **6** after resolidification showed it to be a mixture of *cis* (**6**, R_f 0.75, 2H-s for H-3/H-4 at 6.40) and *trans*-isomer (**10**, R_f 0.57, 2H-s for H-3/H-4 at 7.00), the latter obviously formed by isomerization during melting. By contrast, the *trans* (*E*)-isomer **10** (mp 91–92 °C) is stable on melting.
27 The 3-chloroperbenzoic acid (MCPBA) used for the oxidative furan ring opening **3** → **6**, **4** → **7**, **22** → **24**, **23** → **25** and **35** → **36** was strictly *anhydrous*, *i.e*. the commercially available MCPBA, containing aside 10 % of 3-chlorobenzoic acid 20–40% of water (Fluka, Merck) was freed from water by dissolution in CH_2Cl_2 (5 g in 100 mL of freshly distilled solvent to exclude the presence of small amounts of HCl), separating the aqueous layer, drying of the organic phase (Na_2SO_4), and removal of the solvent *in vacuo* (bath temp. below 35 °C) to yield a fluffy solid, directly to be used.
28 K. Y. Novitskii, N. K. Sadovaya and A. B. Baskina, *Khim. Geterotsikl. Soedin*., 1970, **2**, 57.

Behavior of the solvatochromic probes Reichardt's dye, pyrene, dansylamide, Nile Red and 1-pyrenecarbaldehyde within the room-temperature ionic liquid bmimPF$_6$

Kristin A. Fletcher, Isaiah A. Storey, Ashley E. Hendricks, Shubha Pandey and Siddharth Pandey*

Department of Chemistry, New Mexico Institute of Mining and Technology, Socorro, NM 87801, USA. E-mail: pandey@nmt.edu

Received 23rd April 2001
First published as an Advance Article on the web 30th August 2001

Recently discovered room-temperature ionic liquids (RTILs) show tremendous promise to replace volatile organic compounds (VOC). Investigation of these RTILs as solvents is in very early stages. Before the full potential of these RTILs are realized, much more information about them as solvent systems must be obtained. The dipolarity of one such RTIL, 1-butyl-3-methylimidazolium hexafluorophosphate (bmimPF$_6$) is investigated using both absorbance (Reichardt's betaine dye) and fluorescence (pyrene, dansylamide, Nile Red, and 1-pyrenecarbaldehyde) solvatochromic probes. Results indicate that, in the case of pyrene and 1-pyrenecarbaldehyde the bmimPF$_6$ microenvironment immediately surrounding the probe is similar to the microenvironment sensed in acetonitrile and dimethyl sulfoxide. Dansylamide in bmimPF$_6$ sensed a microenvironment similar to that in acetonitrile. However, calculated $E_T(30)$ values indicate the polarity of bmimPF$_6$ sensed by Reichardt's betaine dye to be similar to ethanol. Nile Red showed that the polarity of the solvent in the immediate vicinity of the probe is similar to neat water and 90 wt% glycerol in water (a solvent with viscosity similar to bmimPF$_6$). The microenvironment sensed by a probe is dependent upon several factors besides polarity such as viscosity, polarizability, the ability to form hydrogen-bonds, *etc*. In light of this, the apparent discrepancies in the polarity of bmimPF$_6$ indicated in this study do not seem so vast.

Introduction

One of the biggest problems posed to the chemical industry is to continuously deal with the fact that all chemical plants rely heavily on toxic, hazardous, and flammable organic solvents. Organic solvents used in most of the synthesis processes in chemical industries evaporate into the atmosphere with detrimental effects on the environment as well as human health. Most of the time, these volatile organic solvents are expensive to purchase, problematic to separate and remove from the desired products, difficult to recycle or reuse, and impractical to dispose of without incurring substantial costs and/or adversely affecting the environment and/or personnel.[1]

Newly rediscovered (in their modified forms) room-temperature ionic liquids (RTILs), with no measurable vapor pressure, can be used as replacements for select organic solvents. RTILs are organic salts composed of anions and cations that are in liquid state at ambient conditions. The new-generation RTILs have potential to act as environmentally benign solvent media for many industrially important chemical processes.[2] Recently, these novel RTILs have shown promise toward important applications such as synthesis,[3] catalysis,[4] polymerization,[5] separation, and extraction processes.[6] However, the basic science involved with fully characterizing these RTILs is still in its infancy, and this may be holding back the complete and most efficient utilization of these green solvents. Before the full potential of RTILs as solvent systems can be explored much more information about their physicochemical properties needs to be gathered. Toward this end, we believe that the effective employment of various solvatochromic probes can provide key information about these RTILs.

In this paper, we present results of our systematic approach to address the lack of physicochemical information about RTILs by exploring the behavior of well-established solvent polarity probes dissolved in a representative RTIL, 1-butyl-3-methylimidazolium hexafluorophosphate (bmimPF$_6$, Fig. 1). The solvatochromic probes used in the current investigation are Reichardt's betaine dye, pyrene, dansylamide, Nile Red and 1-pyrenecarbaldehyde. The molecular structures of all these solvatochromic probes are presented in Fig. 2. In order to compare the results obtained for each solvatochromic probe within bmimPF$_6$ the behavior of the probe in other judiciously selected solvents of varying physicochemical properties are also reported. The solvents investigated as benchmarks for comparison are as follows: cyclohexane and dichloromethane as nonpolar; acetonitrile as polar aprotic; ethanol, methanol and

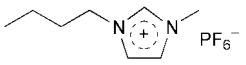

Fig. 1 Molecular structure of the RTIL bmimPF$_6$.

Green Context

Ionic liquids are promising alternative solvents which have the major advantage of being non-volatile, and capable of promoting a wide range of reactions. A greater understanding of their solvent properties is required to aid in their utilisation, and so far this aspect of these compounds has not yet been thoroughly investigated. In this paper, the behaviour of a series of solvatochromic probes has been studied, which contributes to the understanding of the properties of one of the ionic liquid solvents. ***DJM***

 DOI: 10.1039/b103592b

water as polar protic; dimethyl sulfoxide and ethylene glycol as polar and viscous, and finally, 90 wt% glycerol in water as a polar solvent with similar viscosity to that of bmimPF$_6$. Very recently, the viscosity of bmimPF$_6$ is reported to be 330 mNsm^{-2} at 20 °C.[7] To take into consideration the vast differences in the viscosity values of most of the polar solvents.[8] and bmimPF$_6$,[7] we used 90 wt% glycerol in water solution to compare our bmimPF$_6$ results. Using the viscosity values for different wt% glycerol in water solutions at 20 °C reported in the literature,[8] we adopted a simplistic interpolation approach to obtain a viscosity value in the range 320–340 mNsm^{-2} for 90 wt% glycerol in water solution at 20 °C. Selected physicochemical properties of the aforementioned solvents such as density (ρ), static dielectric constant (ε), refractive index (n), dipole moment (D), and viscosity (η) are tabulated in Table 1.[8]

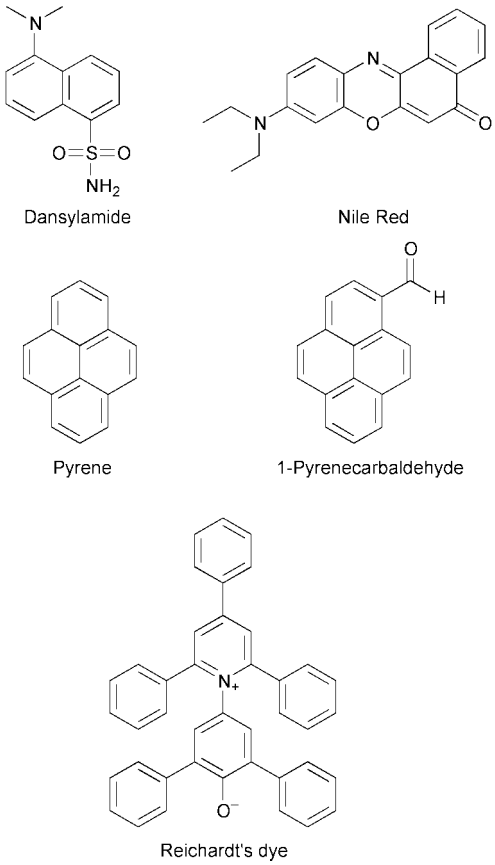

Fig. 2 Molecular structures of the solvatochromic probes used in the present studies.

Results and discussion

Reichardt's Betaine dye

One of the most widely used empirical scales of solvent polarities is the $E_T(30)$ scale based on following expression:

$$E_T(30)(\text{kcal mol}^{-1}) = \frac{28591}{\lambda_{max}^{abs}(\text{nm})} \quad (1)$$

λ_{max}^{abs} is the wavelength of the maximum of the longest wavelength, intramolecular charge-transfer π–π* absorption band of the zwitterionic 2,6-diphenyl-4-(2,4,6-triphenyl-*N*-pyridino)phenolate molecule.[9] This zwitterionic compound, also known as Reichardt's betaine dye (see Fig. 2), exhibits one of the largest observed solvatochromic effects of any known organic molecule. Charge-transfer absorption wavelength shifts amount to several hundred nanometers in going from a polar solvent ($\lambda_{max}^{abs} \approx 453$ nm in water) to a nonpolar solvent ($\lambda_{max}^{abs} \approx 925$ nm in hexane).

While Fig. 3 shows the longest wavelength intramolecular charge-transfer π–π* absorption band of Reichardt's dye in bmimPF$_6$ and selected solvents at ambient conditions, Table 2 tabulates the λ_{max}^{abs} values and calculated $E_T(30)$ polarity values [using eqn. (1)] for 100 μM solutions of Reichardt's dye in all solvents at ambient conditions. A careful examination of the entries in Table 2 reveals that the $E_T(30)$ polarity value obtained for bmimPF$_6$ is similar to that obtained for ethanol. The $E_T(30)$ polarity scale clearly indicates that the microenvironment encountered by Reichardt's dye within bmimPF$_6$ is less polar than that observed for methanol, ethylene glycol, 90 wt% glycerol in water, and neat water; and more polar than acetonitrile, dimethyl sulfoxide, and dichloromethane. Next, we investigated the concentration effects of Reichardt's dye on the $E_T(30)$ polarity scale when dissolved in bmimPF$_6$. The concentration of Reichardt's dye was varied between 50 and 500 μM. The positions of the longest wavelength intramolecular charge-transfer π–π* absorption band were within ±1 nm of each other in the concentration range studied and Beer's law was also obeyed within this concentration range (absorbance *vs.* Reichardt's dye concentration plot was linear with $r^2 = 0.998$, results not shown). This suggests the lack of any aggregation or interaction among Reichardt's dye molecules at concentration ≤500 μM when solubilized in bmimPF$_6$ at ambient conditions.

It is important to mention here that during the preparation of this manuscript, Brennecke and coworkers[10] have reported on the polarity of bmimPF$_6$ utilizing a small and neutral fluorescence probe, 4-(*N*,*N*-dimethylamino)phthalimide (DAP). They correlated the λ_{max}^{fluor} of DAP to the $E_T(30)$ polarity scale and obtained a value of 52.39 kcal mol^{-1} for bmimPF$_6$ at room temperature which is in good agreement with our $E_T(30)$ value

Table 1 Density (ρ), refractive index (n), viscosity (η), static dielectric constant (ε) and dipole moment (D) of the solvents (from ref. 8 unless otherwise stated) investigated in the present studies at ambient conditions (20 °C unless otherwise noted in parentheses)

Solvent	ρ/g ml^{-1}	n	η/mN s m^{-2}t	ε	D
Cyclohexane	0.7786	1.4262	0.980	2.02 (25)	0
Dichloromethane	1.3265	1.4246	0.393 (30)	9.14	1.60
Ethanol	0.7894	1.3611	1.074 (25)	25.3	1.69
Methanol	0.7913	1.3284	0.544 (25)	33.0	1.70
Acetonitrile	0.7875	1.3460	0.329 (30)	36.64	3.924
Dimethyl sulfoxide	1.1014	1.4170	2.4	47.24	3.96
Ethylene glycol	1.113	1.4310	13.35 (30)	41.4	2.28
Water	0.99823	1.3330	1.002	80.20	1.85
90 wt% Glycerol in water	1.2613[a]	1.4746[a]	320–340	46.5[a]	2.68[a]
bmimPF$_6$	1.37 (30)[b]	NA[c]	330[d] 312 (30)[b]	NA	NA

[a] Values are for neat glycerol. [b] From ref. 20. [c] NA = not available. [d] From ref. 7.

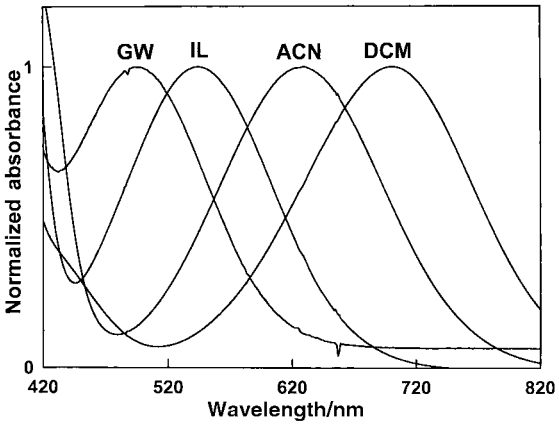

Fig. 3 Longest wavelength intramolecular charge-transfer π π* absorption band of Reichardt's betaine dye in 90 wt% glycerol in water (GW), $bmimPF_6$ (IL), acetonitrile (ACN) and dichloromethane (DCM) under ambient conditions.

Table 2 Intramolecular charge-transfer absorption maxima (λ_{max}^{abs}) and corresponding $E_T(30)$ solvent polarity value for Reichardt's betaine dye dissolved in $bmimPF_6$ and other solvents under ambient conditions

Solvent	λ_{max}^{abs}/nm[a]	$E_T(30)$/kcal mol^{-1}[b]
Dichloromethane	700	40.8
Ethanol	546	52.4
Methano	515	55.1
Acetonitrile	630	45.4
Dimethyl sulfoxide	630	45.4
Ethylene glycol	508	56.3
Water	45	63.1
90 wt% glycerol in water	494	57.9
$bmimPF_6$	545	52.5

[a] Standard deviations associated with λ_{max}^{abs} values are ±2 nm. [b] Calculated from eqn. (1).

of 52.5 kcal mol-1 for $bmimPF_6$ obtained using Reichardt's betaine dye.

Pyrene

While Reichardt's dye is the most common negative solvatochromic charge-transfer absorption probe used to measure the polarity of homogeneous media, neutral fluorescence probe molecules may be preferred when the large size and the charge on the Reichardt's dye pose problems. Another significant advantage of using fluorescent probes is that the concentration of the probe used can be much lower than that required for an absorption probe. This minimizes the possibility of any probe–probe interaction(s) that may occur during absorption probe studies.

Pyrene is one of the most widely used neutral fluorescence probes.[11] Pyrene is constituted of four fused benzene rings and contains no functional group otherwise (Fig. 2). The pyrene solvent polarity scale is defined as I_I/I_{III} emission intensity ratio, where band I corresponds to a $S_1(v = 0) \rightarrow S_0(v = 0)$ transition and band III is a $S_1(v = 0) \rightarrow S_0(v = 1)$ transition. The I_I/I_{III} emission intensity ratio increases with increasing solvent polarity. Karpovich and Blanchard rationalized pyrene's solvatochromic behavior in terms of vibronic coupling between the weakly allowed pyrene first electronically allowed singlet state and the strongly allowed second electronic singlet state.[12] For a detailed description of the origin of the pyrene polarity scale, readers are referred to ref. 12. It is important to mention here that after a detailed investigation, Street, Jr. and Acree, Jr. have reported on the numerous problems associated with the correct determination of the I_I/I_{III} emission intensity ratio.[13] Among the problems listed by the authors are slit width effects, inner-filtering artifacts, excitation wavelengths, and temperature control.

Table 3 presents measured pyrene I_I/I_{III} emission intensity ratios for $bmimPF_6$ and several other solvents at ambient conditions. Fig. 4 shows the pyrene emission spectra in selected solvents; cyclohexane, ethanol, $bmimPF_6$ and neat water. The excitation wavelength was 337 nm in each case and excitation and emission slit widths were fixed at 2 and 1 nm, respectively, for all pyrene solutions as well as appropriate solvent blanks. The concentration of pyrene was ~10 μM in all the solutions.

A careful examination of Table 3 reveals that, contrary to the results obtained during the probe studies with Reichardt's betaine dye, the pyrene I_I/I_{III} value measured in $bmimPF_6$ clearly indicates a completely different microenvironment sensed by excited-state pyrene. The pyrene I_I/I_{III} value in $bmimPF_6$ is significantly higher than those measured in ethanol and dichloromethane. More surprising is the fact that the pyrene I_I/I_{III} value in $bmimPF_6$ is higher than those observed in even methanol, ethylene glycol, and 90 wt% glycerol in water. The only solvents with higher pyrene I_I/I_{III} values than that observed in $bmimPF_6$ are acetonitrile, dimethyl sulfoxide, and neat water, and among these three solvents only neat water shows a significant difference in the measured pyrene I_I/I_{III} values (1.96 for water *vs.* 1.84 for $bmimPF_6$). It is important to mention at

Table 3 Emission band I to III intensity ratio for pyrene (I_I/I_{III}), λ_{max}^{fluor} and Stokes' shift for dansylamide dissolved in $bmimPF_6$ and other solvents under ambient conditions

Solvent	Pyrene I_I/I_{III}[a]	λ_{max}^{fluor}/nm[b]	Stokes' shift/ cm^{-1}[c]
Cyclohexane	0.64 ± 0.01	453.2 ± 0.8	7 106
Dichloromethane	1.45 ± 0.01	507.5 ± 1.3	8 786
Ethanol	1.37 ± 0.01	522.5 ± 1.0	10 247
Methanol	1.50 ± 0.01	525.5 ± 1.0	10 313
Acetonitrile	1.88 ± 0.01	522.3 ± 2.1	9 881
Dimethyl sulfoxide	1.90 ± 0.01	517.3 ± 0.8	9 571
Ethylene glycol	1.55 ± 0.02	534.3 ± 1.0	10 337
Water	1.96 ± 0.05	573.0 ± 0.5	12 668
90 wt% glycerol in water	1.66 ± 0.02	556.2 ± 2.6	11 450
$bmimPF_6$	1.84 ± 0.02	533.5 ± 0.9	9 885

[a] All solutions were ~10 μM in pyrene, except for water (pyrene concentration in water was ~ 0.1 μM). Each sample was excited at 337 nm with excitation and emission slit widths of 2 and 1 nm, respectively. [b] All samples were ~10 μM in dansylamide and excited at 351 nm. [c] Dansylamide Stokes' shifts are calculated using excitation and emission maxima for each sample.

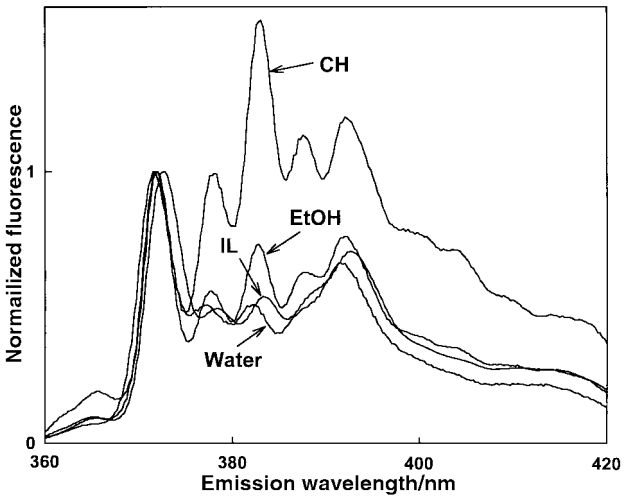

Fig. 4 Normalized fluorescence spectra of pyrene in cyclohexane (CH), ethanol (EtOH), $bmimPF_6$ (IL) and water under ambient conditions.

this point that a comparison of the pyrene I_I/I_{III} values measured in the present studies to the values obtained by Dong and Winnik shows some discrepancies.[11] As mentioned earlier, the pyrene I_I/I_{III} values depend on several experimental variables such as excitation wavelength, excitation/emission slit widths, self-absorption due to pyrene concentration effects, efficiencies associated with double-pass *vs.* single-pass cell compartment designs, procedures involved with data acquisition and manipulation, solvent and pyrene purity, and finally, the temperature of the pyrene solution.[13] In order to minimize the inconsistencies arising from one or more of the aforementioned reasons, we measured pyrene I_I/I_{III} values in all the solvents under more or less similar experimental conditions. All the data were acquired on the same instrument and pyrene concentration, temperature, excitation wavelength, excitation/emission slit widths, and data acquisition and manipulation strategy were identical for each pyrene solution investigated.

Dansylamide

Derivatives of the 5-amino-1-naphthalenesulfonates, particularly the dansyl (5-*N*,*N*-dimethylamino-1-naphthalenesulfonate) group, are used extensively as fluorescence probes of the structures and dynamics of biological macromolecules.[14] These molecules have emission properties which are strongly dependent upon the nature of their environment; in particular, they exhibit a large bathochromic shift on going from a nonpolar to a polar environment. Further, the Stokes' shift ($|\nu^{abs}_{max}$ (cm^{-1}) − ν^{flu}_{max} (cm^{-1})|) of the dansyl group dissolved in a variety of solvents correlates well with the dipolarity of the medium.[14]

Fig. 5 presents dansylamide (5-*N*,*N*-dimethylamino-1-naphthalenesulfonamide) emission spectra in cyclohexane, dichloromethane, ethanol, bmimPF$_6$, 90 wt% glycerol in water, and neat water. Table 3 tabulates measured emission maxima (λ^{fluor}_{max} nm) and Stokes' shifts (in cm^{-1}) for dansylamide dissolved in all the solvents used in the present studies under ambient conditions. A careful examination of the entries in Table 3 reveals that the λ^{fluor}_{max} value for dansylamide within bmimPF$_6$ is higher than those observed for dichloromethane, dimethyl sulfoxide, acetonitrile, ethanol and methanol. Among the solvents investigated, only 90 wt% glycerol in water and neat water show the lowest energy emission maxima positioned at significantly higher wavelengths compared to that observed in bmimPF$_6$. The measured dansylamide λ^{flu}_{max} value within bmimPF$_6$ is similar to that observed in ethylene glycol suggesting a similar microenvironment sensed by dansylamide when dissolved in these two solvents. The dansylamide Stokes' shift observed in bmimPF$_6$, however, is similar to that measured in acetonitrile, lower than the Stokes' shifts observed in ethanol, methanol, and ethylene glycol, and is significantly lower than that in 90 wt% glycerol in water, and neat water. The solvents showing lower dansylamide Stokes' shifts than bmimPF$_6$, are dichloromethane and dimethyl sulfoxide.

Behavior of a solute molecule within its cybotactic region can depend on variety of interactions, *e.g.*, H-bonding, van der Waals forces, dipole–dipole interactions, *etc*. While the dansylamide λ^{fluor}_{max} values depict interaction of excited-state fluorophore with its milieu, measured Stokes' shifts have a complex dependence on different physicochemical properties of the cybotactic region that effects both ground and excited states of the solute.[14] Consequently, the properties of solubilizing media, such as static dielectric constant, refractive index, dipole moment, and viscosity, can have very different effects on λ^{fluor}_{max} and the Stokes' shift. Further, the effect of the specific solvent–solute interactions, most notably H-bonding, on Stokes' shift is shown to be extremely prominent and renders any generalized correlation of either λ^{fluor}_{max} or Stokes' shift meaningless. More specifically, solvent relaxation is manifested through Stokes' shift and, on this basis,[14] a similarity is observed between bmimPF$_6$ and acetonitrile according to our measurements.

Nile Red

Nile Red is a positive solvatochromic dye and shows one of the largest shifts in excitation and emission maxima in going from nonpolar solvents (λ^{ex}_{max} ~ 484 nm, λ^{fluor}_{max} ~ 529 nm) to polar solvents (in water, λ^{ex}_{max} ~ 591 nm, λ^{fluor}_{max} ~ 657 nm). All three of the absorption, excitation, and emission maxima shift to lower energies when the polarity of the medium surrounding Nile Red is increased. Nile Red has been extensively used in many different applications where the dipolarity of the medium needs to be explored. Because of its photochemical stability and strong fluorescence nature, Nile Red has been utilized extensively.[15]

In Table 4 we report λ^{ex}_{max} and λ^{fluor}_{max} values for Nile Red dissolved in bmimPF$_6$ as well as nine other solvents. Fig. 6 shows the emission and excitation spectra of Nile Red in dichloromethane, ethanol, ethylene glycol, and bmimPF$_6$. As mentioned earlier, fluorescence-based probe methods may have advantages over those of absorption-based due to the better sensitivity of the former. This extremely high sensitivity allows studies to be conducted at very low probe concentrations and thus the examination of the host environment in a nearly unperturbed state. A careful look into the entries of Table 4 reveals that both λ^{ex}_{max} and λ^{fluor}_{max} values obtained for Nile Red within bmimPF$_6$ are significantly higher than those obtained for dichloromethane, acetonitrile, ethanol, methanol, dimethyl sulfoxide, and ethylene glycol. Only neat water and 90 wt%

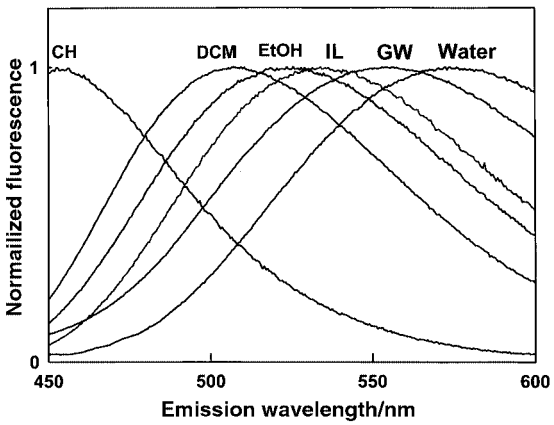

Fig. 5 Normalized fluorescence spectra of dansylamide in cyclohexane (CH), dichloromethane (DCM), ethanol (EtOH), bmimPF$_6$ (IL), 90 wt% glycerol in water (GW), and water under ambient conditions.

Table 4 Excitation and emission maxima of Nile Red (NR λ^{ex}_{max} and NR λ^{fluor}_{max})^{a,b} and the lowest energy emission maxima of 1-pyrenecarbaldehyde (PyCHO λ^{fluor}_{max})^{a,c} dissolved in bmimPF$_6$ and other solvents under ambient conditions

Solvent	NR λ^{ex}_{max}/nm	NR λ^{fluor}_{max}/nm	PyCHO λ^{fluor}_{max}/nm
Cyclohexane	469.0 ± 0.3	570.8 ± 1.6	Highly structured
Dichloromethane	523.4 ± 1.5	606.5 ± 1.3	416 ± 1
Ethanol	539.8 ± 4.7	640.3 ± 0.4	449 ± 1
Methanol	542.9 ± 0.9	641.3 ± 0.9	453 ± 1
Acetonitrile	520.7 ± 1.8	620.0 ± 0.3	416 ± 1
Dimethyl sulfoxide	544.8 ± 0.8	640.0 ± 0.2	418 ± 2
Ethylene glycol	557.3 ± 1.2	655.6 ± 0.4	460 ± 2
Water	584.5 ± 3.0	666.1 ± 3.7	475 ± 2
90 wt% glycerol in water	578.9 ± 2.8	664.9 ± 4.0	466 ± 2
bmimPF$_6$	580.2 ± 6.8	667.0 ± 1.5	428 ± 2

[a] Nile Red and 1-pyrenecarbaldehyde solutions were ~ 10 μM. [b] Nile Red excitation and emission wavelengths were judiciously selected for each solution. [c] 1-Pyrenecarbaldehyde samples were excited at 365 nm.

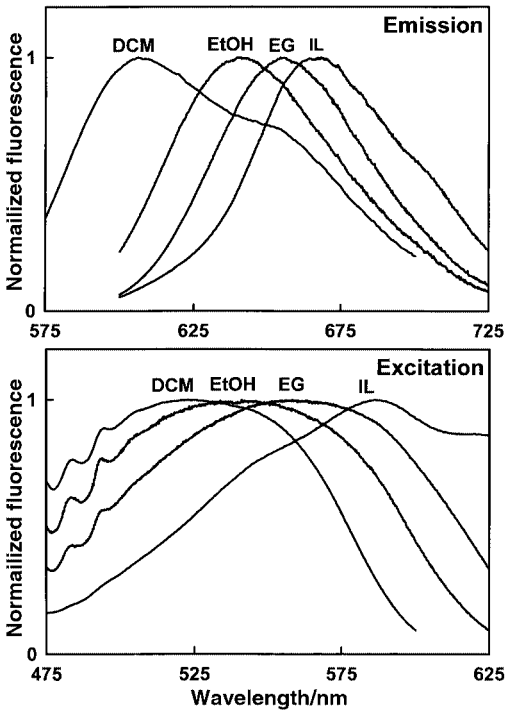

Fig. 6 Normalized fluorescence emission (top panel) and excitation (bottom panel) spectra of Nile Red in dichloromethane (DCM), ethanol (EtOH), ethylene glycol (EG) and bmimPF$_6$ (IL) under ambient conditions.

glycerol in water show λ_{max}^{ex} and λ_{max}^{fluor} values similar to that for bmimPF$_6$. These results suggest that Nile Red experiences a microenvironment within bmimPF$_6$ which is similar to fairly polar solvents such as water and 90 wt% glycerol in water.

Recently, Carmichael and Seddon reported a study of the absorption behavior of Nile Red dissolved in a variety of 1-alkyl-3-methylimidazolium-based RTILs.[16] The λ_{max}^{abs} values obtained for Nile Red in these RTILs were found to be similar to those obtained in short chain alcohols; more specifically, the polarity encountered by Nile Red within bmimPF$_6$ was similar to the polarity in butan-1-ol. Our results are in contrast with observations reported by Carmichael and Seddon based on the absorbance behavior of Nile Red.[16] Our Nile Red λ_{max}^{ex} and λ_{max}^{fluor} values within bmimPF$_6$ and ethanol are significantly different from each other (λ_{max}^{ex} ~ 540 nm for ethanol *vs.* ~580 nm for bmimPF$_6$, and λ_{max}^{fluor} ~ 640 nm for ethanol *vs.* ~667 nm for bmimPF$_6$). It is important to mention at this point that our λ_{max}^{ex} values in solvents other than bmimPF$_6$ vary in a similar fashion as λ_{max}^{abs} values obtained by Carmichael and Seddon within the same solvents. Our λ_{max}^{ex} values, however, are 5–12 nm lower than Carmichael and Seddon λ_{max}^{abs} values in those solvents. Tentatively, we assign these differences to the fact that our measurements are based on an emission-based technique as opposed to the absorbance-based. Furthermore, if we scale our λ_{max}^{ex} values to the Carmichael and Seddon λ_{max}^{abs} values, we obtain an even higher λ_{max}^{ex} value for bmimPF$_6$ suggesting a further increased dipolarity sensed by Nile Red when dissolved in bmimPF$_6$.

1-Pyrenecarbaldehyde

Bredereck *et al*. were the first to report on the solvent-dependent emission characteristics of 1-pyrenecarbaldehyde.[17] This aromatic aldehyde shows two types of closely-spaced excited states, (n,π*) and (π,π*). In nonpolar solvents, the fluorescence spectra of 1-pyrenecarbaldehyde are highly structured and fluorescence quantum yields are fairly low (< 0.001). This type of fluorescence behavior is attributed to be originating from an n-π* transition. However, as the polarity of the surrounding medium is increased, the π–π* energy level becomes lower in energy in comparison to n–π* level as result of solvent relaxation during the lifetime of the excited fluorophore. Thus in polar solvents the π–π* state becomes the fluorescence emitting state and is manifested through a broad, structureless, and moderately intense fluorescence behavior. It has been suggested that a static dielectric constant of ~10 is required to equalize the n-π* and π–π* energy levels. The fluorescence maxima of 1-pyrenecarbaldehyde is known to red-shift with increasing ε of the surrounding milieu for $\varepsilon > 10$.[18] For this reason, 1-pyrenecarbaldehyde has been used as a probe of solvent polarity in various isotropic and complex solubilizing media. Bônhote *et al*. reported the emission spectrum of 1-pyrenecarbaldehyde in 1-ethyl-3-methylimidazolium bis(trifluoromethyl)imide (emimTf$_2$N) at 20 °C.[19] During their investigation, the emission maximum of 1-pyrenecarbaldehyde within emimTf$_2$N appeared at 431 nm, suggesting a solvent environment of very low ε (*i.e*., below 10).

Table 4 tabulates the values of λ_{max}^{fluor} for 1-pyrenecarbaldehyde in bmimPF$_6$ and eight other solvents at ambient conditions. Fig. 7 presents the change in the fluorescence spectral character of 1-pyrenecarbaldehyde in going from nonpolar ($\varepsilon <$ 10; cyclohexane) to polar ($\varepsilon >$ 10; acetonitrile, ethanol, ethylene glycol, and neat water) solvents along with the fluorescence spectrum in bmimPF$_6$. It is clear from Fig. 7 as well as entries in Table 4 that 1-pyrenecarbaldehyde emission maxima in all polar-protic solvents investigated in the present studies, *e.g*., ethanol, methanol, ethylene glycol, 90 wt% glycerol in water, and neat water; are significantly red-shifted in comparison to the emission maximum observed in bmimPF$_6$. However, the two polar-aprotic solvents, acetonitrile and dimethyl sulfoxide, show λ_{max}^{fluor} that are *ca*. 10 nm blue-shifted from the λ_{max}^{fluor} observed within bmimPF$_6$ and considerably blue-shifted from the emission maxima of all polar-protic solvents.

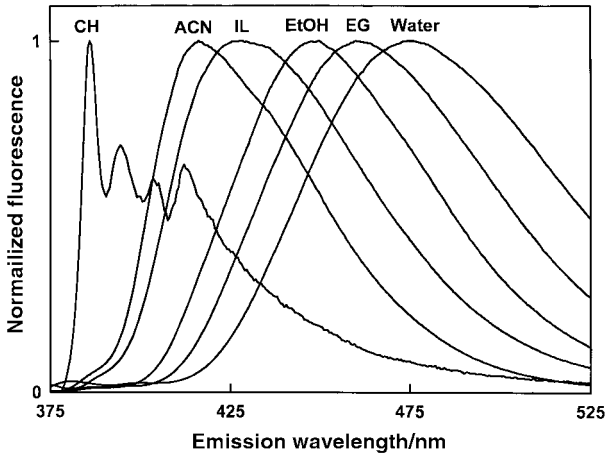

Fig. 7 Normalized fluorescence spectra of 1-pyrenecarbaldehyde in cyclohexane (CH), acetonitrile (ACN), bmimPF$_6$ (IL), ethanol (EtOH), ethylene glycol (EG) and water under ambient conditions.

Conclusions

Whereas defining polarity on an absolute scale is very difficult due to the fact that several different interactions may be involved, one may wish to determine the relative polarity of a particular solvent with respect to different types of functional groups representing possible solvent–solute interactions. In order to investigate the relative polarity of bmimPF$_6$ compared with several organic solvents, absorbance and fluorescence solvatochromic probes were used. Reichardt's betaine dye, a

common zwitterionic absorbance probe, revealed the dipolarity of $bmimPF_6$ in the immediate vicinity of the probe to be similar to that of ethanol. Pyrene, a neutral and small PAH fluorescence probe, showed that relative dipolarities of the microenvironment sensed were comparable in $bmimPF_6$, acetonitrile and dimethyl sulfoxide. Likewise, the Stokes' shift of dansylamide in $bmimPF_6$ was very similar to that in acetonitrile indicating a solvent relaxation behavior of $bmimPF_6$ similar to that of acetonitrile. In the case of Nile Red, the wavelengths of excitation and emission in $bmimPF_6$ were close to those of neat water and 90 wt% glycerol in water. 1-Pyrenecarbaldehyde indicated the polarity of $bmimPF_6$ most closely related to that of acetonitrile and dimethyl sulfoxide.

It would be premature at this time to unequivocally state that the dipolarity of $bmimPF_6$ is similar to acetonitrile or dimethyl sulfoxide under all circumstances, although the data collected in this study strongly suggest that dipolarity of $bmimPF_6$ is greater than or nearly equal to that of acetonitrile or dimethyl sulfoxide for the probes studied.

Experimental

Chemicals and reagents

Pyrene was obtained from AccuStandard, Inc. and was used as received. Dansylamide, 1-pyrenecarbaldehyde, Reichardt's dye, and Nile Red were obtained from Aldrich Chemical Co. and were used as received. Stock solutions of all probes were prepared by dissolving in ethanol in pre-cleaned amber glass vials and stored at ~4 °C. Ionic liquid $bmimPF_6$ was used as received from Covalent Associates, Inc. The following solvents were obtained from Fisher Scientific and used without further purification: acetonitrile (HPLC grade), ethanol (denatured), glycerol (99.99%, certified ACS), ethylene glycol (certified), methanol (99.9%, certified ACS), methylene chloride (99.9%, HPLC grade), dimethyl sulfoxide (99.9%, certified ACS), and cyclohexane (99.9%, certified ACS). Doubly-distilled deionized water was obtained from a Millipore, Milli-Q Academic water purification system.

Methods

Samples for spectroscopic studies were prepared as follows: appropriate aliquots of solvatochromic probe stock solutions were transferred into 1-cm^2 quartz cuvettes and evaporated under argon. Then 3 mL of the appropriate solvent were added to the cuvette, mixed thoroughly and allowed to equilibrate for sufficient time.

Steady-state emission experiments were performed with a PTI QuantaMaster Model C-60/2000 L-format scanning spectrofluorometer with a 75 W xenon arc lamp as the excitation source and single-grating monochromators as wavelength selection devices. All emission spectra were corrected for emission monochromator response and were background subtracted using appropriate blanks. All fluorescence data were measured in a 1 cm^2 quartz cuvette at 25 °C. Absorption spectra were recorded on a Agilent Hewlett-Packard 8453 Photo-Diode Array spectrophotometer in the usual manner with a 1 cm^2 quartz cuvette at 25 °C.

References

1 D. Noble, *Anal. Chem.*, 1993, **65**, 693A; J. Via and L. T. Taylor, *CHEMTECH*, 1993, November 1993, p. 38. A presidential directive published in the *Federal Register* (S8 FR: 65018; Dec. 10, 1993) implemented January 1, 1996.

2 L. A. Blanchard, D. Hancu, E. J. Beckman and J. F. Brennecke, *Nature*, 1999, **399**, 28; K. R. Seddon, *J. Chem. Tech. Biotechnol.*, 1997, **68**, 351; M. Freemantle, *Chem. Eng. News*, 2001, **79**, 21; M. Freemantle, *Chem. Eng. News*, 1998, **76**, 32; M. Freemantle, *Chem. Eng. News*, 2000, **78**, 37; M. Freemantle, *Chem. Eng. News*, 1998, **76**, 12; M. Freemantle, *Chem. Eng. News*, 1999, **77**, 23; M.Freemantle, *Chem. Eng. News*, 1999, **77**, 9; D. Adam, *Nature*, 2000, **407**, 938.

3 J. Howarth, *Tetrahedron Lett.*, 2000, **41**, 6627; T. Welton, *Chem. Rev.*, 1999, **99**, 2071; J. H. Davis, Jr. and K. J. Forrester, *Tetrahedron Lett.*, 1999, **40**, 1621; G. L. Rebeiro and B. M. Khadilkar, *Synth. Commun.*, 2000, **30**, 1605; T. Fischer, A. Sethi, T. Welton and J. Woolf, *Tetrahedron Lett.*, 1999, **40**, 793; T. Kitazume, F. Zulfiqar and G. Tanaka, *Green Chem.*, 2000, **2**, 133.

4 C. E. Song and E. J. Roh, *Chem. Commun.*, 2000, 837; A. J. Carmichael, M. J. Earle, J. D. Holbrey, P. B. McCormac and K. R. Seddon, *Org. Lett.*, 1999, **1**, 997.

5 A. J. Carmichael, D. M. Haddleton, S. A. F. Bon and K. R. Seddon, *Chem. Commun.*, 2000, 1237.

6 D. W. Armstrong, L. He and Y.-S. Liu, *Anal. Chem.*, 1999, **71**, 3873; J. G. Huddleston, H. D. Willauer, R. P. Swatloski, A. E. Visser and R. D. Rogers, *Chem. Commun.*, 1998, 1765; A. E. Visser, R. P. Swatloski and R. D. Rogers, *Green Chem.*, 2000, **2**, 1; S. Dai, Y. H. Ju and C. E. Barnes, *J. Chem. Soc. Dalton Trans.*, 1999, **8**, 1201; A. E. Visser, R. P. Swatloski, W. M. Reichert, S. T. Griffin and R. D. Rogers, *Ind. Eng. Chem. Res.*, 2000, **39**, 3596.

7 C. M. Gordon and A. J. McLean, *Chem. Commun.*, 2000, 1395.

8 J. A. Dean, in *Lange's Handbook of Chemistry*, 1McGraw-Hill, Inc., New York, 15th edn., 1999.

9 C. Reichardt, *Chem. Rev.*, 1994, **94**, 2319; C. Reichardt, *Angew. Chem.*, 1965, **77**, 30; C. Reichardt, *Chem. Soc. Rev.*, 1992, **21**, 147.

10 S. N. V. K. Aki, J. F. Brennecke and A. Samanta, *Chem. Commun.*, 2001, 413.

11 D. C. Dong and M. A. Winnik, *Can. J. Chem.*, 1984, **62**, 2560.

12 D. S. Karpovich and G. J. Blanchard, *J. Phys. Chem.*, 1995, **99**, 3951.

13 K. W. Street, Jr. and W. E. Acree, Jr., *Analyst*, 1986, **111**, 1197.

14 J. R. Lakowicz, in *Principles of Fluorescence Spectroscopy*, Kluwer Academic /Plenum Press, New York, 2nd edn., 1999, ch. 6.

15 .J. F. Deye, T. A. Berger and A. G. Anderson, *Anal. Chem.*, 1990, **62**, 615.

16 A. J. Carmichael and K. R. Seddon, *J. Phys. Org. Chem.*, 2000, **13**, 591.

17 K. Bredereck, Th. Forster and H. G. Oenstein, in *Luminescence of Inorganic and Organic Materials*, ed. H. P. Kallman and G. M. Spruch, Wiley, New York, NY, 1960.

18 K. Kalyanasundaram and J. K. Thomas, *J. Phys. Chem.*, 1977, **81**, 2176.

19 P. Bonhôte, A.-P. Dias, N. Papageorgiou, K. Kalyanasundaram and M. Grätzel, *Inorg. Chem.*, 1996, **35**, 1168.

20 P. A. Z. Suarez, S. Einloft, J. E. L. Dullius, R. F. de Souza and J. Dupont, *J. Chim. Phys. Phys.-Chim. Biol.*, 1998, **95**, 1626; R. Hagiwara and Y. Ito, *J. Fluorine Chem.*, 2000, **105**, 221.

Flow analysis strategies to greener analytical chemistry. An overview

Fábio R. P. Rocha,* Joaquim A. Nóbrega and Orlando Fatibello Filho

Departamento de Química, Centro de Ciências Exatas e de Tecnologia, Universidade Federal de São Carlos, Rodovia Washington Luíz, km 235, P.O. Box 676, 13560-970, São Carlos, SP, Brazil. E-mail: frprocha@cena.usp.br

Received 10th April 2001
First published as an Advance Article on the web 5th September 2001

An overview of the strategies adopted in flow analysis towards cleaner analytical methods is presented. The discussion deals with reagentless procedures, replacement of hazardous chemicals, strategies for waste minimization as well as on-line waste treatment or recycling. The potential of flow approaches such as sequential injection, multicommutation and monosegmented flow is emphasized. Automation, employment of solid-phase reagents and miniaturization are highlighted as alternatives for waste minimization.

Introduction

The growth of environmental responsibility has been inevitable, and the standards towards a well-defined and operated environmental management system are clearly set in the ISO 14000. These standards are gradually regulating interactions among countries and companies, and inevitably will also have a decisive influence on chemists' work. Efforts have been carried out in order to reduce or eliminate the undesirable component of chemical activities: the production of toxic wastes. This has resulted in the development of greener, yet efficient, procedures on the bench or industrial scale.

Nowadays, analytical methods are well established for environmental monitoring. However, a paradoxical situation has emerged because most of the analytical methodologies employed to investigate environmental problems generate chemical wastes, resulting in an environmental impact.[1] In some circumstances, the chemicals employed are even more toxic than the species being monitored. As a consequence, the work of some analytical chemists has been focused on the development of methodologies less harmful to humans and to the environment. Nowadays, in the development of a new analytical procedure, the amount and toxicity of the wastes are as important as any other analytical feature.

Flow analysis encompasses a widespread group of analytical techniques that are extensively employed in routine and research labs. The development of these flow-based techniques has brought a new dimension to analytical chemistry, allowing the measurements to be carried out faster and with minimum intervention of the analyst. Although there are many reliable flow procedures for routine analysis, most of them cannot be considered environmentally friendly, because they produce chemical wastes that can be toxic and need to be suitably managed. Despite this, the potentiality to develop greener analytical procedures is inherent to automated flow-based methodologies. This can be exemplified by the capability to decrease the reagent consumption. Moreover, usual tasks in analytical labs, such as dilutions and implementation of the standard additions method, can be easily attained by gradient exploitation with minimum effluent generation.[2] Sample preparation can be carried out with minimum volumes of acid solutions and in-line monitoring can be implemented to avoid the need for sample preservation.

A priority order can be established for the development of cleaner analytical procedures: (i) chemical wastes should not be produced; (ii) wastes produced should not be toxic; (iii) the amount of wastes should be minimized; (iv) toxic wastes should be recycled and if possible reused and (v) the analytical procedure should include a suitable method for waste treatment and disposal. This work presents an overview about some strategies that can be adopted in flow analysis aiming at the establishment of greener procedures in accord with this priority order.

Reagentless procedures

An ideal green analytical procedure should be implemented without reagents or, in a more realistic approach, by employing only non-toxic chemicals. This holds in some flow methodologies that exploit analyte separation (such as chromatography or electrophoresis) combined with universal detectors (UV spectrophotometers or electrochemical sensors). Moreover, reversible chemical and biosensors can be seen as examples of environmentally friendly analytical approaches. On the other hand, most of the current analytical procedures in flow analysis are reagent based and there are only few examples of reagentless procedures. Of these, electrochemical sensors and spectrometric atomic detectors are the most significant. However, electrochemical procedures usually require previous pH and ionic strength adjustment, and many spectrometric atomic procedures involve the addition of a chemical modifier as well as the combustion of gases and generation of hazardous vapors. Fortunately, some of these experimental requirements can be implemented in a green way, by using non-toxic buffers and

Green Context

Green chemistry does not only apply to the production and use of chemicals, but also to areas such as analytical methodology. While this might be thought of as involving small amounts of materials, there is a definite need to apply the principles of green chemistry here too. This overview analyses some of the current trends in greening analytical chemistry. Advances in reagentless procedures, and the avoidance of toxic reagents are amongst the themes addressed. ***DJM***

 DOI: 10.1039/b103187m

salts as well as reducing drastically the amount of toxic species, as in electrothermal atomic absorption spectrometric techniques.

Replacement of hazardous reagents

Nowadays, the toxicity of the chemicals must be taken into account in the development of new analytical procedures or implementation of existing ones. However, there are many analytically reliable procedures that are not environmentally benign. Many of them are recommended as standard or reference methods.[3,4] Considering the efforts of analytical chemists to develop the current assays, it is not realistic to hope that the replacement of all hazardous chemicals can be made within the near future.[5] However, this should be one of the main goals of the analytical chemists. Some successful examples are presented below.

The replacement of hazardous reagents can be exemplified by the flow-based methodologies for ammonium determination in waters. The procedures based on Nessler[6] or Berthelot (indophenol blue)[7] reactions resulted both in good results but also produced wastes containing high concentrations of mercury(II) or phenol, respectively. A greener procedure was developed by the employment of salicylic acid as the phenolic reagent in the indophenol blue method.[8] Salicylic acid is less reactive than phenol, but the substitution was possible without affecting the analytical performance. However, this procedure still employed a highly pollutant substance (sodium nitroprusside). Nowadays, the most environmentally benign flow-based procedure for ammonium exploits diffusion of gaseous ammonia through a polymeric (PTFE) membrane, followed by conductometric detection in the acceptor stream.[9] Sodium hydroxide is the only necessary reagent and in-line concentration can be exploited for sensitivity improvement. A totally clean method is achieved by on-line neutralization of the donor stream after measurements.

Another example of an efficient, but not environmentally acceptable, procedure is nitrate determination employing a cadmium reducing column and a diazo-coupling reaction.[10] Although the flow-based methodology presents better analytical performance and consumes less reagent in comparison with the batch procedure, the waste still contains Cd(II) and aromatic amine residues. A cleaner flow-based procedure was developed,[11] exploiting nitrate photoreduction and replacement of the diazo-coupling reagent. In the presence of an activator (EDTA), nitrate was in-line reduced in a PTFE tube coiled around a low-pressure 8 W irradiation mercury lamp. The nitrite produced reacted with triiodide ion and the excess of the reagent was biamperometrically detected with two platinum electrodes polarized at 100 mV. The nitrate reduction efficiency was estimated as 50%, which is lower than the mean efficiency achieved with copperized cadmium mini-columns.[10] However, the detection limit is suitable for water analysis.

Ingenious examples of the use of non-toxic reagents are the employment of plant tissues or extracts as enzymatic sources. In this sense, a mini-column containing jack-bean pieces was employed as a source of *urease* for urea determination in serum.[12] The ammonium ions originated from the enzymatic hydrolysis were detected by conductometry after gas diffusion of ammonia through a polymeric (PTFE) membrane. The same column could be used to perform up to 1000 determinations. A clean method for the determination of total phenols in wastewater exemplifies the employment of plant extracts.[13] Phenols were oxidized to *o*-quinones in the presence of dissolved oxygen and *polyphenol oxidase*.[13] A crude extract of sweet potato root prepared in phosphate buffer was employed as a clean enzymatic source, yielding results in agreement with those attained by the established method. The same plant extract has been employed in clean flow-based methodologies for determination of sulfite in wines[14] and L-dopa and carbidopa in pharmaceutical formulations.[15]

Procedures for waste minimization

The residues of analytical labs are usually formed by a mixture of small amounts of several substances. Thus, the replacement of a single reagent is not the most effective alternative to reduce the impact of the total waste on the environment.[5] Moreover, as previously discussed, changing reagents without affecting the analytical performance is not an easy task. Otherwise, general alternatives to minimize the reagent consumption are readily available. As stated in the priority order for establishing of cleaner analytical methods, if the use of toxic reagents cannot be avoided, the involved amounts should be minimized. This approach has also the advantage of reducing operational costs, including those spent on waste treatment and disposal. In this sense, flow-based methodologies combined with a conscientious use of reagents may produce positive results. A brief historical overview on the reagent consumption in flow analysis is presented next and different approaches to minimize the reagent consumption are stressed.

Flow injection analysis

In the first flow injection systems, denoted single-line manifolds [Fig. 1(a)], the reagent solution was employed also as a carrier stream.[2] Thus, the reagent consumption was inherently higher than that necessary to promote the chemical reaction and in some cases the consumption was even higher than in batch procedures. System design was improved by introducing the reagent solutions by confluence,[16] [Fig. 1(b)]. Adopting this strategy, the reagent flow rate could be reduced, without affecting its availability in the sample zone. In addition to the improvement of the analytical performance, this strategy enabled the reduction of the reagent consumed per determination. However, in both systems the solutions were continuously introduced and reagents were consumed even when a sample was not been processed. This drawback was overcome by the merging zones[17] and the intermittent reagent addition[18] approaches. The former consists in the simultaneous introduction of sample and reagent aliquots in independent carrier streams that transport them to a mixing point, in which the solutions merge and the chemical reactions start [Fig. 1(c)]. A discrete reagent aliquot is employed for each sample processed and waste of reagent is avoided. The potentiality of merging zones systems for minimizing reagent consumption was initially demonstrated by phosphate determination in plant digests using the molybdenum blue method.[17] The proposed manifold allowed a decrease of the consumption of the reducing solution

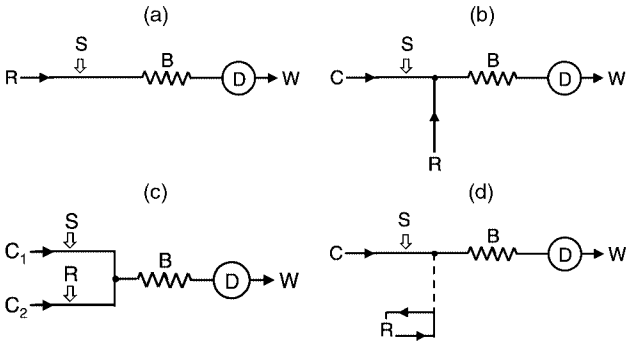

Fig. 1 Flow-injection manifolds: (a) single line; (b) confluent streams; (c) merging zones and (d) intermittent stream. R = reagent; C, C_1, C_2 = carrier streams; S = sample; B = reactor; D = detector; W = waste vessel. Arrows indicate the points of sample or reagent introduction and the flow direction.

to 90% compared with the confluent system. In the intermittent approach, the reagent solutions can be introduced in the analytical path simultaneously with the sample aliquot. During the sampling time, the reagents are recycled to their storing vessels [Fig. 1(d)]. With this strategy, the reagent consumption in spectrophotometric calcium determination was reduced from 40 (confluent system) to 0.27 μg.[19]

Another alternative to reduce the reagent consumption is the employment of systems with reagent injection, which are usually denoted reversed flow systems.[20] These procedures can be implemented by inserting the reagent in a sample carrier stream, with a set-up similar to that shown in Fig. 1(a) (the positions of sample and reagent solutions are inverted). This strategy is very atractive when the sample volume is not a limiting parameter and allows reducing the reagent volume to the μl range. When slow reactions are involved, stopped-flow procedures should be preferred. In these systems, after mixing the sample and reagents, the flow is interrupted by commutation or by stopping the peristaltic pump.[18] In this way, the residence time can be increased without affecting the sample dispersion and the reagent consumption. This strategy also allows performing of kinetic measurements by stopping the flow when the sample zone is inside the flow cell.

Flow systems with solid-phase reagents

In flow systems, solid-phase reagents present some advantages in comparison with reactions performed in homogeneous media. This includes simpler manifolds, improvement of the radial mass transference and possibly reaction with the highest concentration of the reagent.[21] This strategy has been exploited for both sample conversion and on-line reagent production.[21,22] Because only the necessary reagent amount is consumed, greener procedures are inherently achieved. Comprehensive reviews on the strategies for reagent immobilization and applications focusing on pharmaceutical[21] or inorganic analysis[22] have been presented. As an example, a mini-column containing PbO_2 immobilized on polyester was employed for determination of metamizol (dypirone).[23] The Pb(II) ions released by the oxidation of the drug were detected by flame atomic absorption spectrometry. More than 7000 determinations can be carried out with the same oxidizing column, which contains only a few mg of PbO_2. This example deals with the use of a toxic reagent in a more environmentally friendly strategy.

A variant of the use of immobilized reagents is solid-phase spectrophotometry, which is implemented by placing the solid support inside the flow cell, in order to perform the analyte retention and detection simultaneously. The main goal is to increase sensitivity, though selectivity improvement and even simultaneous measurements are also feasible. In some circumstances, it is possible to design the solid support to achieve reversible retention of the analyte, thus resulting in a substantial decrease in reagent consumption. This characteristic was exploited for Zn(II) determination in pharmaceutical preparations by means of its reaction with 1-(2-thiazolylazo)-2-naphthol immobilized on C_{18}-bonded silica.[24] Complete Zn(II) elution was achieved with 400 μl of a 0.5 mol l^{-1} HCl solution and more than 200 measurements were performed without affecting the analyte retention. This corresponds to reagent consumption lower than 1 μg per determination.

In addition to the reduced reagent consumption, the employment of solid-phase reagents also facilitates the storage of chemicals, reducing the risks of environmental accidents.

Monosegmented flow analysis

In monosegmented flow analysis, the sample aliquot is inserted in the carrier stream sandwiched by two air bubbles, generating a monosegment. The air bubbles in front and in the rear of the sample reduce axial sample dispersion.[25] Thus, desirable features of the segmented flow analysis (low sample dispersion) are matched with those of flow injection (*e.g.* simplicity, versatility and high sample throughput). In the original work,[25] the sample was mixed with the reagents by differential pumping before its introduction in the analytical path. As observed in confluent flow injection systems, reagent solutions were consumed even when a sample was not being processed. This drawback was overcome by employing opto-switches to detect the air bubbles in order to constrain the reagent addition to the monosegment.[26] This exemplifies the exploitation of feedback mechanisms to reduce the reagent consumption. An alternative procedure consisted in the introduction of small sample aliquots in tandem with reagent aliquots between the air bubbles.[27] Both strategies led to good analytical performance with minimum reagent consumption.

The employment of opto-switches in monosegmented flow systems was also exploited to reduce the total effluent volume in a manifold for nitrite determination.[28] The air bubbles limiting the monosegmented enabled the localization of the zones containing the reagents. A computer-controlled solenoid valve was used to manage the waste with feedback of the opto-switches. The zones containing reagents were directed to a photodegradation unit for on-line decomposition of the aromatic amines. The water carrier stream, separated from the toxic waste, was directly discarded.

Sequential injection analysis

Sequential injection analysis is a robust alternative to flow injection that allows implementation of different flow methodologies without modification of the manifold.[29] A selection valve is employed to manage all solutions. Aliquots of sample and reagents are aspirated towards a holding coil; then the pumping direction is inverted to increase the overlap between the sample and reagent and to direct the sample zone to the detector.[29] Because the mixing between sample and reagent occurs only by dispersion, the volumes cannot be increased at will, and usually only a few μl of each solution are employed. System operation can be designed to achieve an analytical performance comparable to that attained by usual flow injection systems. The capability to reduce the reagent consumption can be observed in Fig. 2.

Multicommutation-based flow systems

Multicommutation consists in the employment of discrete commutation devices (solenoid valves, for example) to build up dynamic manifolds that can be reconfigured by software.[30] This approach greatly increases the versatility of the flow systems because each analytical step can be independently implemented. Usually, one commutation device is employed to manage each solution and thus only the necessary reagent volume is introduced for sample processing.

The potential of the multicommutation approach to reduce reagent consumption was exemplified by the development of a greener procedure for determination of carbaryl pesticide.[31] The amount of the main reagent (*p*-aminophenol) consumed per determination was reduced from 0.14 mg in a confluent flow injection system to 5.0 μg with the multicommutation approach. A sequential injection system also allowed reduction of reagent consumption (11 μg per determination) but the sensitivity was 3-fold lower. Similar results were observed in a multicommutation-based flow system for sequential determination of anions in waters.[32] The consumption of the reagents was reduced from 3- to 40-fold and from 20- to 760-fold in

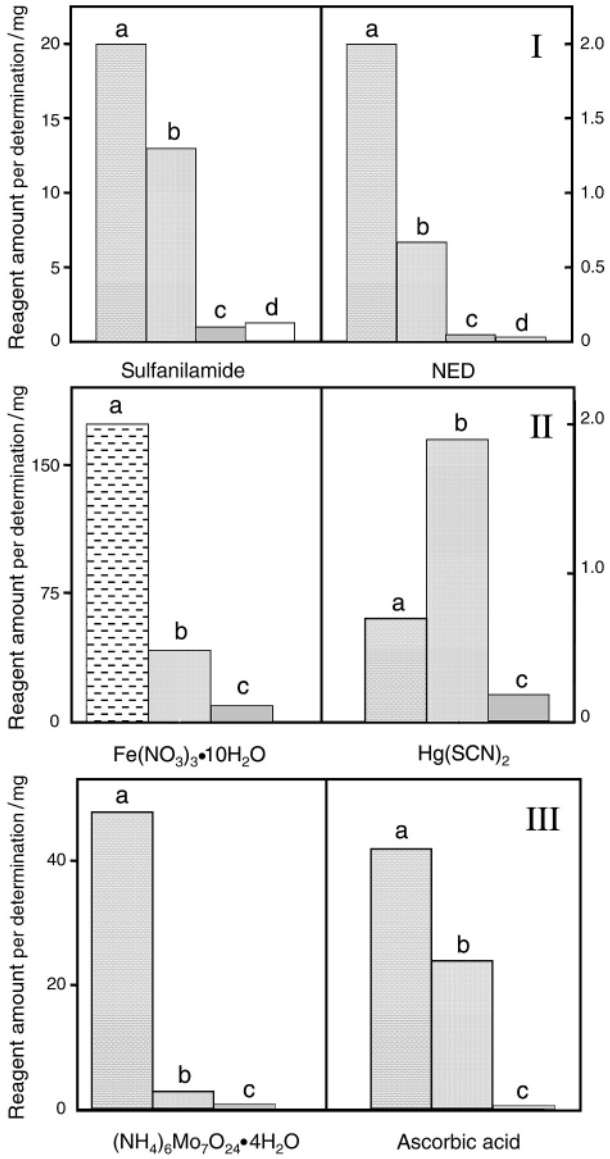

Fig. 2 Reagent consumption in spectrophotometric procedures for determination of (I) nitrate and nitrite, (II) chloride and (III) phosphate, employing (a) batch procedures; (b) flow systems with continuous reagent addition, (c) multicommutation-based flow systems and (d) sequential injection systems.[33]

comparison with confluent flow systems and batch procedures, respectively (Fig. 2).

System miniaturization

All current procedures could become more environmentally benign if the amounts of the reagents were considerably reduced. This task can be readily attained downscaling the manifold components and possibly arranging them in a single device.[33] This resulted in the application of the concept of micro total analytical systems (μTAS) to flow analysis. The central idea of μTAS is to arrange all the steps of sample processing in a single device of a few square centimeters.[33] In flow analysis, this aim can be reached with micro flow injection systems (μFIA), which exploit microelectronics techniques to integrate pumps, mixing and reaction chambers as well as detectors in a single chip.[34,35] With flow rates of some μl min^{-1}, the analytical performance of the usual flow systems can be maintained, consuming sample and reagents in the nanoliter range.[34,35]

The limitation of most μFIA system is the lack of versatility, because developed manifolds are not for general use. In order to circumvent this drawback, the so-called 'lab-on-valve' approach was proposed.[36] The reagent based assays were downscaled to the microliter level, by matching a microconduit system integrating injection ports, working channels and flow-through cell with conventional sized commercially available components, such as sequential injection systems, optical fibers, spectrophotometers and fluorometers. Sample and reagent addition, mixing, incubation and reversed and stopped flow regimes can be directly implemented. Thus, in principle, any flow based methodology with spectrophotometric or fluorometric detection can be carried out. Reagent volumes of about 10 μl and waste generation of 250 μl per determination were reported,[36] highlighting its potential to the development of greener methodologies.

Other ingenious examples of greener analytical procedures designed by downscaling system dimensions and reagent amounts are the employment of falling liquid drops for analytical measurements.[37,38] This approach exploits the reproducible formation of liquid drops at the end of tubes to carry out analytical operations on a fresh reaction surface for every sample. Because of the μl volumes involved and the low flow-rates (< 1 ml min^{-1}), the drop approach minimizes both sample and reagent consumption. This was demonstrated by the development of a procedure for solvent extraction.[38] The sodium dodecyl sulfate surfactant was determined by ion-pair formation with methylene blue, which was extracted in a $CHCl_3$ microdrop (1.3 μl). The analytical signal was directly measured in the drop surface by using a light-emitting diode and an optical fiber to transport the radiation to the detector. With the proposed arrangement, the detection limit was estimated as 50 μg l^{-1} with a coefficient of variation of 5%.

Wastes recycling and reuse

A very attractive alternative considering ecological and economic aspects is to recycle and reuse the waste produced during a chemical analysis. Generally, this is not practical because, as previously mentioned, the waste from an analytical lab is very diversified. However, solvent recycling can be easily implemented in procedures involving solvent extraction for separation or analyte concentration. Generally, phase separation and distillation are suitable to recover the solvents in order to reuse them. Because most of the organic solvents are toxic, this procedure is also environmentally benign.

On-line solvent recycling has been implemented in flow systems. Examples are the simultaneous determination of propyphenazone and caffeine[39] and of ketoptofen[40] in pharmaceuticals by Fourier transform infrared spectrometry. The analytical procedures involve the dissolution of the drugs in chlorinated solvents ($CHCl_3$ or CCl_4), which are transparent in the IR range. The same organic solvent needs to be used as carrier stream, resulting in a pollutant waste (*ca.* 1 ml min^{-1}). This drawback was circumvented by developing a closed flow system incorporating a distillation unit for on-line recycling of the organic solvent. After cooling the distillate, the solvent could be again employed, reducing the costs and side-effects on the environment. The closed flow system has also the advantage to minimize the risks of analyst exposure to carcinogen solvents.

In-line waste treatment

If the use of toxic substances cannot be avoided, clean analytical procedures can be developed by including a waste treatment procedure after analytical measurements. The incorporation of

an additional step for in-line waste treatment in a flow system can make this task less dangerous and tedious. Despite the potential of the flow systems to achieve this goal, only few examples have been presented. The general strategy is to introduce an additional reagent after the flow cell in order to destroy or passivate the toxic species in the effluent.

Detoxification of wastes can be achieved by photochemical, chemical, thermal or microbiological degradation processes.[41] Photochemical degradation has been the most common, because several dangerous organic compounds can be destroyed by photodegradation processes in time intervals compatible with the residence time in flow systems. Generally, the treatment is carried out in the presence of semiconductors such as CdS or TiO_2, which under UV irradiation can generate electron–hole pairs and catalyze the photo-assisted degradation.[41] In this sense, several flow-injection cleaner procedures have been developed by Spanish researchers, which include the detoxification of wastes generated by the determination of carbamate pesticides[41,42] and resorcinol.[43] These procedures involved the continuous introduction of a TiO_2 slurry after the flow cell. The mixture was transported towards a UV-irradiated coil to destroy both the unreacted species and the reaction products. The residence times in the treatment coil and the detoxification efficiency were carefully evaluated. The reported results indicate that complete mineralization of the organic compounds was readily achieved.[41–43] In principle, the procedures could be extended for detoxification of other organic aromatic residues. As the TiO_2 catalyst can be filtered and reused, the treatment step did not produce additional wastes.

Other efficient procedures for waste treatment, such as chemical or physical adsorption, precipitation and co-precipitation, ozonization, bacterial as well as thermal processes have potential to be accomplished in flow systems.[44] If high residence times are necessary, the waste of the flow system can be connected to a batch waste treatment unit.[28] The combined action of the minimization of the reagent consumption and in-line treatment is very attractive for developing greener analytical procedures.

Conclusions

Green analytical chemistry is in its initial stage of development but there is a clear trend towards fast and consistent growth. Analytical methods with high performance but which are not environmentally friendly tend to be unacceptable and this will stimulate the development of cleaner methods. The progress of flow methodologies has contributed to a greener analytical chemistry but there is a long road to go and the potentialities have not been fully exploited. This also holds in the context of education in chemistry. The replacement of old experimental practices by attractive procedures exploiting available instrumentation will result in the immediate reduction of wastes as well as develop an essential environmental conscience for the future.

Acknowledgements

We acknowledge the Brazilian agencies FAPESP (Process 00/04188-4) and CNPq for grants and financial support.

References

1 P. T. Anastas, *Crit. Rev. Anal. Chem.*, 1999, **29**, 167.
2 J. Ruzicka and E. H. Hansen, *Flow Injection Analysis*, Wiley, New York, 2nd edn., 1988.
3 A. D. Eaton, L. S. Clesceri and A. E. Greenberg, *Standard Methods for the Examination of Water and Wastewater*, American Public Health Association, Washington, 19th edn., 1995.
4 *Compilation of EPA's sampling and analysis methods*, ed. L. H. Lawrence, Lewis publishers, Boca Raton, FL, 2nd edn., 1996.
5 M. de la Guardia and J. Ruzicka, *Analyst*, 1995, **120**, 17N.
6 F. J. Krug, J. Ruzicka and E. H. Hansen, *Analyst*, 1979, **104**, 47.
7 F. J. Krug, B. F. Reis, M. F. Giné, J. R. Ferreira, A. O. Jacintho and E. A. G. Zagatto, *Anal. Chim. Acta*, 1983, **151**, 39.
8 J. A. Nóbrega, A. A. Mozetto, R. M. Alberici and J. L. Guimarães, *J. Braz. Chem. Soc.*, 1995, **6**, 327.
9 C. Pasquini and L. C. de Faria, *Anal. Chim. Acta*, 1987, **193**, 19.
10 M. F. Giné, H. Bergamin Filho, E. A. G. Zagatto and B. F. Reis, *Anal. Chim. Acta*, 1980, **114**, 191.
11 I. G. Torró, J. V. G. Mateo and J. M. Calatayud, *Anal. Chim. Acta*, 1998, **366**, 241.
12 L. C. Faria, C. Pasquini and G. Oliveira-Neto, *Analyst*, 1991, **116**, 357.
13 I. C. Vieira and O. Fatibello-Filho, *Anal. Chim. Acta*, 1998, **366**, 111.
14 O. Fatibello-Filho and I. C. Vieira, *Anal. Chim. Acta*, 1997, **354**, 51.
15 O. Fatibello-Filho and I. C. Vieira, *Analyst*, 1997, **122**, 345.
16 E. A. G. Zagatto, B. F. Reis, M. Martinelli, F. J. Krug, H. Bergamin Filho and M. F. Giné, *Anal. Chim. Acta*, 1987, **198**, 153.
17 H. Bergamin Filho, E. A. G. Zagatto, F. J. Krug and B. F. Reis, *Anal. Chim. Acta*, 1978, **101**, 17.
18 A. Ríos and M. Valcárcel, *Talanta*, 1991, **38**, 1359.
19 F. R. P. Rocha, P. B. Martelli, R. M. Frizzarin and B. F. Reis, *Anal. Chim. Acta*, 1998, **366**, 45.
20 K. S. Johnson and R. L. Petty, *Anal. Chem.*, 1982, **54**, 1185.
21 J. M. Calatayud and J. V. G. Mateo, *Trends Anal. Chem.*, 1993, **12**, 428.
22 J. M. Calatayud and J. V. G. Mateo, *Chem. Anal.*, 1993, **38**, 1.
23 L. L. Zamora and J. M. Calatayud, *Talanta*, 1993, **40**, 1067.
24 L. S. G. Teixeira, F. R. P. Rocha, M. Korn, B. F. Reis, S. L. C. Ferreira and A. C. S. Costa, *Anal. Chim. Acta*, 1999, **383**, 309.
25 C. Pasquini and W. A. Oliveira, *Anal. Chem.*, 1985, **57**, 2575.
26 I. M. Raimundo and C. Pasquini, *Analyst*, 1997, **122**, 1039.
27 M. Smiderle, B. F. Reis and F. R. P. Rocha, *Anal. Chim. Acta*, 1999, **386**, 129.
28 A. P. S. Paim, M. S. S. Pereira, M. F. Giné and B. F. Reis, Book of abstracts, *8th Conference on Flow Analysis*, Warsaw, 2000.
29 J. Ruzicka and G. D. Marshall, *Anal. Chim. Acta*, 1990, **237**, 329.
30 B. F. Reis, M. F. Giné, E. A. G. Zagatto, J. L. F. C. Lima, and R. A. Lapa, *Anal. Chim. Acta*, 1994, **293**, 129.
31 B. F. Reis, A. Morales-Rubio and M. de la Guardia, *Anal. Chim. Acta*, 1999, **392**, 265.
32 F. R. P. Rocha, P. B. Martelli and B. F. Reis, *Anal. Chim. Acta*, 2001, **438**, 11.
33 *Analytical Chemistry*, ed. J. M. Mermet, M. Otto and H. M. Widmer, Wiley, Weinheim, 1998, p. 857.
34 S. J. Haswell, *Analyst*, 1997, **122**, 1R.
35 G. N. Doku and S. J. Haswell, *Anal. Chim. Acta*, 1999, **382**, 1.
36 J. Ruzicka, *Analyst*, 2000, **125**, 1053.
37 H. Liu and P. K. Dasgupta, *Trends Anal. Chem.*, 1996, **15**, 468.
38 H. Liu and P. K. Dasgupta, *Anal. Chem.*, 1996, **68**, 1817.
39 Z. Bouhsain, S. Garrigues and M. de la Guardia, *Analyst*, 1997, **122**, 441.
40 M. J. Sánchez-Dasi, S. Garrigues, M. L. Cervera and M. de la Guardia, *Anal. Chim. Acta*, 1998, **361**, 253.
41 M. de la Guardia, K. D. Khalaf, V. Carbonell and A. Morales-Rubio, *Anal. Chim. Acta*, 1995, **308**, 462.
42 M. J. Escuriola, A. Morales-Rubio and M. de la Guardia, *Anal. Chim. Acta*, 1999, **390**, 147.
43 M. de la Guardia, K. D. Khalaf, B. A. Hasan, A. Morales-Rubio and V. Carbonell, *Analyst*, 1995, **120**, 231.
44 G. Lunn and E. B. Sansone, *Destruction of hazardous chemicals in the laboratory*, Wiley, New York, 2nd edn., 1994.

Laser bleaching of cellulosic fabrics by sodium borohydride aqueous solution; a total chlorine free process

Akihiko Ouchi,* Toru Obata, Hitoshi Sakai and Masako Sakuragi

National Institute of Advanced Industrial Science and Technology, Tsukuba, Ibaraki 305-8565, Japan. E-mail: ouchi.akihiko@aist.go.jp

Received 21st May 2001
First published as an Advance Article on the web 30th August 2001

Water-insoluble natural colored compounds adsorbed or chemically bound on cellulosic fabrics were bleached effectively by a selective photolysis of the colored compounds by a KrF excimer laser in the presence of $NaBH_4$ aqueous solutions.

Introduction

Bleaching of natural cellulosic fibers is one of the most important chemical processes in textile[1] and pulp[2] industries. In these processes, halogenated oxidizing agents, such as $NaClO_2$ and NaClO, are widely used in large quantities.[3] However, such halogenated oxidizing agents are reported to form harmful compounds, known as adsorbable organically bound halogens (AOX), in the bleaching processes.[4,5] Therefore, development of total chlorine free (TCF) processes is of an urgent importance to avoid the formation of AOX.

The bleaching process can be interpreted as decomposition or decolorization of natural colored compounds adsorbed or chemically bound on cellulosic fibers. In the case of scoured cotton fabrics, these colored compounds are practically insoluble in water because most of the water-soluble compounds are removed by treatment with hot alkaline aqueous solutions before bleaching. The natural colored compounds remaining on the scoured cotton fabrics are still not identified. However, in analogy with the structure of known natural dyes in plants, the remaining colored compounds on the scoured cotton fabrics are expected to have extended π-electron systems mainly consisting of aromatic, olefinic, carbonyl and carboxylic moieties, and some ether linkages. The decolorization of the colored compounds can be accomplished by cleaving the extended π-electron systems.

We report here an efficient TCF bleaching of cotton fabrics by using a combination of UV laser irradiation and $NaBH_4$ aqueous solution. The reaction can be rationalized as a photochemical hydrogen transfer to the extended π-electron systems. A KrF excimer laser (248 nm) was used as the light source because, considering the chromophore of the cellulosic fibers, the laser was selectively absorbed by the colored compounds and not by the cellulosic fibers themselves.

Results and discussion

The sample used was a scoured cotton fabric (**SF**) [G poplin (J6220), scoured by Awazu Rensen Kogyo]. A sheet of the fabric was padded in a $NaBH_4$ aqueous solution; the uptake of the $NaBH_4$ solution by 1 g of **SF** was 1.6 g. The sheet was then irradiated with a KrF excimer laser (Lambda Physik LPX210i) at room temperature, washed with water, dried, and its whiteness (W),[6] yellow index (YI),[6] reflectance and absorption spectra were measured by a UV spectrophotometer (Shimadzu UV-2400PC) equipped with an integration sphere (Shimadzu ISR-2200). The measurements were conducted by using $BaSO_4$ (Merck, for white standard DIN 5033) as a reference. A sheet of **SF** had values W and YI of 29.12 and 10.77, respectively, and those of the conventionally bleached cotton fabric (**CF**) were 51.57 and 1.72. The **CF** was produced by using $NaClO_2$ from the same batch of the scoured cotton fabric used in the laser experiments [G poplin (J6220), bleached by Awazu Rensen Kogyo].

Fig. 1(a) shows W and YI of the laser bleached cotton fabrics (**LF**) as a function of laser irradiation time. Even after 1 min irradiation, W and YI were better than those of **CF**. The required time for the laser bleaching was much shorter than that of the conventional processes which generally take *ca.* 60 min.[7] It should be also noted that the laser process was conducted at room temperature in contrast to the conventional processes which are generally operated at 94–99 °C.[7]

When **SF** was immersed in a 6% $NaBH_4$ aqueous solution for 2 min at room temperature, W and YI were 37.00 and 7.85, respectively. This result indicates that the irradiation of the laser was essential for the bleaching.

Fig. 1(b) shows W and YI of **LF** as a function of laser frequency. Similarly, Fig. 1(c) shows W and YI of **LF** as a function of laser pulse energy; in this experiment, the total energy irradiated at a unit area was kept constant so that the number of laser pulses decreased with the increase of the laser pulse energy. The effect of laser frequency and pulse energy was small but a slight decrease of the bleaching efficiency, especially in YI, was observed with increasing laser frequency and pulse energy.

Fig. 1(d) shows W and YI of **LF** as a function of $NaBH_4$ concentration. Considerable improvement on W and YI was observed by increasing the concentration up to 2% but then

Green Context

The use of enormous quantities of bleach in the pulp and paper and textile industries leads to the generation of huge quantities of chlorine-containing waste. Alternative, non-chlorine processes have been investigated in the past, but have met with only limited success. The research described here involves the use of laser induced reduction of the unsaturated systems involved in the colour systems, with the H-donor being sodium borohydride. This process is efficient for cellulose fabrics. While the boron waste is not without toxicity problems, it may be seen as a step towards a more efficient bleaching system involving more benign H sources.

DJM

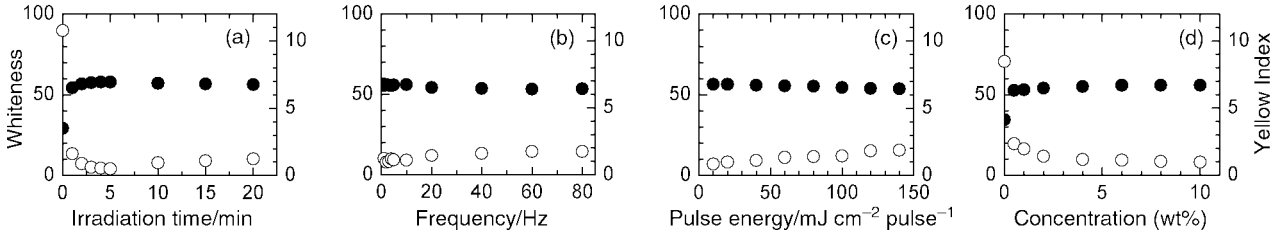

Fig. 1 Whiteness (W) and yellow index (YI) of KrF excimer laser-bleached cotton fabrics (**LF**) as a function of (a) irradiation time (40 mJ·cm^{-2}·pulse^{-1}; 5 Hz; 6 wt% $NaBH_4$ (aq), (b) laser frequency (40 mJ cm^{-2} pulse^{-1}; 600 pulses; 6 wt% $NaBH_4$ (aq), (c) laser pulse energy (24 J cm^{-2}; 5 Hz, 6 wt% $NaBH_4$ (aq), and (d) $NaBH_4$ concentration (40 mJ cm^{-2} pulse^{-1}; 5 Hz; irradiation time: 2 min). Number of cotton cloths: 1 sheet. Whiteness (●); yellow index (○).

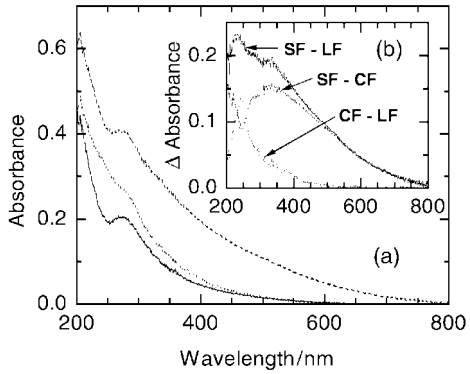

Fig. 2 Absorption (a) and difference absorption (b) spectra of cotton fabrics. (a): (----): scoured fabric (**SF**), (·····): conventionally bleached fabric (**CF**), (—) laser bleached fabric (**LF**).(b) (----): (**SF** − **CF**), (—) (**SF** − **LF**), (·····) (**CF** − **LF**). Laser bleaching condition: KrF laser, 40 mJ cm^{-2} pulse^{-1}, 5 Hz, 2 min, 6 wt% $NaBH_4$ (aq) Number of cotton cloths: 5 sheets.

leveled off at concentrations over 2%. Some extent of bleaching was also observed in pure water ($NaBH_4$ concentration of 0%). When a sheet of dry **SF** was irradiated with the KrF laser (40 mJ cm^{-2} pulse^{-1}, 5 Hz, 3 min), W and YI of the fabric were 31.55 and 9.43, respectively; the values were almost the same as those before irradiation. These results indicate that water is indispensable in the laser bleaching processes.

Back coloration was tested by prolonged standing of **LF** in air; the change of W and YI after one year was 57.42 to 55.69 and 0.62 to 0.82, respectively. In addition, irradiation of a 500W Xe lamp to a **LF** in air for 24 h led only to a small change in the color; the change of W and YI was 55.94 to 57.25 and 0.67 to 0.27, respectively. The change of W and YI values indicates further bleaching of **LF** by the Xe lamp irradiation.

Fig. 2(a) shows the absorbance of five sheets of **SF**, **CF**, and **LF**.[8] The figure shows the presence of a considerable absorption of **SF** in the UV to visible region. By contrast, a significant decrease of the absorption especially in the visible region was observed with **CF** and **LF**. This decrease indicates the decomposition or the shortening of the extended π-electron systems of the colored compounds.

Fig. 2(a) also shows that the absorbance of the laser-bleached fabric has a maximum at 270 nm. The corresponding absorption maximum and a shoulder were also observed in **SF** and **CF**, respectively. This absorption maximum can be assigned to substituted benzene moiety.[9] The presence of this maximum in **LF** indicates the difficulty in the further reduction of the substituted benzene moieties.

Fig. 2(b) shows the absorption differences between **SF**, **CF**, and **LF**, namely, **SF** − **LF**, **SF** − **CF**, and **CF** − **LF**. The absorption differences **SF** − **LF** and **SF** − **CF** show the decrease of the natural colored compounds by the laser and conventional bleaching, respectively. They also show that the colored compounds had broad absorption in UV to visible region, which is evidence for the existence of extended conjugation. Difference absorption **CF** − **LF** in Fig. 2(b) also shows that the extent of laser and conventional bleaching was almost the same at > 500 nm but the laser bleaching was more effective at < 500 nm, especially around 250 nm. This result indicates that short π-conjugations that have absorptions at *ca.* 250 nm, most likely aromatic moieties, decreased more effectively by the KrF laser bleaching than $NaClO_2$ treatments.

The reaction can be rationalized in terms of selective excitations of the natural colored compounds and successive hydrogen transfer from $NaBH_4$ to them. Such reactions have been reported for water-insoluble low-molecular-weight organic compounds in organic or organic–water mixed solvents by using conventional UV lamps.[10–12] The mechanism is still not clear at the moment but can be explained either by a hydride abstraction by the excited colored molecules or by an electron transfer and successive proton transfer from $NaBH_4$ to the colored molecules.[11] However, these reported photolyses were all conducted in homogeneous phases while reactions in heterogeneous phases, like our experiments reported here, have not been reported so far.

Although boron compounds exist in natural sea water (4.44 mg B L^{-1}),[13] they are reported to have some toxicity[14] but often much less than those of some AOX.[14] However, to develop less hazardous bleaching process, the use of less toxic photo-induced H-transfer reagents is now under investigation.

Acknowledgement

We thank Mr Sadao Tamura for conducting preliminary experiments.

References

1 M. Lewin, in *Handbook of Fiber Science and Technology, Chemical Processing of Fibers and Fabrics, Fundamentals and Preparation,* ed. M. Lewin and S. B. Sello, Marcel Dekker, Inc., New York, 1984, vol. 1, Part B, ch. 2.
2 V. Lorås, in *Pulp and Paper*, ed. J. P. Casey, John Wiley & Sons, Inc., New York, 1980, vol. I, ch. 5.
3 Hydrogen peroxide and some peracids are also used in the bleaching processes but with less efficiency: see ref. 1.
4 For textiles: see, for example: G. Schulz, H. Herlinger and P. Schäfer, *Textilveredlung*, 1992, **27**, 167.
5 For pulps: see, for example: J. Rutkowski, *Cellul. Chem. Technol.*, 1997, **31**, 485.
6 Whiteness and yellow index are as defined in CIE 1986c (JIS Z 8715) and JIS K 7103, respectively. Better bleaching is indicated by larger W and smaller YI.
7 See, for example: B. A. Evans, *Textile Chem. Colorist*, 1981, **13**, 254.
8 The number of the sheets of **SF** was varied from one to ten; the reflectance increased with the increase of the number of the sheets

until four but leveled off over five. The increase of the reflectance by increasing the number of the sheets is due to the suppression of transmitted light.

9 H. H. Jaffé and M. Orchin, *Theory and Application of Ultraviolet Spectroscopy*, John Wiley & Sons, Inc., New York, 1962, ch. 12.

10 J. A. Waters and B. Witkop, *J. Am. Chem. Soc*., 1967, **89**, 1022; D. H. Paskovich, A. H. Reddoch and D. F. Williams, *J. Chem. Soc., Chem. Commun*., 1972, 1195.

11 J. A. Barltrop, *Pure Appl. Chem*., 1973, **33**, 179.

12 O. Yonemitsu, P. Cerutti and B. Witkop, *J. Am. Chem. Soc*., 1966, **88**, 3941; G. Ballé, P. Cerutti and B. Witkop, *J. Am. Chem. Soc*., 1966, **88**, 3946.

13 *Handbook of Chemistry and Physics*, ed. D. R. Lide, CRC Press, Boca Raton FL, 81st edn. 2000–2001, 14–14.

14 *The Merck Index*, ed. S. Budavari, Merck & Co., Inc., Whitehouse Station, 12th edn., 1996; I. G. Sipes, C. A. McQueen and A. J. Gandolfi, *Comprehensitive Toxicology*, ed. A. J. Gandolfi, Pergamon, Cambridge, 1997.

Green photochemistry: the solar-chemical 'Photo–Friedel–Crafts acylation' of quinones†

Christian Schiel,[a] Michael Oelgemöller,[b] Jürgen Ortner,[c] and Jochen Mattay*[a]

[a] *Organische Chemie I, Fakultät für Chemie, Universität Bielefeld, Postfach 10 01 31, D-33501 Bielefeld, Germany. E-mail: mattay@uni-bielefeld.de*
[b] *Inoue Photochirogenesis Project, ERATO, JST, 4-6-3 Kamishinden, Toyonaka-shi, Osaka, 560-0085, Japan*
[c] *Deutsches Zentrum für Luft- und Raumfahrt e.V. (DLR), Solare Energietechnik, D-51170 Köln, Germany*

Received 19th July 2001
First published as an Advance Article on the web 2nd October 2001

The photoreactions between 1,4-quinones (**1** and **4**) and aldehydes (**2** and **5**), yielding acylated hydroquinones as sole products, were investigated under artificial and solar irradiation conditions. Three different solar reactors were used for the photochemical syntheses with sunlight (PROPHIS, CPC and a flat bed reactor), and the CPC system was found to be the most robust one in terms of weather dependence. The solar reactions can be easily performed on a half-kilogram scale using cheap and commercially available starting materials.

Introduction

During his general lecture before the International Congress of Applied Chemistry in New York in 1912, Giacomo Ciamician, one of the pioneers of modern organic photochemistry, presented his spectacular vision on 'The Photochemistry of the Future':[1]

> *'On arid lands there will spring up industrial colonies without smoke and without smokestacks, forests of glass tubes will extend over the plains, and glass buildings will rise everywhere; inside of these will take place the photochemical processes that hitherto have been the guarded secret of the plants, but that will have been mastered by human industry which will know how to make them bear even more abundant fruit than nature, for nature is not in a hurry and mankind is.'*

During that time,[2] organic photochemistry was closely linked to the use of the sun as the source of radiation, and therefore took mostly place on the roof tops of chemical institutes (*e.g.* at Ciamician's roof laboratory in Bologna/Italy) or in southern countries (*e.g.* by Alexander Schönberg's group in Cairo/Egypt). With the development of powerful artificial light-sources, photochemistry moved into the laboratories and became an important and successful research field.[3] However, photochemical applications for the production of chemicals on large industrial scale remained rare, and Ciamician's vision seemed unfulfilled. Recently, the call for 'sustainable developments', reduction of CO_2-emission and the growing requirement for environmentally friendly technologies led to an increasing interest in (and remembrance of) the sun as an energy *and* light source.[4] Owing to their absorption at wavelengths above 350 nm, quinones are especially versatile substrates for the use of sunlight,[5] and can be utilized in the field of *green* photochemistry.[6] In terms of the solar-chemical synthesis of fine chemicals,[7] we have selected the photochemical reaction between quinones and aldehydes (the so-called 'Photo–Friedel–Crafts acylation') as a mild and efficient alternative to thermal Friedel–Crafts acylations (Scheme 1).[8] The classical method often suffers from the use of acid chlorides and equimolar amounts of harmful Lewis acids (usually $AlCl_3$), the formation of undesired byproducts (especially volatile hydrochloric acid) and certain restrictions on functionalities in the starting materials.

The extremely useful photochemical alternative was firstly reported by Heinrich Klinger in 1891, who exposed the starting materials to natural sunlight over several months.[9] He also splendidly described the experimental difficulties an early photochemist had to deal with, and, for instance, apologized for presenting older results due to the loss of his reaction flask

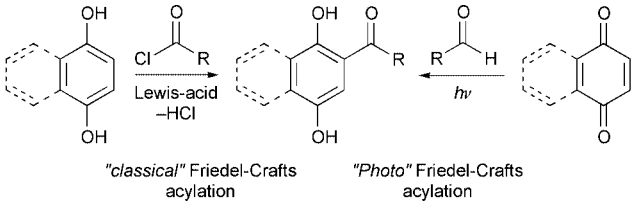

Scheme 1

Green Context

Photochemistry not only represents an alternative energy source, it also offers a way of activating molecules towards selective chemical reactions. If we can develop efficient chemical synthesis with the sun as an energy and molecular activation source, then we truly have sustainable, green chemical processing. Here, an important chemical reaction with real commercial value, the acylation of quinones is investigated under solar-chemical conditions. The ability to react quinones which have been activated by photons has been known for over 100 years but has since been neglected. Here, different solar reactors are applied to the photochemical synthesis of some acylated hydroquinones. The results are certainly encouraging and include success at scale-up, further demonstrating commercial potential. Chemistry can indeed be greener under the sun! ***DJM***

† Dedicated to Prof. Günther O. Schenck on the occasion of his 88th birthday on May 14th, 2001.

 DOI: 10.1039/b106425h

during a storm.[9c] In the following 100 years, however, this photoacylation found only little synthetic attention until in 1992, Kraus *et al.*[10] used it for multigram preparations.

The photoproducts, acylated quinones and their derivatives are important natural compounds (*e.g.* alkannin or shikonin),[11] and serve as useful key intermediates for pharmaceuticals (*e.g.* Nanoamycin A or Frenolicin B).[12] Therefore, a bulk production under economically acceptable and hazard-free conditions represents a highly desirable goal. Since a number of solar reactors are already available at present,[7,13] the solar photochemical approach (as a modern version of Klinger's early experiments and a realization of Ciamician's vision) allows the large scale synthesis of fine chemicals in combination with sunlight as an environmentally friendly source of radiation. For some selected examples, cost estimates have been reported showing that the industrial production of specific fine chemicals (*e.g.* rose oxide or ε-caprolactam) is indeed economical.[14]

Results and discussion

To find optimal reaction conditions for the solar-chemical application, the photoreaction of 1,4-naphthoquinone **1** with butyraldehyde **2** was chosen as a model system using an artificial light source (Scheme 2).[15] Following the original protocol described by Kraus *et al.*,[10] prolonged photolysis for 5 days in benzene and on a multigram scale gave the corresponding acylated hydroquinone **3** in a good yield of 78%. The required prolonged irradiation time is in accord with quantum yield determinations reported by Maruyama and Miyagi.[16] These authors found a drastic decrease with increasing conversion due to self-quenching by the photoproduct (*e.g.* Φ = 0.37–0.51 for the 1,4-naphthoquinone–propionaldehyde system). For the 'outdoor' solarchemical application of this reaction, an exchange of the toxic solvent (benzene) was necessary. Toluene, which was first used as an alternative, had also to be excluded due to its toxicity and sensitivity towards radical side-processes (the yield for **3** dropped to 35%). Pure *tert*-butyl alcohol or a mixture with acetone turned out to be an acceptable alternative and the photoproduct **3** was isolated in 84% yield (laboratory experiment with pure *tert*-butyl alcohol).

All solar experiments described here were performed at the German Aerospace Center (DLR) in Cologne/Germany (latitude 50.5 °N, 70 m above sea level) as a part of the AG Solar program. In all cases examined, the presence of oxygen could be tolerated and thus degassing with an expensive inert gas was not necessary.

For the first solar experiment, a line-focusing parabolic trough collector based on a MAN-Helioman module (PROPHIS plant,[13] Fig. 1) was used, which enables a concentration factor (CF) corresponding to an illumination level 15 times that of the sun in practice at this location, but which can only concentrate (and thus use) the direct part of the global radiation. The whole loop comprises the MAN-Helioman module and the feeding equipment (storage vessel, pump, heat exchanger, gas fitting, *etc.* placed nearby in a separated building).

With the optimized reaction conditions, we have scaled up the reaction of 1,4-naphthoquinone **1** with butyraldehyde **2** to a 500 g (**1**) scale under solar-chemical conditions (80 l of a 3 : 1 *tert*-butyl alcohol–acetone mixture). During the experiment, the PROPHIS reactor followed the sun by a three-dimensional tracking system, whereas the concentrating mirrors faced the ground overnight. Following this procedure and using three troughs (with 24 m^2 reflecting area), irradiation of **1** in the presence of an excess of butyraldehyde **2** and in a *tert*-butyl alcohol–acetone mixture for three days gave **3** in 90% yield and in high purity. The experiment took place on August 20th– 22nd 1996 for a total illumination time of 24 hs (Table 1), and the final conversion was determined by GC. The weather conditions were varying, and only the first day was optimal for the solar-chemical experiment. This can be clearly seen by

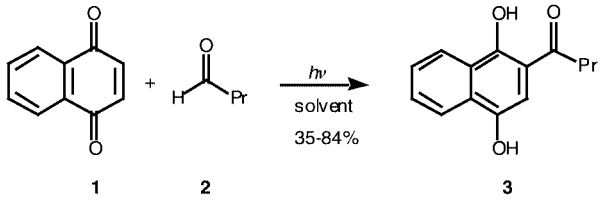

Scheme 2

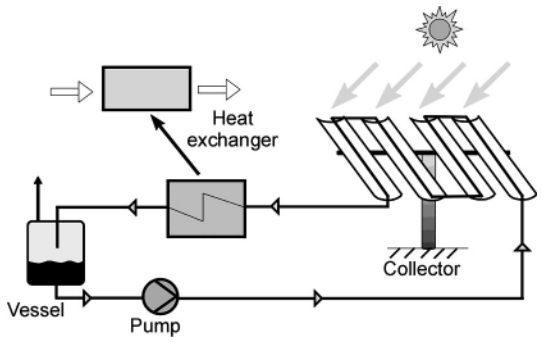

Fig. 1 Schematic diagram of the PROPHIS plant.

Table 1[17]

Day	Illumination time	Radiation powder[a]/ kWh	Precipitation/min	Sunshine[b]/h	Medium day temp./°C	Max./min. day temp./°C
20th Aug. 1996	9:00 am to 5:00 pm	5.3	None	12.75	23.6	30/16
21st Aug. 1996	9:00 am to 5:00 pm	1.7	24	1/2	19.3	24/15
22nd Aug. 1996	9:00 am to 5:00 pm	2.9	1	4.25	16.9	23/15

[a] On 1 m^2 horizontal area. [b] Max. *ca.* 14.5 h.

Table 2[17]

Day	Illumination time[a]	Precipitation/mm	Sunshine[b]/h	Medium day temp./°C	Max./min. day temp./°C
12th Sept. 2000	11:20 am (P), 1:00 pm (C) to 5:00 pm	< 1	7.5	21.1	27/16
13th Sept. 2000	10:00 am to 5:00 pm	None	4	16.3	21/14
14th Sept. 2000	10:30 am to 4:30 pm	< 1	2.2	16.5	22/12

[a] P: PROPHIS loop, C: CPC reactor. [b] Max. *ca.* 12.75 h.

Table 3

Day[a]	Reactor (reflecting area/m²)	Amount of photons/mol 300–400 nm	400–500 nm
20th Aug. 1996	PROPHIS (24)	38.3	226.7
21st Aug. 1996		1.2	6.7
22nd Aug. 1996		3.7	22.2
12th Sept. 2000	PROPHIS (3)	1.5	8.8
13th Sept. 2000		1.0	6.1
14th Sept. 2000		0.4	2.3
12th Sept. 2000	CPC (3)	2.9	10.6
13th Sept. 2000		4.1	14.9
14th Sept. 2000		2.0	7.1

[a] Illumination times: see Tables 1 and 2.

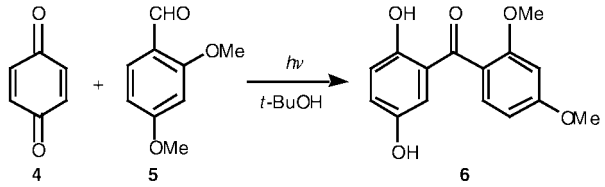

Scheme 3

comparing the radiation power (global radiation, Table 2) and the amount of photons (Table 3, *vide infra*) collected by the mirrors for each day.

As the second model reaction, the photoacylation of 1,4-benzoquinone **4** with 2,4-dimethoxybenzaldehyde **5** was chosen (Scheme 3). The photoproduct **6** is of specific interest, since it may serve as a potential calixarene precursor. With an artificial light-source and pure *tert*-butyl alcohol as solvent, the corresponding aroylated product **6** was readily obtained in 66% yield.

For the comparison of three different sunlight-collecting systems, this reaction was also performed in large scale under solar-chemical conditions (September 2000). Besides the described PROPHIS system (Fig. 2), two more simple reactors were selected,[13] *i.e.* a CPC reactor (compound parabolic collector, Fig. 3) and a double sheet flat bed reactor[18] (Fig. 4). In all cases, the reactor was loaded with 175 g of **4** and 566 g of **5** in 58 l *tert*-butyl alcohol, and the illuminated (flat bed) or reflecting area (PROPHIS, CPC) was 3 m².

Fig. 2 The PROPHIS reactor. The building for the feeding platform can be seen in the background. Only one trough (3 m² reflecting area) was used for the experiment, and the brown–yellowish color of the photosolution can be clearly seen in the absorber tube.

Fig. 3 CPC reactor with 3 m² reflecting area.

Fig. 4 Flat bed reactor with 3 m² of total reflecting area.

The CPC system represents a low concentrating collector (CF = 2–3) that can also use part of the diffuse solar radiation. In addition, it has already been successfully applied to [2 + 2] cycloadditions of several olefins to 1,4-naphthoquinones.[19] In contrast to the PROPHIS plant, this reactor type does not allow tracking of the sun. With a fixed slope of 50° to the position of the sun, the reaction mixture was passed through the absorber tubes during the experiment. Overnight, the reactor was covered with a plastic foil.

The double sheet flat bed reactor (Makrolon®, CF = 1) can be regarded as a modern version of early solar chemical equipment (*e.g.* Schenck's pilot plant for the chlorophyll-sensitized photooxidation of α-terpinene to ascaridol[20] in Ziegelhausen/Germany). The main advantages of this one-sun reactor are its simple design and its ability to use direct and diffuse solar radiation. In contrast to the PROPHIS plant and the CPC reactor, a stationary system was selected (two reactors, each 1.5 m² illuminated area) with a fixed slope of 30° to the position of the sun. As it turned out during the experiment, the selected construction had two major disadvantages. The reacting components were not properly mixed (as *via* pumping), and the solution readily solidified overnight during the cold weather period (melting range of pure *tert*-butyl alcohol: +23–26 °C). Since no reaction occurred in the solid state, most of the solar radiation in the morning was required for the melting process. For the other two reactor types, these problems could be avoided or circumvented by circulation of the reaction mixture.

The illuminations were conducted during September 12th–14th 2000 (Table 2), and the progress of each reaction was monitored by GC. As not untypical for the location and time of year, the weather conditions were varying and cold, and were therefore not optimal for reaching high conversions in short periods of time. The reactions performed with the PROPHIS and the CPC reactor are summarized in Fig. 5.

Since the CPC reactor is less dependent on direct radiation than the PROPHIS loop, it gave better results in terms of

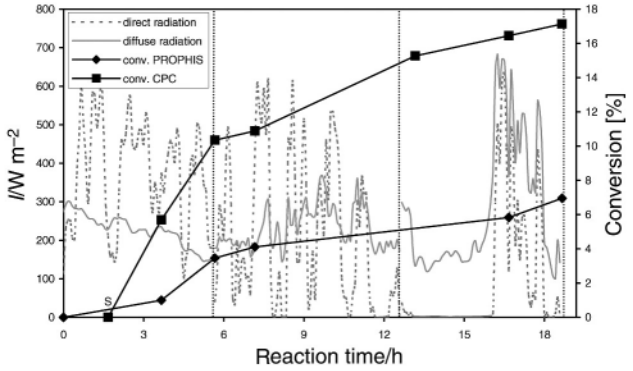

Fig. 5 Reaction progress for the formation of **6**. The single days are separated from each other by vertical, dotted lines. S marks the starting point of the CPC experiment.

conversion and product yield. After a total irradiation time of 17 h, a conversion of 17% was obtained, whereas the PROPHIS system gave a lower conversion of 7% after a slightly longer total irradiation period of *ca.* 19 h. The conversion ratio (PROPHIS *vs.* CPC) of 30 : 70 shows a good agreement with the calculated 35:65 ratio of direct (used by PROPHIS) *vs.* direct + diffuse (used by CPC) radiation (Fig. 6). This ratio is also reflected in the number of collected photons for each system (Table 3).‡ During the experimental period, the PROPHIS plant collected 20.1 mol photons in the range 300–500 nm (the important absorption region of 1,4-quinones within the solar spectrum) while the CPC reactor collected 41.6 mol. The calculated ratio of 33 : 67 again closely matches the conversion ratio.

As can be seen by comparison with the first solar experiment (**1** + **2**), the reactions could have been driven to almost complete conversion with longer irradiation times, more reflecting (mirror) area, more irradiation stages or during more optimal weather conditions.

The flat bed reactors gave the lowest total conversion of *ca.* 3.6% after *ca.* 20 h of irradiation, which can be explained by the difficulties in their construction and the choice of the solvent (relatively high freezing point) without circulation.

In conclusion, the results from the described experiments clearly show that the solarchemical bulk production of specific fine chemicals can serve as a useful and environmentally friendly alternative to existing technical processes.[21] In the present study, not all conditions (*e.g.* large excess of aldehyde, solvent freezing range) were optimal to reach the goal of *green* photochemistry and thus need to be further modified.

Although the CPC reactor can sufficiently operate even in regions with less ideal weather conditions (*e.g.* in central Europe), a solar production plant in southern regions (as *e.g.* at the Plataforma Solar de Almeria/Spain: latitude 37.1° N, 500 m above sea level) should operate more economically. The PROPHIS loop is more dependent on direct radiation but its construction allows a larger reflecting area (max. 32 m^2), which can partly compensate this disadvantage. In general, the space–time yields of concentrating systems (PROPHIS) are higher than those of non-concentrating systems (flat bed).

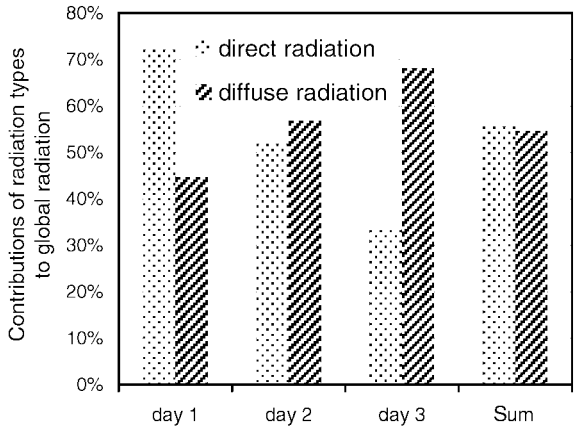

Fig. 6 Direct and diffuse contributions to the global radiation.§

Acknowledgements

We thank the *Arbeitsgemeinschaft Solar des Landes Nordrhein-Westfalen* for supporting this research project. We especially thank Mr Hartmut Kraatz from Deutscher Wetterdienst (DWD), Dr Hans Jochen Kuhn and Dipl.-Met. Heike Hübener for help in the preparation of the manuscript. We are also grateful to Professor Martin Demuth (MPI Mülheim) for providing the flat bed reactor.

Notes and references

‡ The amount of collected photons depends on both the type of radiation (direct *vs.* diffuse) and the selected system (tracked *vs.* fixed to the sun).
§ Global and diffuse radiation are measured horizontally whereas the measurement system for direct radiation is tracked to the sun. Thus the sum of diffuse and direct radiation is larger than the global radiation.

1 G. Ciamician, *Science*, 1912, **36**, 385.
2 For interesting reviews on the beginnings of organic photochemistry see: H. D. Roth, *Angew. Chem.*, 1989, **101**, 1220; H. D. Roth, *Angew. Chem., Int. Ed.*, 1989, **28**, 1193; H. D. Roth, *EPA Newslett.*, 2001, **71**, 37; H. D. Roth, *Pure App. Chem.*, 2001, **73**, 395.
3 A selection of some recent books on photochemistry: D. Wöhrle, M. W. Tausch, W.-D. Stroher, *Photochemie*, Wiley-VCH, Weinheim, 1998; M. Klessinger and J. Michl, *Excited States and Photochemistry of Organic Molecules*, John Wiley & Sons, New York, 1995; C. E. Wayne and R. P. Wayne, *Photochemistry*, Oxford University Press, Oxford, 1996; J. Mattay and A. G. Griesbeck, *Photochemical Key Steps in Organic Chemistry*, VCH, Weinheim, 1994; N. J. Turro, *Modern Molecular Photochemistry*, University Science Books, Mill Valley, CA, 1991.
4 G. Knör, *ChemBioChem*, 2001, **2**, 593.
5 J. M. Bruce, in *The Chemistry of the Quinoid Compounds*, ed. S. Patai, John Wiley & Sons, New York, 1974, vol. 1, p. 465; K. Maruyama and A. Osuka, in *The Chemistry of Quinoid Compounds*, ed. S. Patai, John Wiley & Sons, New York, 1988, vol. 2, p. 759; J. M. Bruce, *Quart. Rev.*, 1967, **21**, 405.
6 For a different concept using a 308 nm excimer radiation source and aqueous media see: A. G. Griesbeck, W. Kramer and M. Oelgemöller, *Green Chem.*, 1999, 205.
7 P. Esser, B. Pohlmann and H.-D. Scharf, *Angew. Chem.*, 1994, **106**, 2085; P. Esser, B. Pohlmann and H.-D. Scharf, *Angew. Chem., Int. Ed.*, 1994, **33**, 2009; K. H. Funken, J. Ortner, K.-J. Riffelmann and C. Sattler, *J. Inf. Recording*, 1998, **24**, 61.
8 G. A. Kraus, H. Maeda, P. Lui, A. Melekhov and Y. Lu, in *Green Chemistry: Frontiers in Benign Chemical Syntheses and Processes*, ed. P. T. Anastas and T. C. Williamson, Oxford University Press, Oxford, 1998, p. 72.
9 (*a*) H. Klinger and O. Standke, *Ber. Dtsch. Chem. Ges.*, 1891, **24**, 1340; (*b*) H. Klinger and W. Kolvenbach, *Ber. Dtsch. Chem. Ges.*, 1898, **31**, 1214; (*c*) H. Klinger, *Justus Liebigs Ann. Chem.*, 1888, **249**, 137.
10 G. A. Kraus and P. Liu, *Tetrahedron Lett.*, 1994, **35**, 7723; G. A. Kraus and M. Kirihara, *J. Org. Chem.*, 1992, **57**, 3256.
11 R. H. Thompson, *Naturally Occurring Quinones*, Academic Press, New York, 2nd edn., 1971; R. H. Thompson, *Naturally Occurring Quinones III, Recent Advances*, Chapman & Hall, London, 1987; V. P. Papageorgiou, A. N. Assimopoulou, E. A. Couladouros, D. Hepworth and K. C. Nicolaou, *Angew. Chem.*, 1999, **111**, 280; *Angew. Chem., Int. Ed.*, 1999, **38**, 270.
12 For 1,4-benzodiazepines, see: G. A. Kraus and H. Maeda, *Tetrahedron Lett.*, 1994, **35**, 9189; for pyrano[2,3-*c*]naphthoquinones, see: M. A. Brimble and S. M. Lynds, *J. Chem. Soc., Perkin Trans. 1*, 1994, 493; for lapachones see: K. Maruyama and Y. Naruta, *Chem. Lett.*, 1977, 847.

13 K. H. Funken and J. Ortner, *Z. Phys. Chem.*, 1999, **213**, 99; J. Ortner, D. Faust, K. H. Funken, T. Lindner, J. Schulat, C. G. Stojanoff and P. Fröning, *J. Phys. IV Fr.*, 1999, **9**, Pr3.
14 N. Monnerie and J. Ortner, *J. Sol. Energy Eng.*, 2001, **123**, 171.
15 C. Schiel, M. Oelgemöller and J. Mattay, *Synthesis*, 2001, 1275.
16 K. Maruyama and Y. Miyagi, *Bull. Chem. Soc. Jpn.*, 1974, **47**, 1303.
17 The weather data was recorded for the nearby Cologne/Bonn-Airport, and was used with permission of the Deutscher Wetterdienst DWD (source: DWD, station: Flughafen Köln/Bonn).
18 This reactor type was designed by Prof. M. Demuth at the Max-Planck-Institut für Strahlenchemie, Mülheim/Germany.
19 C. Covell, A. Gilbert and C. Richter, *J. Chem. Res. (S)*, 1998, 316.
20 (*a*) G. O. Schenck, *Angew. Chem.*, 1952, **64**, 12; G. O. Schenck and K. Ziegler, *Naturwissenschaften*, 1944, **32**, 157.
21 C. Sattler, F.-J. Müller, K.-J. Riffelmann and K. H. Funken, in *Int. Conf. ASME, KSME, JSME, SAREK, JSES and KESE, Renewable and advanced energy systems for the 21st century*, ed. R. Hogan, Y. Kim, S. Kleis, D. O'Neil and T. Tanaka, Maui/Hawaii, April 1999, RAES99-7692; K. H. Funken, G. Luedtke, J. Ortner and K. J. Riffelmann, *J. Inf. Recording*, 2000, **25**, 3; K. H. Funken, F. J. Müller, J. Ortner, K. J. Riffelmann and C. Sattler, *Energy*, 1999, **24**, 681.

Water, a clean, inexpensive, and re-usable reaction medium. One-pot synthesis of (*E*)-2-aryl-1-cyano-1-nitroethenes

D. Amantini, F. Fringuelli, O. Piermatti, F. Pizzo* and L. Vaccaro

Department of Chemistry, University of Perugia - Perugia, Italy. E-mail: pizzo@unipg.it; Fax: +39 075 5855560; Tel: +39 075 5855546

Received 25th June 2001
First published as an Advance Article on the web 13th September 2001

The Knoevenagel addition of aryl aldehydes **1** with nitroacetonitrile **2** in water followed by dehydration of β-nitroalcohols **3**, allows (*E*)-2-aryl-1-cyano-1-nitroethenes **4** to be prepared by a *one-pot* procedure without using organic solvents. The reuse of the aqueous medium makes this process inexpensive and highly environmentally friendly. The protocol was used to synthesize the benzo[*b*]pyrane [4,3-*d*][1,2]oxazine-2-oxide skeleton by a domino Knoevenagel–Diels–Alder process.

Introduction

Nowadays chemical processes employ large amounts of hazardous and toxic solvents. The choice of pursuing a low waste route and reusable reaction media, to minimize the economic cost and environmental impact of a chemical process, is becoming ever more urgent for the future.

Organic chemists are requested to investigate clean, economical and environmentally safer methodologies.

One of the most promising approaches uses water as reaction medium.[1] The use of aqueous medium in organic synthesis is not long-standing and, because of its advantages, a strong development in the future is expected.

We are interested in performing organic reactions in water, and we have investigated epoxidation reactions,[2] Diels–Alder cycloadditions,[3] aldol-like condensations,[4] and oxidation reactions,[5] and most recently the use of Lewis acids in nucleophilic ring opening of oxiranes[6] and the reduction of the azido group.[7]

As a part of our research to develop a *green chemistry* by *one-pot* syntheses of target molecules in water alone as the reaction medium, we report here the Knoevenagel condensation of arylaldehydes **1** and **5** with nitroacetonitrile **2**, for the preparation of (*E*)-2-aryl-1-cyano-1-nitroethenes **4** and benzo[*b*]pyrane[1,2]oxazine-2-oxide **7** and **8**, performed in water, and the reuse of the aqueous reaction medium.

Results and discussion

For several years conjugated nitroethenes have been attracting the attention of organic chemists.[8] They are present in nature,[9] are endowed with valuable biological and pharmacological properties,[10] and are used as both 4π or 2π components in Diels–Alder reactions, and as Michael acceptors for the addition of carbon nucleophiles such as enamines and enolates.[8–11] The straightforward conversion of the nitro group to an amino or carbonyl group gives easy access to a large variety of building-blocks exploitable for the synthesis of target molecules.

Conjugated nitroethenes are usually prepared by a two-step synthesis that first implies an aldol-type addition of a nitroalkane to a carbonyl compound (Henry reaction), followed by dehydration of the resultant β-nitroalcohol. Generally the nitroaldolic reaction is performed in organic media in the presence of a base.[10,12] An accurate control of the basicity of the reaction medium is necessary to avoid side-reactions such as aldol condensations and the Cannizzaro reaction.[10,12] Recently, the Henry reaction was performed[13] in aqueous NaOH (0.025 M) in the presence of cetyltrimethylammonium chloride. Under these conditions neither side reactions nor dehydration of β-nitroalcohols were observed. The dehydration step has been performed in organic solvents, sometimes at high temperature by using basic alumina,[14] phthalic anhydride,[11*b*] dicyclohexylcarbodiimide,[15] $MeSO_2Cl$,[16] Me_3CCOCl[17] or PPh_3.[18]

Conjugated nitroethenes have also been prepared in the absence of solvent by using Al_2O_3[19] or Envirocat EPZG[20] as a heterogeneous catalyst.

Recently we showed that conjugated cyanonitroethenes are very reactive oxaazadienes in inverse electron-demand Diels–Alder cycloadditions, carried out in water, with both achiral and enantiopure vinyl ethers.[21] They are also active dienophiles in normal electron-demand Diels–Alder reactions with alkyl- and alkoxy-1,3-butadienes.[22]

Because of these encouraging results we decided to prepare a variety of cyanonitroethenes **4** using water as the sole reaction medium.

Arylaldehydes **1** react at room temperature with nitroacetonitrile **2** in heterogeneous aqueous media to give cyanonitroethenes **4** in high yields (Table 1). The intermediate β-nitroalcohols **3** are not observed and the reactions are always highly diastereoselective giving only the *E* diasteroisomers as products.

This protocol does not require the use of any organic solvent. In fact the cyanonitroethenes **4** were isolated in a practically pure form by simple Buchner filtration of the final aqueous mixture. The reactions occur in a short time (7 h) and do not require the use of a catalyst. The final aqueous phase was recovered and reused in four subsequent runs. In all cases, the

Green Context

Water is a very attractive solvent for reaction chemistry. It is inexpensive, safe to use and environmentally benign. However, its use can still lead to a waste (aqueous) stream that can be particularly difficult to deal with. In this article the synthetically useful Knoevenagel condensation route to substituted nitroethenes is described using an aqueous medium. The aqueous medium is easily recovered and can be reused with little difference in the yield or quality of the product. ***JHC***

Table 1 Synthesis of conjugated cyanonitroethenes 4 in water

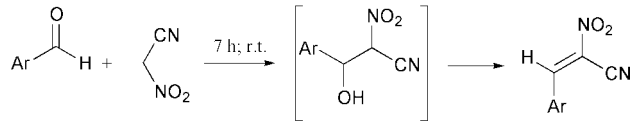

1 2 3 4

Entry	Ar		Yield **4** (%)
1	**a**	Ph	90
2	**b**	*p*-ClC_6H_4	95
3	**c**	*p*-$MeOC_6H_4$	89
4	**d**	*m*-$MeOC_6H_4$	93
5	**e**	*o*-$MeOC_6H_4$	91
6	**f**	*p*-MeC_6H_4	90
7	**g**	*p*-$MeSC_6H_4$	90
8	**h**	2-Furyl	93
9	**i**	2-Thienyl	88
10	**j**	*p*-HOC_6H_4	94
11	**k**	3,4-$(OCH_2O)C_6H_3$	90

yields obtained were excellent. As an example we report the results obtained with **1a** (Table 2). The cyanonitroethene **4g** is a new compound, while all the others except for **4a** and **4c**,[23] are known[24] but characterization is not complete. Their structure was confirmed by ^{1}H, ^{13}C NMR and GC-MS analyses (see Experimental section). The (*E*)-geometry of compounds **4** was assigned by the ^{1}H NMR chemical shift of the C-2 protons which have expected values of δ 8.45–9.20, as a consequence of their *cis* disposition with the nitro group. The corresponding protons of the (*Z*)-isomers are expected to have δ values of *ca.* 8.[25]

Table 2 Reuse of water in the reaction of **1a** and **5** with **2**

Entry	Yield **4a** (%)	Yield **7** (%)
1	90	60
2	88	58
3	92	59
4	91	58
5	90	60

This procedure allows the *one-pot* synthesis of complex molecules by the Koevenagel–Diels–Alder domino process.

Thus the reaction between 2-(3′,3′-dimethyl)allyloxybenzaldehyde **5** with nitroacetonitrile **2** in water at room temperature allows the adducts **7** and **8** to be obtained in a 16:1 ratio, respectively, after 3 h. The intermediate nitroethene **6** immediately gives rise to the *cis*-4a,10b-dihydro-1-cyano-4,4-dimethylbenzo[*b*]pyrane[4,3-*d*][1,2]oxazine-2-oxide **7** and its 4a-epimer **8** by *endo* and *exo* intramolecular inverse electron-demand Diels–Alder reaction, respectively (Scheme 1). Pure **7** was isolated with an overall yield of 60% and the aqueous phase was reused for four more runs with excellent results (see Table 2).

The structure of **7** was established by ^{1}H and ^{13}C NMR spectroscopy. Owing to the small amounts of **8**, its structure was based on the mechanistic reaction route.

The benzo[*b*]pyrane[1,2]oxazine **7** can be converted in water to a 3,4-*cis*-disubstituted-3,4-dihydrobenzo[*b*]pyrane. The generalization of this latter process and performing it by a *one-pot* procedure is under study.

Conclusions

In conclusion we report a high yield *one-pot* procedure, at room temperature in water alone as reaction medium, for the synthesis of (*E*)-2-aryl-1-cyano-1-nitroethenes **4**, by reaction of arylaldehydes **1** with nitroacetonitrile **2** and of benzo[*b*]pyrane[1,2]oxazine-2-oxide **7** by a Knoevenagel–Diels–Alder domino process.

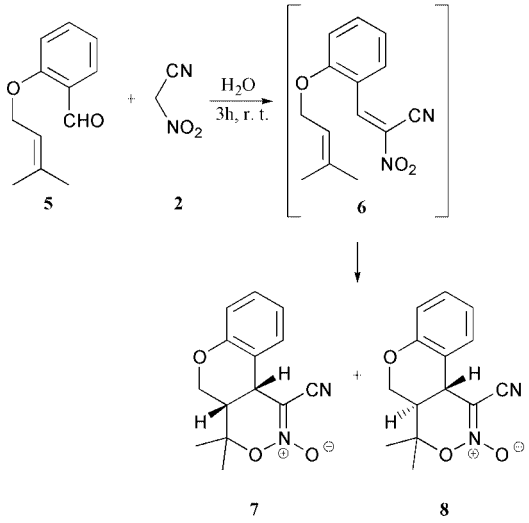

Scheme 1

The reuse of the aqueous medium and the absence of any catalyst make this protocol clean, inexpensive and valuable from an environmental point of view.

Experimental

General

All chemicals were purchased and used without any further purification. Aldehyde **5**[26] and the nitroacetonitrile **2**[27] were prepared following the procedures reported in the literature. GC analyses were performed using an SPB-5 fused silica capillary column (30 m, 0.25 mm diameter), an 'on column' injector system, an FID detector and hydrogen as the carrier gas. GC–MS analyses were performed with 70 eV electron energy. ^{1}H and ^{13}C NMR spectra (200 and 50.3 MHz, respectively) were recorded in ppm (δ) downfield from Me_4Si (δ 0.00) in $CDCl_3$ and CD_3COCD_3 as solvents.

Typical procedure for the preparation of cyanonitroethenes 4

To a solution of nitroacetonitrile **2** (150 mmol) in 500 mL of water was added aldehyde **1** (100 mmol). The resulting mixture was vigorously stirred at room temperature for 7 h, and then left to stand for 3–4 h at 0 °C to obtain a crystalline product. The cyanonitroethenes **4** were isolated by filtration under vacuum. The purity of the products was always at least 98%. Products with a higher purity grade can be obtained by crystallization from 95% ethanol. The aqueous phase obtained after filtration was reused as the reaction medium for one more run and the cyanonitroethenes **4** were isolated once again with a purity >98%. The reuse of the aqueous medium was repeated and excellent yields were obtained during four subsequent runs. As an example, we report the results obtained in the reuse of the aqueous medium in the reaction of **1a** with **2** in Table 2.

(*E*)-2-(4′-Chlorophenyl)-1-nitro-1-cyanoethene 4b. Orange solid, mp 115–116 °C. δ_H($CDCl_3$ 7.54–8.01 (m, 4H, aromatic); 8.64 (s, 1H, H-2). δ_C(CD_3COCD_3) 110.9, 123.7, 126.5, 129.8, 133.3, 140.5, 147.2. MS: *m*/*z* (%) 208 (55, M$^+$), 161 (84), 127 (100), 75 (60). Anal. Calc. for $C_9H_5ClN_2O_2$ (208): C, 51.82; H, 2.42; N, 13.43. Found: C, 51.89; H, 2.33; N, 13.34%.

(*E*)-2-(3′-Methoxyphenyl)-1-nitro-1-cyanoethene 4d. Yellow solid, mp 119–122 °C. $\delta_H(CDCl_3)$ 3.89 (s, 3H, OMe); 7.21–7.59 (m, 4H, aromatic); 8.63 (s, 1H, H-2). $\delta_C(CD_3COCD_3)$ 55.6, 111.9, 116.7, 121.9, 124.3, 125.2, 129.7, 131.4, 149.3, 160.8. MS: *m*/*z* (%) 204 (100, M^+). 143 (62), 115 (66). Anal. Calc. for $C_{10}H_8N_2O_3$ (204): C, 58.82; H, 3.95; N, 13.72. Found: C, 58.89; H, 3.88; N, 13.65%.

(*E*)-2-(2′-Methoxyphenyl)-1-nitro-1-cyanoethene 4e. Yellow solid, mp 130–132 °C. $\delta_H(CDCl_3)$ 4.00 (s, 3H, OMe); 6.97–8.30 (m, 4H, aromatic); 9.20 (s, 1H, H-2). $\delta_C(CD_3COCD_3)$ 55.9, 111.5, 112.4, 116.4, 121.3, 123.1, 129.5, 137.7, 142.5, 160.7. MS: *m*/*z* (%) 204 (100, M^+). 157 (64), 143 (86), 115 (47), 103 (64). Anal. Calc. for $C_{10}H_8N_2O_3$ (204): C, 58.82; H, 3.95; N, 13.72. Found: C, 58.91; H, 3.92; N, 13.88%.

(*E*)-2-(4′-Methylphenyl)-1-nitro-1-cyanoethene 4f. Yellow solid, mp 92–95 °C. $\delta_H(CDCl_3)$ 2.50 (s, 3H, Me); 7.39 (br d, 2H, *J* 8.8 Hz, aromatic); 7.91 (br d, 2H, *J* 8.8 Hz, aromatic); 8.62 (s, 1H, H-2). $\delta_C(CD_3COCD_3)$ 21.7, 112.0, 123.1, 125.8, 131.1, 132.9, 147.7, 149.3. MS: *m*/*z* (%) 188 (51, M^+), 141 (44), 140 (60), 115 (100), 103 (52). Anal. Calc. for $C_{10}H_8N_2O_2$ (188): C, 63.82; H, 4.28; N, 14.89. Found: C, 63.91; H, 4.92; N, 14.88%.

(*E*)-2-(4′-Thiomethylphenyl)-1-nitro-1-cyanoethene 4g. Orange solid, mp 117–118 °C. $\delta_H(CDCl_3)$ 2.57 (s, 3H, Me); 7.36 (br d, 2H, *J* 8.8 Hz, aromatic); 7.92 (br d, 2H, *J* 8.8 Hz, aromatic); 8.57 (s, 1H, H-2). $\delta_C(CD_3COCD_3)$ 14.1, 112.3, 122.2, 124.1, 126.1, 133.1, 148.7, 151.2. MS *m*/*z* (%) 220 (98, M^+), 174 (100), 173 (53), 159 (66), 127 (49). Anal. Calc. for $C_{10}H_8N_2O_2S$ (220): C, 54.53; H, 3.66; N, 12.72. Found: C, 54.49; H, 3.68; N, 12.65%.

(*E*)-2-Furyl-1-nitro-1-cyanoethene 4h. Golden–brown solid, mp 125–127 °C. $\delta_H(CDCl_3)$ 6.78–7.94 (m, 3H, aromatic); 8.42 (s, 1H, H-2). $\delta_C(CD_3COCD_3)$ 111.3, 115.9, 120.0, 129.3, 133.6, 145.5, 152.6. MS: *m*/*z* (%) 164 (31, M^+), 83 (78), 63 (100). Anal. Calc. for $C_7H_4N_2O_3$ (164): C, 51.23; H, 2.46; N, 17.07; O, 29.25. Found: C, 51.09; H, 2.32; N, 17.25%.

(*E*)-2-Thienyl-1-nitro-1-cyanoethene 4i. Golden–brown solid, mp 146–148 °C. $\delta_H(CD_3COCD_3)$ 7.45–7.50 (m, 3H, aromatic); 9.16 (s, 1H, H-2). $\delta_C(CD_3COCD_3)$ 112.0, 120.6, 130.4, 132.5, 140.6, 142.5, 143.2. MS: *m*/*z* (%) 180 (55, M^+), 134 (100), 133 (63), 112 (62), 90 (76), 84 (46), 63 (47). Anal. Calc. for $C_7H_4N_2O_2S$ (180): C, 46.66; H, 2.24; N, 15.55. Found: C, 46.79; H, 2.22; N, 15.45%.

(*E*)-2-(4′-Hydroxyphenyl)-1-nitro-1-cyanoethene 4j. Yellow solid, mp 216–217 °C. $\delta_H(CD_3COCD_3)$ 7.12 (br d, 2H, *J* 8.8 Hz, aromatic); 8.13 (br d, 2H, *J* 8.8 Hz, aromatic); 8.79 (*s*, 1H, H-2); 9.98 (br s, 1H, OH-phenolic). $\delta_C(CD_3COCD_3)$ 112.3, 117.3, 119.6, 120.1, 135.9, 148.8, 164.8. MS: *m*/*z* (%) 190 (62, M^+), 144 (53), 143 (100), 116 (46), 89 (100). Anal. Calc. for $C_9H_6N_2O_3$ (190): C, 56.85; H, 3.18; N, 14.73. Found: C, 56.79; H, 3.25; N, 14.65%.

(*E*)-2-(1′,3′-Benzodioxol-5′-yl)-1-nitro-1-cyanoethene 4k. Yellow solid, mp 142–143 °C. $\delta_H(CDCl_3)$ 6.17 (s, 2H, OCH_2O); 6.94–7.70 (m, 3H, aromatic); 8.56 (s, 1H, H-2). $\delta_C(CD_3COCD_3)$ 103.9, 109.2, 110.0, 112.5, 118.8, 122.6, 133.0, 149.0, 149.8, 155.1. MS: *m*/*z* (%) 218 (55, M^+), 172 (46), 114 (100). Anal. Calc. for $C_{10}H_6N_2O_4$ (218): C, 55.05; H, 2.77; N, 12.84. Found: C, 55.09; H, 2.72; N, 12.85%.

***cis*-4a,10b-Dihydro-1-cyano-4,4-dimethylbenzo[*b*]pyrane[4,3-*d*][1,2]oxazine-2-oxide 7.** To a solution of nitroacetonitrile **2** (0.85 g, 10 mmol in 50 mL of water) was added the 2-(3′,3′-dimethylallyloxy)benzaldehyde **5** (0.95 g, 5.0 mmol) The resulting mixture was vigorously stirred at room temperature for 3 h. The final reaction mixture was extracted with ethyl acetate (2 × 50 mL). The organic phase was dried over anhydrous Na_2SO_4, and concentrated *in vacuo* to give a mixture of **7** and **8** in a 16 : 1 ratio. Pure **7** was obtained by preparative HPLC chromatography using a 30 cm C-18 column and eluting with methanol–water (55 : 45), and isolated in 60% yield. The aqueous phase was re-used for four more times giving excellent yields in all runs.

$\delta_H(CDCl_3)$ 1.55 (s, 3H, Me-4); 1.62 (s, 3H, Me-4); 2.39 (ddd, 1H, *J* 3.6, 5.6, 11.3 Hz, H-4a); 3.82 (dd, 1H, *J* 11.3, 11.3 Hz, H-5β); 4.07 (dd, 1H, *J* 1.4, 5.6 Hz, H-10b); 4.52 (ddd, 1H, *J* 1.4, 3.6, 11.3 Hz, H-5α); 6.88–7.45 (m, 4H, aromatic). $\delta_C(CDCl_3)$ 23.6, 24.6, 33.8, 35.0, 62.6, 85.9, 101.5, 112.4, 115.1, 117.1, 121.3, 153.8. Observed NOE correlations: H-4a–H10b; H-5β–H4a.

Aknowledgements

The Ministero dell'Università e della Ricerca Scientifica e Tecnologica (MURST) and the Consiglio Nazionale delle Ricerche (CNR) are thanked for financial support.

References

1 *Pure Appl. Chem.*, 2000, **72**, entire issue; *Organic Synthesis in Water*, ed. P. A. Grieco, Blackie Academic and Professional, London, 1998; C. J. Li and T. H. Chang, in *Organic Reactions in Aqueous Media*, Wiley, New York, 1997; F. Fringuelli, O. Piermatti, F. Pizzo and L. Vaccaro, *Eur. J. Org. Chem.*, 2001, 439; S. C. Stinson, *Chem. Eng.*, 1996, **74**, 39.
2 D. Ye, F. Fringuelli, O. Piermatti and F. Pizzo, *J. Org. Chem.*, 1997, **62**, 3748.
3 F. Fringuelli, O. Piermatti and F. Pizzo, in *Trends in Heterocyclic Chemistry*, ed. O. A. Attanasi and D. Spinelli, SCI, Roma, 1998, p. 57.
4 F. Fringuelli, O. Piermatti and F. Pizzo, in *Organic Synthesis in Water*, ed. P. A. Grieco, Blackie Academic and Professional, London, 1998, p. 250.
5 F. Fringuelli, O. Piermatti and F. Pizzo, in *Organic Synthesis in Water*, ed. P. A. Grieco, Blackie Academic and Professional, London, 1998, 223.
6 F. Fringuelli, F. Pizzo and L. Vaccaro, *Synlett*, 2000, 311; F. Fringuelli, F. Pizzo and L. Vaccaro, *J. Org. Chem.*, 2001, **66**, 3554; F. Fringuelli, F. Pizzo and L. Vaccaro, *Tetrahedron Lett.*, 2001, **42**, 1131; D. Amantini, F. Fringuelli, F. Pizzo and L. Vaccaro, *J. Org. Chem.*, 2001, **66**, 4463; F. Fringuelli, F. Pizzo and L. Vaccaro, *J. Org. Chem.*, 2001, **66**, 4719.
7 F. Fringuelli, F. Pizzo and L. Vaccaro, *Synthesis*, 2000, 646.
8 A. G. M. Barrett and G. G. Graboski, *Chem. Rev.*, 1986, **86**, 751; S. E. Denmark and A. Thorarensen, *Chem. Rev.*, 1996, **96**, 137.
9 H. Feuer, in *The Chemistry of Nitro and Nitroso Groups*, Parts 1 and 2, ed. S. Patai, Wiley Interscience, New York, NY, 1969/70.
10 K. Zee-Cheng and C. Cheng, *J. Med. Chem.*, 1969, **12**, 157; S. B. Sloway, A. C. Henry, W. D. Kallmeyer, J. E. Padgett, S. A. Roman, C. H. Tieman, R. A. Corey and C. A. Horne, *Abstract of the 4th International Congress of Pesticide Chemistry*, IUPAC, Zurich, 1978, 114.
11 (*a*) D. Ranganathan, C. Bhushan Rao, S. Ranganathan, A. K. Mehrotra and R. Iyengar, *J. Org. Chem.*, 1980, **45**, 1185; (*b*) A. G. M. Barrett, *Chem. Soc. Rev.*, 1991, **20**, 95; (*c*) G. W. Kobalka and R. S. Varma, *Org. Prep. Proced. Int.*, 1987, **19**, 283; (*d*) R. Ballini and G. Bosica, *Tetrahedron Lett.*, 1996, **37**, 8027; (*e*) J. Ji, D. M. Barnes, J. Zhang, S. A. King, S. J. Wittenberg and H. E. Morton, *J. Am. Chem. Soc.*, 1999, **121**, 10215; (*f*) D. Seebach, I. M. Lyapkalo and R. Dahinden, *Helv. Chim. Acta*, 1999, **82**, 1829; (*g*) A. R. Martinez and G. Y. Moltrasio Iglesias, *J. Chem. Res. (S)*, 1998, 169.
12 D. A. K. Seebach, A. K. Beck, T. Mukhopadhyay and E. Thomas, *Helv. Chim. Acta*, 1982, **65**, 1101.
13 R. Ballini and G. Bosica, *J. Org. Chem.*, 1997, **62**, 425.
14 R. Ballini, R. Castagnani and M. Petrini, *J. Org. Chem*, 1992, **57**, 2160.

15 P. Knochel and D. Seebach, *Synthesis*, 1982, 1017.
16 J. Melton and J. E. McMurry, *J. Org. Chem.*, 1975, **40**, 2138.
17 D. Seebach and P. Knochel, *Helv. Chim. Acta*, 1984, **67**, 261.
18 A. K. Saikia, N. C. Barna, R. P. Sharma and A. C. Ghosh, *Synthesis*, 1994, 685.
19 G. Rosini, R. Ballini, M. Petrini and P. Sorrenti, *Synthesis*, 1985, 515.
20 B. P. Bandgar, M. B. Zirange and P. P. Wadgaonkari, *Synlett*, 1996, 149.
21 F. Fringuelli, M. Matteucci, O. Piermatti, F. Pizzo and M. C. Burla, *J. Org. Chem.*, 2001, **66**, 4661.
22 F. Fringuelli and F. Pizzo, unpublished results.
23 N. Nishiwaki, T. Nogami, C. Tanaka, F. Nakashima, Y. Inoue, N. Asaka, Y. Tohda and M. Ariga, *J. Org. Chem.*, 1999, **64**, 2160.
24 V. P. Kislyi, V. N. Nesterov, A. M. Shestopalov and V. V. Semenov, *Russ. Chem. Bull.*, 1999, **48**, 1135; T. Mechkov, Z. Demireva and T. Panaiotova, *Dokl. Bolg. Akad. Nauk.*, 1986, **39**, 51; Ts. Mechkov and Z. Demireva, *Z. Chem.*, 1985, **25**, 169; A. S. Polyanskaya, V. V. Perekalin, N. I. Aboskalova, Z. I. Demireva, L. N. Sokolova and Z. A. Abdulkina, *Zh. Org. Khim.*, 1979, **15**, 2057; R. A. Sheldon and J. A. Van Doorn, *J. Organomet. Chem.*, 1975, **94**, 115; J. C. Dore, P. Rumpf and C. Viel, *Chem. Ther.*, 1973, **8**, 80.
25 N. Otto, A. Kamimura, T. Kawai and A. Kaji, *J. Chem. Soc., Chem. Commun.*, 1987, 1550; T. Hayama, S. Tomoda, Y. Takeuchi and Y. Namoura, *Chem. Lett.*, 1982, **23**, 4733; T. Hayama, S. Tomoda, Y. Takeuchi and Y. Namoura, *Chem. Lett.*, 1982, **23**, 1109.
26 D. L. Boger and W. L. Corbett, *J. Org. Chem.*, 1993, **58**, 2068.
27 W. Ried and E. Köhler, *Ann. Chim.*, 1956, **598**, 145.

A single step synthesis of 2-phenylpyridine from acetophenone, ethanol, formaldehyde and ammonia over molecular sieve catalysts†

D. Venu Gopal and M. Subrahmanyam*

Catalysis Division, Indian Institute of Chemical Technology, Hyderabad, 500 007, India.
E-mail: subrahmanyam@iict.ap.nic.in

Received 12th July 2001
First published as an Advance Article on the web 7th September 2001

The vapor phase cyclization of acetophenone, ethanol, formaldehyde and ammonia to 2-phenylpyridine was carried out over HZSM-5, Hβ,HY and modified HY catalysts at 400 °C. The catalytic activity followed the order: HZSM-5 < Hβ < HY. The influence of catalyst modification, temperature, molar ratio of feed, weight hour space velocity and time on stream on the catalytic activity and selectivity for the cyclization product are investigated. The effect of pore size of the catalyst and acidity of modified zeolites on cyclization activity is discussed. The maximum yield of 2-phenylpyridine was obtained over 3 wt% cobalt-modified HY zeolite.

Introduction

Phenylpyridines are important intermediates in the synthesis of drugs, agrochemicals, herbicides, insecticides, desiccants, surfactant agents and anti-inflammatory agents.[1,2] 2-Phenylpyridine and its derivatives are widely used as ligands in the preparation of coordination complexes. It is also a starting material for the drug BMS-232632, which is a potent azapeptide HIV protease inhibitor that has shown high anti-HIV activity.[3] Traditionally 2-phenylpyridine is synthesized by the arylation of pyridine with phenyllithium[4,5] and also by the Grignard reaction.[6] It has also been photocatalytically synthesized from benzonitrile and ethylene in presence of light using a cobalt(I) complex as a catalyst.[7] However these reactions are performed in homogeneous catalysis mode with problems of catalyst recovery and tedious work up procedures. Zeolites with crystalline and uniform pore structure have proved to be efficient catalysts in acid-mediated reactions. The characteristics that make zeolites as attractive heterogeneous catalysts are a well-defined crystalline structure, a high internal surface area, uniform pores with one or two discrete sizes, the possibility of tuning acidity to a wide range, good thermal stability, shape selectivity and ease of separation. Many pyridine bases such as pyridine, picolines, lutidines and collidines have been synthesized from carbonyl compounds/alcohols with ammonia over zeolite catalysts.[8–14] However, no attempts have been made on the synthesis of large molecular size pyridine bases such as phenylpyridine and substituted phenylpyridines. Recently large pore zeolites and mesoporous molecular sieve catalysts are reported to be excellent catalysts especially for the synthesis of large molecules.[15–19] Previous work in our laboratory has established that the combination of acidity, thermal stability and uniform pore structure of a molecular sieve catalyst provides a good opportunity for the synthesis of large size molecules such as 2-methyl-6-phenylpyridine[20] and 5-methyl-2-phenylpyridine.[21] To the best of our knowledge, this is the first report of the synthesis of 2-phenylpyridine from acetophenone, ethanol, formaldehyde and ammonia over various molecular sieve catalysts in vapor phase reactions.

Experimental

The HZSM-5 (30) zeolite was obtained from Conteka (Sweden), Hβ (20) was obtained from Sud-chemie (India) and HY (2.6) zeolite was obtained from PQ Corporation (USA). The catalyst powders were pelletized and sized (18–30-mesh). A required amount of metal nitrate in aqueous medium was added to the sized catalyst to modify the surface by impregnation followed by calcination in air at 400 °C for 4 h.

Vapor phase cyclization reactions were carried out using a tubular down flow Pyrex glass reactor with 20-mm internal diameter. The catalyst (4 g) was used in the form of granules and placed in the middle of the reactor. The reactor was placed inside a temperature-controlled furnace with a thermocouple placed at the center of the catalyst bed for measuring the reaction temperature. The reaction mixture was fed from the top using a B. Brown (Germany) syringe pump. The product was cooled in a water cooled (ice-cold) condenser, collected in a receiver and analyzed by gas chromatography (Chemito 3865) using 10% SE-30 on a chromosorb HIWP packed column and products were confirmed by GC–MS and NMR spectroscopy. The best hour and fourth hour values are given in the tables. Comparison is made between different catalysts/conditions at 4 h reaction time.

Temperature programmed desorption (TPD) measurements were carried out to measure the acidity of the catalyst using ammonia as an adsorbate. In a typical run, a 0.150 g portion of catalyst was placed in a quartz tubular reactor and heated at

Green Context

One of the major causes of waste in organic reaction chemistry is multi-stage synthesis. Each step will lead to the production of waste made more damaging by the use of traditional separation methods such as solvent extraction and washing. Thus single step syntheses are very attractive. Here the novel single step synthesis of 2-phenylpyridine using solid catalysts is described. The large pore HY zeolite is particularly effective. Phenylpyridines have widespread uses in areas such as medicine and agriculture. ***JHC***

† IICT Communication No. 4718.

400 °C under a nitrogen flow of 30 cm^3 min^{-1} for 3 h and the reactor was then cooled to 25 °C and adsorption conducted at that temperature by exposing the sample to ammonia for 2 h. Physically adsorbed ammonia was removed by purging the sample with a nitrogen stream flowing at 30 cm^3 min^{-1} for 1 h at 80 °C. The acid strength distribution was obtained by raising the catalyst temperature (10 °C min^{-1}) from 80 to 600 °C in a flow of nitrogen (10 cm^3 min^{-1}). The NH_3 gas evolved was quantified by gas chromatography using a thermal conductivity detector.

Results and discussion

Catalyst characterization

The acidity of the modified HY zeolites were measured by temperature programmed desorption of ammonia and values are given in Table 1. The three peaks observed at 150–250, 250–350 and 350–450 °C correspond to desorption of NH_3 gas from weak, medium and strong acid sites, respectively, as observed also by several other groups.[22–24] The total acidity of the catalysts order followed as CuHY < PbHY < CrHY < CoHY < HY < FeHY < LaHY. As reported earlier, the HY catalyst modified by rare earth cations such as La showed slightly higher acidity than the unmodified zeolite.[25–27] The framework of the modified zeolites was checked by X-ray diffraction and FTIR measurements and crystallinity found to be retained. The surface areas of the modified zeolites were measured by the BET method and values are given in Table 1. The decrease in the surface area of the metal modified zeolites relative to the unmodified zeolite is due to the presence of metal ion and its oxide species in the cavity of the zeolites. The surface area of cobalt metal-modified HY zeolite decreases with increased loading of cobalt.

Table 1 Physical characteristics of modified HY zeolites

Catalyst	Surface area/ m^2 g^{-1}	Acidity (NH_3 desorbed) (mmol g^{-1}) 150–250	250–350	350–450 °C	Total acidity
3 wt% metal-modified HY zeolites					
HY	457.19	1.73	0.64	0.45	2.82
CrHY	411.41	1.09	0.38	0.62	2.09
FeHY	377.27	1.81	0.83	0.52	3.16
CoHY	447.16	1.62	0.61	0.23	2.46
CuHY	432.17	0.44	0.68	0.05	1.17
PbHY	448.38	0.89	0.54	0.12	1.55
LaHY	355.71	1.87	0.85	0.69	3.41
Cobalt loading on HY zeolite					
wt %	Surface area/m^2 g^{-1}				
1	450.78				
5	428.00				
10	348.35				

Catalytic activity

The vapor phase cyclization reaction of acetophenone, ethanol, formaldehyde and ammonia was carried out over HZSM-5, Hβ and HY zeolites at 400 °C with a weight hour space velocity (WHSV) of 0.5 h^{-1} and the results are given in Table 2. HZSM-5, Hβ and HY showed conversions of acetophenone of 70.4, 96.5 and 92.0% respectively. The yield of 2-phenylpyridine for HZSM-5, Hβ and HY are 12.0, 14.5 and 25.0%, respectively. The catalytic activity order with respect to the yield of 2-phenylpyridine is HZSM-5 < Hβ < HY. The yield of 2-phenylpyridine increased with increase of pore size from HZSM-5 (5.4 Å) to HY (7.4 Å). Even though a good conversion level for the HZSM-5 catalyst is seen, the low yield of the product may be due to inaccessibility or slower diffusion of the product 2-phenylpyridine through the pores of the ZSM-5 zeolite (5.4 Å). Diffusion restriction through the pores is observed only for 2-phenylpyridine with no constraints on the diffusion of other products such as pyridine, picolines and lutidines. On the other hand, the large pore HY zeolite (7.4 Å) shows higher yields of the product compared to HZSM-5, with no diffusion constraint towards 2-phenylpyridine. The lower yield of 2-phenylpyridine over Hβ compared to HY is due to secondary reactions and also may be due to slower diffusion of the product[28,29] through the pores of different geometry (pore sizes 7.6 × 6.4 and 5.5 × 5.5 Å). The pore size of the catalyst must be accessible to reactant and product molecules in order for the reaction to occur.

Reactions were then carried out over 3 wt% La, Pb Co, Cu, Cr and Fe metal ion-modified HY zeolites at 400 °C at 0.5 h^{-1} weight hour space velocity and results are given in Table 3. The cyclization activity as reflected in the yield of 2-phenylpyridine followed the order: CoHY > CrHY > FeHY > PbHY > HY > CuHY > LaHY. No drastic change in the catalytic activity was observed upon modification by metal ions which may be attributed to the presence of several competitive and parallel reactions in a multi-reactant process. The high acidity of LaHY and FeHY enhances the formation of side products thus leading to a lower selectivity and yield of 2-phenylpyridine. The maximum yield of 2-phenylpyridine was obtained over medium acidic 3 wt% CoHY catalyst. Earlier reports on the synthesis of pyridine, picolines and lutidines from carbonyl compounds and ammonia also reveal that the cobalt-modified zeolites are active for this type of aminocyclization reaction.[12,30] In order to gain more insight into the cyclization reaction the process parameters like effect of wt% of metal, variation of molar ratio of the reactants, weight hour space velocity, and time on stream product distribution have been studied over the 3 wt% CoHY catalyst.

The effect of variation of cobalt loading on HY zeolite on the cyclization reaction is shown in Fig. 1. The optimum percentage of loading was found to be 3 wt%.

Further increase in the amount of cobalt decreased the conversion of acetophenone and yield of the 2-phenylpyridine

Table 2 Synthesis of 2-phenylpyridine from acetophenone, ethanol, formaldehyde and ammonia over modified HY zeolites. Reaction temperature = 400 °C; WHSV = 0.5 h^{-1}. Feed = acetophenone–ethanol–formaldehyde–ammonia = (1 : 1 : 1 : 5) (mole ratio)

Catalyst	TOS/h	Conversion of acetophenone (wt%)	Yield (wt%) 2-PP	Alkylpyridines	5,2-MPP	Others
HZSM-5	2	92.9	19.8	24.2	11.6	37.3
	4	70.4	12.0	28.4	—	30.2
Hβ	1	97.2	20.6	24.7	9.2	42.7
	4	96.5	14.5	29.9	7.7	44.4
HY	1	92.7	31.1	18.3	14.2	28.8
	4	92.0	25.0	22.1	11.2	33.7

2-PP = 2-phenylpyridine; 5,2-MPP = 5-methyl-2-phenylpyridine; alkylpyridines = pyridine, isomers of picoline and lutidine; others = isomers of alkylphenylpyridine, 2,6-diphenylpyridine and acetophenone aldol condensation products. TOS = time on stream (best 1 h and 4 h values).

which may be due the decrease in surface area of the catalyst (Table 1).

The reaction temperature was varied from 300 to 425 °C for the reaction of acetophenone, ethanol, formaldehyde and ammonia over 3 wt% CoHY zeolite and the results are shown in Fig. 2. The maximum yield of 2-phenylpyridine was observed at 400 °C. The yield of 2-phenylpyridine increased with an increase in the reaction temperature from 300 to 400 °C. This may be due to the adsorption of ammonia at lower temperatures, thus blocking the active sites for the reaction to proceed. As the temperature was increased, ammonia starts desorbing making the active sites available for the reaction to occur. Further increase in the temperature above 400 °C decreases the conversion levels and yield of 2-phenylpyridine which may be due to coke formation.

The effect of the molar ratio for the synthesis of 2-phenylpyridine was studied from 0.5:1 to 2:1 molar ratio of acetophenone to ethanol while keeping the formaldehyde and ammonia levels constant, and the results are shown in Fig. 3. The maximum yield of 2-phenylpyridine was obtained at 1:1 molar ratio of acetophenone to ethanol. An increase of either of the reactants leads to decrease in the yield of 2-phenylpyridine. An increase in the molar ratio of acetophenone to ethanol decreases the acetophenone conversion and yield of 2-phenylpyridine due to the non-availability of the required number of ethanol molecules for the cyclization reaction to occur. The decrease in the yield of 2-phenylpyridine is also due to the aldolization of acetophenone giving side products. A decrease in the molar ratio of acetophenone to ethanol in the feed leads to an increase in the formation of pyridine and isomers of picolines and lutidine compounds formation and thus decreases the yield of 2-phenylpyridine.

Variation of weight hour space velocity (WHSV) on the aminocyclization of acetophenone, ethanol, formaldehyde and ammonia was studied in the range 0.25–1 h^{-1} and the results are given in Fig. 4. The yield of 2-phenylpyridine decreased with an increase of WHSV beyond 0.5 h^{-1} due to the decrease in the contact time between reactants and active sites of the catalyst. The maximum yield of 2-phenylpyridine was obtained at a WHSV of 0.5 h^{-1}.

The effect of time on stream on cyclization reaction was studied for 10 h over 3 wt% CoHY catalyst at 400 °C and 0.5 h^{-1} weight hour space velocity and the results are given in Fig. 5. The catalytic activity was found to be constant for the first 5 h, with subsequent deactivation probably due to coke formation.

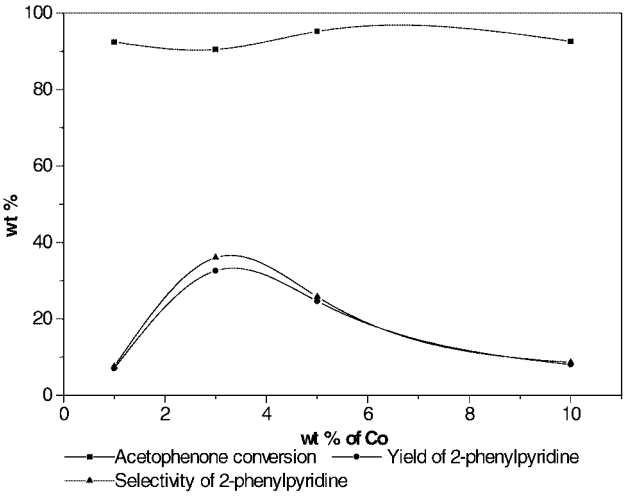

Fig. 1 Effect of wt% of Co in HY zeolite on the synthesis of 2-phenylpyridine. Reaction temperature = 400 °C; WHSV = 0.5 h^{-1}; time on stream = 4 h. Feed = acetophenone–ethanol–formaldehyde–ammonia (1:1:1:5) (mole ratio).

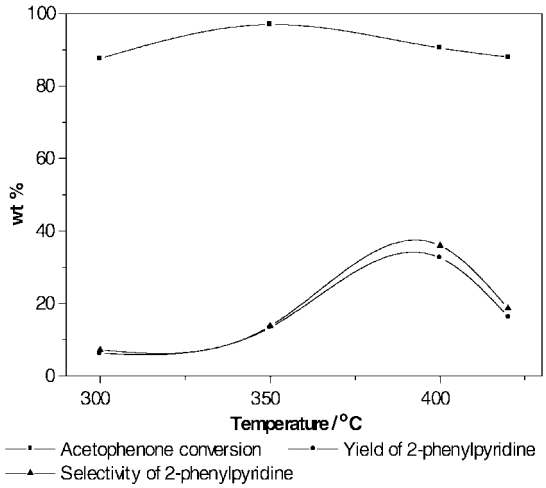

Fig. 2 Effect of temperature on synthesis of 2-phenylpyridine over 3 wt% CoHY zeolite. Feed = acetophenone–ethanol–formaldehyde–ammonia (1:1:1:5) (mole ratio); WHSV = 0.5 h^{-1}; time on stream = 4 h.

Table 3 Synthesis of 2-phenylpyridine over 3 wt% metal-modified HY zeolites. Reaction temperature = 400 °C; WHSV = 0.5 h^{-1}. Feed = acetophenone–ethanol–formaldehyde–ammonia = (1:1:1:5) (mole ratio)

Catalyst	TOS/h	Conversion of acetophenone (wt%)	Yield (wt%)					Selectivity of 2-PP (%)
			2-PP	Alkylpyridines	2,6-MPP	5,2-MPP	Others	
HY	1	92.7	31.1	18.3	0.3	14.2	28.8	33.5
	4	92.0	25.0	22.1	1.9	11.2	21.8	28.3
CrHY	4	91.9	30.1	22.1	1.4	10.5	27.8	32.7
FeHY	1	91.9	29.1	20.1	0.2	10.1	32.4	31.7
	4	91.6	26.5	14.5	0.3	10.0	40.6	28.9
CoHY	2	94.5	38.6	16.6	0.1	12.2	27.1	40.8
	4	90.5	32.6	19.1	0.2	8.6	29.9	36.0
CuHY	1	93.2	34.4	10.2	2.9	11.6	34.1	36.9
	4	94.0	24.4	13.6	0.8	11.5	43.7	26.0
PbHY	4	92.2	26.1	14.5	0.2	10.0	41.4	28.3
LaHY	4	94.2	20.8	25.7	2.3	16.7	28.7	22.8

2-PP = 2-phenylpyridine; 2,6-MPP = 2-methyl-6-phenylpyridine; 5,2-MPP = 5-methyl-2-phenylpyridine; alkylpyridines = pyridine, isomers of picoline and lutidine; others = isomers of alkylphenylpyridine, 2,6-diphenylpyridine and acetophenone aldol condensation products. TOS = time on stream (best 1 h and 4 h values).

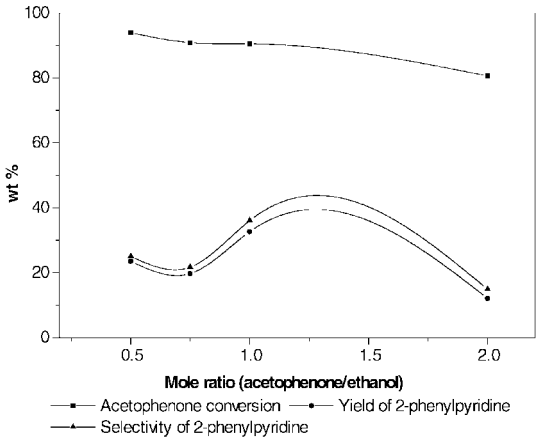

Fig. 3 Effect of molar ratio of acetophenone to ethanol on the synthesis of 2-phenylpyridine over 3 wt% CoHY zeolite. Reaction temperature = 400 °C; WHSV = 0.5 h^{-1}; time on stream = 4 h.

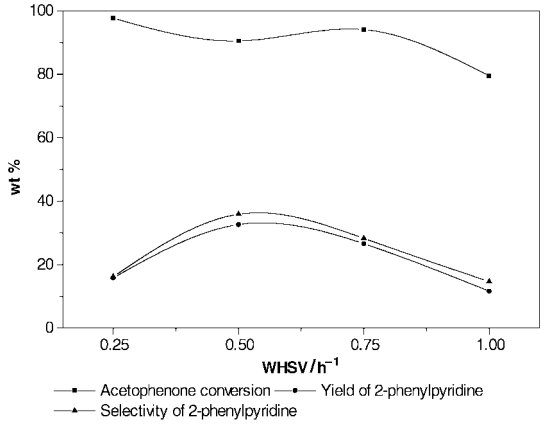

Fig. 4 Effect of weight hour space velocity (WHSV) on the synthesis of 2-phenylpyridine over 3 wt% CoHY zeolite. Feed = acetophenone–ethanol–formaldehyde–ammonia = (1 : 1 : 1 : 5) (mole ratio), reaction temperature = 400 °C; time on stream = 4 h.

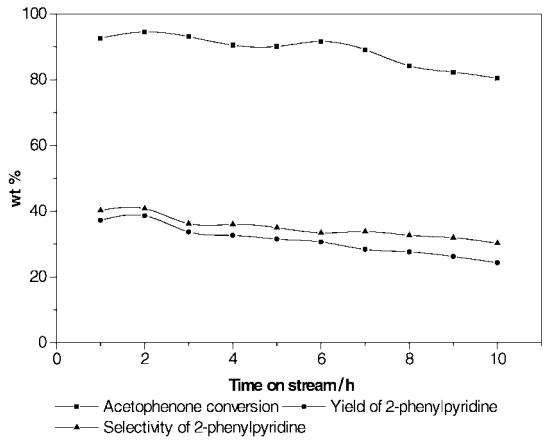

Fig. 5 Effect of time on stream on the synthesis of 2-phenylpyridine over 3 wt% CoHY zeolite. Feed = acetophenone–ethanol–formaldehyde–ammonia = 1 : 1 : 1 : 5 (mole ratio); reaction temperature = 400 °C; WHSV = 0.5 h^{-1}.

Reaction mechanism

A plausible mechanism for the reaction of acetophenone, ethanol, formaldehyde and ammonia over zeolite catalyst is shown in Scheme 1. The reaction of acetophenone with ammonia gives rise to the formation of corresponding imine. Ethanol may be oxidized to acetaldehyde and the subsequent reaction with ammonia results in the formation of the corresponding imine. Thus formed, two molecules of imine react with formaldehyde. The resulting cyclization and dehydrogenation lead to the formation of 2-phenylpyridine. The formation of pyridine, picolines and lutidines from the reaction of ethanol, formaldehyde and ammonia has been reported earlier.[12–14,30]

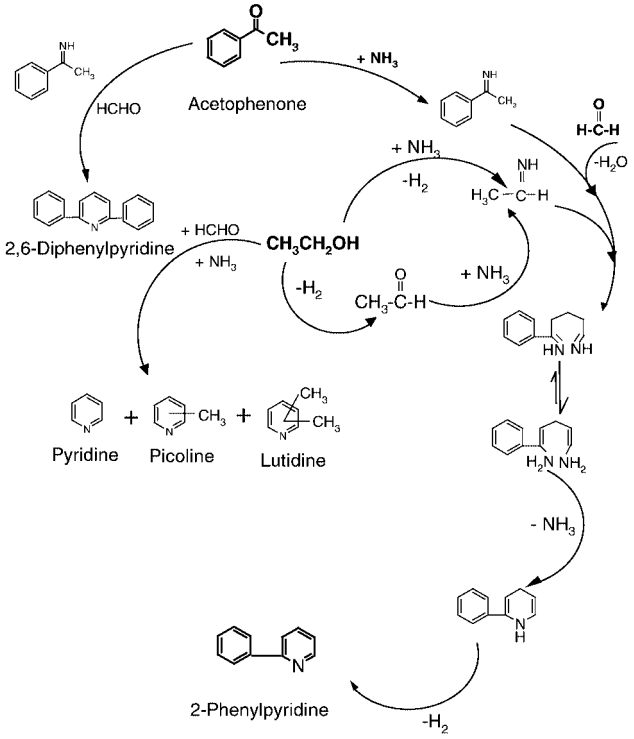

Scheme 1 A plausible reaction mechanism for the synthesis of 2-phenylpyridine from acetophenone, ethanol, formaldehyde and ammonia over molecular sieve catalysts.

Conclusions

Vapor phase cyclization of acetophenone, ethanol, formaldehyde and ammonia involves multiple reactions, which leads to the formation of 2-phenylpyridine as the major product as well as other products such as isomeric substituted phenylpyridines, pyridine, picolines and lutidines *etc*. The large pore size of the HY zeolite offers no constraints for the diffusion of the product and thus shows high activity compared to the medium pore HZSM-5 catalyst. High acidity/temperatures result in eventual deactivation. The maximum yield of 2-phenylpyridine was obtained over a medium acidic 3 wt% CoHY catalyst at 400 °C.

References

1 S. Shimizu, N. Abe, N. Goto, T. Niwa and A. Iguchi, *Jpn. Pat*., JP 01261367A, 1998.
2 S. Peter, H. Gerhard, H. Elisabeth, K. Ralf, K. Hartmann, H. Albrecht, G. Norbert, W. Helmut, W. Karl-Otto and M. Ulf, *US Pat*., US 5 733 850, 1998.
3 X. Rabasseda, J. Silverstre and J. Castaner, *Drugs Fut*., 1999, **24**, 375.
4 M. T. Dupriest, C. L. Schmidt, D. Kuzmich and S. B. Williams, *J. Org. Chem*., 1986, **51**, 2021.
5 F. Littke, C. Dai and G. C. Fu, *J. Am. Chem. Soc*., 2000, **122**, 4020.
6 Daniel. Comins and Abdul H. Abdullah, *J. Org. Chem*., 1982, **47**, 4315.
7 B. Heller and G. Oehme, *J. Chem. Soc., Chem. Commun*., 1995, 179.
8 S. E. Golunski and D. Jackson, *Appl. Catal. A*, 1986, **23**, 1.

9 S. J. Kulkarni and M. Subrahmanyam, *Indian J. Chem. A*, 1991, **30**, 1041.
10 S. J. Kulkarni, *Stud. Surf. Sci. Catal*., 1998, **113**, 151.
11 A. V. Rama Rao, S. J. Kulkarni and M. Subrahmanyam, *Appl. Catal. A*, 1994, **111**, 101.
12 S. Shimizu, N. Abe, A. Iguchi, M. Dohba, H. Sato and K. Hirose, *Microporous Mesoporous Mater*., 1998, **21**, 447.
13 S. J. Kulkarni, R. Ramachandra Rao, M. Subrahmanyam and A. V. Rama Rao, *Appl. Catal. A*, 1994, **113**, 1.
14 R. Ramachandra Rao, S. J. Kulkarni, M. Subrahmanyam and A. V. Rama Rao, *React. Kinet. Catal. Lett*., 1995, **56**, 301.
15 E. Armengol, M. L. Cano, A. Corma, H. Garcia and M. T. Navarro, *J. Chem. Soc., Chem. Commun*., 1995, 519.
16 Rodriguez, M. J. Climent, S. Iborra, V. Fornes and A. Corma, *J. Catal*., 2000, **192**, 441.
17 A. Corma, V. Fornes, J. Matinez-Triguero and S. B. Pergher, *J. Catal*., 1999, **186**, 57.
18 M. J. Climent, A. Corma, I. Rodriguez, S. Iborra, S. Miquel, J. Primo and F. Rey, *J. Catal*., 1999, **183**, 76.
19 J. P. G. Pater, P. A. Jacobs and J. A. Martens, *J. Catal*., 1999, **18**, 262.
20 D. Venu Gopal, N. Srinivas, B. Srinivas, S. J. Kulkarni and M. Subrahmanyam, *Green Chem*., 2001, **3**, 65.
21 D. Venu Gopal and M. Subrahmanyam, *Green Chem*., 2001, **3**, 181.
22 J. R. Anderson, K. Foger, T. Mole, R. A. Rajadhyaksha and J. V. Sanders, *J. Catal*., 1979, **58**, 114.
23 N. Topsoe, K. Pedersen and E. G. Derouane, *J. Catal*., 1981, **70**, 41.
24 G. P. Babu, S. G. Hegde, S. B. Kulkarni and P. Ratnasamy, *J. Catal*., 1983, **81**, 471.
25 P. Ram Reddy, M. Subrahmanyam and S. J. Kulkarni, *Catal. Lett*., 1998, **54**, 95.
26 P. Ram Reddy, M. Subrahmanyam and V. Durga Kumari, *Catal. Lett*., 1999, **60**, 161.
27 F. O. J. Connor and T. P. Rodney, *Zeolites*, 1985, **5**, 158.
28 J. Aguilar , A. Corma, F. V. Melo and E. Sastre, *Catal. Today*, 2000, **55**, 225.
29 J. Horniakova, D. Mravec, S. Fabokova, M. Hronec and P. Moreau, *Appl. Catal. A*, 2000, **203**, 47.
30 S. Shimizu, N. Abe, A. Iguchi and H. Sato, *Catal. Surv. Jpn*., 1998, **2**, 71.

Low-toxicity red ceramic pigments for porcelainised stoneware from lanthanide–cerianite solid solutions

A. García, M. Llusar, J. Calbo, M. A. Tena and G. Monrós

Dpt. of Inorganic and Organic Chemistry, University Jaume I, Castellón, Spain.
E-mail: monros@qio.uji.es

Received 3rd July 2001
First published as an Advance Article on the web 13th September 2001

$Ln–CeO_2$ (Ln = Pr, Tb, Eu) and $M–CeO_2$ solid solutions (reference samples with M = Cr or In, as transition and main group elements, respectively) have been prepared by ceramic and coprecipitation routes. The resulting coloured materials have been checked as potential pigments for porcelainised stoneware. The colouring mechanism is based on the introduction of an additional electronic level of energy in cerianite forbidden band, arising from unpaired 4f electrons of lanthanide ions. The red ceramic pigments obtained have been found to be interesting alternatives for the coloration of porcelainised stoneware bodies. In addition, they present a much lower toxicity than classical cadmium sulfoselenide or chromium–$LnAlO_3$ based red pigments, because both the chromophoric agent (praseodymium and europium ions) and ceramic matrix (cerianite) contain lanthanide elements.

Introduction

The designation 'rare earth' attributed to lanthanide elements could be considered inadequate because of their relative abundance on earth. In fact, they are much more abundant than other considered 'ordinary' elements (*i.e.* cerium is more abundant than copper and neodymium goes beyond lead or cobalt). Lanthanides appear in clays as carbonates, phosphates, oxides or as absorbed ions. Monacite and bastanesite minerals are a mixture of carbonates or phosphates of light lanthanides [from La (Z = 57) to Eu (Z = 63)] rich in cerium, called ceric ores in contrast to yttric ores which are rich in yttrium. Monazite is a complex thorium–lanthanide orthophosphate ($LnThPO_4$), found as a by-product in ilmenite ores, and bastnaesite is a fluoride carbonate of lanthanide elements ($LnFCO_3$), relatively rich in europium. The similar and relatively high ionic radius of trivalent ions from cerium to europium is the main cause of their simultaneous presence in minerals, and their separation is often very difficult.[1]

Industrial utilisation of lanthanides is growing very rapidly because of their known low toxicity. The main industrial application in the field of lanthanides is the ceramic industry, which consumes up to 31% world production of lanthanide compounds. CeO_2 promotes opacity in ceramic glazes, and the so-called yellow of praseodymium–zircon colour is the best commercial yellow ceramic pigment. Similarly, cerium sulfide has substituted the orange and red colours based on the cadmium sulfoselenide pigment used in the ceramic and painting industries.

The electronic configuration of the valence layer of the trivalent lanthanide ions, $[Xe]4f^n$, involves the activity of internal f electrons, strongly protected by 5s and 5p electrons. Therefore, the resulting crystalline field caused by their interaction with neighbouring ions is very low and usually optical spectra of lanthanide compounds present weak and profuse bands.

The use of low-toxicity raw materials in the chemical industry is becoming increasingly favored in order to prevent both health hazards in the workplace and/or environmental damage. In order to satisfy these requirements, research on the utilisation of lanthanide compounds should be encouraged, because of their proven low toxicity.[2]

In the field of ceramic pigments, it is necessary to obtain pigments with some desired properties: (a) high thermal stability at temperatures around 1200 °C (reached during the single firing of porcelainised stoneware), (b) chemical stability towards the vitreous phases coloured by the pigment, and (c) low toxicity, in order to satisfy health and environmental requirements.

Only a limited number of structures exhibit these properties, and this number is even more restricted in the case of red or pink pigments.[3] $Fe_2O_3–ZrSiO_4$ and $Cd(S_xSe_{1-x})$-$ZrSiO_4$ heteromorphic pigments, based on inclusion in to the zircon structure of hematite or cadmium sulfoselenide, respectively, are employed traditionally. Zircon crystals protect the occluded red Fe_2O_3 or $Cd(S_xSe_{1-x})$ chromophore crystals from vitreous phases. However, the resulting colour of both pigments does not achieve the desired colour intensity and/or pure shades.[4,5] Recently, a red colour based on a $Ln_x(Al_{2-x-y}Cr_y)O_3$ (Ln = lanthanide element) perovskite solid solution has been reported[6] using chromium(III) oxide or sometimes chromium(VI) salts. Chromium(III) compounds do not show inherent toxicity but their use is being controlled, *e.g.* Decision 2001/118/CE (CEOJ 2001-2-16) of the European Commission related to hazardous wastes, owing to the possibility of oxidation to Cr(VI) which is a proven carcinogenic substance.

Green Context

Growing concern over the safety and environmental compatibility of consumer goods is making product substitution one of the most important aspects of green chemistry. The use of chemicals to produce colours for various applications is one of the oldest examples of applied chemistry but the requirements for colours will become increasingly demanding. For ceramic pigments for example, the products must be thermally stable to very high temperatures, chemically stable and meet health and safety requirements. Few currently used pigments properly satisfy these requirements but here is described a new low-toxicity red ceramic pigment for procelain. It is based on readily available lanthanides.
JHC

 DOI: 10.1039/b105830b

Since 1960, the red pigment based on a cerianite lattice doped with praseodymium has been known.[7] However, the red colour is lost when working at the relatively high temperatures (1200 °C) employed during the enamel firing of ceramic bodies such as porcelainised stoneware. Indeed, the colour becomes orange when the working temperature is increased, but high firing temperatures (1000–1300 °C) and/or long soaking time (15–48 h) are necessary to attain the colour.

On the other hand, addition of halides as flux agents is necessary in the preparation of the above three pigments, and the colouring mechanism leading to the red colour becomes very different in each case.

In heteromorphic pigments based on zircon lattice, the colour is due to the inclusion of red crystals (hematite or cadmium sulfoselenide) into zircon crystals.

In the red perovskite pigments $Ln_x(Al_{2-x-y}Cr_y)O_3$,[8,9] the colour is due to the introduction of Cr^{3+} ions into AlO_6 octahedra of the $LnAlO_3$ perovskite lattice, substituting for Al^{3+} ions. The chromium(III) ion has a larger ionic radius than the aluminium(III) ion (Pauling ionic radius values for six-coordination of 0.69 and 0.5 Å respectively). In an octahedral crystalline field of oxygen ions, as in Cr_2O_3 oxide, Cr(III) presents two absorption bands due to the $^4A_{2g}\rightarrow{}^4T_{1g}$ transition (blue) and $^4A_{2g}\rightarrow{}^4T_{2g}$ transition (yellow). In the perovskite $LnAlO_3$ lattice, the crystalline field around Cr^{3+} can be controlled by the ionic radius of Ln^{3+} ion located in the centre of the fcc lattice described by Al^{3+} (edge positions) and O^{2-} ions. If the Ln^{3+} size is increased (La, Sm, Gd, Y), the Cr–O distance decreases, and the resulting high tetragonal distortion of d orbitals of chromium(III) enhances the crystalline field over the ion. Consequently the absorption bands shift to higher frequencies and the yellow $^4A_{2g}\rightarrow{}^4T_{2g}$ transition shifts to green wavelengths resulting in a red reflection. $Y(AlCr)O_3$ solid solutions are found to show the best red colour of the $Ln_x(Al_{2-x-y}Cr_y)O_3$ series.

Finally in cerianite doped red pigments, the colouring mechanism is based on the shift of the charge transfer band of the semiconductor CeO_2 to higher wavelengths, introducing an additional electronic level by doping. CeO_2 crystallises in the fluorite structure, where fcc packed Ce^{4+} ions are surrounded by eight oxygens, occupying alternate centres of tetrahedral cavities in the fcc lattice.[7,10,11] The 4f valence shell of Ce^{4+}([Xe]) in cerianite is empty, and that of O^{2-} ([Ne]$2s^22p^6$) is full: adjacent Ce^{4+} ions are virtually in contact in the fluorite lattice and, as a result, 4f orbitals overlap in a cationic conduction band; similarly, overlap of 2p orbitals of oxygen ions gives to an anionic valence band. The band gap between the anionic band and the cationic band is 2.76 eV. By doping CeO_2 with Pr^{4+} ions, the $4f^1$ electron of the praseodymium valence shell introduces an additional electronic level of energy between the O^{2-} valence band and Ce^{4+} conduction band, and a reduced band gap of 1.94 eV is observed. The CeO_2 band gap falls in indigo region of visible wavelengths, and a complementary light yellow colour is observed. By contrast, Pr^{4+}–CeO_2 absorbs in the wavelength region below 600 nm producing a red colour.[9,10]

In this work Ln–CeO_2 solid solutions (Ln = Pr, Tb, Eu), and also M–CeO_2 samples used as reference (M = Cr or In as transition and main group elements respectively), have been prepared by ceramic and by hydroxide coprecipitation routes. The resulting coloured materials have been checked as potential low-toxicity red pigments for porcelainised stoneware bodies.

Preparation and characterisation of samples

The composition of the prepared samples and the precursors (supplied by IMATRA S.A.) used in the preparation of the samples are given in Table 1.

In the ceramic method, precursors were homogenised in a planetary ball mill in acetone media. In the coprecipitation route, the steps followed to prepare the samples are shown in Fig. 1. The necessary amount (to obtain 10 g of the final oxide product), of the precursor of chromophore ion (M = Pr, Tb, Eu, Cr, In), was dissolved in 20 mL of concentrated HCl continuously stirred at 60 °C until complete dissolution (this was not necessary for the chromium sample). This chromophore solution was added to $CeCl_3{\cdot}7H_2O$ previously dissolved in 200 mL of water, and then precipitated with a solution of concentrated ammonia until pH 8. The obtained coprecipitate was dried in a heater at 110 °C and then mixed with the flux agent in acetone media using a ball mill.

All samples were fired at 1150 °C with 6 h of soaking time. Since at this temperature the ceramic samples remain unreacted and colorless, they were fired at 1300 °C for 6 h in order to attain the pigment.

The characterisation of samples was carried out by several techniques. XRD patterns were obtained in an Philips D-500 diffractometer in order to detect the crystalline phases present in the samples and to measure the cell unit parameters. For the calculation of the cell parameters, XRD runs using α-Al_2O_3 as internal standard were carried out, and the results were analysed with the POWCAL and LSQC programs.[12]

In order to analyse the properties as ceramic pigments, the samples were 2% weight enamelled in porcelainised stoneware and fired for 5 min at 1185 °C in a single-firing cycle of 47 min (cold-to-cold). UV–VIS–NIR spectra of samples were collected by the diffuse reflectance technique using a Lambda 2 spectrophotometer supplied by Perkin Elmer. Colour parameters of enamelled samples were measured using the same spectrophotometer following the CIE-$L^*a^*b^*$ convention:[13] in this system, L^* measures the brightness, a^* the amount of green(−)→red(+) colour, and b^* the amount of blue(−)→yellow(+). Finally, SEM-EDX characterisation was carried out using a LEO.2i electronic microscope equipped with an Oxford microanalysis system, in order to analyse the microstructure of the samples.

Experimental results and discussion

The compositions prepared and the precursors (and fluxes) employed are given in Table 1.

Solution of oxide precursor in concentrated HCl
media
↓
(stirring,60 °C)
↓
water addition (up to 250 mL)
↓
addition of precursor of cromophore ion
↓
dropwise addition of concentrated NH_3
until pH 8
↓
drying 110 °C
↓
addition of flux agents
↓
homogenisation in acetone media
↓
firing
1150 °C/6 h

Fig. 1 Preparation of coprecipitated samples for 10 g of final product.

For the praseodymium-doped ceramic sample four types of fluxing agents were tested in order to select the most appropriate mineralisation: (a) a mixture of alkaline-earth fluorides (BaF_2 + MgF_2 sample PrCI), (b) complex halides [Na_3AlF_6 (cryolite) in sample PrCII and Na_2SiF_6 in sample PrCIII], and (c) a mixture of alkaline halides (NaF + NaCl in sample PrCIV).

Samples prepared by the ceramic route had to be annealed at 1300 °C in order to obtain a brown coloured powder; and the Na_2SiF_6-fluxed sample (PrCIII sample) was not suitable as a ceramic pigment, since it produced a highly sintered material.

Colour characterisation

When these ceramic samples were enamelled with a porcelainised stoneware matrix, the colour disappeared in cryolite-fluxed sample (PrCII) and produced a light pink colour in samples fluxed with both BaF_2–MgF_2 (PrCI) and NaF-NaCl (PrCIV) ($L^*/a^*/b^*$ = 85/3/10). By contrast, the red colour remained when the matrix was a glaze for single-firing conventional gres (firing at only 1140 °C, with 5 min of soaking time and 40 min from cold-to-cold). In effect, 5% of the ceramic powder fluxed with BaF_2–MgF_2 (fired at 1300 °C/6 h) produced an orange shade ($L^*/a^*/b^*$ = 84.3/6.8/13.1) enamelled in this glaze. Considering these results, the BaF_2–MgF_2 mixture was selected as mineraliser in the coprecipitation route.

The crystalline phases detected by XRD analysis, the visual colour of the fired powders, and the CIE $L^*a^*b^*$ parameters of enamelled samples (in porcelainised stoneware) are shown in Table 2. The XRD pattern of the PrGI sample is also shown in Fig. 2.

In all samples only CeO_2 was detected by XRD (Fig. 2), and only the coprecipitated samples PrGI, PrGII and EuG exhibited a reddish coloration in the porcelainised stoneware ($L^*/a^*/b^*$ = 75.8/8.2/17.5, 76.3/8.5/17.2 and 78.2/7.2/20.3, respectively). Increasing the amount of praseodymium from 0.1 mol (PrGI sample) to 0.15 (PrGII sample) did not significantly enhance the colour intensity.

UV–VIS–NIR spectroscopy

The UV–VIS–NIR absorption spectra for the enamelled samples are shown in Fig. 3. Some differences may be ascertained in the spectra that can explain the colour performance of the samples.

For CrG and InG samples, no shift of the charge transfer band of CeO_2 is observed, and the threshold wavelength of optical absorption is 450 nm (related to a band gap of 2.76 eV). For the terbium sample (TbG), a new absorption band may be observed around 380 nm, though the threshold wavelength of optical absorption remains at 450 nm, similarly to the CrG and InG samples.

However, doping with Pr results in the appearance of a new charge transfer band centred at 485 nm showing a threshold wavelength at 640 nm (associated with a band gap of 1.94 eV). Finally, in the case of the Eu-doped sample the behaviour is similar to the PrGI sample, though the absorption band is less intense and the threshold wavelength is 620 nm (band gap 1.99 eV).

Cell parameter measurements

The measurement of cell parameter for the PrGI sample indicates that the parameter a increases associated with the incorporation of Pr^{4+} ions (Shannon–Prewitt ionic radius 0.92 Å),[14] substituting Ce^{4+} ions (1.01 Å) in the CeO_2 lattice. The $4f^1$ electron of the Pr^{4+} valence shell introduces an additional electronic level of energy between the O^{2-} valence band and Ce^{4+} conduction band, and the modified band gap is 1.94 eV.[8–10]

In the europium EuG sample, which shows similar optical behaviour to the PrGI sample, cell measurements also indicate a shrinkage when europium ions enter into cerianite lattice, with both Eu^{2+} (1.31 Å) and Eu^{3+} (1.087 Å) being larger than Ce^{4+}. A mechanism of introduction of O^{2-} vacancies can be considered in order to preserve the electroneutrality of the system producing the observed shrinkage of the cell. However, halide anions have been used as mineralisers and the possibility to substitute the oxygen sublattice by halides in other systems is

Table 2 Characteristics of samples fired at 1150 °C/6 h

Sample	XRD	Visual colour (powder)	$L^*/a^*/b^*$ (2 wt% in gres)	a/Å[a]
PrCI (1300 °C/6 h)	CeO_2	Red-brown	85/3/10 84.3/6.8/13.2[b]	—
PrGI	CeO_2	Red-brown	75.8/8.2/17.5	5.370(2)
PrGII	CeO_2	Red-brown	76.3/8.5/17.2	—
CrG	CeO_2	Cream	80.4/2.0/15.6	5.412(1)
TbG	CeO_2	Light pink	85.4/1.7/13.1	5.417(1)
EuG	CeO_2	Brown	78.2/7.2/20.3	5.396(1)
InG	CeO_2	Cream	83.0/2.0/15.3	5.410(1)

[a] a = 5.41134 Å in CeO_2 (JCPDS 43-1002). [b] 5% in glaze.

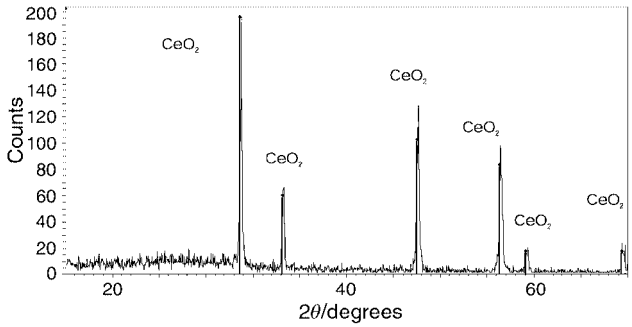

Fig. 2 XRD diffractogram of the PrGI sample fired at 1150 °C/6 h.

Table 1 Composition, flux agents and precursors for samples

	Sample	Composition	Flux (mol%)	Method	Precursor(s)
	PrCI	$Ce_{0.9}Pr_{0.1}O_2$	0.2 BaF_2/0.2 MgF_2	Ceramic	CeO_2/Pr_6O_{11}
	PrCII	$Ce_{0.9}Pr_{0.1}O_2$	0.2 Na_3AlF_6	Ceramic	CeO_2/Pr_6O_{11}
	PrCIII	$Ce_{0.9}Pr_{0.1}O_2$	0.2 NaF/0.3 Na_2SiF_6	Ceramic	CeO_2/Pr_6O_{11}
	PrCIV	$Ce_{0.9}Pr_{0.1}O_2$	0.3 NaF/0.6 NaCl	Ceramic	CeO_2/Pr_6O_{11}
	PrGI	$Ce_{0.9}Pr_{0.1}O_2$	0.2 BaF_2/0.2 MgF_2	Coprecipitation	$CeCl_3/Pr_6O_{11}$
	PrGII	$Ce_{0.85}Pr_{0.15}O_2$	0.2 BaF_2/0.2 MgF_2	Coprecipitation	$CeCl_3/Pr_6O_{11}$
	CrG	$Ce_{0.9}Cr_{0.1}O_2$	0.2 BaF_2/0.2 MgF_2	Coprecipitation	$CeCl_3/CrCl_3{\cdot}7H_2O$
	TbG	$Ce_{0.9}Tb_{0.1}O_2$	0.2 BaF_2/0.2 MgF_2	Coprecipitation	$CeCl_3/Tb_4O_7$
	EuG	$Ce_{0.9}Eu_{0.1}O_2$	0.2 BaF_2/0.2 MgF_2	Coprecipitation	$CeCl_3/Eu_2O_3$
	InG	$Ce_{0.9}In_{0.1}O_2$	0.2 BaF_2/0.2 MgF_2	Coprecipitation	$CeCl_3/In_2O_3$

well known.[15] Oxygen vacancies or halide substitution can explain the observed cell shrinkage in europium–cerianite solid solutions and crystallographic studies should be accomplished in the future in order to establish the true mechanism. The unpaired $4f^7$ electrons of the Eu^{2+} or $4f^6$ of the Eu^{3+} valence shell introduce an additional electronic level of energy, and the modified band gap is 1.99 eV.

The TbG sample presents higher cell parameters than the CeO_2 undoped sample (Table 2). The introduction of the relatively large Tb^{3+} can explain this behaviour, and is associated with the band observed at 380 nm in the UV–VIS spectra of TbG samples (Fig. 3 and 4 show enamelled and powder TbG sample spectra, respectively). Introduction of Tb^{4+} produces an additional band in the visible region around 480 nm and the powder has a reddish colour (Fig. 4). However, in the enamelling porcelainised stoneware firing process sample loses the colour owing to destabilisation of Tb^{4+} (the 480 nm band disappears but the 380 nm shoulder is observed in Fig. 3).

Finally with Cr (transition metal) and In (main group) elements, the cell parameter (CrG and InG samples in Table 2) is the same as in the undoped sample, indicating that Cr and In do not enter into solid solution with the cerianite lattice.

Microstructure characterisation (SEM-EDX)

SEM micrographs of samples are shown in Fig. 5. All samples show micrometric particles (0.5–1 μm particle size range) which aggregate into clusters especially in lanthanide-coprecipitated samples (5–20 μm) more than in Cr and In samples (3 μm). Ceramic samples show high aggregation [30–100 μm in Fig. 5(a)].

EDX microanalysis indicates a segregation of Mg (flux agent) in samples (Fig. 6). The lanthanide ions Pr, Tb and Eu are homogeneously distributed in the particles at a molar concentration of *ca.* 7.6% (the amount initially introduced in the raw samples is 10%). Cr and In ions were not detected by the EDX technique, probably owing to volatilisation in the firing process. The homogeneous distribution of the lanthanides is in accord with solid solution formation into the cerianite lattice as discussed above.

The coprecipitation route of preparation of raw powders leads to solid solutions being obtained at lower temperatures

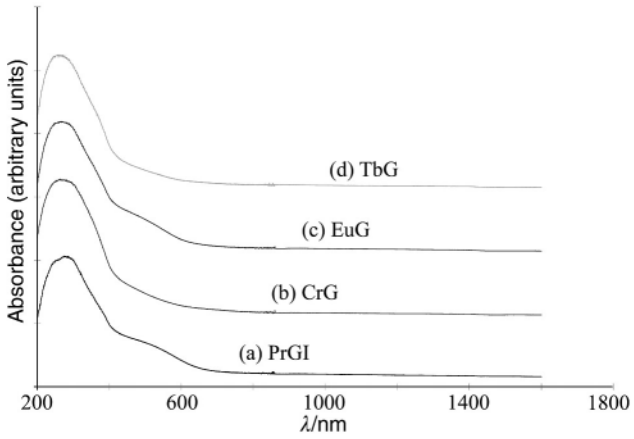

Fig. 3 UV–VIS–NIR spectra: (a) PrGI, (b) CrG, (c) EuG, (d) TbG.

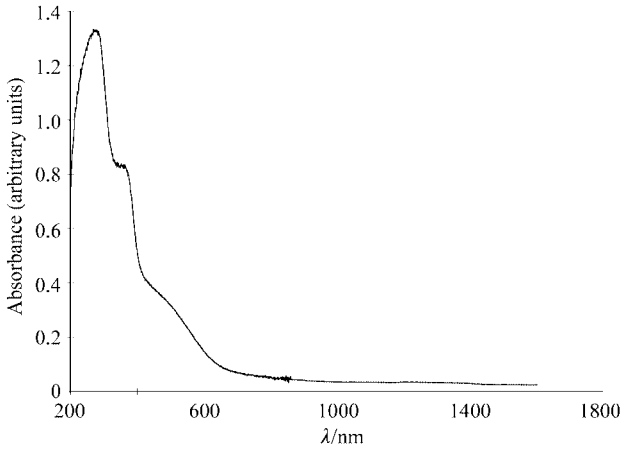

Fig. 4 UV–VIS–NIR spectrum of powdered TbG sample fired at 1150 °C/6h.

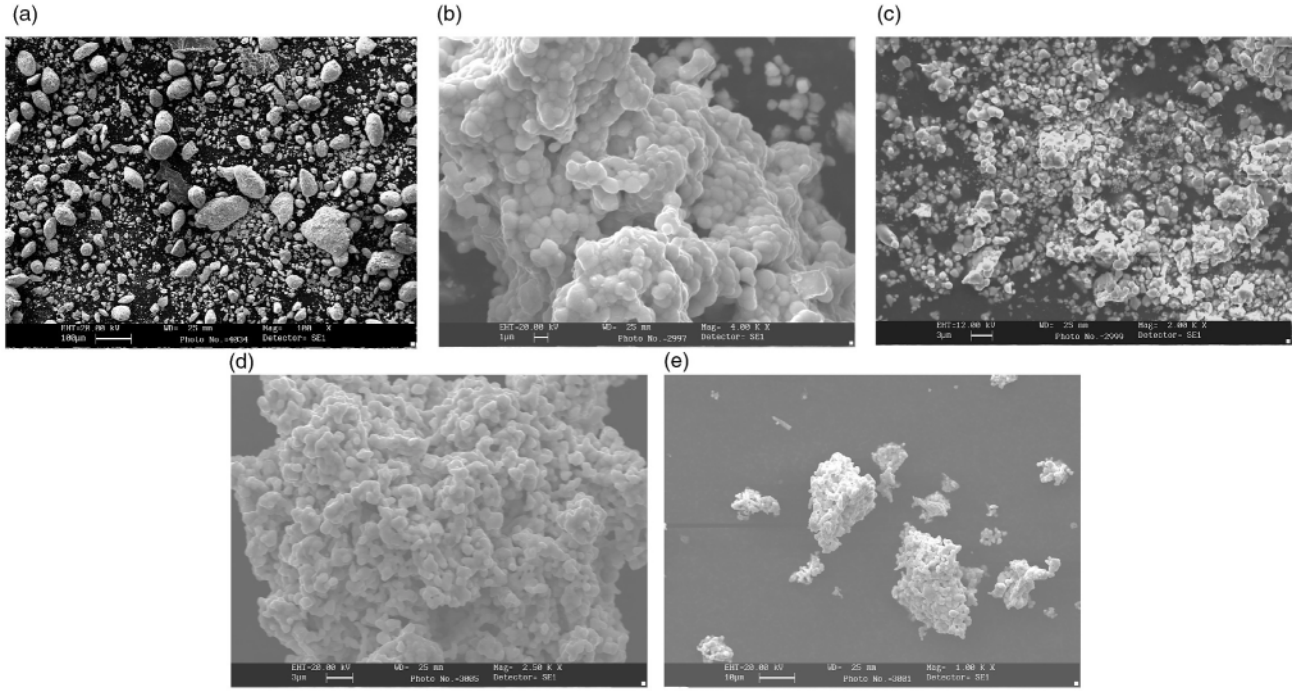

Fig. 5 SEM micrographs of samples fired at 1150 °C/6 h. (a) PrCI (1250 °C/6 h) (b) PrGI, (c) CrGI, (d) TbGI, (e) EuGI.

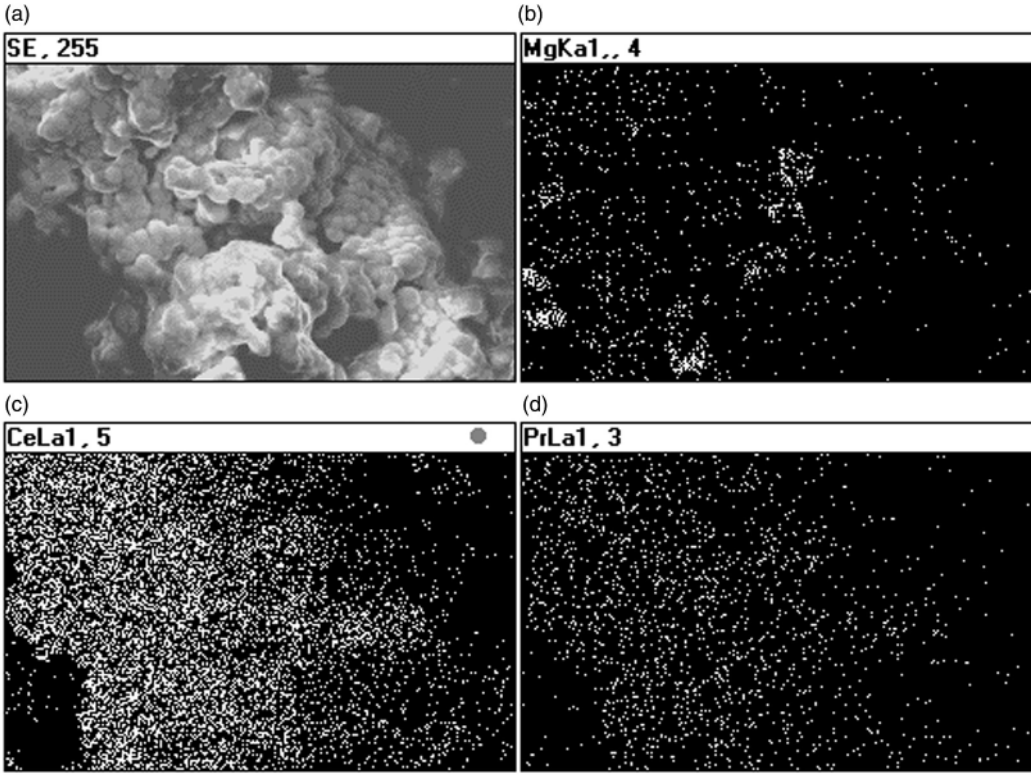

Fig. 6 Mapping analysis of the PrGI sample: (a) SEM micrograph (×4000) of the analyzed microscopic field; (b) magnesium distribution showing the presence of particles of the mineraliser; (c) distribution of cerium on the particles; (d) distribution of praseodymium.

(1150 °C) than the ceramic route (1300 °C), due to the high degree of homogeneity in the first process.

Conclusions

From above discussion some conclusions can be pointed out:

(1) In order to obtain red Pr–cerianite pigments from ceramic mixtures, the addition of flux agents and relatively high temperatures is rquired (1300 °C) but leads to pigments which are unstable in porcelainised stoneware.

(2) Using the coprecipitation route, Pr^{4+}–cerianite and Eu^{2+}/Eu^{3+}–cerianite solid solutions were obtained at relatively low temperatures (1150 °C/6 h) giving a red colour in porcelainised stoneware.

(3) The colouring mechanism is based in the introduction of an additional electronic level of energy in the cerianite forbidden band, from unpaired 4f electrons of lanthanide ions ($4f^1$ of Pr^{4+} and $4f^7/4f^6$ of Eu^{2+}/Eu^{3+}). The modified band gap is 1.94 eV (threshold wavelength 640 nm) for Pr–cerianite and 1.99 eV (threshold wavelength 625 nm) for Eu–cerianite.

(4) The red pigments obtained, which are introduced in to porcelainised stoneware, show low toxicity because both the chromophoric agent (Pr and Eu ions) and the ceramic matrix (cerianite) contain lanthanide elements.

Acknowledgement

We are grateful for financial support of the Spanish CICYT (MAT98-0392 Project).

References

1 L. A. Askin and T. P. Paster, *Geochemistry and Mineralogy of the Rare Earths*., in *Handbook on the Physics and Chemistry on the rare Earths*, ed. K. A. Gschneider and E. Eyring, North Holland, 1979, vol. 3, ch. 21.
2 E. Greinacher, *Industrial Applications of Rare Earths Elements*, ed. K. L. Gschneider, *Am. Chem. Soc. Symp. Serv*., 1981, **164**, 3.
3 K. Hudson, H. Winbow and J. Cowley, *Ceram. Eng. Proc*., 1996, **17**, 102.
4 M. Llusar, J. Calbo, J. A. Badenes, M. A. Tena and G. Monrós, *J. Mater. Sci*., 2000, **35**, 1.
5 *DE Pat*. 2315611, 2312535, 1980 (to Degussa).
6 G. Baldi and N. Dolen, *Synthesis of a new class of red pigments based on perovskite type lattice for use in body stain and high temperature glazes*, International Ceramics Journal supplement of Ceramica Informazione, Faenza, 2000, April, 31.
7 *Rhone Poulenc Fr*. Patent, 1.257.078, 1960 (to Rhone Poulenc).
8 R. Olazcuaga, A. El Kira, G. Le Flem and P. Hagenmuller, *Rev. Chim. Miner*., 1986, **23**, 55.
9 R. Olazcuaga, A. El Kira, G. Le Flem and P. Hagenmuller, *Rev. Chim. Miner*., 1984, **21**, 221.
10 R. Olazcuaga, *Pigmentos rojos con elementos de transición o tierras raras para cerámica de alta temperatura*, in *Nuevos productos y tecnologías de esmaltes y pigmentos cerámicos*, ed. Faenza Editrice Iberica, Castellón, 1992.
11 B. Gonzalbo, J. Romero, F. Fernández and M. J. Torralvo, *Rare Earth Pigments Based on the Fluorite Type structure, VIIth. Euorpean Conference on Solid State Chemistry*, Madrid, 1999, Vol. I, P-30.
12 POWCAL and LSQC programs, Dept. of Chemistry, University of Aberdeen, UK, 1990.
13 CIE Comission International de l'Eclairage, recommendations on Uniform Color Spaces, Colour Difference equations, Psychometrics Colour Terms. Suplement no 2 of CIE Pub. No 15 (E1-1.31) 1971, Bureau Central de la CIE, Paris, 1978.
14 R. D. Shannon and C. T. Prewit, *Acta. Crystallogr*., 1969, **8**, 925.
15 G. Monrós, J. Carda, M. A. Tena, V. Cantavella, P. Escribano and J. Alarcón, *Mater. Res. Bull*., 1992, **27**, 753.

Alumina: a cheap, active and selective catalyst for epoxidations with (aqueous) hydrogen peroxide

Michiel C. A. van Vliet,†[a] Dalmo Mandelli,[b] Isabel W. C. E. Arends,[a] Ulf Schuchardt[c] and Roger A. Sheldon*[a]

[a] *Biocatalysis and Organic Chemistry, Delft University of Technology, Julianalaan 136, 2628 BL Delft, The Netherlands. E-mail: secretariat-ock@tnw.tudelft.nl*
[b] *Instituto de Ciências Biológicas e Química, Pontifícia Universidade Católica de Campinas, P.O. Box 1111, 13020-904, Campinas, SP, Brazil*
[c] *Instituto de Química, Universidade Estadual de Campinas, P.O. Box 6154, 13083-970, Campinas, SP, Brazil*

Received 2nd May 2001
First published as an Advance Article on the web 7th September 2001

Chromatography alumina catalyses the epoxidation of alkenes with hydrogen peroxide under nearly anhydrous conditions. A variety of different aluminas show a similar catalytic behaviour. The hydrogen peroxide can be used as a preformed anhydrous solution in ethyl acetate, or it can be dried *in situ* by conducting the reaction under reflux with Dean–Stark water separation. The presence of a small amount of water in the reaction medium was shown to be of crucial importance.

Introduction

Olefin epoxidation constitutes a pivotal reaction in organic synthesis. Epoxidations using hydrogen peroxide as the terminal oxidant are very attractive since this cheap and readily available oxidant gives water as the by-product. Hydrogen peroxide generally requires a catalyst to achieve an acceptable reaction rate in epoxidation. Established catalytic methods are mostly based on transition metals, notably titanium,[1] manganese,[2] tungsten[3] and rhenium[4] and, to a lesser extent, main group elements such as arsenic[5] and selenium.[6]

A major disadvantage of all these methods, however, is that for optimum results, both in rate and yield, highly polar, non-coordinating solvents are required.[3,4] These solvents, mostly chlorinated hydrocarbons or highly fluorinated alcohols, are expensive and environmentally unattractive. Catalytic epoxidations in more benign solvents, such as hydrocarbons, alcohols, ethers or esters, generally proceed with a much lower rate.[7] Epoxide selectivity can also be a problem if acidic reaction conditions are used and water is present in the organic phase.[7,8]

Moreover, problems of recovery of the, often expensive, catalyst and contamination of the product are associated with the use of homogeneous catalysts.

The ideal catalyst, therefore, should be a stable heterogeneous catalyst that gives optimum activity in environmentally acceptable solvents.

During our research on heterogenised rhenium catalysts for epoxidation, we noticed that in some cases the alumina support itself showed considerable catalytic activity.[9] The epoxidation activity of alumina has been published before,[10] but the activity that we observed was much higher. In a few initial experiments reasonable epoxide yields were obtained for several alkenes ranging from unreactive (terminal) alkenes to the highly reactive terpenes.[11] Starting with these results a systematic investigation of the important parameters influencing the catalytic activity was conducted.

† Present address: Department of Organic Chemistry, Weizmann Institute of Science, Rehovot, 76100 Israel.

Results and discussion

α-Pinene is a reactive olefin for electrophilic epoxidation and forms an epoxide that is very sensitive towards (acid-catalysed) solvolysis, hydrolysis and rearrangement reactions. Therefore, this alkene was chosen as a probe for the investigation of reaction parameters influencing the catalytic activity (and selectivity) of several types of chromatography alumina.

High yields of the epoxide were obtained with acidic, neutral and basic aluminas (Table 1). The rate of the reaction decreased strongly with increasing conversion. This gives an apparent non-linear influence of the amount of catalyst on the reaction rate. However, at very low conversion a first order influence of the amount of catalyst on the reaction rate was observed. No reaction occurred without catalyst. A filtration experiment at high temperature showed that the catalyst was heterogeneous; *i.e.* no further reaction took place in the filtrate. No significant

Green Context

Epoxidation is a key transformation in organic synthesis and the reagent of choice in the fine chemicals industry is hydrogen peroxide. Many different catalytic systems have been developed in recent years, *e.g.* based on titanium, manganese, tungsten and rhenium. It has become increasing clear for those working in this area that no one system is effective for the wide variety of olefin substrates of relevance to the fine chemicals industry. In this manuscript an elegantly simple system is described. The catalyst is chromatography alumina, which is cheap and readily recyclable. It is also highly effective with a range of industrially relevant olefins. It is less effective than some of the other systems mentioned above, with relatively unreactive terminal olefins. On the other hand, it is a very effective catalyst, for example, with a variety of industrially relevant terpene substrates. This represents an economic and green method for the epoxidation of a range of interesting olefin substrates with H_2O_2. ***JHC***

DOI: 10.1039/b103952k

blank reaction can be observed in ethyl acetate under similar conditions.[12] Recovered alumina showed a similar activity and selectivity as fresh alumina.

The amount of water had a critical influence on the rate of the reaction. Almost no activity was observed in the case of 60% hydrogen peroxide. Anhydrous hydrogen peroxide (for safety reasons this was prepared by azeotropic drying of a diluted ethyl acetate solution; pure anhydrous hydrogen peroxide is extremely shock sensitive and not available commercially; see **warning** in experimental part) gave a much higher rate. The *in situ* drying of aqueous hydrogen peroxide by conducting the catalytic experiment under Dean–Stark conditions gave the opportunity to start with the commercially available 60% hydrogen peroxide and to avoid the use of moderately concentrated solutions of anhydrous hydrogen peroxide. The two procedures gave almost identical results (Table 1). The first procedure gives slightly higher yields, but the second procedure is based on a much more readily available oxidant. Ethyl acetate is the solvent of choice, since it is readily available, cheap, environmentally benign and forms a favorable azeotrope with water and mixes with hydrogen peroxide.

The procedure starting with anhydrous hydrogen peroxide is suited for a wide range of alkenes (Table 2). Even volatile alkenes, that would give problems with the Dean–Stark procedure, can be epoxidised under reflux. Although yields are mostly in the range 70–90%, the remaining part is not only unconverted alkene. A large number of by-products are formed, some in the same boiling range as the desired epoxide. Several attempts were made to increase the selectivity of the reaction. Addition of radical inhibitors or buffers that could block the strongly acidic sites of the alumina did not show a significant influence on the selectivity of the reaction.

A more advantageous epoxidation procedure is based on the use of aqueous hydrogen peroxide. The water in the starting oxidant and the water produced by the reaction could be removed by conducting the epoxidation under Dean–Stark conditions. In this case even a lower average water content can be reached than in the procedure starting with anhydrous hydrogen peroxide. A range of alkenes was epoxidised (see Table 3).

Terpenes were epoxidised in moderate to high yields. γ-Terpinene (1-isopropyl-4-methylcyclohexa-1,4-diene) afforded the monoepoxide or diepoxide, depending on the reaction time. However 30–35% of *p*-cymene (1-isopropyl-4-methylbenzene) was also formed, presumably by oxidative dehydrogenation. Epoxidation of limonene (1-methyl-4-isopropenylcyclohexene) gave the usual mixture of stereoisomers of the two monoepoxides and the diepoxide, with a clear preference for the 1,2-monoepoxide. This is consistent with the accepted electrophilic mechanism for peracid mediated and (hydro)peroxometal catalysed epoxidation, electron rich alkenes having the highest reactivity.

The range of 1-alkylcyclohexenes demonstrated a disadvantage of this procedure. The volatile 1-methylcyclohexene was epoxidised in high chemical selectivity (almost no by-products observed) but, nevertheless, gave a low yield. About 40% of the alkene was lost by evaporation and condensation in the Dean–Stark trap. The higher alkylcyclohexenes had almost the same reactivity, but gave a much better yield, since the volatility of these alkenes was low enough to prevent evaporation losses. The same effect was observed with the volatile 2-methylhept-2-ene and the less volatile 2-methylocta-

Table 1 Influence of different conditions and types of alumina on the epoxidation of α-pinene with anhydrous hydrogen peroxide in ethyl acetate[a]

			t/h		
Alumina	Weight/g	H_2O_2 source	0.5	2	4
Weakly acidic	0.25	H_2O_2–EtOAc	22 (83)	43 (91)	52 (85)
Weakly acidic	0.25	H_2O_2–EtOAc[b]	22 (80)	47 (85)	51 (78)
Weakly acidic	0.50	60% H_2O_2	7	18 (79)	21 (71)
Weakly acidic	0.50	60% H_2O_2[b]	24 (81)	49 (81)	56 (75)
Acidic	0.50	H_2O_2–EtOAc	32 (85)	54 (85)	63 (75)
Basic	0.50	H_2O_2–EtOAc	32 (86)	53 (85)	65 (83)
Neutral	0.50	H_2O_2–EtOAc	32 (83)	54 (84)	63 (83)
Weakly acidic	0.50	H_2O_2–EtOAc	30 (84)	54 (84)	65 (85)
Weakly acidic[c]	0.50	H_2O_2–EtOAc	34 (86)	54 (86)	69 (87)

[a] *Reagents and conditions*: 10 mmol α-pinene, 1 mmol dibutyl ether, 10 ml ethyl acetate, indicated type and amount of chromatography alumina, 20 mmol H_2O_2, reflux under N_2. Results are yield (selectivity). [b] Dean–Stark adapter. [c] 1 mol% 2,6-di-*tert*-butyl-4-methylphenol is added.

Table 2 Alumina catalysed epoxidation of (volatile) alkenes by anhydrous hydrogen peroxide[a]

Alkene	*t*/h	Yield (%)
1-Methylcyclohexene	4	88
Limonene	4	77[b]
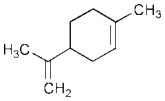		
2-Methylhept-1-ene	3	73
2-Methylhept-1-ene	24	82
Cyclohexene	6	76
Cycloheptene	24	77
Cyclooctene	24	92
Oct-1-ene	24	58

[a] *Reagents and conditions*: 10 mmol alkene, 1 mmol dibutyl ether, 0.50 g alumina (Aldrich, weakly acidic), 10 ml ethyl acetate, 20 mmol H_2O_2–EtOAc, reflux under N_2. Analysis by GLC. [b] Sum of mono- and di-epoxides.

Table 3 Alumina catalysed epoxidation of alkenes with aqueous hydrogen peroxide under Dean–Stark conditions[a]

Alkene	*t*/h	Yield (%)
α-Pinene	4	69
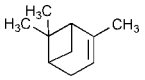		
γ-Terpinene	4	41[b]
	22	40[c]
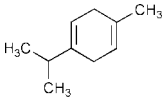		
3-Carene	3	87
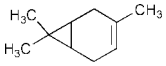		
Limonene	4	83[d]
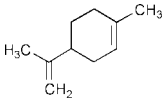		
1-Methylcyclohexene	4	42
1-Isopropylcyclohexene	4	79
1-*tert*-Butylcyclohexene	4	91
2-Methylocta-2,7-diene	3	80[e]
2-Methylocta-2,7-diene[f]	3	79[e]
2-Methylhept-2-ene	2	58
Cyclooctene	8	90

[a] *Reagents and conditions*: 10 mmol alkene, 1 mmol dibutyl ether, 0.50 g alumina (Aldrich, weakly acidic), 10 ml ethyl acetate, 20 mmol 60% H_2O_2, reflux with a Dean–Stark trap under N_2. Analysis by GLC. [b] Monoepoxides accompanied by 31% cymene. [c] Diepoxide accompanied by 36% cymene. [d] Sum of mono- and di-epoxides. [e] Only 2,3-epoxide formed. [f] 0.50 g of recovered alumina was used.

2,7-diene. The lowest atmospheric boiling point for which this procedure gives acceptable results is about 130 °C.

The alumina could be recycled, without the need for reactivation. Alumina was recovered from a large-scale reaction with cyclooctene, washed with ethyl acetate and dried under vacuum. The recovery was >99%. This alumina was used in the catalytic epoxidation of 2-methylocta-2,7-diene. The same yield and selectivity was obtained compared to fresh alumina.

A number of functionalised alkenes were epoxidised to explore the influences of functional groups on the reaction. Functionalised cyclohexenes had a low reactivity. A lower epoxide yield was obtained than for the non-substituted cyclohexene. However, if slightly more reactive functionalised methylcyclohexenes were used, a yield comparable to the non-functionalised 1-alkylcyclohexenes was obtained. In most cases a (*cis*/*trans*) isomer ratio comparable to that of MTO (methyl trioxorhenium) catalysed epoxidation was obtained (1.4–1.5 : 1).[13] No special influence of the functional group on rate or selectivity was observed (see Table 4).

Alumina is known to catalyse solvolysis and rearrangement reactions of epoxides,[14] so the high selectivity towards the unstable α-pinene oxide or other sensitive epoxides is remarkable. Fig. 1 shows some control experiments with preformed α-pinene oxide. Anhydrous alumina indeed decomposed the epoxide quite efficiently, only 27% of the epoxide remained after 4 h reflux. This catalytic activity, however, was almost completely suppressed by 1 equivalent of water and 91% of epoxide remained after 4 h. The decomposition of the epoxide by alumina and aqueous hydrogen peroxide was somewhat stronger. A large number of side-products was observed. Most likely the alumina catalyses the perhydrolysis of the epoxide, to form a hydroxyhydroperoxide, that can decompose in a variety of ways.

The amount of remaining epoxide (80%) corresponds well with the selectivity observed in the catalytic reactions. Hence, we conclude that secondary reactions of the epoxide on the alumina catalyst in a medium containing water and H_2O_2 are causing the selectivity to be reduced from 100%.

A second observation was that after the catalytic reaction no remaining hydrogen peroxide was present. It is known from literature[15] that hydrogen peroxide adsorbed on alumina slowly loses its active oxygen content. No results have been published on hydrogen peroxide decomposition by catalytic amounts of alumina. Fig. 2 shows the remaining hydrogen peroxide in a boiling ethyl acetate solution with 25 mol% alumina, conditions that are comparable to the catalytic reaction.

Table 4 Alumina catalysed epoxidation of functionalised (methyl)-cyclohexenes[a]

Alkene	*t*/h	Yield (%)
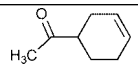	6	61
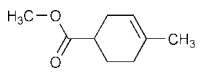	4	85
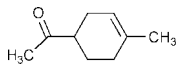	3	85
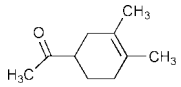	2	86

[a] *Reagents and conditions*: alkene (5 or 10 mmol), dibutyl ether (1 mmol), alumina (50 mg per mmol alkene), ethyl acetate (1 ml per mmol alkene). Reflux with a Dean–Stark trap; 2 equiv. 60% H_2O_2 were added dropwise in 15 min. Analysis by GLC.

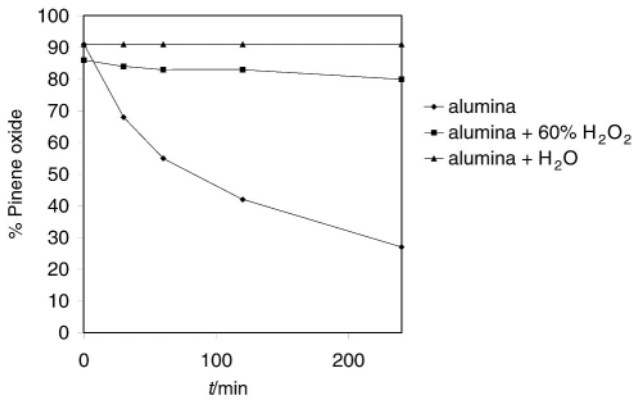

Fig. 1 α-Pinene oxide decomposition over alumina. *Reagents and conditions*: 10 mmol α-pinene oxide, 0.50 g alumina (Aldrich, weakly acidic), 1 mmol dibutyl ether, 10 ml ethyl acetate, (when indicated) 10 mmol 60%H_2O_2 or 10 mmol H_2O. Reflux under N_2. Analysis by GLC.

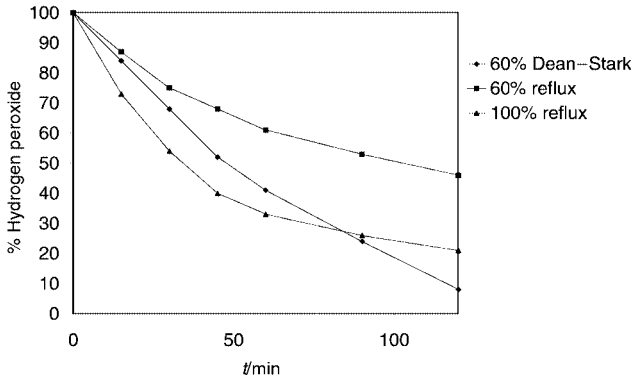

Fig. 2 Hydrogen peroxide decomposition over alumina. *Reagents and conditions*: 20 mmol H_2O_2 (60% or anhydrous in ethyl acetate), 0.50 g alumina (Aldrich, weakly acidic), 10 ml ethyl acetate. Reflux or reflux with Dean–Stark water separation. Analysis by iodometric titration of small aliquots.

The decomposition of hydrogen peroxide was retarded by the presence of water. Under the (anhydrous) Dean–Stark conditions the decomposition was completed in a few hours. The epoxidation of unreactive alkenes therefore, requires a large excess of hydrogen peroxide or the slow addition of hydrogen peroxide to the reaction mixture. In an experiment with cyclooctene as the substrate the slow addition of 2 equivalents of hydrogen peroxide indeed resulted in a higher epoxide yield of 94%, compared to the 90% shown in Table 2. An experiment on a slightly larger scale, without addition of internal standard, gave a yield of 97%, or 83% after aqueous work-up and distillation.

The extensive decomposition of hydrogen peroxide constitutes a possible safety problem. Vast amounts of oxygen gas are produced and mixed with the ethyl acetate vapor. This can result in the formation of explosive mixtures. For a safe operation the reaction vessel needs to be purged with inert gas. This gas flow can disturb the azeotropic distillation leading to a different rate of water separation. In an experiment with α-pinene with a high nitrogen flow (100 ml min^{-1}), the rate of the reaction was slightly higher than the normal procedure under a nitrogen blanket, but selectivity was much lower. The high nitrogen flow caused a very efficient water separation. From the results in Figs. 1 and 2 it is clear that operation under a strictly anhydrous regime is not advantageous. A low water content is necessary to prevent alumina catalysed epoxide and hydrogen peroxide decompostion.

A simplified mechanism for the epoxidation of alkenes catalysed by alumina is depicted in Fig. 3. From the experiments it is clear that the reaction takes places on the alumina surface, since filtration removes all catalytic activity from the reaction mixture. The formation of surface hydroperoxo-species on alumina has been observed and described.[15] The Lewis acidic

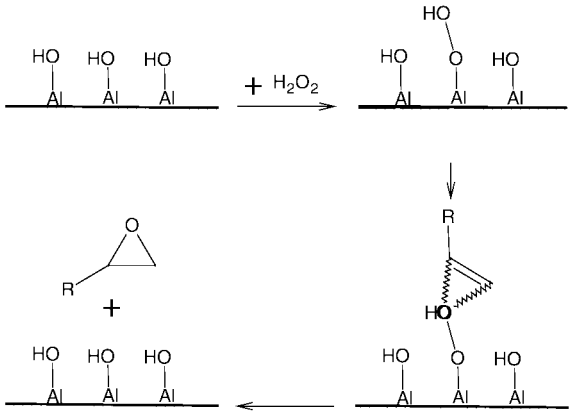

Fig. 3 Proposed mechanism for alumina catalysed epoxidation.

aluminium centre activates the hydroperoxo group for electrophilic epoxidation of the alkene. After reaction the surface hydroxy group is restored. The actual mechanism has to be much more complicated. Chromatography alumina has a bulk structure with numerous crystallographic planes exposed on the surface. Even simplified models for alumina show that for a single crystallographic plane there are several surface hydroxy groups present.[16] Each of these different Al–OH groups has a different acidity and reactivity. From the results with different types of alumina, it can be excluded that the strongly acidic or basic sites are involved in the catalysis. Also sites produced by dehydration (mostly strong Lewis acidic sites) are not likely to be involved in the epoxidation, since a small amount of water is needed for a good catalytic performance. On the other hand, these sites are probably involved in the undesired epoxide and hydrogen peroxide decomposition.

In conclusion, chromatography alumina is a versatile, reusable catalyst for epoxidation of alkenes with hydrogen peroxide under nearly anhydrous conditions. A very small amount of water is necessary in the reaction medium to prevent epoxide and hydrogen peroxide decomposition.

Experimental

WARNING: solutions of hydrogen peroxide in flammable organic solvents should be considered dangerous. A general rule for safe handling is to limit the concentration of hydrogen peroxide to 20 wt% of the reaction mixture.[17] In general, the procedures described in this paper do not reach this concentration, although care should be taken when preparing the anhydrous hydrogen peroxide solution in ethyl acetate. The *in situ* method never exceeds hydrogen peroxide concentrations of 2 M (about 7 wt%). Additional consideration should be given to the oxygen generated by hydrogen peroxide decomposition and the possibility of forming explosive gas mixtures of solvent and oxygen.

Chromatography alumina was Camag type[18] obtained from Aldrich or Fluka. Alkenes were used without prior treatment. Analysis was conducted by GLC on a Varian Star 3600 with a CP Sil 5 CB column of 50 m length and 0.53 mm inner diameter using an internal standard technique with predetermined response factors.

Cyclooctene oxide by alumina catalysed epoxidation

Cyclooctene (2.32 g; 20 mmol) and alumina (Aldrich, weakly acidic; 1 g) were mixed with ethyl acetate (20 ml). The mixture was heated under reflux with a Dean–Stark water separator. Aqueous hydrogen peroxide (2 ml; 60%; 40 mmol) was slowly added over 4 h. The mixture was heated for another 18 h. GLC showed complete conversion at 97% selectivity. The mixture was cooled and filtered. The residue was washed with ethyl acetate (2 × 10 ml). The combined organic filtrates were washed with 1 M sodium hydrogensulfite solution (25 ml) and saturated sodium chloride solution (20 ml). The aqueous layers were back extracted with ethyl acetate (2 × 25 ml). The combined organic extracts were dried on Na_2SO_4. Evaporation of the solvent gave a colourless oil (2.75 g). This oil was distilled on a Kugelrohr apparatus. An oil (2.08 g; 16.5 mmol; 83%) that solidified on standing was obtained at 80–90 °C (10 mmHg). GLC: 97% purity. δ_H (400 MHz, $CDCl_3$) 1.38 (m, 2H), 1.5 (m, 8H), 2.15 (m, 2H), 2.9 (m, 2H). δ_C (100 MHz, $CDCl_3$) 25.6, 26.3, 26.6, 55.7.

Acknowledgement

This research was sponsored by the Dutch Innovation Oriented Research Program on Catalysis (IOP Catalysis, IKA 96018).

References

1 B. Notari, *Adv. Catal.*, 1996, **41**, 253.
2 P. L. Anelli, S. Banfi, F. Montanari and S. Quici, *J. Chem. Soc., Chem. Commun.*, 1989, 779; D. de Vos and T. Bein, *Chem. Commun.*, 1996, 917; D. E. de Vos, B. F. Sels, M. Reynaers, Y. V. Subba Rao and P. Jacobs, *Tetrahedron Lett.*, 1998, **39**, 3221; A. Berkessel and C. A. Sklorz, *Tetrahedron Lett.*, 1999, **40**, 7965.
3 C. Venturello and R. D'Aloisio, *J. Org. Chem.*, 1988, **53**, 1553; Y. Ishii, K. Yamawaki, T. Ura, H. Yamada, T. Yoshida and M. Ogawa, *J. Org. Chem.*, 1988, **53**, 3587; K. Sato, M. Aoki, M. Ogawa, T. Hashimoto and R. Noyori, *J. Org. Chem.*, 1996, **61**, 8310; K. Sato, M. Aoki, M. Ogawa, T. Hashimoto, D. Panyella and R. Noyori, *Bull. Chem. Soc. Jpn.*, 1997, **70**, 905.
4 J. Rudolph, K. L. Reddy, J. P. Chiang and K. B. Sharpless, *J. Am. Chem. Soc.*, 1997, **119**, 6189; C. Copéret, H. Adolfsson and K. B. Sharpless, *Chem. Commun.*, 1997, 1565; W. A. Herrmann, R. M. Kratzer, H. Ding, W. R. Thiel and H. Glas, *J. Organomet. Chem.*, 1998, **555**, 293; M. C. A. van Vliet, I. W. C. E. Arends and R. A. Sheldon, *Chem Commun.*, 1999, 821.
5 S. E. Jacobson, F. Mares and P. M. Zambri, *J. Am. Chem. Soc.*, 1979, **101**, 6946; R. A. W. Johnstone and E. Francsicsné-Czinege, *World Pat.*, WO 98/17640, 1998, to Solvay Interox Limited; M. C. A. van Vliet, I. W. C. E. Arends and R. A. Sheldon, *Tetrahedron Lett.*, 1999, **40**, 5239.
6 T. Hori and K. B. Sharpless, *J. Org. Chem.*, 1978, **43**, 1689; H. J. Reich, F. Chow and S. L. Peake, *Synthesis*, 1978, 299; R. T. Taylor and L. A. Flood, *J. Org. Chem.*, 1983, **48**, 5160; B. Betzemeier, F. Lehrmitte and P. Knochel, *Synlett*, 1999, 489.
7 K. Sato, M. Aoki, M. Ogawa, T. Hashimoto, D. Panyella and R. Noyori, *Bull. Chem. Soc. Jpn.*, 1997, **70**, 905.
8 C. Venturello and R. D'Aloisio, *J. Org. Chem.*, 1988, **53**, 1553; A. L. Villa de P., B. F. Sels, D. E. de Vos and P. A. Jacobs, *J. Org. Chem.*, 1999, **64**, 7267.
9 D. Mandelli, M. C. A. van Vliet, U. Arnold, R. A. Sheldon and U. Schuchardt, *J. Mol. Catal. A*, 2001, **168**, 165.
10 J. Rebek and R. McCready, *Tetrahedron Lett.*, 1979, 4337.
11 D. Mandelli, M. C. A. van Vliet, R. A. Sheldon and U. Schuchardt, *Appl. Catal.*, in press.
12 M. C. A. van Vliet, I. W. C. E. Arends and R. A. Sheldon, *Synlett*, 2001, 248.
13 M. C. A. van Vliet, I. W. C. E. Arends and R. A. Sheldon, *Synlett*, 2001, **8**, 1305.
14 G. H. Posner, *Angew. Chem.*, 1978, **90**, 527.
15 J. E. Leffler and D. W. Miller, *J. Am. Chem. Soc.*, 1977, **99**, 480.
16 H. Knözinger and P. Ratnasamy, *Catal. Rev.-Sci. Eng.*, 1978, **17**, 31.
17 A variety of brochures on the safe handling of hydrogen peroxide are available from the Solvay Interox website: www.solvayinterox.com/resource.htm
18 *Aldrichim. Acta*, 1984, **17**, 42.

Montmorillonite K-10 catalyzed synthesis of β-keto esters: condensation of ethyl diazoacetate with aldehydes under mild conditions

B. P. Bandgar*, S. S. Pandit and V. S. Sadavarte

Organic Chemistry Research Lab., School of Chemical Sciences, Swami Ramanand Teerth Marathwada University, Nanded-431606, India. E-mail: bandgar_bp@yahoo.com

Received 10th May 2001
First published as an Advance Article on the web 27th September 2001

A simple and efficient synthesis of β-keto esters using montmorillonite K-10 catalyzed condensation of ethyl diazoacetate with various aldehydes at room temperature is described.

Introduction

β-Keto esters, an important class of versatile synthetic intermediates, are extensively used in the agrochemical, pharmaceutical and dyestuff industries and for efficient syntheses of complex natural products.[1] Apart from the classical Claisen condensation[2] and related reactions,[3] the most direct method involves the condensation of aldehydes with ethyl diazoacetate. This transformation is achieved either thermally[4] or in the presence of Lewis acids[5,6] or by using a two-step sequence which involves an aldol-type condensation of ethyl diazoacetate with aldehyde followed by oxidative elimination of nitrogen.[7] Recently Sonwane and coworkers[8] described the synthesis of β-keto esters using a zeolite catalyzed condensation of ethyl diazoacetate with aldehydes in moderate to good yields. However this method requires drastic conditions and long reaction times. Thermal condensation or methods involving drastic conditions are not clean and provide side products along with the β-keto esters. Although the Lewis acid catalyzed method is convenient there are some limitations. Of the different Lewis acids, only tin(II) chloride gives good yields for aliphatic aldehydes.[5] For aromatic and sugar aldehydes this method gives low yields. Another drawback is the known toxicity of tin compounds. A solid-phase reaction of aliphatic and aromatic aldehydes with ethyl diazoacetate over alumina under solvent-free conditions is also reported for the synthesis of β-keto esters in high yields.[9] However, the use of a large excess (10 times) of specially activated alumina as a reagent makes it less attractive in scale-up operations.

In recent years, there has been considerable growth of interest in the catalysis of organic reactions by clays. Clays have many advantages such as ease of handling, non-corrosiveness, low cost and ease of regeneration. Owing their Bronsted and Lewis acidities, clays, both in their natural and ion exchanged forms, function as efficient catalysts for various organic transformations.[10] We have recently reported the catalytic properties of natural kaolinitic clay for selective deprotection of thioacetals,[11] transesterification of β-keto esters[12] and cleavage of aryl acetates.[13] We report herein a simple and practical method for the preparation of β-keto esters involving montmorillonite K-10 catalyzed condensation of ethyl diazoacetate with aldehydes under mild conditions [eqn. (1)].

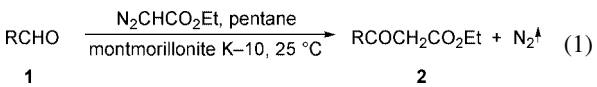

(1)

When treated with ethyl diazoacetate in the presence of montmorillonite K-10 as a catalyst, a variety of aldehydes gave the corresponding β-keto esters in high yields (Table 1). Both aliphatic and aromatic aldehydes react equally well under these reaction conditions, while alkyl and aryl ketones were found to be practically unreactive. Aromatic aldehydes with electron-donating as well as -withdrawing groups undergo smooth condensation with ethyl diazoacetate in the presence of this catalyst. An important aspect is that the conditions are mild and acidic enough to catalyze the condensation but not too acidic so as to cleave methoxy, methylenedioxy or ester functional groups. This method is useful for gram-scale synthesis of β-keto esters. The most noteworthy feature is the generality of the reaction leading to the formation of various β-keto esters in high yields.

The formation of β-keto esters appears to proceed through a α-diazo-β-keto ester type of intermediate generated by electrophilic attack on ethyl diazoacetate of species formed upon complexation of the aldehyde with the acid sites of the catalyst. Loss of nitrogen followed by a 1,2-hydride shift is then expected to lead to the observed β-keto ester.

In conclusion, we have developed a simple and efficient method for the synthesis of β-keto esters using montmorillonite K-10 catalyzed condensation of ethyl diazoacetate with aldehydes under mild conditions. The superiority and flexibility of this method over the existing methods coupled with the ease of operation and simplicity of work-up makes this catalyst potentially very useful. The catalyst can be recovered and reused at least three times without appreciable loss of activity.

Green Context

β-Keto esters have a remarkably wide range of uses that cover several industrial sectors including pharmaceuticals, agrochemicals and dyestuffs. Their synthesis has attracted considerable attention and this has developed a distinctly clean synthesis focus in more recent years. Thus alternatives for environmentally unacceptable catalysts for β-keto ester forming condensation reactions are now being put forward. However, while solid catalysts such as zeolites and alumina have some activity, drastic conditions or large catalyst quantities restrict the value of the methods. Here a clean, efficient and very general route to β-keto esters using a clay catalyst is described. The new method would certainly seem to have more widespread value, and general environmental benefits compared to many others described in the literature. ***JHC***

Experimental

IR spectra were recorded on a Bomem MB 104 FT-IR spectrometer and ^{1}H NMR spectra were recorded on a Bruker ACc 300F NMR spectrometer (300 MHz). Montmorillonite K-10 is a yellowish-gray dusty powder the principal constituents of which are bentonite and Fuller's earth. The approximate formula is $M^+_{0.33}(Al, Mg)\ Si_4O_{10}(OH)_2{\cdot}nH_2O$, where M^+, in the natural material includes one or more cations such as Na^+, K^+, Mg^+, Ca^+ and possibly others.[14] The characteristics of montmorillonite K-10 are: (1) surface area = 220–270 $m^2\ g^{-1}$, (2) bulk density = 300–370 g l^{-1} (3) specific gravity = 2.5 g ml (4) refractive index = 1.51, (5) crystal system, monoclinic.

Table 1 Montmorillonite K-10 catalyzed synthesis of β-keto esters

Entry	Aldehyde **1**	β-keto ester **2**	Reaction time/h	Yield[a,b] (%)
a	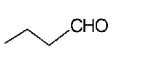	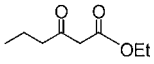	3.0	92
b	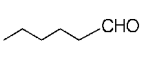	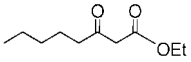	4.0	89
c	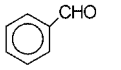	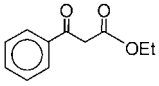	6.0	87
d	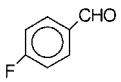	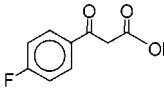	8.5	82
e	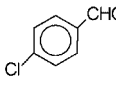	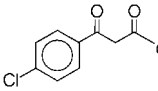	6.5	92
f	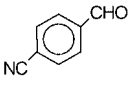	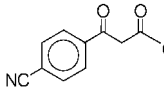	3.5	89
g	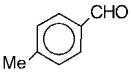	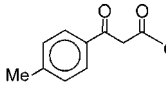	4.0	68
h	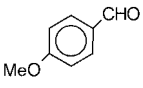	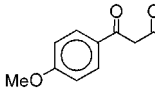	5.0	88
i	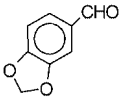	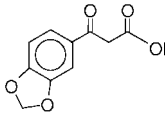	6.0	69
j	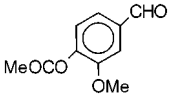	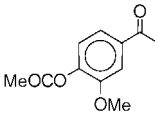	9.0	69
k	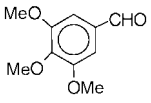	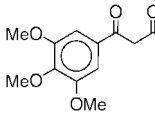	2.0	70
l	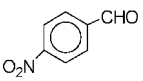	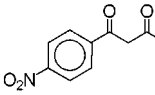	6.0	85
m	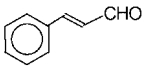	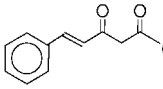	4.0	89
n	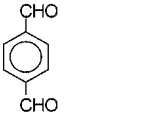	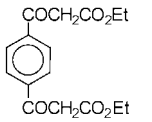	6.0	87

[a] Yields of isolated products. [b] Products are characterized by spectral analysis and comparison with authentic samples.[1]

Montmorillonite K-10 is a strong Bronsted and Lewis acidic catalyst and modification is carried out by exchanging the cations present in the clay with other suitable cations such as Fe, Zn, Pd, Cu, Ru, Rh, Ce *etc*., or by increasing the interlameller space by pillaring.[14]

Montmorillonite K-10 may show complexation towards carbonyl groups and thus may enhance the electrophic character of the aldehydes.

General procedure

A mixture of aldehyde (5 mmol), ethyl diazoacetate (7.5 mmol) and montmorillonite K-10 (100 mg) in pentane (10 ml) was stirred at room temperature (25 °C) for a specified time (Table 1). After completion of the reaction (TLC), the catalyst was removed by filtration and washed with pentane (3 × 5 ml). The solvent was removed under reduced pressure to obtain the crude product which was further purified by column chromatography on silica gel [ethyl acetate light petroleum (bp 40–60°) = 1 : 9].

Spectroscopic data of some selected compounds: 2i: mp 41 °C; IR (KBr) ν/cm^{-1}, 1630, 1682, 1740; δ_H ($CDCl_3$, 300 MHz) : 1.22 (t, 3H), 3.90 (s), 5.62 (s), 12.6 (s) (2H), 4.3 (q, 2H), 6.1 (s, 2H), 6.98 (d, 1H), 7.40 (d, 1H), 7.61 (dd, 1H); δ_C ($CDCl_3$, 75 MHz): 14.2 (1), 46.3 (t), 61.4 (t), 104.0 (t), 108.0 (d), 108.1(d), 126.1(d), 132.4(s), 149.8(s), 153.9(s), 171.5(s), 195.9 (s).

2k: (KBr): ν/cm^{-1}, 1020, 1140, 1210, 1640, 1710, 1735, 2920; δ_H ($CDCl_3$, 300 MHz): 1.25 (t, 3H), 3.85 (s), 5.55 (s), 12.4 (s) (2H), 3.88 (s, 6H), 3.95 (s, 3H), 4.25 (q, 2H), 7.1 (s, 2H); δ_C ($CDCl_3$, 75 MHz): 15.2 (q), 45.7 (t), 58.9 (q, strong), 65.9 (q), 67.8 (t), 107.3 (s), 112.1 (d, strong), 118.6 (s, weak), 121.5 (s, weak), 174.2 (s), 191.6 (s).

2m: IR (KBr): ν/cm^{-1}, 1040, 1120, 1650, 1715, 1741, 2905; δ_H ($CDCl_3$) 300 MHz): 1.28 (t 3H), 3.92 (s), 5.62 (s), 12.4 (s) (2H), 4.37 (q, 2H), 6.2 (d, 1H), 6.5 (d, 1H), 7.5 (m, 5H); δ_C ($CDCl_3$, 75 MHz): 14.1(q), 44.7 (t), 62.9 (t), 101.4 (d), 101.5 (s, weak), 102.3 (d), 105.1 (d, strong), 111.2 (d, strong), 112.7 (d), 177.4 (s, weak), 187.8 (s, weak).

Acknowledgement

S. S. P. thanks UGC, New Delhi for a teacher fellowship and V. S. S. thanks CSIR, New Delhi for a junior research fellowship.

References

1 S. Benetti, R. Ramagnoli, C. De-Risi, G. Spalluto and V. Zanirato, *Chem. Rev*., 1995, **5**, 1065; G. Sartori, F. Bigi, G. Canali, G. Casnati and X. Tao, *J. Org. Chem*., 1993, **58**, 840; J. J. Landi, L. M. Garofalo and K. Ramig, *Tetrahedron Lett*., 1993, **34**, 277; X. Smith, E. P. Mazzola, J. J. Sims, S. L. Midland, N. T. Keen, V. Burton and M. M. Staytan, *Tetrahedron Lett*., 1993, **34**, 223; G. Sartori, F. Bigi, R. Maggi, D. Baraldi and G. Casnati, *J. Chem. Soc., Perkin Trans. 1*, 1992, 2985; L. Brehm, J. S. Johansen and P. K. Larsen, *J. Chem. Soc., Perkin Trans. 1*, 1992, 2059; J. Zhang and D. P. Curran, *J. Chem. Soc., Perkin Trans. 1*, 1991, **47**, 1137; M. A. Willims, C. N. Hsiao and M. J. Miller, *J. Org. Chem*., 1991, **56**, 2690; D. P. Curran, T. M. Morgan, C. E. Schwartz and B. B. Snider, *J. Am. Chem. Soc*., 1981, **113**, 6607
2 C. R. Hauser and B. E. Hudson, *Org. React*., Jr., 1942, **1**, 266.
3 J. Schaefer and J. Bloomfield, *Org. React*., 1967, **15**, 1; M. Rathe, *Org. React*., 1975, **22**, 423; R. Barhdadi, J. Gal, M. Heintz and M. Troupel, *J. Chem. Soc., Chem. Commun*., 1992, 50.
4 T. Curtius and E. Buchner, *Chem. Ber*., 1885, **18**, 2371; F. Schlotterbeck, *Chem. Ber*., 1909, **42**, 2565; W. Dieckman, *Chem. Ber*., 1910, **43**, 1024; C. Gutsche, *Org. React*., 1954, **8**, 364.

5 C. R. Holmquist and E. J. Rosekamp, *J. Org. Chem.*, 1989, **54**, 3258.
6 F. J. Aparicio, F. J. Herrera and M. V. Fernandez, *An Quim.*, 1978, **74**, 1516; M. V. Fernandez, F. J. G. Herera and C. G. Perez, *Carbohydr. Res.*, 1983, **124**, 333.
7 E. Wenkert and A. J. McPherson, *J. Am. Chem. Soc.*, 1954, **76**, 8084; R. Pellicciari, R. Fringuelli, P. Ceccherelli and E. Sisani, *J. Chem. Soc., Chem. Commun.*, 1979, 959; R. Pellicciari, B. Natalini, R. Fringuelli and P. Ceccherelli, *J. Chem. Soc., Perkin Trans. 1*, 1985, 493; E. Wenkert, P. Ceccherelli and R. A. Fugiel, *J. Org. Chem.*, 1978, **43**, 3983.
8 S. G. Sudrik, B. S. Balaji, A. P. Singh, R. B. Mitra and H. R. Sonawane, *Synlett*, 1996, 369.
9 D. D. Dhavale, P. N. Patil and R. S. Mali, *J. Chem. Res. (S)*, 1994, 152.
10 D. Ponde, H. B. Borate, A. Sudlai, T. Ravindranathan and V. H. Deshpande, *Tetrahedron Lett.*, 1996, **37**, 4605; T. T. Upadhya, T. Daniel, A. Sudlai, T. Ravindranathan and K. R. Sabu, *Synth. Commun.*, 1996, **26**, 4539; G. K. Janeshwara, N. B. Barhate, A. Sudlai, V. H. Deshpande, A. S. Gajare, M. S. Shingare and R. Sukumar, *J. Chem. Soc., Perkin Trans. 1*, 1998, 965; N. S. Shaikh, A. S. Gajare, V. H. Deshpande and A. V. Bedekar, *Tetrahedron Lett.*, 2000, **41**, 385.
11 B. P. Bandgar and S. P. Kasture, *Green Chem.*, 2000, **2**, 154.
12 B. P. Bandgar, L. S. Uppalla and V. S. Sadavarte, *Green Chem.*, 2001, **3**, 39.
13 B. P. Bandgar, L. S. Uppalla, A. D. Sagar and V. S. Sadavarte, *Tetrahedron Lett.*, 2001, **42**, 1163.
14 M. D. Nikalje, P. Phukan and A. Sudalai, *Org. Prep. Proc. Int.*, 2000, **32**, 1; Merk Index, 12th edn., 1999.

Use of water as a direct hydrogen donor in supercritical carbon dioxide: a novel and efficient Zn–H_2O–CO_2 system for selective reduction of aldehydes to alcohols

Guoping Li, Huanfeng Jiang* and Jinheng Li

LCLC, Guangzhou Institute of Chemistry, Chinese Academy of Sciences, P. O. Box 1122, Guangzhou 510650, China. E-mail: jhf@mail.gic.ac.cn

Received 18th June 2001
First published as an Advance Article on the web 7th September 2001

This is the first report that Zn–H_2O–CO_2 is an excellent reducing reagent for the reduction of aldehydes in supercritical carbon dioxide ($scCO_2$). The corresponding alcohols were obtained in good yields and excellent selectivity. The experimental results showed that $scCO_2$ plays an important role in this reduction.

Introduction

In recent years, green chemistry has received increased attention.[1] The general areas of investigation in green chemistry include selections of feedstocks, reagents, solvents, reaction conditions, catalysts and the design of safer chemicals. Moreover, supercritical carbon dioxide, as a green reaction medium substitute for some toxic and volatile organic solvents, has played a significant role in raising conversions and improving selectivities of reactions.[2,3] On the other hand, alternative reagents are also the focus of attention in green chemistry circles. Water is the ultimate hydrogen source. Therefore it is clearly valuable to use water as one of the fundamental feedstocks in contemporary chemical industry.

For several years, the reduction of carbonyls to the corresponding alcohols with zinc dust was known to occur under acidic conditions.[4,5] Unfortunately, the reaction gives low chemoselectivity, for example, the reduction of aromatic aldehydes only gives a mixture of arylmethyl acetates and pinacols. Although the Zn–H_2O system was found later to reduce aldehydes to the corresponding alcohols, it was necessary to add Pd catalysts and other toxic solvents into the system.[6,7]

As a part of our research on searching for more environmentally benign methods to reduce carbonyls, we have found a new and efficient method to reduce aldehydes to alcohols, using Zn–H_2O–CO_2 as the reducing reagent in $scCO_2$ without use of other toxic solvents.

Results and discussion

In our first experiment, *p*-tolualdehyde was chosen as the model and the reduction was carried out in $scCO_2$, in the presence of zinc dust and water. After the reaction was complete, the reaction mixture was extracted, separated and characterized by ^{1}H NMR, IR and GC–MS. 4-Methylbenzyl alcohol was obtained in good yield and excellent selectivity, and the solid inorganic product was $ZnCO_3$, which is detected by XRD and IR.

To the best of our knowledge, this is the first example where aldehydes are reduced to alcohols using Zn–H_2O–CO_2 as the reducing reagent without the use of catalysts.

Table 1 shows that CO_2 plays a central role in this reaction since no reaction occurred in the absence of CO_2 (Table 1, entry 1). In the presence of CO_2, even at normal atmosphere pressure, the reaction was accelerated (entry 2). When the pressure of carbon dioxide reached the supercritical point, the rate of reaction was substantially enhanced (entry 3). These results showed that CO_2 takes part in the reaction, with a solution equilibrium between CO_2 and water, especially in $scCO_2$, leading to acidic conditions (pH value lower to 5),[8] which will promote the reaction.

As can be seen in Table 1, the reaction times, reaction temperatures and the pressure of carbon dioxide obviously influence the yields of 4-methylbenzyl alcohol. When the pressure was lower than the critical pressure or higher than 15 MPa, the yields were decreased (entries 6 and 7). The optimum reaction time was 6 h with a temperature of 65 °C (entries 3, 4 and 7). Comparing our results with the observations of Sasson and coworkers,[6], it is obvious that use of $scCO_2$ decreases the reaction temperature and shortens the reaction time.

Table 1 Reduction of *p*-tolualdehyde to 4-methylbenzyl alcohol under various conditions[a]

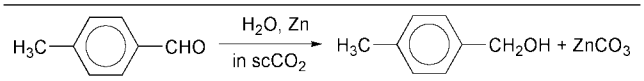

Entry	*P*/MPa	*t*/h	*T*/°C	Yield[b] (%)
1[c]	0	6	60	Trace
2[d]	0.1	8	65	18
3	8	1.5	65	88
4	8	6	65	100[e]
5	12	6	65	99
6	15	6	63	28
7	8	6	43	31

[a] Tolualdehyde (2 mmol), zinc dust (2.5 mmol), water (0.1 ml). [b] Determined by gas chromatography. [c] Without carbon dioxide. [d] Carbon dioxide was introduced by use of a baloon. [e] Isolated yield was 71%.

Green Context

This article brings together two very important green chemistry technologies—the use of carbon dioxide as a solvent for reaction chemistry and the use of water as a reagent. A new method for the selective reduction of aldehydes to alcohols is described. The use of supercritical carbon dioxide avoids the use of toxic organic solvents. Water is used as a hydrogen donor. Avoiding a catalyst further reduces the potential for hazardous waste. Overall the reaction is environmentally benign. ***JHC***

 DOI: 10.1039/b105307h

On the basis of these results, we further investigated this reduction reaction with different aldehydes employed under the optimized reaction conditions. As shown in Table 2, aromatic aldehydes could be converted into the corresponding alcohols in yields of 82–100%.

The electronic effects of phenyl ring substituents were also explored. The experimental results showed the presence of electron-withdrawing-releasing groups on the substrates had only a slight influence on the yields.

Aliphatic aldehydes could be reduced to yield the corresponding alcohols under the same conditions, although the conversion is only 17% for hexanal (Table 2, entry 6). When a catalytic amount of hydrochloric acid (10 mol%) was added, the conversion was raised to 68% (entry 7). These results indicate that the activity of aliphatic aldehydes in this reaction was lower than that of aromatic aldehydes, and furthermore, increasing the system acidity accelerated the reaction.

The reaction mechanism of this reaction is not yet clear and is therefore the subject of current investigation. Based on two experimental results, *i.e.*, the non-catalytic conditions and the action of the carbon dioxide in $scCO_2$, the mechanism of this reducing reaction is quite different from that of Sasson's. The following mechanism seems to be possible: hydrogen-transfer takes place from 'zinc and carbon dioxide activated' water to the substrate, rather than a dehydrogenation–hydrogenation sequence involving molecular hydrogen. This was supported by the following findings: (i) the normal condition experiment (Table 1 entry 1) could be carried out in an open vessel, and no free hydrogen gas was detected; (ii) when free hydrogen gas, *p*-tolualdehyde and $ZnCO_3$ or ZnO were placed together in supercritical carbon dioxide, no reaction occurred.

In conclusion, the advantage of the presented hydrogen transfer reaction can be delineated as follows: (i) aromatic aldehydes can be reduced with high yields and excellent selectivity; (ii) the reaction is simple and free of traditional organic solvents; (iii) this method of reduction is in full accord with the principles of green chemistry.

Table 2 Reduction of aromatic and aliphatic aldehydes under optimal reaction conditions[a]

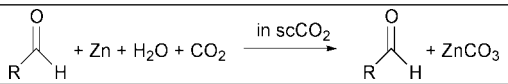

Entry	Aldehyde	*t*/h	Yield[b] (%)	Isolated yield (%)
1	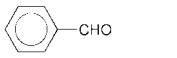	6	90	70
2	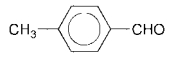	6	100	71
3	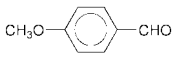	6	82	63
4[c]	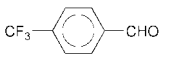	24	100	69
5	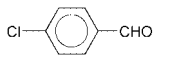	24	100	63
6[d]	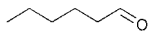	6	17	9
7[de]	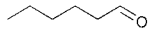	14	68	41

[a] Aldehyde (2 mmol), zinc dust (2.5 mmol), water (0.1 ml). [b] Yields were determined by gas chromatography. [c] *p*-Trifluoromethylbenzaldehyde (1 mmol), zinc dust (1.5 mmol), water (0.1 ml). [d] The presence of Hexanol is confirmed by GC–MS and NMR. [e] 10 mol% of HCl was added to initiate the reaction.

Experimental

A 15 ml stainless reaction vessel was charged with aldehyde (2 mmol), water (6 mmol) and zinc dust (2.5 mmol). The vessel was sealed and then liquid carbon dioxide was introduced from a cylinder. The reaction system was heated to the selected temperature using an oil-bath and stirred magnetically for the required reaction time. When the reaction was complete, the vessel was cooled with an ice-bath and the pressure was released slowly to atmospheric pressure. The residual was extracted and separated. The products were detected by gas chromatography and identified by ^1H NMR, IR and MS.

Acknowledgements

We are grateful to the National Science Foundation of China for financial support of this work (29872039).

References

1 P. Anastas and T. Williamson, *Green Chemistry*, Oxford University Press, New York, 1998.
2 P. G. Jessop, T. Kariya and R. Noyori, *Chem. Rev*., 1999, **99**, 475; A. Baiker, *Chem. Rev*., 1999, **99**, 453.
3 L. Jia, H. Jiang and J. Li, *Green Chem*., 1999, **1**, 91; H. Jiang, L. Jia and J. Li, *Green Chem*., 2000, **2**, 161; L. Jia, H. Jiang and J. Li, *Chem.Commun*., 1999, 985.
4 R. C. Selm, *Org. Prep. Int*., 1973, **5**, 303.
5 B. R. Rani, M. Ubukata and H. Osada, *Bull. Chem. Soc. Jpn*., 1995, **68**, 282.
6 S. Mukhopadhyay, G. Rothenberg, H. Wiener and Y. Sasson, *New J. Chem*., 2000, **24**, 305.
7 W. B. Wang, L. L. Shi and Y. Z. Huang, *Tetrahedron Lett*., 1990, **31**, 1185.
8 R. Kruse and E. V. Franck, *Ber. Bunsenges. Phys. Chem*., 1982, **86**, 1036.

Solvent-free reactions of solid substances using solid catalysts: estimation of physical states of substrate–product mixtures by the BET method and the SEM observation

Toshiyuki Kitamura and Tadao Harada*

Faculty of Science and Technology, Ryukoku University, Seta, Otsu 520-2194, Japan.
E-mail: harada@rins.ryukoku.ac.jp

Received 9th September 2001
First published as an Advance Article on the web 1st October 2001

Surface area estimations by the BET method and SEM observations were applied to the investigation of the physical states of substrates and products during the solvent-free reactions of solid substances using supported metal catalysts. The solvent-free hydrogenolysis of *trans*-oxirane-2,3-dicarboxylic acid (*trans*-epoxysuccinic acid) or its disodium salt and the solvent-free hydrogenation of thymol were used as the sample reactions in this study. These reactions were postulated to proceed in the fused state, based on specific surface areas and micrographs of the catalyst–substrate–product mixtures. This study revealed that the combination of the BET method and SEM observations was a promising tool for the mechanistic investigation of solvent-free reactions.

Introduction

Organic syntheses directed toward 'Green Chemistry' have attained increasing interest in recent years[1] which should lead to new environmentally benign procedures to save resources and energy. Solvent-free reactions promise to be an essential facet of 'Green Chemistry'. This type of organic reaction possesses some advantages over traditional reactions in organic solvents. Solvent-free reactions make it possible to reduce the consumption of environmentally unfriendly solvents and utilize scaled-down reaction vessels. Moreover, the use of a catalyst for solvent-free reactions can achieve energy savings. Recently, several techniques for the efficient use of solvent-free reactions have been developed. For example, Wang *et al*. succeeded in the solvent-free reaction of C_{60} to dumbbell-shaped C_{120} using KCN as a catalyst.[2] They found that the use of a vibrating mill was efficient for the smooth progress of the solvent-free reaction while this molecule can not be prepared from C_{60} using reactions in solvents. Varma *et al*. have carried out the solvent-free oxidation of benzoins using $CuSO_4/Al_2O_3$[3] promoted by microwave irradiation within 2–3 min. The symmetrical and unsymmetrical benzoins were efficiently oxidized to the corresponding diketones (yield >90%).

In spite of significant advances in solvent-free reactions, some aspects remain equivocal. It has been well documented that some reactions proceed more smoothly under solvent-free conditions than in solvents, even when solid compounds are used as the substrates. Nozoe *et al*. have performed solvent-free hydrogenations of solid alkenes and alkynes using supported Pd catalysts.[4] These reactions were carried out at room temperature under a hydrogen stream (0.1 MPa, 2.4×10^{-2} m^3 h^{-1}). When diphenylacetylene (mp 59–61 °C) was used as the substrate, bibenzyl was obtained as the main hydrogenated product. The solvent-free hydrogenation proceeded more smoothly than that in THF. However, the rate of the solvent-free hydrogenation of *trans*-stilbene (mp 122–124 °C) into bibenzyl was slower than that in THF. Based on these facts, Nozoe *et al*. suggested that diphenylacetylene was hydrogenated to bibenzyl *via cis*-stilbene, which has a lower melting point (mp 5–6 °C) than the reaction temperature, and that the substrate was in the fused state during most of the reaction process. Lamartine *et al*. reported the results of the solvent-free hydrogenation of thymol using various metal catalysts.[5] The substrate was hydrogenated to menthones and menthols under solvent-free conditions and 99% conversion was attained using a Pt/C catalyst. Lamartine *et al*. suggested that the dissociated hydrogen generated on the metal migrates to the inner area of the solid thymol particles *via* the support, to hydrogenate all the substrate molecules in the particles.

It is possible to assume that there are two types of solvent-free reactions of solid substrates using solid catalysts; reactions occurring in the fused state and in the solid state. When substrates are in the fused state during solvent-free reactions using solid catalysts, the substrate molecules, as in a solvent, should migrate to the surface of the catalyst. On the other hand, when substrates are in the solid state, active species such as dissociated hydrogen must migrate from the catalyst surface to the inner area of the substrate particles since no substrate molecules in the inner area can come in contact with the catalyst surface. The product distribution of this type of reactions may reflect the crystal structures of the substrates. These dependences on the crystal structures of the substrates are characteristic

Green Context

There is a great deal of interest in carrying out solvent-free organic reactions. The possible environmental benefits are obvious with no concerns over solvent emissions or any by-products derived from the solvent. However, solventless reactions represent a major change to traditional chemical processing for companies used to operating in the batch mode. It is very important that we seek to understand better how these reactions work and how the physical state of the solid mixtures changes during reaction, how it effects reaction and how it can be studied. In this way chemical engineers can gain the information needed for them to consider developing processes suitable for exploiting solvent-free reactions. Here, surface area measurement and SEM observation are used to study the physical states of substrate-catalyst-product mixtures. Remarkable changes in surfaces areas are observed which can be used to help understand the reaction processes but also reveal a simple method for following the reactions. ***JHC***

 DOI: 10.1039/b106031g

of solvent-free reactions of solid compounds. Thus, information relating to the physical states of substrates during solvent-free reactions is indispensable for mechanistic studies of solvent-free reactions over solid catalysts. However, the physical states of the substrates during the reactions have not been systematically investigated.

In a previous paper, we attempted the solvent-free hydrogenolysis of *trans*-oxirane-2,3-dicarboxylic acid (*trans*-epoxysuccinic acid, H_2TES) using supported Pd catalysts.[6] The substrate was hydrogenolyzed to malic, diglycolic and succinic acids using a Pd/C catalyst. The yield of malic acid was found to be highest with Pd/SiC. The physical states of the substrate and products during the reaction were investigated using scanning electron microscopy (SEM). Gummy masses of the catalyst–substrate–product mixtures were observed after the reaction. Based on the idea that the catalyst particles were intimately mixed with the fused substrate and product, we suggested that the substrate was in the fused state during the reaction. Furthermore, it was assumed that the solvent-free hydrogenolysis of the disodium salt of H_2TES (Na_2TES) using supported Pd catalysts proceeded in the solid state since no gummy masses were formed during the reaction.[7]

In this paper, we propose another method to estimate the physical states of the substrates and products during solvent-free reactions using heterogeneous catalysts based on the measurement of specific surface areas of the catalyst–substrate and catalyst–substrate–product mixtures by the Brunauer–Emmett–Teller (BET) method.[8] In this method, surface areas are determined by the measurement of the amount of N_2 gas adsorbed. Our approach is based on the idea that the fused substrates and products on the catalyst surface enter the pores of the catalyst particles and decrease their surface area, whereas solid-state substrates and products show no decrease.

Results and discussion

Scheme 1 depicts the solvent-free hydrogenolysis of *trans*-oxirane-2,3-dicarboxylic acid (*trans*-epoxysuccinic acid, H_2TES) and its disodium salt (Na_2TES) using supported Pd catalysts.

Table 1 shows the results of the solvent-free hydrogenolysis of H_2TES and Na_2TES using Pd/Al_2O_3 or Pd/C. The reactions were carried out at room temperature under a hydrogen pressure of 0.1 MPa. The hydrogenolysis proceeded with all combinations of substrates and catalysts examined in this study, although the reaction conditions were much milder than those for previously reported solvent-free hydrogenolysis of H_2TES and Na_2TES.[6,7] The reaction yields, {1.0 − (non-reacted substrate/added substrate)} × 100, were >50% after 2 days. When H_2TES was used as the substrate, succinic and diglycolic acids were obtained rather than malic acid. For Na_2TES, no formation of the succinate and the diglycolate were observed. Differences in the product distributions were also observed in the solvent-free hydrogenolysis of H_2TES and Na_2TES at higher temperatures under a higher hydrogen pressure.[7] It is likely that the sodium ions protect the C–C bond in the epoxide

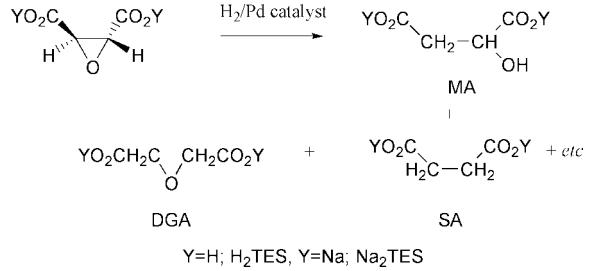

Scheme 1 Solvent-free hydrogenolysis of H_2TES or Na_2TES using the Pd catalyst.

Table 1 Solvent-free hydrogenolysis of H_2TES or Na_2TES using supported Pd catalysts[a]

		Organic components (%)				
Substrate	Catalyst	Substrate	MA[b]	SA[c]	DGA[d]	Others
H_2TES[e]	$5\%Pd/Al_2O_3$	44	27	20	6	3
	5%Pd/C	19	31	41	8	1
Na_2TES[f]	$5\%Pd/Al_2O_3$	26	70	0	0	4
	5%Pd/C	42	53	0	0	5

[a] *Reaction conditions*: substrate (0.1 g), catalyst (0.1 g), reaction temperature (room temperature), hydrogen pressure (0.1 MPa), reaction time (2 days). [b] MA = malic acid or its Na salt. [c] SA = succinic acid or its Na salt. [d] DGA = diglycolic acid or its Na salt. [e] H_2TES = *trans*-epoxysuccinic acid. [f] Na_2TES = disodium *trans*-epoxysuccinate.

ring and the hydroxy group in the formed malate over the Pd catalysts. This role of the sodium ions would reduce the formation of diglycolate and succinate.

Table 2 shows the results of the hydrogenolysis of H_2TES or Na_2TES using supported Pd catalysts in a solvent. When the hydrogenolysis of H_2TES or Na_2TES was carried out in methanol or deionized water, the reactions proceeded more slowly than under solvent-free conditions. These findings can be explained on the basis that the concentration of the substrate molecules on the catalyst surface during the hydrogenolysis in a solvent was lower than that during the solvent-free hydrogenolysis.

It can be assumed that the specific surface area of the catalysts after the solvent-free reactions reflect the physical states of the substrates and products during the reactions; *i.e.* fused substrate–product mixtures fill the catalyst pores to decrease the specific surface area of the catalyst, whereas the solid substrate–product mixtures have no influence on the specific surface area. On this basis, we attempted to estimate the specific surface area of the catalyst–substrate and the catalyst–substrate–product mixtures in order to investigate the physical states of the substrates and products during the reactions.

In the presence of hydrogen gas, a mixture of H_2TES and Pd/Al_2O_3 was allowed to stand at room temperature. The influence of the hydrogen on the specific surface area of the catalyst–organic component mixture was examined by comparing the specific surface area of the mixture in an atmosphere of hydrogen with that in an argon atmosphere. The specific surface area of the catalyst was presumed to decrease in the presence of hydrogen, since the solvent-free hydrogenolysis of H_2TES is known to proceed in the fused state.[6] Table 3 lists the specific surface area of H_2TES, Pd/Al_2O_3 and their mixture. It can be seen that the specific surface area of H_2TES is <10% of the specific surface area of the catalyst. This suggests that when the specific surface area of the mixture is significantly changed during the solvent-free reactions, the change is mostly attributable to the change in the specific surface area of the catalyst. As

Table 2 Hydrogenolysis in solvent of H_2TES or Na_2TES using supported Pd catalysts[a]

			Organic components (%)				
Substrate	Catalyst	Solvent	Substrate	MA[b]	SA[c]	DGA[d]	Others
H_2TES[e]	$5\%Pd/Al_2O_3$	MeOH	93	0	0	0	7
	5%Pd/C	MeOH	91	2	2	2	3
Na_2TES[f]	$5\%Pd/Al_2O_3$	H_2O	81	16	0	1	2
	5%Pd/C	H_2O	93	5	0	0	2

[a] *Reaction conditions*: substrate (0.1 g), catalyst (0.1 g), reaction temperature (room temperature), hydrogen pressure (0.1 MPa), reaction time (2 days). [b] MA = malic acid or its Na salt. [c] SA = succinic acid or its Na salt. [d] DGA = diglycolic acid or its Na salt. [e] H_2TES = *trans*-epoxysuccinic acid. [f] Na_2TES = disodium *trans*-epoxysuccinate.

Table 3 BET specific surface area of H_2TES, 5%Pd/Al_2O_3 and their mixture

Sample	BET specific surface area/$m^2\ g^{-1}$	
	Before reaction	After reaction
H_2TES	8.2	—
5%Pd/Al_2O_3	96.8	—
H_2TES + 5%Pd/Al_2O_3[a]	57.3	21.6
H_2TES + 5%Pd/Al_2O_3[b]	57.3	53.9

[a] *Reaction conditions*: at room temperature (30 °C) in the presence of hydrogen (0.1 MPa). [b] *Reaction conditions*: at room temperature (30 °C) in the presence of argon (0.1 MPa).

can be seen in Table 3, the specific surface area of the catalyst–organic component mixture significantly decreased during the hydrogenolysis of H_2TES, whereas the surface area was unchanged under an argon atmosphere. These findings support the validity of our view that the specific surface area of the catalysts after solvent-free reactions reflects the physical states of the substrates and products during the reactions.

Table 4 lists the specific surface area of the catalyst–organic component mixture before and after the hydrogenolysis of Na_2TES using Pd/Al_2O_3 and also lists the specific surface area of the mixture allowed to stand in an argon atmosphere. The specific surface area significantly decreased in the hydrogen atmosphere, whereas it was unchanged in an argon atmosphere. These findings suggested that the hydrogenolysis during the solvent-free reaction of Na_2TES proceeded in the fused state.

This conclusion based on the BET data is in conflict with the conclusion based on the SEM observation that the hydrogenolysis of Na_2TES under solvent-free conditions proceeded in the solid state.[7] However, there are some differences between the present experimental conditions and the previous conditions. The typical experimental conditions are as follows:

(1) Previous conditions: reaction temperature (100 °C), hydrogen pressure (9.0 MPa) and weight ratio of catalyst to Na_2TES (5 : 1).

(2) Present conditions: reaction temperature (30 °C), hydrogen pressure (0.1 MPa) and weight ratio of catalyst to Na_2TES (1 : 1).

The 5 : 1 Pd/Al_2O_3–Na_2TES mixture was thus subjected to the previous reaction conditions and the resulting mixture employed for the estimation of the specific surface area by the BET method. The appearance of the catalyst–organic component mixture thus obtained was similar to that of the catalyst–substrate mixture before the reaction and no formation of a gummy mass was observed. Entry 3 in Table 4 shows the specific surface area of the catalyst–organic component mixtures before and after the reaction. The specific surface area of the mixture decreased by about a half during the reaction. This fact supports the idea that the hydrogenolysis of Na_2TES using Pd/Al_2O_3 proceeded in the fused state, though SEM did not register the formation of a gummy mass. It is reasonable to assume that when the weight ratio of the catalyst to the substrate is high (5 : 1), most of the substrate–product mixture enters the pores and only a small amount of the mixture is present on the outside surface of the catalyst. In such a situation, the mixture on the outside surface would not be able to glue the catalyst particles together. In order to substantiate this hypothesis, we conducted SEM observations of the mixture after the hydrogenolysis of Na_2TES (at 30 °C under 0.1 MPa of hydrogen, Pd/Al_2O_3 : Na_2TES = 1 : 1 or 5 : 1). When the weight ratio of the catalyst : substrate was 1 : 1, the catalyst–substrate–product mixture after the reaction appears to be a gummy mass (Fig. 1). On the other hand, for a catalyst : substrate ratio of 5 : 1, no drastic change in appearance was observed in the mixture of the organic components and the catalyst after the reaction (Fig. 2). These findings show that when the weight ratio of the catalyst to the substrate was low (1 : 1), the substrate–product mixture glued the catalyst particles together to form a gummy mass. It is thus apparent that the use of a small amount of the substrate did not result in the formation of a gummy mass even though the reaction occurred in the fused state.

We next attempted the solvent-free hydrogenation of solid thymol using Rh/Al_2O_3.[5] Quantitative reaction was found to occur under solvent-free conditions (Table 5). The specific surface areas of the catalyst–organic component mixture are listed in Table 5. The specific surface area of the Rh/Al_2O_3–thymol mixture before the reaction was quite low compared with that of the Rh/Al_2O_3 catalyst. This fact suggested that the thymol was fused during the mixing process using a mortar and pestle. The finding that the specific surface area of the mixture appeared to increase during the reaction can be interpreted in terms of hydrogenation to menthones and menthols under the

Table 4 BET specific surface area of the 5%Pd/Al_2O_3–Na_2TES mixture

Entry	Atmosphere	BET specific surface area/$m^2\ g^{-1}$	
		Before reaction	After reaction
1	H_2[a]	50.8	3.0
2	Ar	50.8	48.7
3	H_2[b]	89.9	47.5

[a] *Reaction conditions*: Na_2TES (0.1 g), 5%Pd/Al_2O_3 (0.1 g), at 30 °C in the presence of hydrogen (0.1 MPa). [b] *Reaction conditions*: Na_2TES (0.1 g), 5%Pd/Al_2O_3 (0.5 g), at 100 °C in the presence of hydrogen (9.0 MPa).

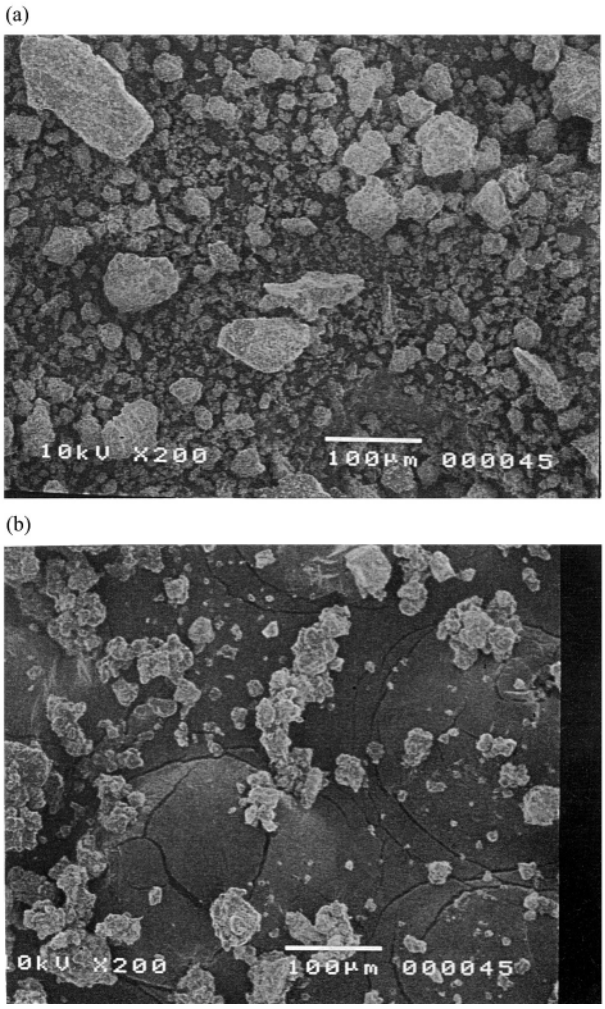

Fig. 1 Micrographs of Na_2TES–5%Pd/Al_2O_3 mixture (wt. ratio; catalyst : substrate = 1 : 1): (a) before the solvent-free reaction, (b) after the solvent-free reaction.

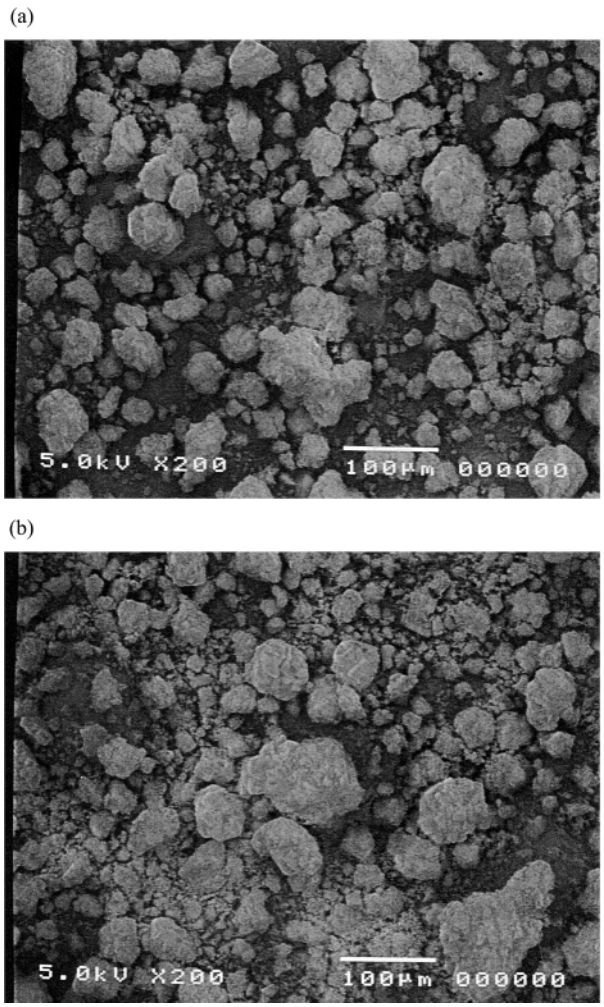

Fig. 2 Micrographs of the Na_2TES–5%Pd/Al_2O_3 mixture (wt. ratio; catalyst : substrate = 5 : 1): (a) before the solvent-free reaction, (b) after the solvent-free reaction.

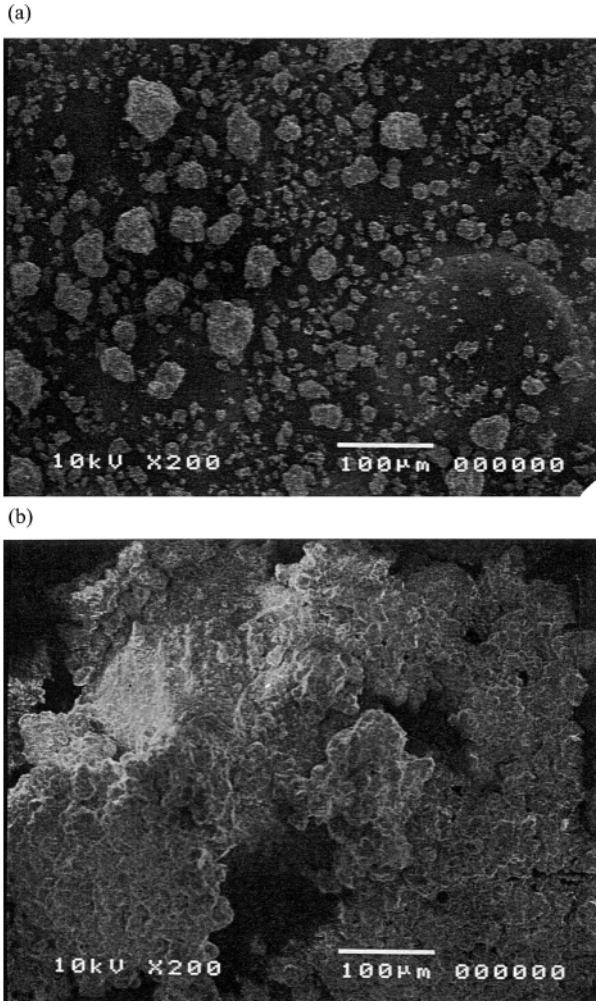

Fig. 3 Micrographs of the thymol–5%Rh/Al_2O_3 mixture: (a) before the solvent-free reaction, (b) after the solvent-free reaction.

Table 5 BET specific surface area of 5%Rh/Al_2O_3 and the 5%Rh/Al_2O_3-thymol mixture

Sample	Yield[a] (%)	BET specific surface area/$m^2\ g^{-1}$	
		Before reaction	After reaction[b]
5%Rh/Al_2O_3	—	89.5	—
Thymol + 5%Rh/Al_2O_3	98	9.2	50.6

[a] Yield: {1.0 − (non-reacted substrate/added substrate)} × 100. [b] *Reaction conditions*: room temperature (30 °C) in the presence of hydrogen (0.1 MPa), thymol (0.1 g), 5%Rh/Al_2O_3 (0.1 g).

solvent-free conditions. It is well known that these compounds are readily sublimed even at room temperature. Most of products in the catalyst pores would be sublimed during the BET procedure *in vacuo* so leading to an increase in the surface area. Thus, the increase in the specific surface area does not reflect the physical states of the substrate and the products during the reaction. Fig. 3 shows micrographs of the catalyst–organic component mixture. The features of the catalyst–organic component mixture changed from a fine powder to a gummy mass during the reaction. This situation is similar to that of the mixture during the solvent-free hydrogenolysis of H_2TES using Pd/SiC, which proceeds in the fused state.[6] Based on the SEM observations, we propose that the solvent-free hydrogenation of thymol proceeds, at least partially, in the fused state. Taking into account Lamartine and Perrin's postulation based on polarimetry,[5] the hydrogenation of thymol should proceed in the presence of both fused and solid thymols.

All the results of the BET method and the SEM observations can be interpreted based on the view that the solvent-free hydrogenolysis of H_2TES or Na_2TES proceeds in the fused state. It is apparent that the BET method is more sensitive for detection of fused-state processes than is SEM. We believe that the estimation of surface area of the catalyst–substrate(–product) mixtures is a promising tool for the investigation of the solvent-free reaction mechanism of solid substances using heterogeneous catalysts.

Experimental

All chemicals were used as received. The supported palladium catalysts were purchased from N. E. CHEMCAT, Japan.

Solvent-free hydrogenolysis of *trans*-epoxysuccinic acid (H_2TES) and its disodium salt (Na_2TES) using supported palladium catalysts

A supported Pd catalyst (0.1 g) was pretreated at 200 °C for 30 min with a H_2 stream. The resulting catalyst was mixed with H_2TES or Na_2TES (0.1 g), and the mixture was ground to a fine powder using a mortar and pestle. The mixture was placed in a Schlenk tube, and then the air in the tube was replaced by hydrogen gas. The reaction vessel was allowed to stand at 30 °C in the presence of hydrogen (0.1 MPa) for 2 days.

Hydrogenolysis in solvents of H_2TES and Na_2TES using supported palladium catalysts

The hydrogenolysis was carried out in the presence of solvent. H_2TES or Na_2TES (0.1 g) was dissolved in methanol or deionized water (5.0 ml). The H_2-pretreated Pd catalyst (0.1 g) was then added to the solution. The reaction conditions, other than the use of the solvent, were the same as those for the solvent-free hydrogenolysis.

Product analyses of the hydrogenolysis of H_2TES or Na_2TES by GC and GC–MS

After the solvent-free reaction, the remaining H_2 gas in the Schlenk tube was replaced by Ar. The extraction solvent (10 ml) was poured into the catalyst–organic component mixture in the tube. Methanol and deionized water were used as the extraction solvents for the H_2TES and Na_2TES, respectively. The resulting suspension was then stirred for 10 min at room temperature. The solvent–insoluble materials were removed by filtration and the filtrate was concentrated to dryness *in vacuo*. The residue was esterified, and the resulting samples were subjected to GC analyses for the estimation of the product distribution. The esterification and GC analyses were carried out according to a previously reported procedure.[6,7]

The identifications of the methyl esters of the substrates and the products were carried out using GC–MS (Shimadzu GC-17A/QP-5000, Column: DB-1, 30 m). The MS spectra of the esters were compared to those of esterified samples of the commercial chemicals. Dimethyl ester of H_2TES: *m*/*z* (%) 101 ([M − CO_2Me]$^+$; 100), 85 (5), 69 (48), 59 (63), 41 (43); dimethyl malate; *m*/*z* 103 ([M − CO_2Me]$^+$; 63), 71 (73), 61 (40), 43 (100); dimethyl glycolate: *m*/*z* (%) 103 ([M − CO_2Me]$^+$; 48), 74 (26), 45 (100); dimethyl succinate: *m*/*z* (%) 115 ([M − 2Me]$^+$; 100), 87 (26), 55 (95), 45 (13).

Solvent-free hydrogenation of thymol using Rh/Al_2O_3

5%Rh/Al_2O_3 (0.1 g) pretreated with H_2 at 200 °C for 30 min was mixed with thymol (0.1 g), and the mixture was ground to fine powder with a mortar and pestle. The reaction variables other than the reaction time were the same as those for the solvent-free hydrogenolysis of H_2TES or Na_2TES. The reaction time was 24 h.

Specific surface area estimation by the BET method

The catalyst–organic component mixture (*ca.* 0.05 g) was placed in a glass tube previously dried *in vacuo*. The air in the glass tube was evacuated to 5.3×10^{-4} MPa and then the mixture was subjected to specific surface area measurement by the BET method (Shimadzu Micromeritics ASAP-2000).

Micrographic observation of catalyst–organic component mixture using a SEM

A small portion of the catalyst–organic component mixture was sputtered with Au to prepare a sample for SEM. After the sputtering, the sample was observed using the SEM (JSM-5410).

Acknowledgements

We thank Professor Yoshiaki Goto and Mr Yasuji Akazawa of Ryukoku University for their kind help with the surface area estimations using the BET method. We also appreciate Ms Hiromi Nakano of Ryukoku University for her advice during the SEM observations.

References

1 D. C. Dittmer, *Chem. Ind.*, 1997, 779; K. Tanaka and F. Toda, *Chem. Res.*, 2000, **100**, 1025; K. Hara, in *Organic Synthesis at High Pressures*, ed. K. Matsumoto and R. M. Acheson, Wiley, New York, 1991, p. 423; Y. Ogo, *Petrotech.*, 1988, **11**, 307.
2 G.-W. Wang, K. Komatsu, Y. Murata and M. Shiro, *Nature*, 1997, **387**, 583.
3 R. S. Varma, D. Kumar and R. Dahiya, *J. Chem. Res. (S)*, 1998, 324.
4 T. Nozoe, K. Tanimoto, T. Takemitsu, T. Kitamura, T. Harada, T. Osawa and O. Takayasu, *Solid State Ionics.*, 2001, **141–142**, 695.
5 R. Lamartine and R. Perrin, in *Spillover of Adsorbed Species*, ed. G. M. Pajonk, S. J. Teichner and J. E. Germain, Elsevier, Amsterdam, 1983, p. 251.
6 T. Kitamura, T. Harada and T. Osawa, in *Spillover and Migration of Surface Species on Catalysts*, ed. C. Li and Q. Xin, Elsevier, Amsterdam, 1997, p. 491.
7 T. Kitamura and T. Harada, *J. Mol. Catal. A: Chemical*, 1999, **148**, 197.
8 S. Brunauer, P. H. Emmet and E. Teller, *J. Am. Chem. Soc.*, 1938, **60**, 309.

Layered double hydroxide fluoride: a novel solid base catalyst for C–C bond formation

B. M. Choudary,*[a] M. Lakshmi Kantam,*[a] V. Neeraja,[a] K. Koteswara Rao,[a] F. Figueras[b] and L. Delmotte[c]

[a] *Inorganic chemistry division, Indian Institute of Chemical Technology, Hyderabad-500 007, India. E-mail: Choudary@iict.ap.nic.in*
[b] *Institut de Recherches sur la Catalyse du CNRS, 2 Av. A. Einstein, 69626 Villeurbanne Cedex, France*
[c] *E.N.S.C. Mu, Laboratoire de Materiaux Mineraux, 3, rue Alfred Werner, F-68093 Mulhouse Cedex, France*

Received 6th August 2001
First published as an Advance Article on the web 10th September 2001

LDH-F hydrotalcite catalysts are found to be an efficient, environmentally attractive and selective solid base catalysts for 1,4-Michael addition and also for simple synthesis of α,β-unsaturated esters and nitriles by Knoevenagel condensation. The catalyst displayed unprecedented catalytic activity both in Knoevenagel and Michael reactions under mild liquid phase conditions at a greater rate compared with known solid bases and fluoride catalysts. The present ecofriendly catalyst is a potential alternative to soluble bases.

Introduction

The employment of solid bases dispensing the use of soluble bases in order to reduce effluents to environmentally acceptable limits in the fine chemical industry is of topical interest. The utility of fluoride salts as potential bases in a variety of synthetic reactions is well known.[1] However, the low solubility of fluoride salts in ordinary solvents hampers their wide application in organic synthesis. Solid bases such as anionic resins, KO^{t}Bu/xonotlite,[2] Amberlyst[3] or activated hydrotalcites,[4] zeolites and MCM materials containing alkali metals,[5] and especially bases sourced from fluorides such as KF/alumina[6] and KF/18-crown-6,[7] designed to overcome solubility problems have been developed and found to be excellent catalysts. The versatile Michael and Knoevenagel reactions have numerous applications in the elegant synthesis of fine chemicals[1,8] and are classically catalysed by bases[9] or suitable combinations of amines and carboxylic or Lewis acids under homogeneous conditions. The employment of these bases/acids in these reactions, however, leads to two main problems affecting the environment; *i.e.* the necessity to dispose of huge amounts of organic waste due to formation of undesirable side products resulting from polymerisation, bis-addition and self condensation, and total dissolved salts formed following the neutralisation of soluble bases with acids or acids with bases. There are a few reports concerning heterogeneous catalysis for Michael additions and Knoevenagel condensations mediated particularly by aluminium oxide,[10] xonotlite/potassium *tert*-butoxide,[2] KF/alumina,[6] cation exchanged zeolites,[11] alkali metal containing MCM-41[5] and $AlPO_4$–Al_2O_3[12] catalysts. The incorporation of alkali metal cations[5] such as Cs^+ or Na^+ in zeolites and mesoporous molecular sieves by cationic exchange provides low basicity which is useful for only a small range of organic reactions. Na^+ clusters introduced in zeolites by impregnation with sodium azide[13] afford strongly basic sites, which catalyse side-chain alkylation reactions, but these are easily deactivated by moisture. In view of these limitations, the development of efficient and selective solid acid–base catalysts for the construction of C–C bonds continues to be a challenging area in organic synthesis. With this background, we envisaged the use of solid bases in the form of layered double hydroxides (LDHs),[14] which possess an intrinsic basicity, in view of their potential usefulness as basic catalysts.[15,16] The introduction of hydroxy groups in the interlayers by rehydration of the calcined LDH provided enhanced activity in C–C bond formation reactions[17,18] over as-synthesised LDHs due to increased basicity.

We conceived and designed LDH fluoride (LDH-F) since the highly polarised fluoride anion in the interlayers of LDH possibly exhibits higher basicity. We report here, for the first time, the preparation of LDH-F through a novel exchange of OH^- obtained *in situ* by calcination (450 °C) followed by rehydration of the LDH in an effort to develop highly basic materials.

Experimental

Mg–Al–NO_3 LDHs with Mg : Al ratios of 2 : 1, 2.5 : 1 and 3 : 1 were prepared as described.[19] The samples of Mg–Al–NO_3 LDHs synthesised as above were first calcined at 450 °C for 8 h in a flow of air (ramping at a rate of 10 °C per min^{-1}), then cooled to room temperature under a flow of nitrogen. Then the samples of the calcined LDHs (1 g each) were treated separately with solutions of KF (0.1 M, 0.5810 g) in 100 mL of deionised and decarbonated water under stirring at room temperature for 24 h to obtain solids of LDH-F with Mg : Al ratios of 2 : 1, 2.5 : 1

Green Context

Solid bases are in many respects the poor cousins to solid acids. While the literature is abundant with examples of the latter, many of which have been utilised commercially, relatively few successful solid bases are known. Here a novel solid base catalyst for C–C bond formation is described. The highly polarised basic fluoride in LDH displays unprecedented catalytic activity in both the important Knoevenagel and Michael reactions. It also offers the other potential advantages of solid catalysts, including easy separation and low reactor corrosion. ***JHC***

and 3:1 which were filtered under nitrogen atmosphere and washed with 400 ml of deionised water and vacuum dried at 80 °C (yield: 1.380 g).

Knoevenagel condensation

In a typical procedure, 2-methoxybenzaldehyde (1 mmol, 0.12 mL) and 0.035 g of as-synthesised LDH-F were stirred in 5 mL DMF for 5 min under a nitrogen atmosphere. Then malononitrile (1 mmol, 0.06 mL) was added and stirring was continued until the completion of the reaction, as monitored by TLC. The catalyst was filtered off and the filtrate concentrated under reduced pressure (162 mg, 100% yield).

Michael reaction

In a typical reaction procedure, acetylacetone (1 mmol, 0.10 mL) and 0.1 g of as-synthesised LDH-F hydrotalcite were stirred in 5 ml of dry acetonitrile for 5 min under a nitrogen atmosphere. Then methyl vinyl ketone (1 mmol, 0.08 mL) was added and stirring continued at room temperature until the completion of the reaction as monitored by thin layer chromatography. The catalyst was filtered off and the filtrate concentrated under reduced pressure. The crude product was purified by column chromatography using hexane–ethyl acetate (9:1) as eluent (164 mg, 85% yield).

Chemical analysis (ICP) of LDH-F samples with Mg:Al ratios of 2:1, 2.5:1 and 3:1 showed fluoride contents of 2.73, 3.57 and 4.11%, respectively, and a potassium content of <0.1% in all samples. The solid state ^{19}F MAS NMR spectra† of the LDH-F samples (Fig. 1) show chemical shifts centered at −175, −172 and −170 ppm, respectively. Thus with a decrease of Mg content, the fluoride signal is shifted upfield. This indicates that the electronic density on fluoride increases with decrease in Mg content and the polarisability is enhanced. As the Mg content increases, the fluoride peak is intensified, which is in agreement with the increased fluoride content as revealed by ICP. The other minor broad peak in the range of −154 to −149 ppm indicates the presence of AlF_3[20] in LDH-F samples.

† ^{19}F MAS NMR spectra were recorded at 8.5 kHz on a DSX400 Bruker spectrometer, with a 2.5 mm NMR probe from Bruker. The chemical shifts were referenced relative to external $CFCl_3$.

It is well established that the ^{19}F chemical shifts for KF[21] and KF/alumina[22] appear at −123 and −155 ppm, respectively. Hence, the upfield chemical shift is assigned to highly ionised F^- anions, most probably bound to Al in LDH-F.

ESCA results of LDH-F (Mg:Al ratio 3:1, 2.5:1 and 2:1) as well as of the used catalyst show binding energies of fluoride at 685.6, 685.1, 685.4 and 684.5 eV respectively. The binding energies of fluoride observed in these LDHs are in accord with the ECSA binding energies of fluoride in KF and KF/alumina at 684.8 eV. The TGA/DTA data display two stages of weight loss, *viz*., at 210–250 and 410–460 °C accompanied by two endothermic transformations characteristic of LDHs.[17]

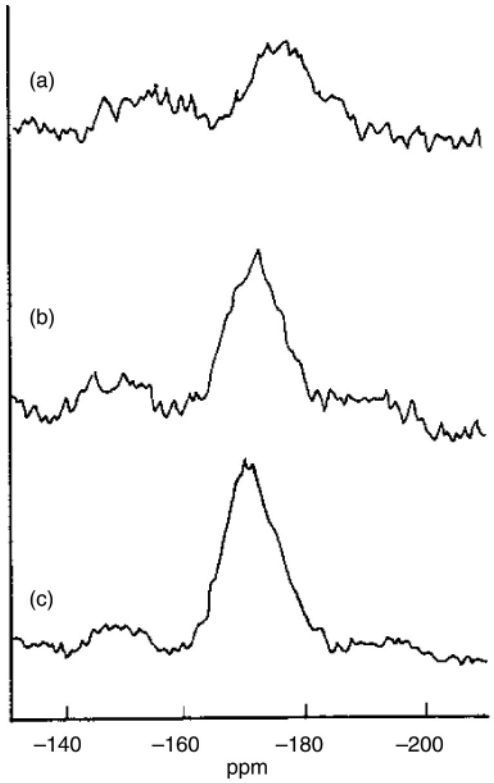

Fig. 1 Solid state ^{19}F MAS NMR spectra of LDH-F: (a) Mg:Al = 2:1, (b) Mg:Al = 2.5:1 and (c) Mg:Al = 3:1.

Table 1 Knoevenagel condensation catalysed by LDH-F catalyst (Mg:Al = 3:1)[a]

Entry	R^1	R^2	Y	Solvent	Time/h	Yields[b] (%)	STY[c]	Ref.
1	Ph	H	CN[d]	DMF	0.25	100	17.6	
					3[e]	86[e]	1.13	6
					1[f]	100[f]	10.6	23
					24[g]	81[g]	0.48	24
2	Ph	H	CO_2Et[h]	DMF	2	92	2.64	
					7[i]	81[i]	0.07	5
3	4-$NO_2C_6H_4$	H	CN[d]	MeCN	1.5	100	3.52	
					24[g]	80[g]	0.66	24
4	4-$NO_2C_6H_4$	H	CO_2Et[h]	MeCN	1.5	100	4.41	
					24[g]	94[g]	0.91	24
5	*c*-C_5H_{10}	H	CN[d]	DMF	2	100	2.08	
					15[e]	55[e]	0.13	6
					6[f]	75[f]	1.25	23
6	*c*-C_5H_{10}		CO_2Et[h]	DMF	2	21	0.57	
7	4-ClC_6H_4	H	CN[d]	DMF	0.25	100,95[j]	21.5	
					24[g]	65[g]	0.47	24
8	4-ClC_6H_4	H	CO_2Et[h]	DMF	2	86	2.89	
					24[g]	85[g]	0.83	24

[a] All reactions were performed with 1 mmol of substrate and 1 mmol of active methylene compound using 0.035 g of catalyst in 5 mL of DMF or MeCN in the specified time. [b] ^{1}H NMR yields based on aldehyde. [c] Space time yield (STY): g of product obtained per g of catalyst per h. [d] Reactions carried out at room temperature. [e] Reaction with KF/alumina as catalyst. [f] Reaction with KF as catalyst. [g] Reaction with untreated xonotlite as catalyst. [h] Reactions carried out at 60 °C. [i] Alkali metal containing MCM-41 as catalyst. [j] Yield after 5th cycle.

Results and discussion

Since no simple method has yet been agreed for the determination of basicity, we chose the base catalysed[9] Knoevenagel and Michael reactions to further characterize the surface chemistry. LDH-F as a catalyst in Knoevenagel condensations (Scheme 1) displays superior activity when compared with other bases (Table 1).

The LDH-F catalyst with an Mg : Al ratio of 3 : 1 shows higher activity than the LDH-F catalysts with Mg : Al ratios of 2 : 1 or 2.5 : 1, which is ascribed to the larger fluoride loading. Aromatic aldehydes readily condensed with malononitrile to afford excellent space-time yields (STY), while with ethyl cyanoacetate, the STY is low. This lower reactivity may be due to the lower acidity of the active methylene group of ethyl cyanoacetate. As can be seen from Table 1, all reactions proceed selectively to give the dehydrated products with high atom economy without formation of any by-products. It may be noted that LDH-F displays much higher activity than KF and KF/alumina in the condensation of benzaldehyde and cyclohexanone, respectively, with malononitrile (Table 1, entries 1 and 5). The Knoevenagel condensation using solid support catalysts such as $AlPO_4$–Al_2O_3[12] or Al_2O_3,[10] required a large amount of the catalyst and afforded poor yields of adducts. Though the reaction is relatively facile with rare-earth NaY zeolite,[11] longer reaction times were required. The recyclability of the catalyst in Knoevenagel reactions is well established with consistent selectivity and activity being displayed for five cycles.

The activity of LDH-F was also compared with that of solid bases in the Michael reaction (Table 2) involving various donors and acceptors (Scheme 2).

Significantly the Michael reaction of α,β-unsaturated ketones with nitroalkanes catalysed by LDH-F shows much higher activity (as indicated by STY) than with other solid bases which usually require a large excess of nitroalkanes and high catalyst loading (Table 2, entries 1, 3 and 6). Similarly, the Michael reaction of α,β-unsaturated ketones with other donors catalysed by LDH-F manifests STYs in the range of 1.6–16 times that of KO^{t}Bu/xonotlite (Table 2, entries 4 and 5), rehydrated hydrotalcite (Table 2, entry 2) or KF/alumina (basic). The higher basicity of the LDH-F over other fluoride catalysts as displayed both in Knoevenagel and Michael reactions is correlated to the highly polarised F^- anion in LDHs when compared with KF and KF/alumina as revealed by the solid state ^{19}F NMR data of the LDH-F catalysts.

A plausible reaction mechanism (Scheme 3) involves the abstraction of the proton to generate a carbanion stabilised in the LDH with its cationic charge, both in Knoevenagel and Michael reactions. Since the enhanced basicity increases the rate of these reactions, the generation of the carbanion is assumed to be the rate-determining step. The HF formed due to the abstraction of protons interacts with water to regenerate F^- to sustain catalytic activity along with H_3O^+. The vital role of water is confirmed by the fact that the Michael reaction conducted with a sample of LDH-F preheated at 250 °C to remove hydrate water shows a poor performance. In the Michael reaction, the carbanion–LDH further adds to the α,β-unsaturated ketone to form an intermediate enolate, which in turn abstracts a proton from *in situ* formed H_3O^+ to afford the final product and regenerate LDH-F. Similarly, in the case of the Knoevenagel condensation, the carbanion–LDH reacts with the carbonyl compound and on subsequent dehydration gives the Knoevenagel product.

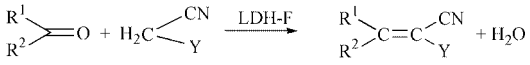

Scheme 1

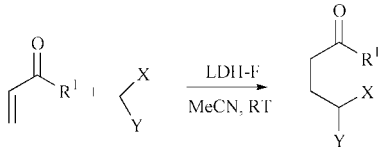

Scheme 2

Table 2 Michael additions catalysed by LDH-F catalyst (Mg : Al = 3 : 1)[a]

Entry	Acceptor	Donor[b]	Time/h	Product	Yield (%)	STY[c]	Ref.
1	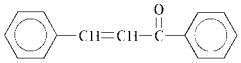	NM	2.0 3.5[d]	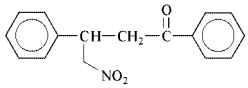	90 74[d]	1.21 0.09	6
2	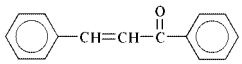	DEM	2.0 6.0[e]	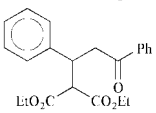	95 96[e]	1.74 0.11	18
3		NE	1.5 2.0[f]	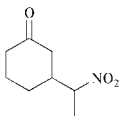	98 100[f]	1.11 0.14	6
4		AA	2.0 96[g]	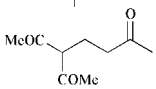	85 79[g]	0.72 0.34	2
5		DEM	2.0 72[g]	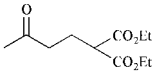	80 70[g]	0.92 0.34	2
6		NM	2.0[h] 2.0	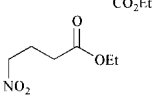	77[h] 98	0.11 0.78	6

[a] All reactions were performed with 1 mmol of acceptor and 1 mmol of donor using 0.1 g of catalyst in 5 mL of MeCN at room temperature in the specified time. [b] NM = nitromethane, NE = nitroethane, DEM = diethyl malonate, AA = acetylacetone. [c] Space time yield (STY): g of product obtained per g of catalyst per h. [d] KF/alumina (basic) as catalyst. [e] Rehydrated Mg–Al hydrotalcite as catalyst, 1 g of catalyst per 2 mmol of substrate. [f] KF/alumina (basic) as catalyst, 3 g of catalyst per 5 mmol of substrate. [g] KO^{t}Bu/xonotlite as catalyst. [h] KF/alumina (basic) as catalyst, 5 g of catalyst per 9.2 mmol of substrate.

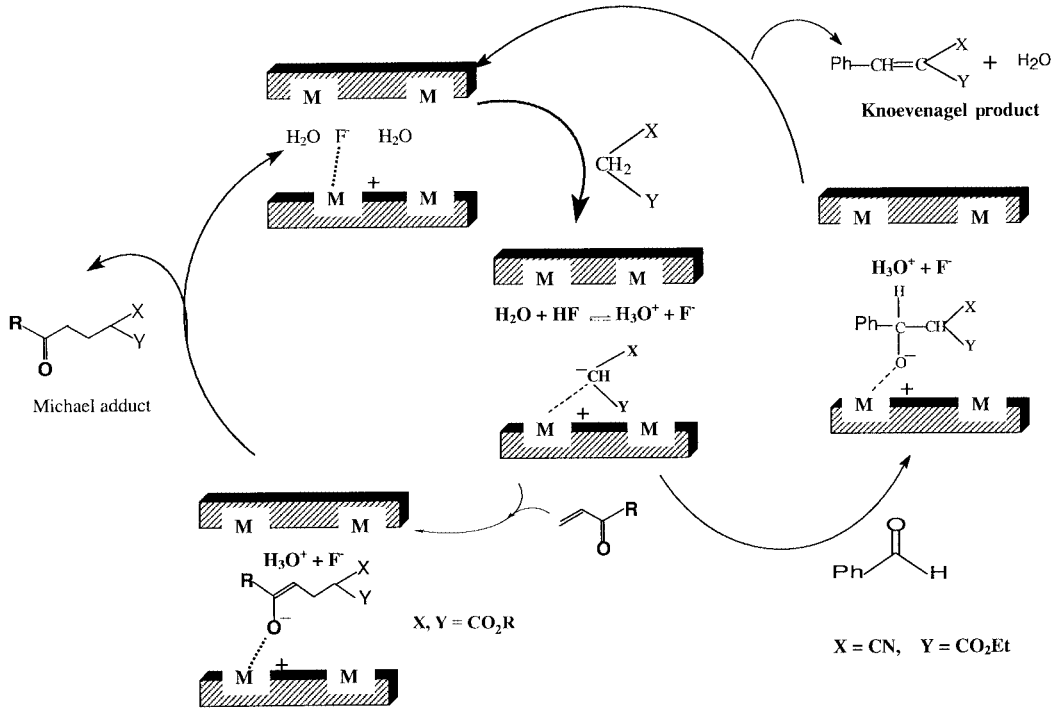

Scheme 3 Plausible mechanism for Michael and Knoevenagel reactions.

Conclusions

The highly polarised basic fluoride ions in our developed LDHs, display unprecedented catalytic activity both in Knoevenagel and Michael reactions among the family of solid bases, in general, and known fluoride catalysts, in particular, under very mild liquid phase conditions. The other advantages of LDH-F include easy separation of the catalyst by simple filtration, high atom economy to enable waste minimization, reduced corrosion and reusability thus making the catalyst an attractive and potential candidate for commercial realisation in C–C coupling reactions addressed in this work. Thus this method offers an environmentally safer alternative to the existing methods.

This work was realised in the framework of an Indo–French co-operative programme, funded by IFCPAR (project No. IFC/1106-2/96/2460).

References

1 J. H. Clark, *Chem. Rev.*, 1980, **80**, 429; B. M. Trost in *Comprehensive Organic Synthesis*, Pergamon, Oxford, 1991, Vol. 2, p. 133–340.
2 P. Laszlo and P. Pennetreau, *Tetrahedron Lett.*, 1985, **26**, 2645; S. Chalais, P. Laszlo and A. Mathy, *Tetrahedron Lett.*, 1985, **26**, 4453; A. Garcia-Raso, J. Garcia-raso, B. Campaner, R. Mestres and J. V. Sinisterra, *Synthesis*, 1982, 1037; M. Iglesias, J. M. Marinas and J. V. Sinisterra, *Tetrahedron*, 1987, **43**, 2335.
3 R. Ballini, P. Marziali and A. Mozzica Freddo, *J. Org. Chem.*, 1996, **61**, 3209.
4 E. Suzuki and Y. Ono, *Bull. Chem. Soc. Jpn.*, 1988, **61**, 1008.
5 A. Corma and R. M. Martin-Aranda, *J. Catal.*, 1991, **130**, 130; K. R. Kloetstra and H. Van Bekkum, *J. Chem. Soc., Chem. Commun.*, 1995, 1005.
6 T. Ando, J. Yamawaki, T. Kawabe, S. Sumi and T. Hanufusa, *Bull. Chem. Soc. Jpn.*, 1982, **55**, 2504; J. H. Clark, D. G. Cork and M. S. Robertson, *Chem. Lett.*, 1983, 1145; J. H. Clark, D. G. Cork and H. W. Gibbs, *J. Chem. Soc., Perkins Trans. 1*, 1983, 2253; D. E. Bergbreiter and J. J. Lalonde, *J. Org. Chem.*, 1987, **52**, 1601; J. Yamawaki, T. Kawabe, T. Ando and T. Hanafusa, *Bull. Chem. Soc. Jpn.*, 1983, 1885.
7 I. Belsky, *J. Chem. Soc., Chem. Commun.*, 1977, 237.
8 S. Ganesh and A. Sarkar, *Tetrahedron Lett.*, 1991, **32**, 1085; S. Machida, Y. Hashimoto, K. Saigo, J. Inoue and M. Hasegawa, *Tetrahedron*, 1991, **47**, 3737.
9 E. D. Bergman, D. Ginsburg and R. Pappo, *Org. React.*, 1959, **10**, 179; D. A. Oare and C. H. Heathcock, *Top. Stereochem.*, 1989, **19**, 277; E. Knoevenagel, *Chem. Ber.*, 1894, **27**, 2345.
10 F. Texier-Boullet and A. Foucaud, *Tetrahedron Lett.*, 1982, **26**, 4453.
11 A. Corma, V. Frones, R. M. Martin-Aranda, H. Garcia and J. Primo, *Appl. Catal.*, 1990, **59**, 237; T. Indrasena Reddy and R. S. Varma, *Tetrahedron Lett.*, 1997, **38**, 1721.
12 J. A. Cabello, J. M. Campelo, A. Garcia, D. Luna and J. M. Marinas, *J. Org. Chem.*, 1984, **49**, 5195.
13 L. Martens, P. Grobet and P. A. Jacobs, *Nature*, 1985, **315**, 568.
14 F. Cavani, F. Trifiro and A. Vaccari, *Catal. Today*, 1991, **11**, 173.
15 W. T. Reichle, *J. Catal.*, 1985, **94**, 547; C. Busetto, G. DelPiero, G. Manara, F. Trifiro and A. Vaccari, *J. Catal.*, 1984, **85**, 260.
16 J. G. Numan, P. B. Himelfarb, R. G. Herman, K. Klier, C. E. Bogdan and G. W. Simmons, *Inorg. Chem.*, 1989, **28**, 3868.
17 K. K. Rao, M. Gravelle, J. Sanchez and F. Figueras, *J. Catal.*, 1998, **173**, 115; M. L. Kantam, B. M. Choudary, Ch. V. Reddy, K. K. Rao and F. Figueras, *Chem. Commun.*, 1998, 1033.
18 B. M. Choudary, M. L. Kantam, Ch. V. Reddy, K. K. Rao and F. Figueras, *J. Mol. Catal. A: Chem.*, 1999, **146**, 279.
19 S. Miyata, *Clays Clay Miner.*, 1975, **23**, 369.
20 J. R. Schlup and W. Vaughan, *J. Catal.*, 1986, **99**, 304.
21 J. H. Clark, E. M. Goodman, D. K. Smith, S. J. Brown and J. M. Miller, *J. Chem. Soc., Chem. Commun.*, 1986, 657.
22 C. V. A. Duke and J. M. Miller, *J. Mol. Catal.*, 1990, **62**, 233.
23 L. Rand, J. V. Swisher and C. J. Cronin, *J. Org. Chem.*, 1962, **27**, 3505.
24 S. Chalais, P. Laszlo and A. Mathy, *Tetrahedron Lett.*, 1985, **26**, 4453.

Potassium fluoride doped alumina: an effective reagent for ester hydrolysis under solvent free conditions

George W. Kabalka,* Lei Wang and Richard M. Pagni

Departments of Chemistry and Radiology, The University of Tennessee, Knoxville, TN 37996-1600 USA. E-mail: kabalka@utk.edu

Received 19th July 2001
First published as an Advance Article on the web 1st October 2001

A microwave-enhanced hydrolysis of esters utilizing potassium fluoride doped alumina in the absence of solvents has been developed. Carboxylic acids are produced in excellent yields along with the corresponding alcohols.

Introduction

Protection and de-protection of functional groups are widely used procedures in organic synthesis. Esters are used to protect carboxylic acids as well as alcohols since they are moderately stable but yet can be hydrolyzed in a variety of ways.[1] However, hydrolytic procedures often proceed in moderate yields and the requisite solvents can pose waste handling problems. Recently, a solventless ester deprotection sequence utilizing alumina and microwave irradiation was reported for use with benzyl and acetyl esters.[2]

We have found potassium fluoride alumina mixtures to be particularly useful in organic synthesis.[3] For example, using a commercially available alumina–potassium fluoride mixture to which we added either palladium powder or copper(II) chloride, we were able to carry out Suzuki, Sonogashira and Glaser coupling reactions on a wide variety of aromatic moieties without the use of solvent[4] under microwave irradiation.[5,6]

We now wish to report a general, solventless, microwave-enhanced hydrolysis reaction utilizing potassium fluoride doped alumina which can be utilized on a wide variety of esters to generate the corresponding carboxylic acids and alcohols in excellent yields [eqn. (1)].

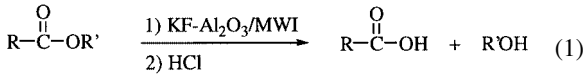

(1)

Results and discussion

We first investigated the generation of acids from a variety of esters. The results are summarized in Table 1. The data indicate that, in the presence of potassium fluoride doped alumina under microwave irradiation (MWI) and solvent free conditions, a wide variety of esters derived from aromatic, vinyl and aliphatic acids readily undergo hydrolysis. Esters of primary, secondary and tertiary alcohols are cleaved to generate the corresponding carboxylic acids in excellent yields. The results also suggest that the reaction is relatively insensitive to the electronic characteristics of the substituent in an aromatic acid.

The hydrolysis reaction can be carried out in the absence of microwaves by simply heating the ester on the potassium fluoride doped alumina but reaction times are relatively long. As an example, the hydrolysis of ethyl benzoate requires 4 h at 80 °C whereas the reaction requires only 2 min under microwave irradiation.

We made no attempt to isolate the low molecular weight alcohol co-products in the reactions listed in Table 1, although gas chromatographic analyses of the reaction mixtures indicated essentially quantitative yields of both acid and alcohol products. Since esters are frequently used to protect alcohols, we carried out a series of experiments in which the alcohol products were isolated *via* hydrolysis of a series of acetate and benzoate derivatives. The results are summarized in Table 2. The ease of isolation is especially noteworthy. The product alcohols are

Table 1 Generation of carboxylic acids from esters using KF doped alumina[a]

Entry	R	R′	Yield(%)[b]
a	Ph	Me	97
b	Ph	Et	98
c	Ph	Bu^n	97
d	Ph	Pr^i	95
e	Ph	Bu^t	96
f	*o*-IC_6H_4	Et	96
g	*p*$MeOC_6H_4$	Et	98
h	*p*-$NO_2C_6H_4$	ET	94
i	$Me(CH_2)_{12}$	Et	90
j	$Me(CH_2)_{12}$	Pr^i	94
k	$Me(CH_2)_{12}$	Bu^t	90
l	$Et(Me)_2C$	Bu^n	92
m	CH_2=CH	Pr^i	96
n	Ph	Et	98

[a] Ester (2 mmol) and potassium fluoride doped alumina (1.00 g, 40 wt% KF) were mixed and then subjected to microwave irradiation (2 min, 100% power). The product was isolated by washing with 5 mL of water, filtration and acidification of the filtrate. [b] Isolated yield of carboxylic acid.

Green Context

Protection and de-protection of functional groups in organic molecules remain important procedures for the synthetic chemist. If such methods are required then it is important that the intermediates are benign and the protection and de-protection methods require minimum resource inputs and waste outputs. Esters are among the safer and more acceptable intermediates in this context but their conversion back to the carboxylic acid and alcohol can be less than efficient. Low product yields and solvent-intense procedures are commonplace but unacceptable in these environmentally conscious days. Here, the use of the established support reagent KF-Al_2O_3 in ester saponification reactions is described. Only the ester and the reagent are required for the reaction which can be carried out thermally or more effectively under microwave irradiation. Only acidic water is required in the extraction. ***JHC***

Table 2 De-protection of alcohols using KF doped alumina[a]

Entry	R	R′	Yield(%)[b]
a	Ph	$PhCH_2$	96
b	Me	$PhCH_2$	97
c	Ph	Ph	95
d	Me	Ph	97
e	Ph	n-C_8H_{17}	94
f	Me	n-C_8H_{17}	92
g	Me	$Me_2C{=}CHCH_2CH_2(Me)C{=}CHCH_2$	94

[a] A mixture of ester (2 mmol) and KF/alumina (1.00 g, 40 wt% KF) was subjected to microwave irradiation (2 min, 100% power). The alcohol was removed by rinsing the alumina with a mixture of hexane and diethyl ether (1 : 1). [b] Isolated yield of alcohol.

simply washed off the solid matrix and then isolated by evaporation of the solvent.

Experimental procedure

A commercially available Sharp Model R-4A38, 1000-watt microwave oven was used in this study at 100% power. Requisite esters were obtained from the Aldrich Chemical Company or were prepared *via* standard procedures. KF/Al_2O_3 was purchased from the Aldrich Chemical Co.

The hydrolysis of ethyl benzoate is representative. Ethyl benzoate (0.300 g, 2.00 mmol) was added to KF/Al_2O_3 (1.00 g, 40 wt% KF) contained in a 10 mL round-bottomed flask. The mixture was stirred at room temperature to ensure efficient mixing. The flask was then fitted with a septum, placed in the microwave oven and irradiated at 100% power for 2 min. (**CAUTION:** heating volatile materials in commercial microwave ovens for extended periods can be hazardous.) After cooling, water (5 mL) was added to the solid and stirred for 10 min (to ensure the potassium carboxylate was removed from the surface) and the mixture filtered. The filtrate was neutralized by addition of aqueous HCl. The product was filtered off and dried under vacuum to afford benzoic acid (0.240 g, 98%).

The procedure for regeneration of alcohols from esters is even more straightforward. *n*-Octyl benzoate (0.468 g, 2.00 mmol) was added to KF/Al_2O_3 (1.00 g, 40 wt% by weight) contained in a 10 mL round-bottomed flask. The mixture was stirred at room temperature to ensure efficient mixing. The flask was then fitted with a septum, placed in the microwave oven and irradiated at 100% power for 2 min. After cooling, hexane–diethyl ether (1 : 1 v/v, 2 × 5 mL) was added and the mixture stirred for 10 min prior to filtration. The filtrate was concentrated under reduced pressure to yield the crude alcohol, which was purified by column chromatography (silica gel, ethyl acetate–hexane) to afford *n*-octyl alcohol (0.244 g, 94%).

Conclusion

A reliable, rapid and practical procedure for the deprotection of esters has been developed which involves the use of a solvent-free mixture of potassium fluoride doped alumina under microwave irradiation. The reaction is environmentally friendly and results in excellent yields of desired products.

Acknowledgments

We wish to thank the U. S. Department of Energy and the Robert H. Cole Foundation for support of this research.

References

1 T. W. Greene and P. G. M. Wuts, *Protective Groups in Organic Synthesis*, John Wiley and Sons, New York, 3rd Edn., 1999.
2 R. S. Varma, A. K. Chatterjee and M. Varma, *Tetrahedron Lett.*, 1993, **34**, 4603; R. S. Varma, M. Varma and A. K. Chatterjee, *J. Chem. Soc., Perkin Trans. I*, 1993, 999.
3 G. W. Kabalka and R. M. Pagni, *Tetrahedron*, 1997, **53**, 7999; M. B. McGinnis, K. Vagle, J. F. Green, L.-C. Tan, R. Palmer, L. Siler, R. M. Pagni and G. W. Kabalka, *J. Org. Chem.*, 1996, **61**, 3496; W. R. Sponholtz, III, R. M. Pagni, G. W. Kabalka, J. F. Green and L.-C. Tan, *J. Org. Chem.*, 1991, **56**, 5700; C. Pala-Wilgus, S. Downing, E. Moliter, S. Bains, R. M. Pagni and G. W. Kabalka, *Tetrahedron Lett.*, 1995, **36**, 3469.
4 G. W. Kabalka, R. M. Pagni and C. M. Hair, *Org. Lett.*, 1999, **1**, 1423; G. W. Kabalka, R. M. Pagni, L. Wang, V. Namboodiri and C. M. Hair, *Green Chem.*, 2000, **2**, 120; G. W. Kabalka, L. Wang, V. Namboodiri and R. M. Pagni, *Tetrahedron Lett.*, 2000, **41**, 5151; G. W. Kabalka, L. Wang and R. M. Pagni, *Synlett*, 2001, 108.
5 R. A. Abramovich, *Org. Prep. Proc. Int.*, 1991, **23**, 683; C. G. Blettner, W. A. Koenig, A. Wilfried, W. Stenzel and T. Schotten, *J. Org. Chem.*, 1999, **64**, 3885; D. S. Bose and B. Jayalakshmi, *J. Org. Chem.*, 1999, **64**, 1713; S. Caddick, *Tetrahedron*, 1995, **51**, 10403; G. Majetich and K. Wheless, in *Microwave-Enhanced Chemistry*, ed. H. M. Kingston and S. J. Haswell, American Chemical Society, Washington, D.C., 1997, pp. 455–505.
6 R. S. Varma, *Green Chem.*, 1999, **1**, 43; V. V. Namboodiri and R. S. Varma, *Green Chem.*, 2001, **3**, 146; R. S. Varma, *Pure Appl. Chem.*, 2001, **73**, 193; R. S. Varma and V. V. Namboodiri, *Chem. Commun.*, 2001, 643; R. S. Varma and K. P. Naicker, *Green Chem.*, 1999, **1**, 247.

Microwave mediated solvent-free acetylation of deactivated and hindered phenols

Nabajyoti Deka, Anne-Marie Mariotte and Ahcène Boumendjel*

Département de Pharmacochimie Moléculaire, UMR-CNRS 5063, UFR de Pharmacie de Grenoble, 38706 La Tronche, France. E-mail: Ahcene.Boumendjel@ujf-grenoble.fr

Received 28th August 2001
First published as an Advance Article on the web 19th September 2001

Deactivated and sterically hindered phenols have been acetylated with acetic anhydride under microwave irradiation and using iodine as catalyst in an eco-friendly process. The reaction was carried out under solvent-free conditions and the acetates were obtained in nearly quantitative yields with dramatic reduction of reaction time compared to standard oil-bath heating.

Introduction

Functional group protection strategies are central to target molecule synthesis. The protection of alcohols, phenols and amines as their acetates is one of the most fundamental, useful and widely used transformations in organic synthesis. Although numerous methods are available for the preparation of acetates, an acetic anhydride–pyridine mixture is commonly used.[1] In our ongoing research program dealing with the synthesis and Structure Activity Relationship studies[2] of 5-hydroxyflavones, we found that acetic anhydride–pyridine is not suitable for acetylation of the 5-OH group (Fig. 1) due to poor yield and long reaction time. The low reactivity of 5-OH is due to the adjacent carbonyl to which it may form a hydrogen bond and thus result in a non-covalent six-membered ring.[3] Generally, the acetylation or alkylation of such a proton, requires more drastic conditions, *e.g.* using acetyl chloride with strong bases, or by using phase transfer catalysis; a further drawback is longer reaction times (up to 40 h).[1]

Recently, iodine has been used as an efficient catalyst for acetylation of alcohols.[4] It is likely that the role of iodine is in activation of acetic anhydride as a Lewis acid which promotes the acetylation reaction. Using iodine as a catalyst for the acetylation of 5-hydroxyflavones is not advantageous as the reaction takes a long time at room temperature or under reflux.

In order to generalize the use of iodine as an efficient catalyst for acetylation of phenols and especially those of low reactivity, we now report the coupling of microwave irradiation with the use of iodine for acetylation of deactivated or hindered phenols. The use of microwave energy in organic synthesis is becoming very popular and many reactions are becoming accessible. An advantage of microwave-catalyzed reactions, is that they can take place under solvent-free conditions (eco-friendly process) compared to conventional heating; in addition, lower reaction times and higher yields are generally obtained.[5]

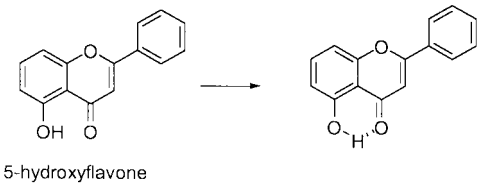

5-hydroxyflavone

Fig. 1

Results and discussion

In the present article, we report the acetylation of the deactivated and sterically hindered phenols shown in Fig. 2.

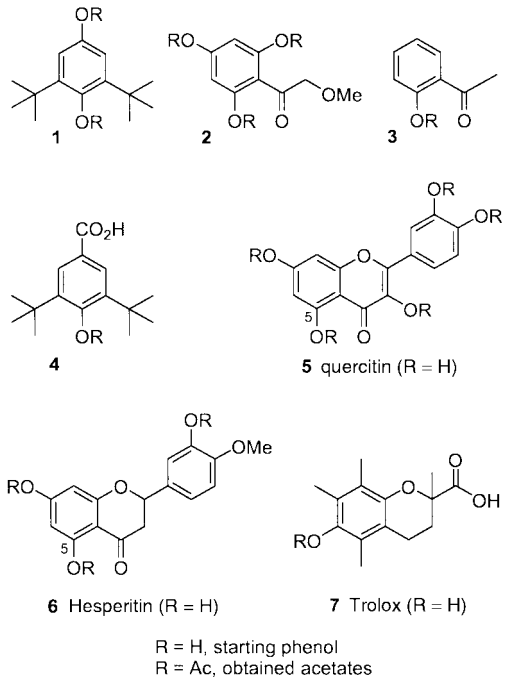

Fig. 2 Phenols acetylated according to the reported method.

Green Context

Functional group protection strategies are fundamental in the synthesis of many target molecules but they are intrinsically wasteful. If they are to be used then it is very important that we utilise the cleanest possible protection methods. Solvents and toxic reagents, as well as very heavy groups (lowering overall process atom efficiency) should be avoided. Here a green procedure for acetylation (relatively small added weight) is described that avoids solvent and uses a widely available safe reagent. ***JHC***

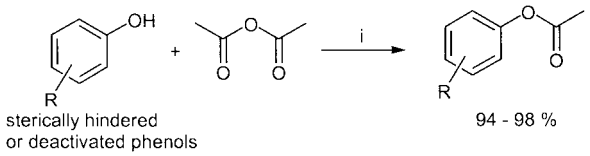

Scheme 1 *Reagents and conditions*: i, I_2 (10%), microwaves 2–4 min.

Table 1 Acetylation of phenols shown in Fig. 2. Comparison of microwave and oil-bath heating

Entry[a]	t^b/min at 500 W (≈ 65 °C)	Yield (%)[c] (microwave)	Yield (time/h) at 65 °C (oil bath)
1	2	97	70(3)
2	2	95	63(4)
3	2	98	68(3)
4	4	96	63(3)
5	4	94	53(5)
6	4	94	56(5)
7	4	97	50(5)

[a] All compounds gave satisfactory NMR and MS analysis. [b] At 500 W power (≈ 65 °C). [c] Yields are for isolated pure products.

The procedure is easy to perform and the reaction can be conducted in solvent free conditions and leads to quantitative yields of products (Scheme 1, Table 1).

Acetylation does not take place when microwave energy is used in the absence of iodine. When the procedure was tested by simply using iodine (without microwave irradiation), very low yields were obtained and the 5-hydroxy group of quercitin and hesperitin was not acetylated, as deduced by ^{1}H NMR spectroscopy.

In order to show the usefulness of the microwaves, control experiments were carried out using the same amount of reactants and at the same temperature reached in a microwave oven (65 °C). As shown in Table 1, acetylated derivatives were obtained after a minimum of 3 h heating and the yields were generally lower. In this case, yields can be increased by using chloroform as a solvent.

In conclusion, we have demonstrated that combining iodine with microwave energy is an efficient method for acetylation of deactivated phenols. This eco-friendly method offers scope for the practical synthesis of protected polyphenols and, especially, the biologically active 5-hydroxyflavones.

Experimental

General procedure

In a microwave oven. A catalytic amount of iodine (0.1 mmol) was added to a mixture of the phenolic compound (1 mmol) and acetic anhydride (5 mmol). The mixture, placed in a 100 mL round bottomed flask, was irradiated in a microwave reactor for 2–4 min at 500 W power. Immediately upon completion, the flask was removed from the oven and the temperature recorded with a thermometer (60–65 °C).[6] The mixture was poured into water and extracted with CH_2Cl_2. The extract was washed successively with sodium thiosulfate solution, hydrogencarbonate solution and water. The extract was then dried over anhydrous sodium sulfate and evaporated to yield the pure phenol acetate. The reaction was conducted in solvent free conditions except for **5** and **6**, for which dichloromethane (2 mL mmol^{-1}) was added to help solubilization. Even when performed on a large scale (2 or 3 g) the reaction was complete in the same time without affecting the yield (Table 1).

In an oil-bath. The reactants were mixed in the same manner as in the microwave oven and heated in an oil-bath at 65 °C. After cooling to room temperature, dichloromethane was added and the mixture poured into water and the product extracted with dichloromethane and treated as above. The crude product was column chromatographed on silica gel and eluted with cyclohexane–ethyl acetate (8 : 2).

Acknowledgements

N. D. is a receipient of a fellowship from Le Ministère de la Recherche du Gouvernement Français to whom we are grateful.

References

1 T. W. Greene and P. G. M. Wuts, *Protective Groups in Organic Synthesis*, John Wiley and Sons, Inc., New York, 1991.
2 F. Bois, A. Desfougéres, A. Boumendjel, A.-M. Mariotte, G. Bessard, F. Caron and P. Devillier, *Bioorg. Med. Chem. Lett.*, 1997, **7**, 1323; F. Bois, C. Beney, A. Boumendjel, A.-M. Mariotte, G. Conseil and A. Di Pietro, *J. Med. Chem.*, 1998, **41**, 4161; A. Boumendjel, F. Bois, C. Beney, A.-M. Mariotte, G. Conseil and A. Di Pietro, *Bioorg. Med. Chem. Lett.*, 2001, **11**, 75.
3 K. P. R. Kartha and R. A. Field, *Tetrahedron*, 1997, **53**, 11 753.
4 R. Borah, N. Deka and J. Sarma, *J. Chem. Res. (S)*, 1997, 110.
5 Some recent references dealing with microwave catalyzed reactions: S. Caddick, *Tetrahedron*, 1995, **51**, 10 403; A. Loupy, A. Petit, J. Hamelin and F. Texier-Boullet, *Synthesis*, 1998, 1213; P. Jacquault, D. Mathé, T. Vidal, T. A. Petit, A. Loupy and R. N. Gedye, *Tetrahedron*, 2000, **56**, 5473; A. Y. Usyatinsky and Y. L. Khmelnitsky, *Tetrahedron Lett.*, 2000, **41**, 5031; A. D. Sagar, N. A. Shinde and B. P. Bandgar, *Org. Prep. Proc. Int.*, 2000, **32**, 269; N. Tesson and S. Deshayes, *Org. Prep. Proc. Int.*, 2000, **32**, 41; S. Deshayes, M. Liagre, A. Loupy, J.-L. Luche and A. Petit, *Tetrahedron*, 1999, **55**, 10 851; R. S. Varma, *Green Chem.*, 1999, **1**, 43; R. S. Varma, *Pure Appl. Chem.*, 2001, **73**, 193.
6 The microwave reactor used was a Normatron® 112 from Normandie Labo S.A. Lintot, France, equipped with magnetic stirring plate and a reflux condenser.

Organic reactions in aqueous medium: FeF_3 catalyzed chemoselective addition of cyanotrimethylsilane to aldehydes

B. P. Bandgar* and V. T. Kamble

Organic Chemistry Research Laboratory, School of Chemical Sciences, Swami Ramanand Teerth Marathwada University, Nanded-431 606, India. E-mail: vtkd@rediffmail.com

Received 22nd February 2001
First published as an Advance Article on the web 25th September 2001

Chemoselective addition of TMSCN to various aldehydes in water using FeF_3 as a new catalyst is carried out giving the corresponding cyanohydrins in good to excellent yields.

Introduction

Cyanohydrins are versatile intermediates bearing two functional groups which can be easily manupulated into a wide range of other products such as α-hydroxy aldehydes, α-hydroxy ketones, β-hydroxy amines and α-amino acid derivatives.[1] Use of cyanotrimethylsilane (TMSCN) instead of HCN as a cyano anion source provides a promising and safer route to these compounds.[2] Nowadays, much attention is focused on the development of practical, novel and versatile methods for the synthesis of cyanohydrins including the most recently developed asymmetric version of this reaction.[3] There are various methods reported for the synthesis of cyanohydrins involving the addition of TMSCN to an aldehyde in an organic solvent catalyzed by a Lewis acid.[4] Where a solvent must be used, water is, without doubt, the most acceptable in terms of cost and environmental impact. However, despite its large liquid range and extremely high specific heat capacity, it is frequently overlooked as a solvent for organic reactions. Therefore, efforts to carry out organic reactions in water poses an important challenge in the area of reaction design. This communication describes our studies directed towards the development of FeF_3 catalyzed selective addition of TMSCN to aldehydes in water (Scheme 1).

Results and discussion

When a mixture of an aldehyde, TMSCN and a catalytic amount of FeF_3 in water is stirred vigorously overnight at room temperature, the corresponding cyanohydrin is formed in high yield and results are given in Table 1. In the absence of Lewis acid (FeF_3) catalyst, no reaction was observed when 4-nitrobenzaldehyde was treated with TMSCN in water (entry 1). This indicates that TMSCN does not decompose in water to generate HCN *in situ*. Similarly, in the presence of potassium fluoride (entry 2), tetrabutylammonium fluoride (entry 3), polyvinylpyridinium fluoride (entry 4), HF (entry 5) or $FeCl_3$ (entry 6) there was no reaction even after stirring the reaction mixture for a longer time (48 h) at room temperature. In search of a more efficient catalyst, we found that FeF_3, a commercially available and water-stable Lewis acid is a highly effective catalyst for this reaction. After much study on the catalytic effect of FeF_3 on cyanohydration of 4-nitrobenzaldehyde, we found that when a stoichiometric amount of FeF_3 (entry 7) is used, it resulted in low yield of the corresponding cyanohydrin. However, 30 mol% of FeF_3 led to complete conversion of the reactants giving excellent yields of the products (entries 10–16). The use of < 30 mol% of FeF_3 for this reaction gave a low yield of the product (entry 8). It is also important to note that there was no reaction when using organic solvents such as $CHCl_3$ or diethyl ether. The reactions were clean and the respective cyanohydrins were obtained in good to excellent yields with total conversion of the starting material. It is of note that in all cases the reaction proceeded smoothly under extremely mild conditions with aliphatic aldehydes (entry 10) and aromatic aldehydes (entries 11–16) or heterocyclic aldehyde (entry 14) as well as dialdehyde (entry 15) and α,β-unsaturated aldehyde (entry 12) giving the corresponding cyanohydrins in high yields. It should be noted that only the 1,2-addition product was observed with cinnamaldehde (entry 12).

The superiority of this protocol can be clearly visualized in the chemoselectivity of this reaction between aldehydes and ketones. It is interesting that only aldehydes underwent selective cyanohydration in the presence of ketones (entry 16 and eqns. 1–4). Thus under these conditions aliphatic, cyclic and aromatic ketones did not undergo addition reactions with TMSCN. The unreacted ketones can also be easily recovered.

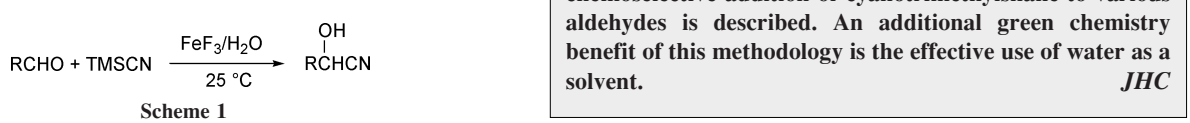

Scheme 1

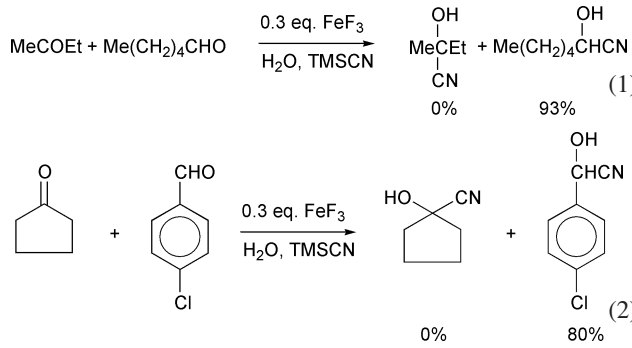

Green Context

Cyanohydrins are very useful synthetic intermediates but the traditional use of HCN makes their preparation hazardous. Cyanotrimethylsilane is a much safer alternative and effective methods to utilise this reagent are needed. Here the use of novel Lewis acid, FeF_3, to catalyze the chemoselective addition of cyanotrimethylsilane to various aldehydes is described. An additional green chemistry benefit of this methodology is the effective use of water as a solvent. ***JHC***

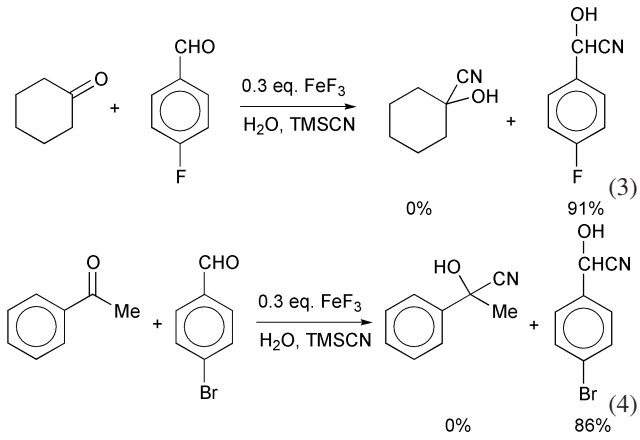

Most Lewis acids cannot be used in this reaction because they decompose or are deactivated in the presence of water. In this connection, the present catalyst is superior because of its stability and higher activity in water relative to organic solvents.

When 4-nitrobenzaldehyde was treated with TMSCN in the presence of KF (1 eqiv.), TBAF (1 equiv.), PVP.HF (1 equiv. w/w) or HF (1 equiv.) the corresponding cyanohydrin was not obtained. These experiments exclude the possibility that a fluoride catalization process is operative.

In conclusion, this work demonstrates that the Lewis acid FeF_3 is a highly efficient catalyst for the addition of TMSCN to aldehydes in water.

Table 1 FeF_3 catalyzed preparation of cyanohydrins from aldehydes with TMSCN in water

Entry	Aldehyde	Catalyst	Product	Yield[ab] (%)
1	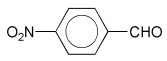	—	No reaction	—
2	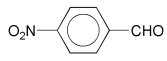	KF (1 equiv.)	No reaction	—
3	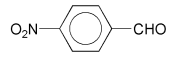	TBAF (1 equiv.)	No reaction	—
4	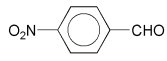	$PVP{\cdot}(HF)_n$ (1 equiv.)	No reaction	—
5	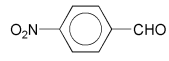	HF (1 equiv.)	No reaction	—
6	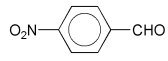	$FeCl_3$ (1 equiv.)	No reaction	—
7	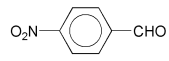	FeF_3 (1 equiv.)	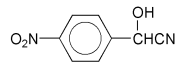	60
8	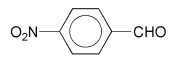	FeF_3 (0.5 equiv.)	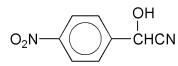	75
9	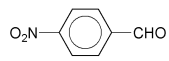	FeF_3 (0.2 equiv.)	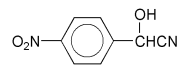	80
10	$Me(CH_2)_7CHO$	FeF_3 (0.3 equiv.)	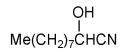	93
11	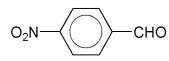	FeF_3 (0.3 equiv.)	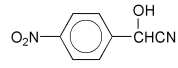	95
12	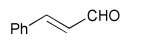	FeF_3 (0.3 equiv.)	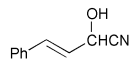	80
13	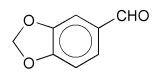	FeF_3 (0.3 equiv.)	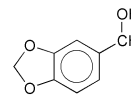	82
14	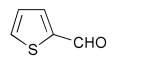	FeF_3 (0.3 equiv.)	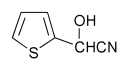	87
15	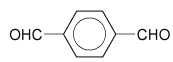	FeF_3 (0.3 equiv.)	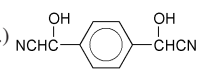	86
16	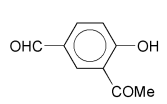	FeF_3 (0.3 equiv.)	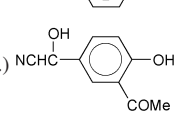	80

[a] Yield of pure isolated product. [b] Product characterized by spectral analysis.

Experimental

All reactions were carrried out in oven-dried flasks. All chemicals were of analytical grade. IR spectra were recorded on a Bomem MB 104 FT-IR spectrometer and ^1H NMR spectra were recorded on an AC 300F NMR spectrometer (300 MHz).

Typical procedure

A mixture of 4-nitrobenzaldehyde (1 mmol), TMSCN (2 mmol) and FeF_3 (0.3 mmol) in water (5 ml) was stirred vigorously for 25 h at room temperature. After completion of the reaction (TLC), the product was extracted with ethyl acetate (2 × 5 ml). After drying organic layer (anhydrous Na_2SO_4), the solvent was removed under reduced pressure to isolate the cyanohydrin of 4-nitrobenzaldehyde.

IR (ν/cm^{-1}): 1108, 1189, 1229, 1345, 1525, 1600, 1610, 2241, 2851, 2922, 3117 and 3339 δ_H($CDCl_3$, TMS): 3.5 (1H, br, OH); 5.7 (s, 1H, CH); 7.75 (d, 2H, ArH); 8.3 (d, 2H, ArH); Anal. Calc. for $C_8H_6N_2O_3$ (178.1449); C, 53.94; H, 6.05; N, 15.73 Found : C, 54.01; H, 6.09; N, 15.65%.

References

1 B. R. Matthews, H. Gountzos, W. R. Jackson and K. G. Watson, *Tetrahendron Lett*., 1989, **30**, 5157; W. R. Jackson, H. A. Jacobs, G. S. Jayatilake, B. R. Matthews and K. G. Watson, *Aust. J. Chem*., 1990, **43**, 2045; W. R. Jackson, H. A. Jacobs, B. R. Matthews, G. S. Jayatilake and K. G. Watson, *Tetrahendron Lett*., 1990, **31**, 1447; T. Ziegler, B. Horsch and F. Effenberger, *Synthesis*, 1990, 575; F. Effenberger and U. Steizer, *Angew. Chem., Int. Ed. Engl*., 1991, **30**, 873; P. Zandbergen, J. Brussee, A. Van der Gen and C. G. Kruse, *Tetrahedron: Asymmetry*, 1992, **3**, 769; Synthesis of pharmaceuticals: K. G. Watson, Y. M. Fung, M. Gredley, G. J. Bird, W. R. Watson, H. Gountzos and B. R. Matthews, *J. Chem. Soc., Chem. Commun*., 1990, 1018; For recent review: M. North, *Synlett*, 1993, 807 and references therein.

2 Y. M. Shafran, V. A. Bakulev and V. S. Mokrushin, *Russ. Chem. Rev*., 1989, **58**, 148.

3 E. J. Corey and Z. Wang, *Tetrahedron Lett*., 1993, **34**, 4001; K. Narasaka, T. Yamada and H. Minamikawa, *Chem. Lett*., 1987, 2073; H. Minamikawa, S. Hayakawa, T. Yamada, N. Iwasawa and K. Narasaka, *Bull. Chem. Soc. Jpn*., 1988, **61**, 4379; S. Tsuboyama, *Bull. Chem. Soc. Jpn*., 1962, **35**, 1004; H. J. Kim and W. R. Jackson, *Tetrahedron: Asymmetry*, 1992, **3**, 1421; H. Nitta, D. Yu, M. Kudo, A. Mori and S. Inoue, *J. Am. Chem. Soc*., 1992, **114**, 7969; M. Hayashi, Y. Miyamoto, T. Inoue and N. Oguni, *J. Org. Chem*., 1993, **5**, 1515; T. K. Chakraborti. G. V. Reddy and K. A. Hussain, *Tetrahedron Lett*., 1991, **32**, 7597; M. T. Reetz, K. Kesseler and A. Jung, *Angew Chem., Int. Ed. Engl*., 1985, **24**, 989.

4 S. Kobayashi, H. Ishitani and M. Ueno, *Syntlett*, 1997, **115**, 000; M. Kanai, Y. Hamashima and M. Shibasaki, *Tetrahedron Lett*., 2000, **41**, 2405; M. Sandberg and L. K. Sydnes, *Org. Lett*., 2000, **2**, 687.